AN ABSTRACT OF THE DISSERTATION OF

Matthew D. Ramirez for the degree of Doctor of Philosophy in Fisheries Science presented on November 25, 2019.

Title: It's in Their Bones: Ecological Drivers of Kemp's Ridley Sea Turtle (*Lepidochelys kempii*) Somatic Growth and Population Dynamics.

Abstract approved: _____

Selina S. Heppell

Somatic growth variation manifests from the cumulative effects of a suite of biological, ecological, and environmental processes and can have profound effects on individual fitness and species population dynamics. As ectotherms whose growth dynamics are greatly influenced by environmental factors, sea turtles display considerable variation in somatic growth within and among individuals, populations, and species. Given the sensitivity of sea turtle population dynamics to small changes in demographic rates, identifying the proximate drivers of somatic growth variation, and subsequent influences on population dynamics, is of high importance to sea turtle conservation and management. This is particularly true for the critically endangered Kemp's ridley sea turtle (*Lepidochelys kempii*), which displays regional differences in somatic growth rates and whose recovery is now uncertain given recent changes in population growth. Through the integration of multiple skeletal, geochemical, and quantitative analyses, my dissertation aims to identify ecological factors influential to

Kemp's ridley sea turtle somatic growth variation and the potential influence of life history variation on their population dynamics.

In Chapter 2, I used a 20+ year dataset of Kemp's ridley sea turtle somatic growth rates generated through skeletochronology to quantify the influence of the *Deepwater Horizon* oil spill, climate change, and changing population density on age- and region-specific somatic growth rates. These analyses revealed a significant reduction in mean somatic growth rates in 2012–2015 for Age 0 and Age 2–5 turtles that stranded in the U.S. Gulf of Mexico and Atlantic Coasts. Additionally, Age 0 and Age 2–5 growth rates were related to regional climate indices and population abundance estimates, respectively. Integrative analysis determined that the 2012 growth shift explained the greatest variation in somatic growth rates, which I hypothesize may be related to long-term deleterious effects of the *Deepwater Horizon* oil spill. Continued evaluation of growth rates is needed to distinguish the effects of population density and climate indices as drivers of somatic growth variation in this species.

In Chapter 3, I sampled bones processed in Chapter 2 for stable isotope ratios ($\delta^{13}C$, $\delta^{15}N$) to characterize regional variation in diet composition and quantify relationships between diet composition and somatic growth rates. Turtle bone stable isotope date were combined with prey stable isotope data collated from the literature into a Bayesian stable isotope mixing model to estimate the proportional contribution of crustaceans, bivalves, gastropods, fish, and seagrass/macroalgae to turtle diets. I found distinct regional differences in model-derived estimates of diet composition that largely follow known diet patterns. My mixing models indicated that northern

GoM and Atlantic turtles primarily consumed invertebrates, western GoM turtles consumed equal amounts of invertebrates and fish, and eastern GoM turtles consumed equal amounts of invertebrates and basal resources. Growth rates were poorly correlated with $\delta^{15}N$ values and diet composition estimates, suggesting that higher trophic level diets do not cause higher Kemp's ridley growth rates and that diet composition does not drive the apparent regional differences in somatic growth evident in this species.

In Chapter 4, I investigated the ability of complementary lead (Pb) stable isotope, trace element, and growth rate analyses to discriminate regional (GoM vs. Atlantic) Kemp's ridley sea turtle habitat use. Through multiple quadratic discriminant function analyses, I found that ^{208}Pb:^{206}Pb could be used to classify turtles to stranding region with exceptional accuracy (94.1 %), whereas somatic growth rates in conjunction with Sr:Ca, Cu:Ca, Ba:Ca, Mg:Ca, and Zn:Ca had a correct classification success rate of 79.5 %. These results suggest that Pb stable isotopes, and possibly somatic growth rates, may provide a useful tool for studying Atlantic-to-GoM ontogenetic shifts in this and other sea turtle species in the future.

In Chapter 5, I used a spatially explicit, age-structured matrix population model to evaluate the relative contribution of Atlantic Kemp's ridley sea turtles to population growth and recovery prior to 2010. I specifically evaluated sensitivity to changes in key transition probabilities that describe the movement of turtles among habitats and life stages within the western North Atlantic Ocean. My model simulations suggest that Atlantic turtles were a strong contributor to Kemp's ridley population growth during the species' pre-2010 recovery and are unlikely to influence

recovery time, even under the most extreme scenarios evaluated. Future work will include simulations under stable or declining population growth rate indicators, as have been observed in the species since 2010.

Taken together, this study filled some critical knowledge gaps in our understanding of the relationship between multiple ecological and environmental factors (oil spills, climate, population density, foraging ecology, habitat use) and Kemp's ridley sea turtle somatic growth and population dynamics. This research also highlighted the importance of continued collection and study of stranded turtle tissues as they provide a means to investigate otherwise intractable research questions in sea turtle ecology.

©Copyright by Matthew D. Ramirez
November 25, 2019
All Rights Reserved

It's in Their Bones: Ecological Drivers of Kemp's Ridley Sea Turtle (*Lepidochelys kempii*) Somatic Growth and Population Dynamics

by
Matthew D. Ramirez

A DISSERTATION

submitted to

Oregon State University

in partial fulfillment of
the requirements for the
degree of

Doctor of Philosophy

Presented November 25, 2019
Commencement June 2020

Doctor of Philosophy dissertation of Matthew D. Ramirez presented on November 25, 2019

APPROVED:

Major Professor, representing Fisheries Science

Head of the Department of Fisheries and Wildlife

Dean of the Graduate School

I understand that my dissertation will become part of the permanent collection of Oregon State University libraries. My signature below authorizes release of my dissertation to any reader upon request.

Matthew D. Ramirez, Author

ACKNOWLEDGEMENTS

It is hard to believe that just seven years ago I was a budding new graduate student eager to make my mark on the world without becoming a viral internet meme. Had you told me 10 years ago that I would become an expert in the study of sea turtles bones I most certainly would not have believed you. My path to this degree is checkered by the influence of countless people who intentionally or not helped shape me into the scientist I am today. First and foremost, I must thank my graduate advisor Selina Heppell whose wisdom, encouragement, and guidance allowed me to flourish as a researcher. Her suggestion at the beginning of my graduate studies to reach out to Larisa Avens and Jeffrey Seminoff at NOAA to discuss sea turtle bones and stable isotopes was perhaps the single most influential event to putting me on my current career and research trajectory. Thank you to Larisa and Jeff for their willingness to collaborate with me, share samples and data for my graduate studies, and host me at their respective NOAA facilities at various points over the past few years. Your continued support, enthusiasm for science, and creative insight were instrumental to my development and the success of these projects. Thank you to Jessica Miller, Alyssa Shiel, and Jennifer McKay, who exposed me to exciting new areas of research novel to the sea turtle world and who were invaluable to my geochemistry training.

I must also thank the many co-authors on these manuscripts. Thank you to Lisa Goshe for spending a month with me in 2016 to teach me how to perform skeletochronological analyses. The resulting data from those and subsequent efforts were critical to all chapters of my dissertation. Thank you to Melissa Snover for

providing bone growth data and input on manuscripts. Thank you to Melissa Cook for continuing to collect sea turtle humerus bones from stranded turtles long past you were required and for providing valuable insight into the transport of sea turtle carcasses in the ocean. Thank you to Heather Haas for assistance in obtaining funding for some of these projects and providing valuable input that shaped the direction of Chapter 2.

This work would also not have been possible without the assistance of countless individuals who were not listed as co-authors. First, I must thank my indispensable team of undergraduate research assistants: Jason Cordeiro, Meghan Davis, Hanna Hagler, Mathew VanBemmel, Julia Hart, Keira McNeely, and Nate Owens. I might still be working in the lab if it wasn't for all of your hard work. I would also like to thank Kathy Magnusson who allowed me to use her lab and equipment for an entire year to perform skeletochrological analysis. Thank you to Brian Stacy and Jennifer Keene for collecting and providing sea turtle humeri as part of the *Deepwater Horizon* oil spill Natural Resource Damage Assessment. I also thank Andy Ungerer, Chris Russo, and Nansen Olsen for assistance with laser ablation-inductively coupled plasma-mass spectrometry and Beth Rutila, Kali Melby, and Christina Murphy for assistance with Pb isotope analyses. I also extend special thanks to Jeff Moore, Alex Curtis, and Tomo Eguchi for their insight during the development of my population model for Chapter 5.

I would also like to thank the hundreds of federal, state, and private partners that collectively form the Sea Turtle Stranding and Salvage Network (STSSN). Your dedicated work responding to and sampling sea turtle strandings over the past 40

years is the primary reason these projects were even possible. Thank you also to the state and federal coordinators of the STSSN for their permission to use their stranding data in Chapter 5: Wendy Teas, Donna Shaver, Lyndsey Howell, Melissa Cook, Allen Foley, Mark Dodd, Michelle Pate, Sarah Finn, Sarah Rose, Amanda Weschler, Suzanne Thurman, Robert Schoelkopf, Kimberly Durham, Janelle Schuh, Robert Prescott, Connie Merigo, Lynda Doughty, Sean Todd, and Kate Sampson.

I am especially grateful to my family, old and new, for their support throughout this process. I must particularly thank my husband, Wyatt, and our dogs, Ruby and Tusc. Your love and encouragement were instrumental to getting me through this Ph.D., especially during my exams and these last few months of analysis and writing. I am forever indebted to you for putting up with me throughout this endeavor. Also thank you to the Heppell lab and all of my Corvallis friends past and present. You made our time in Corvallis unforgettable and a true adventure. Having to continuously say goodbye to you all has been one the hardest parts of this experience, but I look forward to many more adventures in the future!

Funding for myself and this project were provided by the NSF Graduate Research Fellowship Program, the National Oceanic and Atmospheric Administration National Marine Fisheries Service (NOAA-NMFS), the NOAA Office of Education Educational Partnership Program (# NA16SEC4810007), the PADI Foundation (# 28838), and multiple scholarships from Oregon State University (OSU) and the OSU Department of Fisheries and Wildlife. This publications content is solely the responsibility of the award recipient and do not necessarily represent the official views of the U.S. Department of Commerce, National Oceanic and Atmospheric

Administration. Research was conducted under USFWS permit number TE-676379-5 issued to the NMFS Southeast Fisheries Science Center.

CONTRIBUTION OF AUTHORS

Dr. Larisa Avens provided somatic growth rate data and humerus bone cross-sections used in all chapters. She also provided updated habitat-specific somatic growth curves for estimating age from size in Chapter 5. Ms. Lisa Goshe, Dr. Melissa Snover, Dr. Larisa Avens, and I performed skeletochronological analyses to generate the growth rate dataset. Dr. Melissa Cook provided valuable recent humerus bone samples from Mississippi for 2015–2016 for Chapters 2–4. She also provided valuable insight into the oceanic transport of sea turtle carcasses. Dr. Heather Haas contributed to the analysis of Chapter 2 and was instrumental in obtaining funding for Chapters 3 and 4. Dr. Jessica Miller provided training in trace element analysis for Chapter 4 and provided input on data analysis and interpretation. Dr. Alyssa Shiel assisted with lead isotope analyses and data reduction and analysis for Chapter 4. Dr. Melissa Cook and Dr. Donna Shaver, in addition to numerous state stranding coordinators not included as co-authors, contributed stranding data used in Chapter 5. Dr. Selina Heppell contributed to study design and data analysis and interpretation for Chapters 2–5. All co-authors contributed to manuscript revisions.

TABLE OF CONTENTS

Page

Chapter 1: General Introduction 1

Chapter 2: Regional Environmental Drivers of Kemp's Ridley Sea Turtle Somatic Growth Variation 8

Abstract 9

Introduction 10

Materials and Methods 15

Sample collection and processing 15

Age and growth rate estimation 16

Environmental covariates 18

Data Analysis 20

Results 24

Age and Growth 24

Deepwater Horizon oil spill effects 26

Density-dependent effects 28

Climate effects 29

Integrative effects 30

Discussion 32

Chapter 3: Elucidating Intra-Population Diet Variation and Potential Influence on Somatic Growth in the Kemp's Ridley Sea Turtle (*Lepidochelys Kempii*) Through Complementary Skeletochronological and Stable Isotope Analyses 52

Abstract 53

Introduction 54

Materials and Methods 59

Geographic Breakpoints 59

Prey Stable Isotope Ratios 60

Sea Turtle Stable Isotope Ratios 62

Stable Isotope Mixing Model 66

Somatic Growth Rates 69

Results 71

TABLE OF CONTENTS (Continued)

Page

Prey and Sea Turtle Stable Isotope Ratios 71

Regional Variation in Diet Composition 73

Diet Composition and Somatic Growth Rates 75

Discussion 76

Chapter 4: Classification of Kemp's Ridley Sea Turtles to Marine Ecoregions Through Complementary Skeletal and Geochemical Analyses 98

Abstract 99

Introduction 100

Materials and Methods 105

Sample Collection and Processing 105

Bone Geochemical Analyses 106

Somatic Growth Rates 110

Statistical Analyses 113

Results 115

Regional Variation in Geochemical Markers 115

Trace Element Discriminant Analysis 115

Lead Isotope Discriminant Analysis 117

Discussion 118

Chapter 5: Kemp's Ridley Sea Turtle Life History Variation: Do Atlantic Turtles Matter? 139

Abstract 140

Introduction 141

Materials and Methods 146

Model Structure 146

Model Parameterization 148

Model Implementation, Evaluation, and Projection 156

Results 157

Juvenile Survival Rates 157

Elasticity and Sensitivity Analyses 158

TABLE OF CONTENTS (Continued)

Page

Population Projections 160

Discussion 160

Chapter 6: General Conclusion 179

Bibliography 188

Appendix A: Chapter 2 Supplemental Information 215

Appendix B: Chapter 3 Supplemental Information 224

Appendix C: Chapter 4 Supplemental Information 266

Appendix D: Chapter 5 Supplemental Information 269

LIST OF FIGURES

Figure Page

Figure 2.1. Conceptual model of alternative hypotheses for the size-class-specific growth response of Kemp's ridley sea turtles to environmental factors..... 46

Figure 2.2. Frequency histograms of Kemp's ridley sea turtle back-calculated somatic growth rates by stranding location, age, and year..... 47

Figure 2.3. Time series of mean Kemp's ridley sea turtle growth rate by age class. . 48

Figure 2.4. Von Bertalanffy growth functions estimated for Kemp's ridley sea turtles stranded in the Gulf of Mexico before (1993–2009, *n* = 309) and after (2010–2016, *n* = 459) the *Deepwater Horizon* oil spill. 49

Figure 2.5. Relationship between mean back–calculated growth rate and population density metrics for Age 2–5 Kemp's ridley sea turtles stranded in the Gulf of Mexico. 50

Figure 2.6. Relationships between (**A**-**C**) climate indices and year and (**D**-**F**) mean Age 0 growth rates and annualized climate indices (2-yr lag)..... 51

Figure 3.1. Map of Kemp's ridley sea turtle stranding locations for the humerus bones used in this study and geographic breakpoints used to cluster turtles and prey groups. 93

Figure 3.2. Biplots of $\delta^{13}C$ and $\delta^{15}N$ values for Kemp's ridley sea turtles (open circles) and their potential prey groups (mean ± SD) by geographic region. 94

Figure 3.3. Proportional contribution of each prey group to Kemp's ridley sea turtle diets by geographic region based on MixSIAR models that included an informative prior constructed from published diet proportion data and an uninformative prior that assigned equal probability to all prey groups. 95

Figure 3.4. Generalized Linear Model results examining the relationships between annual Kemp's ridley sea turtle growth rates and $\delta^{15}N$ values, and age and $\delta^{15}N$ values, for individual turtles by geographic region. 96

Figure 3.5. Generalized Linear Model results examining the relationship between annual Kemp's ridley sea turtle growth rates and proportional contribution of fish to western Gulf of Mexico turtle diets. 97

Figure 4.1. Stranding locations for Kemp's ridley sea turtles (n = 82) analyzed for trace element concentrations (n = 73) and Pb isotope ratios (n = 17). 134

LIST OF FIGURES (Continued)

Figure Page

Figure 4.2. Boxplots of weighted annual growth rates (cm yr^{-1}; n = 73), trace element ratios (mg g^{-1} ; n = 73), and lead isotope ratios (n = 17) for Kemp's ridley sea turtles by stranding region (ATL, Atlantic = Florida Atlantic Coast to Virginia; GoM, Gulf of Mexico = Texas to Florida Gulf Coast). 135

Figure 4.3. Posterior probabilities for regional assignments resulting from the reduced quadratic discriminant function models (black points = trace element $QDA_{reduced}$, red points = lead isotope $QDA_{reduced}$). 136

Figure 4.4. Partition plots showing the classifications of turtles to regions based on the reduced trace element QDA. 137

Figure 4.5. Biplots of $^{208}Pb/^{206}Pb$ and $^{206}Pb/^{207}Pb$ for Kemp's ridley sea turtles, potential Pb sources (aerosols, coal), and other animals (oyster, coral) sampled for Pb isotopes within the western North Atlantic Ocean and Gulf of Mexico (GoM)..... 138

Figure 5.1. Conceptual diagram of base spatially explicit, age structured matrix population model. 171

Figure 5.2. Summary of sizes (straightline carapace length, SCL) and ages of stranded Kemp's ridley sea turtles by region. 172

Figure 5.3. Results of region- and age-specific catch curve analyses for Kemp's ridley sea turtles. 173

Figure 5.4. Habitat- and stage-specific survival and fertility elasticities for Kemp's ridley sea turtles (2005–2009). 174

Figure 5.5. Estimated population size by life stage for the base model (Model 1: Atlantic turtles shift to GoM at maturation; base scenario = 15% to Atlantic, ATL, annually). 175

Figure 5.6. **(A)** Predicted nest counts for the base model (Model 1: Atlantic turtles shift to GoM at maturation) ran using varying proportions of turtles entering U.S. Atlantic life stages from the oceanic life stage. **(B)** Percent change in nests counts relative to the base scenario (base scenario = 15% to Atlantic, ATL, annually). Plots for Model 2 and 3 presented in Figure D4. 176

Figure 5.7. Sensitivity of population growth rate (percent change in λ_{nest} for period 2005–2009) to change in the proportion of turtles entering U.S. Atlantic life stages from the oceanic life stage (base scenario = 15% to Atlantic, ATL, annually) for each model evaluated. 177

LIST OF FIGURES (Continued)

Figure Page

Figure 5.8. **(A)** Predicted number of nesting females per year based on projection of base model (Model 1: Atlantic turtles shift to GoM at maturation) and varying proportions of turtles entering U.S. Atlantic life stages from the oceanic life stage. **(B)** Projection for all three models evaluated using base scenario (15% to Atlantic annually). 178

LIST OF TABLES

Table Page

Table 2.1. Summary characteristics for Kemp's ridley sea turtles by stranding location. 41

Table 2.2. Summary statistics for the family of models used to evaluate whether von Bertalanffy growth parameter estimates differed for Kemp's ridley sea turtles stranded in the Gulf of Mexico before (1993–2009, *n* = 309) and after (2010–2016, *n* = 459) the *Deepwater Horizon* oil spill. 42

Table 2.3. Results of complementary breakpoint and cutpoint analyses. 43

Table 2.4. Summary statistics for the family of Generalized Additive Models used to evaluate the influence of covariates [temporal shift (TS), hatchling production (HatchProd), Multivariate El Niño Southern Oscillation Index (MEI)] on mean age class-specific growth rates for Age 0 and Age 2–5 Kemp's ridley sea turtles. 44

Table 2.5. Summary of statistical output for Generalized Additive Models (GAMs) used to evaluate the influence of potential environmental covariates [temporal shift (*TS*), hatchling production (*HatchProd*), Multivariate El Niño Southern Oscillation Index (*MEI*)] on mean age class-specific growth rates for Age 0 and Age 2-5 Kemp's ridley sea turtles. 45

Table 3.1. Summary of literature review for Kemp's ridley sea turtle prey species included in the mixing model. See Table B1 for full dataset..... 88

Table 3.2. Mean ± SD $\delta^{13}C$ and $\delta^{15}N$ values for potential prey groups by geographic region. 89

Table 3.3. Summary characteristics for Kemp's ridley sea turtle bone growth layers sampled for stable isotope analysis. 90

Table 3.4. Median (95% CI) posterior Bayesian mixing model estimates of diet proportion by geographic region for Kemp's ridley sea turtles (n = 153). 91

Table 3.5. Summary of statistical output for Generalized Linear Models used to evaluate the influence of diet on Kemp's ridley sea turtle annual growth rates. 92

Table 4.1. Estimated accuracy [relative standard deviations (RSD)], precision (percent difference from MACS-1 known values; mean ± SD), and limits of detection (LOD; mean ± SD) for trace element data collected via laser ablation-inductively coupled plasma-mass spectrometry. 129

LIST OF TABLES (Continued)

Table Page

Table 4.2. Summary information [mean ± SD (range)] for Kemp's ridley bone growth layers sampled for trace element concentrations (mg g^{-1}, $^{*}\mu g\ g^{-1}$) and lead isotope ratios by stranding region..... 130

Table 4.3. Results of one-way AN(C)OVA comparing elemental concentrations among regions after controlling for age and year effects, where needed. 131

Table 4.4. Predicted regional assignment of Kemp's ridley sea turtles based on cross-validated quadratic discriminant function analysis (QDA). 132

Table 4.5. Results of stepwise variable selection using the Wilk's λ criterion. 133

Table 5.1. Summary of input parameter used across all models. 168

Table 5.2. Age at oceanic-to-neritic habitat shift by stranding region based on bone $\delta^{15}N$ values (‰) [mean ± SD (sample size)]. 169

Table 5.3. Summary of survival rate estimates generated through catch curve analyses of stranding data (non-bolded values) or maximum likelihood estimation (bolded values) for the three models evaluated..... 170

LIST OF APPENDIX FIGURES

Figure Page

Figure A1. Time series of Kemp's ridley sea turtle abundance. 220

Figure A2. Relationship between mean back–calculated growth rate and population density metrics for Age 0 Kemp's ridley sea turtles stranded in the Gulf of Mexico and Atlantic Coast. 221

Figure A3. Relationship between mean back–calculated growth rate and population density metrics for Age 1, Age 2–5, and Age 6–9 Kemp's ridley sea turtles stranded in the Gulf of Mexico. 222

Figure A4. Relationship between mean back–calculated growth rate and population density metrics for Age 1, Age 2–5, and Age 6–9 Kemp's ridley sea turtles stranded along the Atlantic Coast. 223

Figure B1. Map of sampling locations of invertebrate prey groups and geographic breakpoints used to cluster turtles and prey groups. 260

Figure B2. Map of sampling locations of fish and macroalgae/seagrass prey groups and geographic breakpoints used to cluster turtles and prey groups. 261

Figure B3. Informative and uninformative priors used in the mixing models..... 262

Figure B4. Posterior distributions for the proportional contribution of each prey group to Kemp's ridley sea turtle diets. 263

Figure B5. Proportional contribution of each prey group to Kemp's ridley sea turtle diets based on MixSIAR models that included an informative prior constructed from published diet proportion data and an uninformative prior that assigned equal probability to all prey groups. 264

Figure B6. Sensitivity analysis showing how the proportional contribution of each prey group to western GoM-stranded Kemp's ridley sea turtle diets changes when trophic discrimination factors (TDFs) are varied. 265

Figure C1. Conceptual diagram outlining **(A)** decision tree for estimating growth rates and **(B)** weighted growth rate calculation. 268

Figure D1. Transition probabilities for Atlantic-to-GoM ontogenetic shifts used in Model 1 (Atlantic turtles shift to GoM at maturation) and Model 2 (Atlantic turtles shift to GoM beginning at age 7). 271

Figure D2. Kemp's ridley stranding counts by state and year. 272

LIST OF APPENDIX FIGURES (Continued)

Figure Page

Figure D3. Estimated annual mortality estimates for Kemp's ridley stranding counts by state. 273

Figure D4. Predicted nest counts for Model 2 (upper panels; Atlantic turtles shift to GoM beginning at age 7) and Model 3 (lower panels; No Atlantic turtles shift to GoM) ran using varying proportions of turtles entering U.S. Atlantic life stages from the oceanic life stage. 274

LIST OF APPENDIX TABLES

Table Page

Table A1. Summary characteristics for stranded Kemp's ridley sea turtles by stranding state. 216

Table A2. Results of Reverse Helmert Coding schemes used to compare mean age class-specific growth rates of Kemp's ridley sea turtles before and after the Deepwater Horizon oil spill. 217

Table A3. Summary of statistical output for age class-specific Generalized Additive Models (GAMs) used to analyze the influence of population density metrics on mean back–calculated growth rates for Kemp's ridley sea turtles stranded in the U.S. Gulf of Mexico and Atlantic Coasts. 218

Table A4. Cross-correlation coefficients for comparison of age class-specific mean growth rates and lagged climate indices (0- to 5-yr lags). 219

Table B1. Stable carbon and nitrogen isotope values for potential Kemp's ridley sea turtle prey species included in the stable isotope mixing model. 228

Table B2. Summary of studies quantifying Kemp's ridley sea turtle diet composition throughout their range. 254

Table B3. Elemental concentrations of species representative of the prey groups included in the stable isotope mixing models. 255

Table B4. Statistical results for Kruskal-Wallis rank sum tests comparing prey stable carbon and nitrogen isotope ratios **(A)** within and **(B)** among regions. 257

Table B5. Statistical results for Wilcoxon rank sum tests comparing stable carbon and nitrogen isotope ratios among prey groups within regions. 258

Table B6. Statistical results for one-way Analysis of Variance with post-hoc Tukey Honestly Significant Difference Test comparing Kemp's ridley bone stable carbon and nitrogen isotope ratios among regions. 259

Table C1. Predicted regional assignment of Kemp's ridley sea turtles based on cross-validated quadratic discriminant function analysis (QDA). 267

Table D1. Annual nest and hatchling production from the three primary Kemp's ridley sea turtle nesting beaches in Mexico (Rancho Nuevo, Tepehuajes, Playa Dos). Data sourced from Gallaway et al. (2016) (originally provided by La Comisión Nacional de Áreas Naturales Protegidas, CONANP). 270

CHAPTER 1: GENERAL INTRODUCTION

Somatic growth is a fundamental component of an organism's life history that can shape both individual fitness and community and population dynamics (Werner & Gilliam 1984, Stearns 1992, Dmitriew 2011). For ectothermic reptiles, species whose internal body temperatures fluctuate with changes in ambient temperatures (Atkinson 1994), somatic growth rates reflect the integrated effects of a myriad of biological, ecological, and environmental factors. Given that fitness is maximized at habitat-specific optimal growth rates (Werner & Gilliam 1984), intrapopulation variation in somatic growth can have strong effects on key life history features critical to both individual fitness and species population dynamics such as time to maturity (Frazer et al. 1993, Bjorndal et al. 2013a), size-dependent mortality (Werner & Gilliam 1984, O'Brien et al. 2005), and fecundity (Berry & Shine 1980, Frazer & Richardson 1986). Illuminating the proximate drivers of somatic growth variation can thus aid evaluation of population demography, particularly in slow-growing, long-lived species such as sea turtles whose population dynamics are sensitive to changes in demographic rates (Crouse et al. 1987, Gerber & Heppell 2004).

Sea turtle somatic growth rates are highly variable within and among individuals, populations, and species. Yet, our understanding of the specific factors underpinning this variation is poor due to the logistical difficulty of studying growth in such highly mobile, widely distributed species. Because all seven species of this charismatic megafauna are threatened or endangered, considerable resources have

been mobilized over the past 50 years to both protect and study them. However, in-water studies have lagged behind research performed on nesting beaches (Hamann et al. 2010, Rees et al. 2016), resulting in relatively modest evaluation of sea turtles growth rates and underlying mechanisms to date. Recent advances in bone-based studies of sea turtle somatic growth rates using skeletochronology, in conjunction with regular bone collection through the Sea Turtle Stranding and Stranding Network, have greatly enhanced our ability to study sea turtle growth rates across space and time and potentially identify mechanisms underpinning somatic growth variation (Zug et al. 1986, Ramirez et al. 2017, Avens et al. 2017). As sea turtle population dynamics are sensitive to small changes in demographic rates, especially size-specific mortality and time to maturity (Crouse et al. 1987, Crowder et al. 1994, Heppell et al. 2004), identifying the proximate drivers of somatic growth variation and subsequent influences on population dynamics is of high importance to sea turtle conservation and management.

The Kemp's ridley sea turtle (*Lepidochelys kempii*) is an ideal model species to investigate drivers of somatic growth variation and potential influences on sea turtle population dynamics due to its unique ecology and conservation status. First, Kemp's ridleys retain annual records of growth in their humerus bone, which have been collected from dead stranded turtles throughout the species range since the 1990s. The species thereby has a unique 20+ year history of somatic growth against which environmental variables can be compared. Second, the species occupies multiple marine habitats throughout the western North Atlantic Ocean that each have

a unique suite of threats and stressors (Bolten 2003), potentially allowing for the separation of growth effects associated with different environmental factors (e.g., climate, oil spills, population density). Third, the species experienced exponential growth from the 1990s through 2000s following implementation of successful conservation efforts (NMFS & USFWS 2015), providing a natural experiment to seek evidence for density-dependent regulation of somatic growth. Fourth, the species has regionally variable diets and growth rates (Shaver 1991, Seney & Musick 2005, Witzell & Schmid 2005, Avens et al. 2017), providing a means to examine relationships between individual foraging ecology and growth. Lastly, 85 % of annual nest production occurs on only a ~60 km stretch of beach in Mexico (NMFS et al. 2011), which has been heavily monitored since 1978, providing an unprecedented record of nest and hatchling production for nearly an entire species that has served as vital input for population models.

Marine ecosystems have changed rapidly over the past century due to the synergistic effects of multiple environmental and anthropogenic factors. Climate variability, both natural and human-induced, has led to persistent shifts in food web structure and function that have had cascading effects on organisms at all trophic levels (deYoung et al. 2008, Beaugrand et al. 2015). For sea turtles, climate-driven shifts in productivity have impacted the abundance of important food and habitat resources over inter-annual and decadal time scales (Sanchez-Rubio et al. 2011, 2018, Karnauskas et al. 2015), which may be linked to changes in growth rates (Bjorndal et al. 2013b, 2016, 2017) and reproductive rates (Chaloupka et al. 2008, Mazaris et al.

2008, Van Houtan & Halley 2011, del Monte-Luna et al. 2012) for multiple species. Additionally, multiple large oil spills have wreaked havoc on marine habitats (Hall et al. 1983, Peterson et al. 2003, Beyer et al. 2016, Bertrand & Hare 2017). Of particular note was the 2010 *Deepwater Horizon* (*DWH*) oil spill in the Gulf of Mexico (GoM), the largest man-made environmental disaster in United States history (DWH NRDA Trustees 2016). While the full impact of the *DWH* oil spill on sea turtles remains unknown, immediate declines in survival and physiological condition were observed (Mitchelmore et al. 2017, Stacy et al. 2017), and a cascade of indirect effects may have compromised long-term health and growth rates (Stacy 2015, Coleman et al. 2016).

Fully natural processes, such as changing population density and individual foraging behavior, can also strongly influence somatic growth rates. Density-dependent regulation of growth is principally manifested through resource limitation, where per capita food availability declines with increasing population size. This phenomenon has be observed across a wide range of marine species (e.g., Bjorndal et al. 2000, Lorenzen & Enberg 2002, Jansen & Burns 2015, Hammill & Sauvé 2017). The Kemp's ridley population experienced exponential growth (12–19% per year) between 1990 and 2009. However, annual nest counts have fluctuated unpredictably since 2010, prompting investigations into whether the carrying capacity of the GoM has been reached for this species (Gallaway et al. 2016b, Caillouet et al. 2016, 2018). Empirical support for this hypothesis has generally been lacking due to insufficient data (but see Shaver et al. 2016). However, the 20+ year growth time series for

Kemps ridleys generated through skeletochronology provides a means of evaluating support for density dependent growth in this species. Similarly, sea turtle bones contain records of diet in the form of naturally occurring stable isotopes, which when compared to potential prey stable isotope data in mixing models can be used to estimate the contribution of different prey groups to consumer diets. Given the regional differences in diet observed in this species (e.g., fish in western and northern GoM turtle diets, tunicates in eastern GoM turtles diets, invertebrates only in Atlantic turtle diets; Shaver 1991, Seney & Musick 2005, Witzell & Schmid 2005), combined stable isotope and skeletochronological analysis of their bone tissue may allow for determination of the relationship between growth and diet composition, a well-known driver of somatic growth variation (Dunham 1978, Cairns 1988, Abraham & Sydeman 2004).

Integrating life history variation into demographic models can reveal the relative contribution of multiple sources of variation to population growth rates (Caswell 1983, Sæther & Bakke 2000, Beston 2011). Considering the effect of life history variation on population dynamics is particularly important to understanding the dynamics of patchily distributed species with regionally variable demographic rates, such as Kemp's ridleys, where local effects can alter a species' population trajectory if population subgroups are connected (Runge et al. 2014). Understanding the connectivity of population subgroups, in addition to their demographic rates, is thereby critical to demographic modeling and population assessment for conservation and management. Nevertheless, our understanding of the differential recruitment of

Kemp's ridleys to Atlantic versus GoM habitats, and movements in between, is poor. Furthermore, although multiple population models have been implemented for Kemp's ridleys to evaluate extinction risk and estimate time to recovery (e.g., Heppell et al. 2004, NMFS & USFWS 2015, Gallaway et al. 2016, Kocmoud et al. 2019), none have explicitly included a separate Atlantic Kemp's ridley population subgroup nor regionally variable demographic rates.

The primary objectives of my dissertation were to (1) identify environmental factors influential to Kemp's ridley sea turtle somatic growth rates and (2) examine how life history variation influences sea turtle population dynamics. I address these objectives in four primary chapters centered on the analysis of 20+ year collection of Kemp's ridley sea turtle bones originally sourced from dead stranded turtles through the Sea Turtle Stranding and Salvage Network. In Chapter 2, I used the full somatic growth dataset to examine how Kemp's ridley growth rates were influenced by the *DWH* oil spill, climate change, and population density over the past 20 years. In Chapter 3, I sampled a subset of these bones for stable carbon and nitrogen isotope ratios to characterize regional variation in diet composition and quantify relationships between diet composition and somatic growth rates. In Chapter 4, I investigated the ability of complementary lead (Pb) stable isotope, trace element, and growth rate analyses to discriminate regional (GoM vs. Atlantic) Kemp's ridley sea turtle habitat use in order to develop tools to study population connectivity. In Chapter 5, I use a spatially explicit, age-structured matrix population model to examine how life history variation (e.g., habitat-specific demographic rates, variable ontogenetic shifts)

influences Kemp's ridley population growth and to evaluate the relative contribution of Atlantic Kemp's ridley sea turtles to population growth and recovery. My study illustrates the incredible role stranded sea turtles can play in filling important knowledge gaps pertinent to sea turtle conservation and management.

CHAPTER 2: REGIONAL ENVIRONMENTAL DRIVERS OF KEMP'S RIDLEY SEA TURTLE SOMATIC GROWTH VARIATION

Matthew D. Ramirez, Larisa Avens, Lisa R. Goshe, Melissa L. Snover, Melissa Cook, Heather L. Haas, and Selina S. Heppell

In preparation for submission to Marine Biology

Abstract

Environmental conditions are the primary driver of somatic growth variation in wildlife populations, and changes in somatic growth can be an important indicator of environmental perturbations. Yet, identifying specific environmental factors influential to the somatic growth rates of migratory marine megafauna has proven challenging. Using a 20+ year dataset of somatic growth generated through skeletochronology, we evaluated the potential effects of multiple region-wide environmental factors—the 2010 *Deepwater Horizon* (*DWH*) oil spill, climate change, and population density—on age- and region-specific Kemp's ridley sea turtle (*Lepidochelys kempii*) somatic growth rates. We used temporal analyses to identify structural shifts in a time series of growth and fit von Bertalanffy growth curves to explicitly compare somatic growth rates before and after the *DWH* oil spill. Generalized Additive Models (GAMs) and cross-correlation analyses were used to examine relationships between growth rates, population abundance measures, and time-lagged climate indices, and to partition variance explained by the alternate environmental factors. The GAMs showed significant, multi-year reductions in mean somatic growth rates beginning in 2012 for Age 0 and Age 2–5 turtles from both the Gulf of Mexico and Atlantic Ocean. Comparisons of pre- and post-*DWH* von Bertalanffy growth curves indicated that the Brody growth rate coefficient (K) was lower after the *DWH* oil spill. Regional climate indices were correlated with mean Age 0 growth rates with a 2-yr lag (cross-correlation = –0.57 to 0.60), whereas population abundance exhibited significant relationships with mean Age 2–5 growth

rates. In integrative analyses, the temporal shift in growth rates was identified as the greatest predictor of somatic growth variation. We theorize that this shift is related to long-term deleterious effects of the *DWH* oil spill on hatchling and small juvenile turtles. However, there are potential additive influences of both changing climate and population abundance on somatic growth rates for certain age classes. Continued collection and study of sea turtle humerus bones is needed to further identify mechanisms underpinning the observed growth patterns given that the coincidental timing of changes in environmental parameters examined herein made it difficult to assess their individual and combined effects.

Introduction

Marine ecosystems have experienced unprecedented change over the past century due to multiple environmental and anthropogenic stressors that have caused population declines (Myers & Worm 2003, McCauley et al. 2015), persistent shifts in food web structure and function (i.e., ecological regime shifts) (deYoung et al. 2008, Beaugrand et al. 2015), and loss and degradation of habitats (Halpern et al. 2008, Mendelssohn et al. 2012). Numerous studies have characterized effects of single stressors on marine species, but fewer have examined the synergistic effects of multiple environmental factors over extended time scales, particularly in higher order marine megafauna such as sea turtles, marine mammals, and sharks (Crain et al. 2008, Bjorndal et al. 2013b). As the population dynamics of these long-lived species are highly sensitive to small changes in demographic rates (Heppell et al. 2000),

understanding environmental effects on growth, survival, and reproduction is important to their conservation and management.

The Kemp's ridley sea turtle (*Lepidochelys kempii*) is an ideal model species to assess the influence of multiple environmental factors on large marine vertebrate demographic rates due to its ecology and conservation history. First, their humerus bones contain annual records of somatic growth—similar to tree rings and fish otoliths—and have been collected from dead stranded turtles since the early 1990s (Snover & Hohn 2004, Avens et al. 2017). Second, decades of intensive conservation and management following near extinction in the 1980s led to exponential population growth over the past two decades and a robust record of hatchling production from the species' primary nesting beach, allowing for investigations into density dependent population regulation (Caillouet et al. 2016, 2018). Lastly, the species' global distribution is predominantly restricted to the Gulf of Mexico (GoM) and U.S. Atlantic (Musick & Limpus 1997), an area that experienced a climate-driven ecological regime shift in the 1990s (Sanchez-Rubio et al. 2011, Karnauskas et al. 2015) and the largest man-made environmental disaster in United States history with the 2010 explosion and sinking of the *Deepwater Horizon* (*DWH*) oil drilling rig (DWH NRDA Trustees 2016). The presence of a subset of the population outside the geographic footprint of the *DWH* oil spill (i.e., U.S. Atlantic Coast) provides a natural experiment to examine *DWH* oil spill effects and potentially disentangle them from other region-wide stressors such as changing climate and population density.

Environmental impacts of the *DWH* oil spill and response efforts were unprecedented in their temporal, spatial, and ecological scale, as were the subsequent clean-up and impact mitigation (DWH NRDA Trustees 2016, Beyer et al. 2016). Yet, much still remains unknown about the response of sea turtles to this anthropogenic disturbance outside the well-documented short-term effects on survival and oiled turtle physiology (Mitchelmore et al. 2017, Stacy et al. 2017). Negative effects of the *DWH* oil spill on somatic growth rates have been documented in a wide range of fish and invertebrates (e.g., Rozas et al. 2014; Brown-Peterson et al. 2016; Herdter et al. 2017; Perez et al. 2017). Moreover, a cascade of indirect effects followed the exposure of marine habitats to *DWH* oil spill-associated environmental toxins as occurred in the Prince William Sound following the 1989 *Exxon Valdez* oil spill (Peterson et al. 2003). Sublethal or indirect effects on sea turtle health mediated through the food web continue to remain a significant concern (McDonald et al. 2017, Stacy et al. 2017). Such effects may be responsible for the general decline in nutritional condition of stranded sea turtles from 2011 to 2013 and the observation of lower juvenile Kemp's ridley growth rates in Mississippi post–*DWH* relative to pre–*DWH* estimates (Stacy 2015, Coleman et al. 2016).

The Kemp's ridley experienced exponential population growth (12–16% per year) between 1990 and 2009 following decades of conservation and management, resulting in rapid increases in abundance across all life stages (Heppell et al. 2004, NMFS & USFWS 2015). However, in 2010, annual nest counts began to fluctuate unpredictably. Causal factors have been difficult to identify, but one hypothesis is that

the carrying capacity of the GoM has been reached for this species (Gallaway et al. 2016b, Caillouet et al. 2016, 2018). While the current population is less than 10% of its estimated historic size (Bevan et al. 2016), long-term alteration and degradation of GoM ecosystems, as well as reductions in some food resources (e.g., blue crab *Callinectes sapidus*; VanderKooy 2013), may have lowered the potential carrying capacity of the GoM for sea turtles (Heppell et al. 2007, Caillouet 2014). Nevertheless, empirical support for this hypothesis is lacking. Most evidence for density dependent population regulation in this species is based on analyses of nesting trends (Gallaway et al. 2016b, Caillouet et al. 2016, 2018, Kocmoud et al. 2019), which are confounded after 2010 with unknown effects of the *DWH* oil spill. Shaver et al. (2016) provide the only potential empirical support for density dependent effects on reproductive rates with the observation of increasing breeding intervals from 2008 to 2016 in Kemp's ridleys nesting in Texas. However, other environmental factors, such as colder temperatures on the foraging grounds during the winter of 2009–2010 (Lamont & Fujisaki 2014, Gallaway et al. 2016b), could have also contributed to this pattern.

Climate is a primary driver of spatiotemporal variability in ocean productivity, and abrupt changes in bottom-up forcing associated with climate often precipitate ecological regime shifts (deYoung et al. 2008, Beaugrand et al. 2015). Within the North Atlantic Ocean, an ecological regime shift occurred in the late-1990s as a result of an abrupt warming of the ocean that coincided with one of the strongest El Niño Southern Oscillation events ever recorded in 1997/1998 as well as a shift from cool to

warm phase of the Atlantic Multidecadal Oscillation (Sanchez-Rubio et al. 2011, Luczak C. et al. 2011, Reid & Beaugrand 2012, Beaugrand et al. 2013, Karnauskas et al. 2015). This late-1990s regime shift has been linked to reduced blue crab productivity in the GoM (Sanchez-Rubio et al. 2011), an important food source for sea turtles, as well as declining growth rates in loggerhead (*Caretta caretta*), green (*Chelonia mydas*), and hawksbill (*Eretmochelys imbricata*) sea turtles in the western North Atlantic Ocean (Bjorndal et al. 2013b, 2016, 2017). Similar declines in growth were observed in large juvenile and adult Kemp's ridleys in the GoM from 1988 to 2009 and small juveniles from 2004 to 2009 (Avens et al. 2017), although causal mechanisms have yet to be identified.

Here we examined temporal trends in juvenile Kemp's ridley sea turtle growth rates using a 20+ year dataset generated through skeletochronology. The primary objective of this study was to quantify the influence of multiple region-wide environmental factors, including the *Deepwater Horizon* oil spill, changing climate, and increasing population density, on Kemp's ridley sea turtle growth rates. We developed and tested a suite of hypotheses related to the differential effect of these factors (Figure 2.1). Given the observed decrease in nutritional condition of GoM-stranded turtles and significant degradation of offshore and nearshore habitats in the GoM following the 2010 *DWH* oil spill, we predicted that Kemp's ridley growth rates would decline beginning in 2010 for both oceanic and neritic juveniles. Importantly, we predicted *DWH* oil spill effects to be restricted to turtles resident in the GoM only; Atlantic turtle growth rates should not change after 2010 given their spatial isolation

from this anthropogenic stressor. We predicted that density-dependent effects, if present, would result in declining growth rates beginning in the mid- to late-2000s for GoM life stages, when population growth was the highest (NMFS & USFWS 2015); only a small fraction of Kemp's ridleys reside in the Atlantic and we assume they are not strongly influenced by intraspecific population density. Lastly, we predicted that climate effects would cause declining growth rates across all Kemp's ridley life stages beginning in the late-1990s in response to a regional regime shift as observed in other western North Atlantic sea turtle species.

Materials and Methods

Sample collection and processing

Front flippers were collected from Kemp's ridleys that stranded on U.S. beaches from Texas to Massachusetts between 1991 and 2017 by participants of the Sea Turtle Stranding and Salvage Network. Samples were obtained from turtles that either stranded dead or stranded alive but were later euthanized. Stranding location, date, and carapace length were recorded at the time of stranding (see Tables 2.1 and A1 for summary). Carapace length was measured as straightline (SCL) or curved (CCL) carapace length, notch to tip. In cases where only CCL was recorded, CCL was converted to SCL as described by Avens et al. (2017). This study utilizes and extends the growth datasets presented in Avens et al. (2017) (n = 333 turtles, GoM) and Snover et al. (2007a) (n = 144, Atlantic) to include growth histories obtained

from 783 turtles stranded along the U.S. GoM Coast and 453 turtles stranded along the U.S. Atlantic Coast between 1991 and 2017.

Humerus bones were prepared and histologically processed as described by Avens and Snover (2013) and Avens et al. (2017). Tissue was removed from the humerus bones, which were then boiled and air dried for at least two weeks. A low-speed isomet saw (Buehler) was used to cut a 2 to 3 mm thick cross-section from each bone just distal to the deltopectoral muscle insertion scar. Bone sections were fixed and decalcified using Cal Ex II (Fisher Scientific) or 10% neutral buffered formalin followed by RDO (Apex Engineering Corporation) and thin sectioned to 25 microns using a freezing-stage microtome (Leica) or cryostat (Thermo Scientific Microm HM 550). Thin sections were stained using diluted Ehrlich's hematoxylin, mounted onto microscope slides in 100% glycerin, and digitally imaged using a digital camera fitted to a compound microscope. Growth mark analyses were performed using image analysis software (Olympus Microsuite and cellSens) and Adobe Photoshop (Adobe Systems). Two or three readers (of L. Avens, L. R. Goshe, M. Ramirez, M. Snover) independently analyzed the digital bone images to determine the number and placement of lines of arrested growth (LAGs), which delimit the outer edges of each skeletal growth mark (Snover & Hohn 2004), followed by a joint assessment to reach consensus. Once consensus was reached, total humerus section diameter and the diameter of each LAG were measured.

Age and growth rate estimation

Previous analyses validated annual LAG deposition in Kemp's ridleys (Snover & Hohn 2004, Avens et al. 2017), allowing for characterization of age at stranding through skeletochronology. Kemp's ridleys deposit a unique first-year growth mark, or "annulus," that differs from subsequent marks (Snover & Hohn 2004). For bones where the annulus was visible, an initial age estimate was determined directly from LAG counts. However, bone resorption results in the loss of internal LAGs as sea turtles age (Zug et al. 1986), preventing the direct assessment of turtle age in larger individuals where the annulus has been resorbed. Therefore, for turtles where the annulus was not visible, a correction factor was developed based on the relationship between LAG numbers and diameters from known age individuals to estimate the number of LAGs lost to resorption for each bone (Parham & Zug 1997). An initial age estimate was then generated by adding the estimated number of resorbed LAGs to the number visible LAGs. A final age estimate at stranding was made by adjusting initial age estimates to the nearest 0.25 years based on the mean hatch date for the population (June) and individual stranding date. Given that LAG deposition occurs in late winter/early spring and peak hatching for this species occurs during the summer (Snover & Hohn 2004), the first-year growth mark denotes an age of ~0.75 years, the next LAG an age of 1.75 years, and so on. Final age estimates were used to back-assign age estimates to individual LAGs. Similarly, a calendar year was back assigned to each LAG based on the date of stranding.

There is a strong allometric relationship between humerus section diameter (HSD) and SCL for Kemp's ridleys that allows for the back-calculation of body size

estimates for measurable LAGs (Snover & Hohn 2004, Avens et al. 2017). We characterized the HSD:SCL relationship for newly processed turtle bones and combined that with the body proportional hypothesis back-calculation technique (BPH; Francis 1990) to estimate SCL for every measurable LAG, adjusted for turtle-specific SCL and HSD at death. Annual somatic growth rates were then calculated by taking the difference between SCL estimates of successive LAGs. In this way, multiple growth rate estimates were generated from each humerus bone (median = 3 per turtle, range = 1–8). Growth rate estimates were assigned to the calendar year associated with the LAG that begins the growth interval.

Environmental covariates

To separate potential *DWH*-induced growth effects from those derived from other region-wide environmental factors, we examined the influence of population density and climate on Kemp's ridley somatic growth rates. While these are not encompassing of all major environmental phenomena that may influence sea turtle growth rates, we focused on them given the scale of their potential impact.

The relationships between somatic growth rates and population density were investigated using two independently-derived population abundance metrics: (1) annual age class-specific abundance estimates obtained from the most recent Kemp's ridley population model used for status assessment (i.e., model-dependent metric; NMFS and USFWS 2015), and (2) cumulative annual hatchling production from the species' index nesting beach in Tamaulipas, Mexico, which comprises over 85% of

nesting activity by the species (i.e., model–independent metric; data sourced from NMFS & USFWS 2015). This species is unique among sea turtles in that nearly its entire annual reproductive output is concentrated on only a handful of beaches in Mexico and South Texas that have been monitored and protected continuously since 1978. This has allowed for the near-complete census of nests laid and hatchlings produced from these beaches annually, accounting for over 85% of the known population (NMFS & USFWS 2015). The Kemp's ridley population model used to derive age-specific abundance estimates is a deterministic age-based simulation model that uses known hatchling production since 1966 to predict the number of nests laid annually (NMFS and USFWS 2015). Model-derived abundance estimates by age-class are only used through 2009 given model uncertainties beginning in 2010 when nest counts began to fluctuate widely and a large number of Kemp's ridleys are estimated to have been killed by the *DWH* oil spill (Wallace et al. 2017a). Trends in these metrics are summarized in Figure A1.

To elucidate potential relationships between changes in broadscale climate patterns and Kemp's ridley somatic growth variation, we considered three well-known modes of variability [North Atlantic Oscillation (NAO), Atlantic Multidecadal Oscillation (AMO), and the El Niño Southern Oscillation (ENSO)] that exert strong biophysical control on western North Atlantic Ocean ecosystems (Giannini et al. 2001, Greene et al. 2013, Karnauskas et al. 2015). Collectively, they influence ocean temperature, salinity, mixing, and circulation patterns that affect the productivity, distribution, growth, and survival of animals across all trophic levels (Drinkwater et

al. 2003, Edwards et al. 2013, Karnauskas et al. 2015). For the NAO, we used the winter (December to March) NAO index (wNAO) given that the NAO is thought to exert the greatest influence on ocean ecosystems in the boreal winter (Drinkwater et al. 2003). For the ENSO, we used the Multivariate El Niño Southern Oscillation Index (MEI) Version 2, which integrates five meteorological variables: SST, surface air temperature, sea–level pressure, surface zonal winds, surface meridional winds, and Outgoing Longwave Radiation. Monthly AMO and bimonthly MEI data were obtained from NOAA's Earth System Research Laboratory (http://www.esrl.noaa.gov/psd/data/climateindices/) whereas wNAO data were obtained from the National Center for Atmospheric Research (https://climatedataguide.ucar.edu/climate–data/). For the AMO and MEI, monthly or bimonthly data were averaged within a calendar year to create an annualized index used in all analyses.

Data Analysis

We employed a suite of statistical tools to evaluate the independent and synergistic effects of the *Deepwater Horizon* oil spill, population density, and climate on Kemp's ridley growth rates. In most cases, analyses were restricted to juvenile growth data—binned by age class (Age 0, 1, 2–5, 6–9) to increase statistical power—given that adult turtle growth rate data are poorly represented in the dataset. These age classes align with known ontogenetic differences in somatic growth rates and are similar to those used in age-structured population models for this species (Snover et

al. 2007b, NMFS & USFWS 2015). Age 0 (ages 0 to 0.75) and 1 (ages 0.75 to 1.75) align with the oceanic life stage but are separated here because growth rates differ between these ages and a small fraction of Kemp's ridleys begin to recruit to neritic habitats at age 1. All other age classes represent neritic life stages, i.e., small neritic juveniles (2–5), large neritic juveniles (6–9). As pre-2000 data suggest that somatic growth rates differ between Kemp's ridleys that inhabit the U.S. Gulf of Mexico and Atlantic Coast (Avens et al. 2017), growth data were analyzed separately for turtles that stranded on beaches in these regions for all age classes but Age 0—all Age 0 turtles are assumed to occupy the same oceanic habitats in the central GoM prior to migrating to neritic habitats along either the U.S. Gulf or Atlantic Coast.

To investigate *DWH* oil spill effects on somatic growth rates we used two primary approaches: growth curve and temporal analysis. First, to examine population-level growth response, a family of von Bertalanffy growth functions (VBGFs) were fit to size-at-age data for all turtles stranded before (1991–2009) and after (2010–2017) the *DWH* oil spill using non–linear least-squares regression. Eight models were considered to compare von Bertalanffy growth parameters (L_∞, K, t_0) between both time periods that ranged from including identical parameter estimates between the time periods (1 L_∞, 1 K, 1 t_0) to including different parameter estimates for the time periods (2 L_∞, 2 K, 2 t_0), and all model subsets in between (Table 2.2). Akaike information criterion (AIC) and Akaike weights (w_i) were used to evaluate and compare models (Burnham & Anderson 2002). Given that adult turtles primarily reside and nest in the GoM (Morreale et al. 2007), VBGFs were fit using data from

GoM-stranded turtles only. In addition, given the non–independence of the full growth dataset, VBGFs were fit to measured SCL and estimated age at stranding only, eliminating SCL and age data estimated from growth marks. Growth functions were implemented using the *FSA* (Ogle et al. 2018) and *nlstools* (Baty et al. 2015) packages in R (version 3.5.3; R Core Team 2019).

To examine mean age class-specific growth response to the *DWH* oil spill and identify year(s) of statistically significant changes in mean somatic growth, we employed breakpoint and cutpoint structural analyses, followed by regression coding schemes. The breakpoint analysis uses segmented regression to randomly split the time series into two or more segments to identify the optimum number of break points based on minimization of residual sum of squares and Bayesian information criterion (Zeileis et al. 2003). Once the optimal number of break points were identified, the Chow test was used to assess their statistical significance. In addition, maximally selected rank statistics were used to identify the single best cutpoint for each time series. This approach differs from the breakpoint analysis in that it is non–parametric and is robust to small sample sizes (Hothorn & Lausen 2003, Müller & Hothorn 2004). These analyses were restricted to years with a minimum of five growth rate estimates per age class to avoid the influence of anomalous growth rates and were implemented using the *strucchange* and *coin* packages in R (Zeileis et al. 2002, Hothorn et al. 2006). As breakpoint and cutpoint analyses do not account for non–independence of data, Reverse Helmert Coding was used to specifically compare growth rates in the years during and after (2010–2015) the *DWH* oil spill to growth

rates in the 15 years prior (1995–2009). Regression coding schemes were implemented using age class-specific linear mixed-effects models that included estimated annual growth rate, year at the beginning of the bone growth interval, first-order autoregressive [AR(1)] covariance structure for growth increments within turtles, and turtle-specific random effects.

Relationships between population density metrics and mean age class-specific growth rates were examined using Generalized Additive Models (GAMs). Models included age-specific abundance (*Abund*) or cumulative hatchling production (*HatchProd*) as a fixed effect, an identity link, and a quasi-likelihood error function. Within each model, mean growth rates were weighted by sample size (i.e., number of growth rate estimates per year). For the oceanic life stages (Age 0, Age 1), age-specific growth rates were compared to the model-derived cumulative number of 0– and 1–year old turtles predicted to exist in a given year (metric 1) or the cumulative number of hatchlings produced in a given year and the year prior (t_0–t_{-1}) (metric 2). For the neritic life stages (Age 2–5, Age 6–9), age-specific growth rates were compared to the model–derived cumulative number of juvenile turtles (ages 2–9) predicted to exist in a given year (metric 1) or the cumulative number of hatchlings produced two to five years in the past (t_{-2}–t_{-9}) (metric 2). Models were implemented in R using the *mgcv* package (Wood 2006).

Cross-correlation was used to examine relationships between mean age class-specific growth rates and climate indices. Following Bjorndal et al. (2016), GAMs with AR(1) covariance structure were fit to the annualized climate data to reveal

underlying trends in the climate indices since 1950 for the wNAO and AMO and 1979 for the MEI. Mean age class-specific growth rates were then compared to lagged (0- to 5-yrs) smoothing spline fits generated from the GAMs using the *ccf* function in R (version 3.5.3; R Core Team 2019). Cross-correlation coefficients were used to measure the degree of similarity between the two time series.

To partition variance in mean age class-specific growth associated with the alternative region-wide environmental factors, we implemented a family of GAMs that included various combinations of the three factors investigated as fixed effects and used AIC and w_i to evaluate and compare models (Burnham & Anderson 2002). The specific covariates included in the models were determined based on the results of the previous analyses examining the environmental factors independently. As in the previous GAMs, each model included an identity link and a quasi-likelihood error function, and weighted mean growth rates by sample size.

Results

Age and Growth

SCL and age at stranding ranged from 4.2 to 69.1 cm SCL and zero to 30.25 years for turtles stranded on U.S. GoM beaches. Those stranded on U.S. Atlantic Coast beached were 19.3 to 66.7 cm SCL and 1.00 to 18.75 years old (Tables 2.1, A1). Although their contribution to the breeding population is not well understood (NMFS & USFWS 2015), documentation of tagged Atlantic turtles nesting on the species' primary nesting beach in Mexico suggests that Atlantic Kemp's ridleys

ultimately return to the GoM as large juveniles or maturing adults (Caillouet et al. 2015), resulting in relatively few adult animals on the Atlantic Coast. In total, skeletochronological analyses yielded 3600 annual growth rate estimates from 1235 turtles for the years 1988 to 2015 (Figure 2.2). This constitutes the largest and most comprehensive dataset of Kemp's ridley somatic growth rates to date. Annual growth rates span the ages 0 (first year of life) to 28.75 but data from younger ages (< 6 yrs) dominate the dataset (~75%) because younger/smaller turtles are the most abundant Kemp's ridley age classes in the population and thus constitute the majority of stranded turtles (Gallaway et al. 2016b).

For both the GoM and Atlantic Coast, there were distinct spatiotemporal changes in humerus bone collection from dead stranded turtles. Prior to 2010, GoM samples were primarily obtained from turtles stranded in Texas (wGoM) and Florida (eGoM), whereas after 2010 sample collection shifted to turtles stranded in Louisiana, Mississippi, and Alabama (nGoM) as part of the *DWH* oil spill response efforts. Along the U.S. Atlantic Coast, there was a similar shift in sample collection from turtles that stranded primarily in North Carolina and Virginia (sATL) to turtles that stranded in Massachusetts (nATL) in 2014 and 2015. Using a general linear mixed model that accounted for year, age, AR(1) autocorrelation, and turtle-specific random effects, we found somatic growth rates did not differ within regions (Tukey's post hoc > 0.05) but were significantly lower in turtles from the Atlantic Coast (Tukey's post hoc < 0.05). Examination of age class-specific growth rates indicates that these

regional differences in growth manifest as early as Age 1 and extend through the small neritic juvenile life stage (Age 2–5) (Figure 2.3).

The quantity of age class-specific somatic growth rate data was sparse for years preceding 1995, so all temporal growth analyses begin in 1995 and generally extend through 2014/2015. The datasets for Age 0, Age $2–5_{GoM}$, Age $2–5_{Atlantic}$, and Age $6–9_{GoM}$ turtles are the largest and most continuous—all years have at least seven independent growth rate estimates (Figure 2.3). In contrast, significant data gaps exist for Age 1_{GoM}, Age $1_{Atlantic}$, and Age $6–9_{Atlantic}$ turtles and the datasets for Age $6–9_{GoM}$ and Age $6–9_{Atlantic}$ turtles only extend to 2012 and 2010, respectively. Caution is thus warranted when interpreting results from these latter data given that they are relatively incomplete and do not reflect similar time frames as the data for Ages 0 and 2–5.

Deepwater Horizon oil spill effects

Von Bertalanffy growth models fit to stranding length-at-age estimates from turtles that stranded in the GoM were significantly different before and after the *DWH* oil spill (Table 2.2, Figure 2.4). The model with the lowest AIC score and highest Akaike weight (w_i of 0.404) included common L_∞ and t_0 parameters but different K parameters for the two time periods (1993–2009 vs. 2010–2016; Table 2.2). However, the next three best models had ΔAIC scores less than 2.0 and w_i values between 0.152 and 0.237. While the parameters that differed or agreed between the two time periods varied in these models, all included two separate K parameters and

the summed weights of the models that included separate *K* parameters was 0.943, indicating strong evidence for an overall growth rate reduction in the GoM after 2009. Because most Atlantic Kemp's ridley juveniles are thought to emigrate back to the GoM as maturing subadults, we did not conduct a similar growth rate fitting exercise for the Atlantic strandings.

Temporal analyses showed significant decreases in annual somatic growth rates between 2011 and 2012 for turtles in the oceanic (Age 0) and small neritic juvenile life stages in both the U.S. GoM (Age 2–5_{GoM}) and Atlantic Coast (Age 2–$5_{Atlantic}$) (Table 2.3, Figure 2.3). Similar results were obtained using the complementary breakpoint, cutpoint analyses, and Reverse Helmert Coding schemes—all identified a significant structural shift in the growth time series for these two age classes between 2011 and 2012 (Tables 2.3, A2). Growth rates in 2013 (Age 0, Age 2–5_{GoM}) and 2014 (Age 2–5_{GoM}, Age 2–$5_{Atlantic}$) remained significantly lower than pre–*DWH* growth rates. The breakpoint analysis identified a second significant change (increase) in somatic growth for the Age 2–5_{GoM} time series between 2008 and 2009. However, 2011 was identified as the best cutpoint for the time series. No consistent changes ($P < 0.05$) in growth were identified for the Age 1_{GoM}, Age $1_{Atlantic}$, and Age 6–$9_{Atlantic}$ time series across the statistical methods used. Within the GoM and Atlantic age classes that exhibited significant decreases in annual somatic growth rates in 2012, mean annual growth rates declined by 1–2 cm relative to growth rates in years prior to the *DWH* oil spill. Notably, even with a

decrease in growth rates, small neritic juveniles (Age 2–5) still grew faster in the GoM relative to the Atlantic.

Taken together, these analyses provide evidence for a sharp decline in Kemp's ridley growth rates in the years following the *DWH* oil spill. However, the results of the temporal analyses did not align with our original hypotheses that predicted either an acute (H_{1A}) or chronic (H_{1B}) *DWH* oil spill impact on somatic growth rates beginning in 2010 for turtles in the GoM only (Figure 2.1)—a decline is also evident in the turtles that stranded in the Atlantic.

Density-dependent effects

We found little support for density dependent effects of cumulative turtle abundance and hatchling production on mean age class-specific somatic growth rates (Table A3). For all but Age 2–5_{GoM}, GAMs revealed no significant relationship between these population density metrics and somatic growth ($P > 0.05$)—mean annual growth rates did not decline with increasing predicted juvenile abundance nor was there the presence of a threshold above which growth rates declined. The GAM response functions for both population abundance metrics and both GoM and Atlantic stranded turtles were generally similar (Figures A2–A4).

Cumulative hatchling production was a significant ($P = 0.018$) predictor of Age 2–5_{GoM} somatic growth whereas cumulative Age 2–5 abundance was only a marginally significant ($P = 0.051$) predictor (Table A3, Figure 2.5). Growth rates at the highest Age 2–5_{GoM} population abundances were lower on average than those at

lowest predicted population abundance. However, 95% confidence intervals surrounding the annual means at the highest and lowest abundances overlapped extensively. Nevertheless, the shapes of this relationship for Age 2–5_{GoM} did align with our hypothesis related to density-dependent effects (H_2) on somatic growth rates (Figure 2.1), which predicted a threshold above which growth rates begin to decline.

Climate effects

Mean annual growth rates were generally poorly correlated with the annualized climate indices with 0- to 5-year lags (Table A4). Cross correlations for most life stages (Age 1, Age 2–5, Age 6–9) were generally negligible to weak (cross correlations ≤ |0.40|), although cross correlations for Age 6–9_{GoM} with 4- and 5-yr lags were –0.53 and –0.59 for wNAO and 0.52 and 0.60 for AMO. In contrast, mean annual growth rates exhibited moderate to strong correlations with all climate indices for the fully oceanic life stage (Age 0; Figure 2.6). The highest, consistent cross correlation values for Age 0 included a 2-year lag (wNAO = 0.59; AMO = –0.57; MEI = 0.60). Cross correlations values ≥ |0.50| were also observed for the wNAO and AMO with 3- to 4-yr lags, and the MEI with 0- to 1-yr lags. The general consistency in age class-specific growth patterns through time (Figure 2.3) do not align with our predicted climate growth response (Figure 2.1: H_3) of declining growth rates beginning in the late 1990s but do suggest that ocean climate may affect hatchling and oceanic juvenile growth.

For the wNAO, positive cross correlations mean growth rates are higher when winter weather conditions are warmer and wetter in the western North Atlantic (Drinkwater et al. 2003) and during periods of high river discharge, enhanced blue productivity, and reduced *Sargassum* abundance in the GoM (Sanchez-Rubio et al. 2011, 2018). Similar conditions along with cooler ocean temperatures are present during negative AMO phases (Karnauskas et al. 2015), which aligns with our observation of negative correlations between AMO and growth rates (i.e., positive wNAO and negative AMO are coupled). Positive correlations between the MEI and growth rates indicate growth rates increase when ocean temperatures increase (Giannini et al. 2001), which contrasts with correlations with the AMO which suggest the opposite effect. Such differences may relate to system- and taxon-specific responses to climate variability, which can influence organisms both directly through changes physical properties of the environment (e.g., temperature, circulation) as well as indirectly through changes in resource availability (Drinkwater et al. 2003, Edwards et al. 2013, Karnauskas et al. 2015).

Integrative effects

Three sets of GAMs were implemented to determine which environmental factors—either independently or synergistically—were most influential to Age 0, Age 2–5_{GoM}, and Age 2–$5_{Atlantic}$ somatic growth rates. Comparative models were restricted to these age classes because they showed evidence of significant temporal, density, and climate effects. The three specific metrics evaluated in these models were (1) the

temporal shift (*TS*) observed in 2012, included as a categorical variable (TS_{pre} = 1995-–2011, TS_{post} = 2012–2015); (2) cumulative hatchling production (*HatchProd*), included as a continuous variable; and, (3) the annualized GAM trend for the MEI index with a 2-year lag, included as a continuous variable. Cumulative hatchling production and the MEI index displayed high collinearity ($r > 0.90$) during the study period and were modeled separately, resulting in the evaluation of five models for each age class that included all combinations of the above covariates as fixed effects (i.e., *TS* + *MEI, TS* + *HatchProd, TS, MEI, HatchProd*).

For both Age 0 and Age 2–5_{Atlantic}, the top model included *TS* and *MEI* as fixed effects based on AIC score and Akaike weight (Table 2.4). However, in both cases the next two best models were within 1 AIC of the top models. These models included *TS* and *HatchProd* or *TS* only as fixed effects. The cumulative Akaike weights for these top three models were 0.89 for Age 0 and 1.00 for Age 2–5_{Atlantic}. However, *TS* was the only statistically significant predictor of mean Age 0 and Age 2–5_{Atlantic} growth rates in these top three models (Table 2.5).

For Age 2–5_{GoM}, the single best model included *TS* and *HatchProd* as fixed effects with an Akaike weight of 0.71 (Table 2.4). Only *TS* was a statistically significant predictor of mean Age 2–5_{GoM} growth rates for this model (Table 2.5), although *HatchProd* was marginally significant ($P = 0.071$). Unlike Age 0 and Age 2–5_{Atlantic}, no other Age 2–5_{GoM} models had ΔAIC scores less than two.

Discussion

Through an analysis of a 20-year time series, we show that juvenile Kemp's ridley sea turtles have experienced a recent, multi-year reduction in somatic growth from 2012 to 2015 that spanned multiple life stages (oceanic and small neritic juveniles) and habitats (GoM and western North Atlantic). This temporal shift was the strongest predictor of somatic growth variation among the environmental factors investigated. However, it is also possible that regional climate and population density contribute to oceanic and small neritic juvenile somatic growth variation in the GoM, albeit to a smaller degree. Our results contrast with other post–*DWH* oil spill studies that observed immediate effects on growth in invertebrates and fish in 2010 but coincide with observations of declines in stranded turtle nutritional condition in the northern GoM beginning in 2012 (Stacy 2015), a phenomena of unknown origin but that would likely reduce growth rates.

While the growth rate reduction observed in Atlantic-foraging turtles suggests that factors other than *DWH* are affecting juvenile Kemp's ridleys, we theorize that the observed declines in growth across the species' range that begin in 2012 result from both direct and indirect effects of the *DWH* oil spill on GoM ecosystems that ultimately compromised the long-term health of sea turtles. Sea turtle exposure to *DWH*-associated environmental toxins was high both during and after the *DWH* oil spill given its spatial overlap with critical sea turtle foraging grounds (Wallace et al. 2017a). Indeed, sea turtles in the GoM continued to use impacted foraging areas in the years following the *DWH* oil spill (Shaver et al. 2013, Hart et al. 2014), ingested

spilled oil, and absorbed polycyclic aromatic hydrocarbons (PAHs) into their tissues (Ylitalo et al. 2017, Reich et al. 2017). Exposure to PAHs can cause adverse physiological effects in animals, including reduced growth (e.g., Meador et al. 2006; Albers 2006), and likely continues to threaten coastal food webs as a result of leaching and resuspension of oil-contaminated sediments (Murawski et al. 2016, Rouhani et al. 2017, Romero et al. 2017). Following the 1989 *Exxon Valdez* oil spill, chronic exposure to weathered oil entrained in sediments delayed the recovery of a wide range of taxa for decades due to long-term effects on survival, growth, and reproduction (Peterson et al. 2003), and similar effects appear to be compromising the long-term health, reproductive success, and survival of GoM bottlenose dolphins (Schwacke et al. 2014, 2017, Lane et al. 2015, Kellar et al. 2017). Sublethal effects of long-term exposure to PAHs and other *DWH*-associated toxins may include reduced growth rates in sea turtles.

Interestingly, the decline in growth rates herein aligns with a simultaneous decline in the nutritional condition of neritic turtles stranded in the northern GoM. Stacy (2015) necropsied Kemp's ridleys stranded dead in the northern GoM between 2010 and 2014 and observed significantly smaller fat stores in turtles that stranded in 2013 and 2014 relative to turtles that stranded in 2010 and 2011, with this change beginning in 2012. This declining trend was only evident in turtles 25–60 cm SCL at stranding (~2–9 yrs old), which encompasses the small and large neritic juvenile life stages included in our study. Causal factors for this change in nutritional status were not identified, but the spatiotemporal proximity to the *DWH* oil spill is conspicuous.

Alternatively, these changes may relate to the collapse of the Mississippi blue crab fishery in 2011, which has been attributed to freshwater inundation from the opening of the Bonnet Carré Spillway (GSFMC 2015), and may have forced turtles to feed at fishing piers (Rudloe & Rudloe 2005, Coleman et al. 2016). Comparisons of the nutritional status and growth histories of dead stranded turtles may improve our understanding of temporal variability in Kemp's ridley growth dynamics.

The observation of a strong decline in growth for small neritic juveniles in the Atlantic concurrent to that observed in the GoM was unexpected given our initial hypotheses. The specific causal factors for this decline remain unknown. However, this simultaneous change in disparate ocean regions could hint at a common stressor that impacted oceanic-stage turtles and was carried over to later life stages. All Kemp's ridleys associate with floating *Sargassum* within GoM oceanic habitats for the first 1 to 3 years of life before recruiting to neritic habitats along either the U.S. GoM or Atlantic Coast (Turtle Expert Working Group 2000). The *DWH* oil spill is known to have severely compromised these *Sargassum* habitats, which tended to accumulate oil, became hypoxic, and sank (Powers et al. 2013). The loss of this critical oceanic habitat likely led to a cascade of indirect effects that increased predation rates, reduced prey availability, and increased the energetic costs of foraging (Witherington 2002). It is well established that early nutrition can impact life-time growth through 'silver spoon' effects in a wide range of taxa (Larsson & Forslund 1991, Madsen & Shine 2000, McAdam & Boutin 2003, Gaillard et al. 2003). Therefore, it is plausible that although neritic Atlantic Kemp's ridleys were

spatially isolated from the *DWH* oil spill, cumulative impacts on oceanic habitats and life stages compromised the long-term turtle health of sea turtles and were carried into non-impacted marine habitats outside of the GoM (Putman et al. 2015). Our understanding of population connectivity in this species is limited; thus, some Atlantic Kemp's ridleys could have also occupied neritic GoM habitats during the *DWH* oil spill and later been transported to the U.S. Atlantic Coast via the Loop Current and Gulf Stream.

It is also possible that the decline in neritic turtle growth rates in the Atlantic is independent from that in the GoM and was caused by an environmental factor not measured in this study. Our analysis centered on region-wide environmental factors, but many other factors may differentially affect sea turtle growth at a smaller scale including diet, prey availability, interspecific competition, local water temperatures, disease, cold-stunning, and many anthropogenic stressors. Notably, Atlantic Kemp's ridleys likely face greater interspecific competition for resources relative to their GoM conspecifics due to the presence of a large loggerhead sea turtle population. These species generally segregate geographically in the GoM (Hart et al. 2018a b), and limited tracking data suggests they may also partition resources in the Chesapeake Bay (Byles 1988). As Kemp's ridley diet may differ regionally (Shaver 1991, Seney & Musick 2005, Witzell & Schmid 2005), changes in prey availability concurrent to increased intra- and inter-specific competition could decrease nutritional status and lead to reduced growth rates. This indeed may explain why overall growth rates are lower for Kemp's ridleys in the Atlantic relative to those in

the GoM (Avens et al. 2017). An improved understanding of regional differences in diet and resource availability, population connectivity, and competition between Atlantic loggerheads and Kemp's ridleys would greatly aid future investigations into regional differences in sea turtle vital rates.

Given the apparent relationships between oceanic and small neritic juvenile growth rates and regional climate and population abundance, respectively, we cannot rule out these factors as drivers of somatic growth variation in Kemp's ridleys. Recent studies have linked decades-long declines in sea turtle growth rates throughout the Caribbean Basin to a climate-driven ecological regime shift that occurred in the late-1990s (Bjorndal et al. 2013b, 2016, 2017). Patterns of oceanic turtle growth herein generally align with this narrative. However, this does not negate that possibility of *DWH*-induced changes in somatic growth rates for oceanic turtles. Although vast areas of *Sargassum* habitat were damaged and destroyed following the *DWH* oil spill, 2011 and 2012 saw anomalous high *Sargassum* abundance throughout the tropical North Atlantic that should have renewed these habitats and provided oceanic stage turtles with optimal conditions for growth and survival (Witherington et al. 2012, Gower et al. 2013, Powers et al. 2013). That oceanic turtle growth rates were significantly lower in 2012 and 2013 relative to nearly all years prior suggests the presence of an additional factor. Given that oceanic turtles alive in 2012 would not have been directly impacted by the *DWH* oil spill, changes in growth rates for this life stage likely reflect the synergistic effects of lingering impacts of the *DWH* oil spill and changes in regional climate on oceanic habitats.

We similarly cannot rule out the possibility that intraspecific population density is influencing neritic juvenile growth rates. Recent fluctuations in population growth combined with long-term alteration and degradation of GoM ecosystems has prompted hypotheses that the carrying capacity of the GoM has been reached for Kemp's ridleys (Gallaway et al. 2016b, Caillouet et al. 2016, 2018). Nevertheless, empirical support for this hypothesis independent of analyses of the nesting trends, which are confounded after 2010 with unknown effects of the *DWH* oil spill, has been lacking (but see Shaver et al. 2016). We observed more variable, possibly declining, growth at the highest population abundances for GoM small neritic juveniles. While not statistically significant, similar patterns were observed in Atlantic small neritic juveniles. However, our results are equivocal and more research is needed before we can confidently assert Kemp's ridleys population density is influencing somatic growth rates. Importantly, our findings contrast with those that have suggested that density dependent processes have influenced this population as early as the year 2000 (Caillouet et al. 2018, Caillouet 2019). Skeletochronological analysis of turtle bones collected after 2016 will be critical in evaluating density dependent effects on Kemp's ridley growth rates.

Broadly, our findings both align and contrast with previous Kemp's ridley growth studies. In a post–*DWH* mark-recapture study conducted in the Mississippi Sound, Coleman et al. (2016) found that post-*DWH* growth rates were significantly lower than previously reported estimates from turtles in Florida (Schmid 1998, Witzell & Schmid 2004). Outside possible regional differences in somatic growth,

hypothesized causal factors included abnormal diets of turtles around piers and density dependent resource limitation—blood health indicators suggested this was not linked to malnutrition (Coleman et al. 2016). Interestingly, our findings contrast with a previous skeletochronology study based on an analysis of data from pre-*DWH* GoM-stranded turtles which found long-term declines in Kemp's ridley growth rates beginning in 2004/2005 for small juveniles and the late 1980s for large juveniles and adults (Avens et al. 2017). This was presumed to be related to a suite of factors that cumulatively could limit sea turtle resource availability in the GoM (e.g., expanding hypoxic zone in the northern GoM, population declines of preferred prey species, density dependence). No clear long-term declines in growth were evident in our study for these life stages. Given that turtle bones contain multi-year growth histories, the inclusion of data herein from turtles stranded between 2010 and 2016 added a significant amount of new data during the period of apparent juvenile growth decline (2005–2009). Therefore, these contrasting results are likely an effect of this increased sample size. Future studies linking Kemp's ridley somatic growth rates to smaller-scale environmental phenomena (e.g., local temperature, salinity, diet composition, mortality source) would greatly aide our understanding of spatiotemporal somatic growth variation in this species.

Through skeletal analyses of dead stranded sea turtles collected over the past 30 years, we examined the population-level somatic growth response of Kemp's ridley sea turtles to multiple environmental factors. Specifically, we identified a simultaneous decrease in annual growth rates beginning in 2012 for oceanic and small

neritic juveniles across the species' entire range. While we cannot definitively link changes in growth rates observed herein to the *DWH* oil spill, we hypothesize that the declines are due at least in part to deleterious effects of the *DWH* oil spill on sea turtles and their habitats that either directly or indirectly compromised long-term health. For certain life stages, this growth response may result from synergistic effects of the oil spill, climate change, and density-dependent processes. Our understanding of the links between the *DWH* oil spill and sea turtle growth rates would be greatly enhanced through geochemical analyses (e.g. PAHs, trace elements, isotopes) of turtle bone tissues, which may contain evidence of exposure to *DWH*-associated environmental toxins (e.g., Wise et al. 2014; Wilson et al. 2015; López-Duarte et al. 2016; Romero et al. 2018). The integration of our results into updated Kemp's ridley population models would allow for quantification of the effect of the observed growth declines on the species' population dynamics (e.g., time to maturity) and recovery. Most importantly, this study highlights the critical importance of long-term, continuous collection of sea turtle humerus bones for status and threat assessment. To date, the collection of sea turtle humerus bones from dead stranded individuals has been inconsistent across both space and time. Resumption of widespread bone collection from Kemp's ridleys turtles, which ended in 2015, will be necessary to fully evaluate the long-term influence of multiple environmental factors on sea turtle growth rates.

Acknowledgements

We thank the hundreds of federal, state, and private partners that collectively form the Sea Turtle Stranding and Salvage Network for their invaluable work with which this study would not have been possible. We also thank K. Magnusson for providing lab space and equipment for skeletochronological analysis and the Oregon State University Linus Pauling Institute for use of their imaging systems, and B. Stacy and J. Keene (NOAA) for collection of humeri associated with the DWH Natural Resource Damage Assessment. Thank you to J. Cordeiro, M. Davis, H. Hagler, and M. VanBemmel for assistance with laboratory analyses. Thank you also to J. Miller, A. Shiel, J. McKay, and two anonymous reviewers for comments on this manuscript. Funding for M. Ramirez and this project were provided by the NSF Graduate Research Fellowship Program. The contents of this publication are solely the responsibility of the authors and do not necessarily represent the official views of the U.S. Department of Commerce, National Oceanic and Atmospheric Administration. Research was conducted under USFWS permit number TE-676379-5 issued to the NMFS Southeast Fisheries Science Center.

Table 2.1. Summary characteristics for Kemp's ridley sea turtles by stranding location. Western GoM (wGoM) = TX; northern GoM (nGoM) = LA, MS, AL; eastern GoM (eGoM) = western FL); southern Atlantic (sATL) = eastern FL, GA, SC, NC, VA; northern Atlantic (nATL = DE, NJ, NY, MA). See Table A1 for state-specific data.

Location	Stranding data				Growth rate data	
	*n**	SCL (cm) Mean ± SD (range)	Estimated age (yr) Mean ± SD (range)	Year range	*n*	Year range
wGoM	200	55.6 ± 10.9 (4.2 – 69.1)	11.87 ± 6.47 (1.00 – 30.25)	1997 – 2013	915	1988 – 2012
nGoM	439	40.1 ± 11.2 (16.6 – 66.2)	2.86 ± 4.38 (0.75 – 23.00)	1993 – 2016	1055	1990 – 2015
eGoM	142	41.1 ± 11.0 (20.3 – 65.4)	4.62 ± 3.23 (1.00 – 15.75)	1998 – 2013	354	1994 – 2013
sATL	362	38.1 ± 10.4 (19.3 – 66.7)	5.06 ± 3.25 (1.00 – 18.75)	1993 – 2016	1024	1991 – 2015
nATL	77	28.0 ± 4.1 (19.3 – 40.0)	3.67 ± 1.41 (1.00 – 8.50)	2001 – 2017	219	1996 – 2015

*Stranding state unknown for 15 turtles (2 in Gulf of Mexico, 13 in Atlantic)

Table 2.2. Summary statistics for the family of models used to evaluate whether von Bertalanffy growth parameter estimates differed for Kemp's ridley sea turtles stranded in the Gulf of Mexico before (1993–2009, *n* = 309) and after (2010–2016, *n* = 459) the *Deepwater Horizon* oil spill.

Model	*df*	logLik	AIC	ΔAIC	W_i
Common L_∞ and t_0 $(K \neq K)$	5	–2207.80	4425.60	0.00	0.408
Common L_∞ $(K \neq K,\ t_0 \neq t_0)$	6	–2207.34	4426.67	1.07	0.235
Different $L_\infty, K,$ and t_0	7	–2206.78	4427.55	1.95	0.150
Common t_0 $(L_\infty \neq L_\infty,\ K \neq K)$	6	–2207.78	4427.55	1.95	0.150
Common K $(L_\infty \neq L_\infty,\ t_0 \neq t_0)$	6	–2209.50	4431.00	5.40	0.027
Common K and t_0 $(L_\infty \neq L_\infty)$	5	–2210.97	4431.94	6.34	0.017
Common L_∞ and K $(t_0 \neq t_0)$	5	–2211.42	4432.84	7.24	0.011
Common $L_\infty, K,$ and t_0	4	–2225.40	4458.80	33.20	0.000

Table 2.3. Results of complementary breakpoint and cutpoint analyses. Shaded rows identify significant years where there was concordance between the two statistical methods. Excludes years with $N < 5$.

	Breakpoint analysis			Cutpoint analysis		
Age class	Breakdate(s)	sup*F**	*P*	Best Cutpoint	max*T*	*P*
Age 0	2011	15.46	**<0.001**	2011	2.96	**0.014**
Age 1_{GoM}	2001	2.08	0.175			
	2008	3.26	0.096	2008	1.67	0.450
Age $1_{Atlantic}$	None	–	–	1997	1.59	0.542
Age $2–5_{GoM}$	1997	1.15	0.297			
	2005	0.08	0.785			
	2008	8.30	**0.010**			
	2011	15.19	**0.002**	2011	2.98	**0.008**
Age $2–5_{Atlantic}$	2011	19.12	**<0.001**	2011	3.17	**0.007**
Age $6–9_{GoM}$	2009	9.88	**0.006**	2009	2.55	0.062
Age $6–9_{Atlantic}$	None	–	–	2002	1.83	0.328

*Chow test statistic

Table 2.4. Summary statistics for the family of Generalized Additive Models used to evaluate the influence of covariates [temporal shift (TS), hatchling production (HatchProd), Multivariate El Niño Southern Oscillation Index (MEI)] on mean age class-specific growth rates for Age 0 and Age 2–5 Kemp's ridley sea turtles. *TS* is a factor with categorization based on breakpoint identified in temporal analyses (pre-shift = 1995–2011, post-shift = 2012–2015). *HatchProd* is cumulative hatchling production for years, t(x), prior to a given year (Age 0 = $\Sigma\ t_0$–t_{-1}, Age 2–5 = $\Sigma\ t_{-2}$–t_{-5}). *MEI* is the annualized GAM trend for the index with a 2-year lag. The models exclude years with $N < 5$.

Model	*df*	logLik	AIC	ΔAIC	W_i
(a) Age 0					
TS + MEI	4.00	–9.74	27.48	0.00	0.34
TS + HatchProd	4.00	–9.80	27.59	0.11	0.32
TS	3.00	–11.14	28.28	0.80	0.23
MEI	5.34	–9.53	29.74	2.26	0.11
HatchProd	3.00	–18.84	43.69	16.21	0.00
(b) Age 2-5, Gulf of Mexico					
TS + HatchProd	6.74	–9.55	32.57	0.00	0.71
TS + MEI	6.10	–11.93	36.06	3.49	0.12
MEI	6.27	–12.10	36.74	4.17	0.09
TS	3.00	–15.49	36.97	4.40	0.08
HatchProd	5.46	–16.43	43.78	11.21	0.00
(c) Age 2-5, Atlantic					
TS + MEI	4.00	–14.73	37.45	0.00	0.41
TS + HatchProd	4.00	–14.96	37.91	0.46	0.33
TS	3.00	–16.17	38.33	0.88	0.26
MEI	4.94	–19.14	48.16	10.71	0.00
HatchProd	3.00	–22.54	51.09	13.64	0.00

Table 2.5. Summary of statistical output for Generalized Additive Models (GAMs) used to evaluate the influence of potential environmental covariates [temporal shift (*TS*), hatchling production (*HatchProd*), Multivariate El Niño Southern Oscillation Index (*MEI*)] on mean age class-specific growth rates for Age 0 and Age 2-5 Kemp's ridley sea turtles. *TS* is a factor with categorization based on breakpoint identified in temporal analyses (pre-shift = 1995–2011, post-shift = 2012–2015). *HatchProd* is cumulative hatchling production for years, t(x), prior to a given year (Age 0 = $\Sigma\ t_0$–t_{-1}, Age 2–5 = $\Sigma\ t_{-2}$–t_{-5}). *MEI* is the annualized GAM trend for the index with a 2-year lag. *Dev* : deviance explained by the model. *Edf*: estimated degrees of freedom. The models exclude years with $N < 5$ and are ordered by AIC values.

				Smooth terms				Parametric coefficients				
Model	Dev (%)	Adj. R^2	AIC	Var	*Edf*	*F*	Prob(*F*)	Var	Est	SE	t	Pr>|*t*|
(a) Age 0 (n = 20)												
GAM_{TS+MEI}	66.0	0.62	27.5	MEI	1.00	2.56	0.128	TS_{preTS}	0.98	0.26	3.82	**0.001**
GAM_{TS+HP}	65.8	0.62	27.6	HP	1.00	2.45	0.136	TS_{preTS}	1.12	0.22	5.00	**<0.001**
GAM_{TS}	60.9	0.59	28.3	–	–	–	–	TS_{preTS}	1.20	0.23	5.29	**<0.001**
GAM_{MEI}	66.7	0.61	29.7	MEI	2.80	3.47	**<0.001**	–	–	–	–	–
GAM_{HP}	15.5	0.11	43.7	HP	1.00	3.30	0.086	–	–	–	–	–
(b) Age 2-5, Gulf of Mexico (n = 20)												
GAM_{TS+HP}	73.6	0.67	32.6	HP	3.08	2.54	0.071	TS_{preTS}	1.07	0.28	3.84	**0.002**
GAM_{TS+MEI}	66.9	0.60	36.1	MEI	2.42	1.36	0.271	TS_{preTS}	0.94	0.44	2.16	**0.046**
GAM_{MEI}	66.4	0.59	36.7	MEI	3.52	6.80	**0.001**	–	–	–	–	–
GAM_{TS}	53.6	0.51	37.0	–	–	–	–	TS_{preTS}	1.30	0.28	4.68	**<0.001**
GAM_{HP}	49.2	0.41	43.8	HP	2.84	4.12	**0.018**	–	–	–	–	–
(c) Age 2-5, Atlantic (n = 20)												
GAM_{TS+MEI}	53.7	0.48	37.5	MEI	1.00	2.65	0.121	TS_{preTS}	1.73	0.40	4.36	**<0.001**
GAM_{TS+HP}	52.6	0.47	37.9	HP	1.00	2.18	0.155	TS_{preTS}	1.62	0.37	4.37	**<0.001**
GAM_{TS}	46.8	0.44	38.3	–	–	–	–	TS_{preTS}	1.33	0.33	4.09	**<0.001**
GAM_{MEI}	29.5	0.20	48.2	MEI	2.36	2.16	0.150	–	–	–	–	–
GAM_{HP}	2.43	–0.03	51.1	HP	1.00	0.47	0.500	–	–	–	–	–

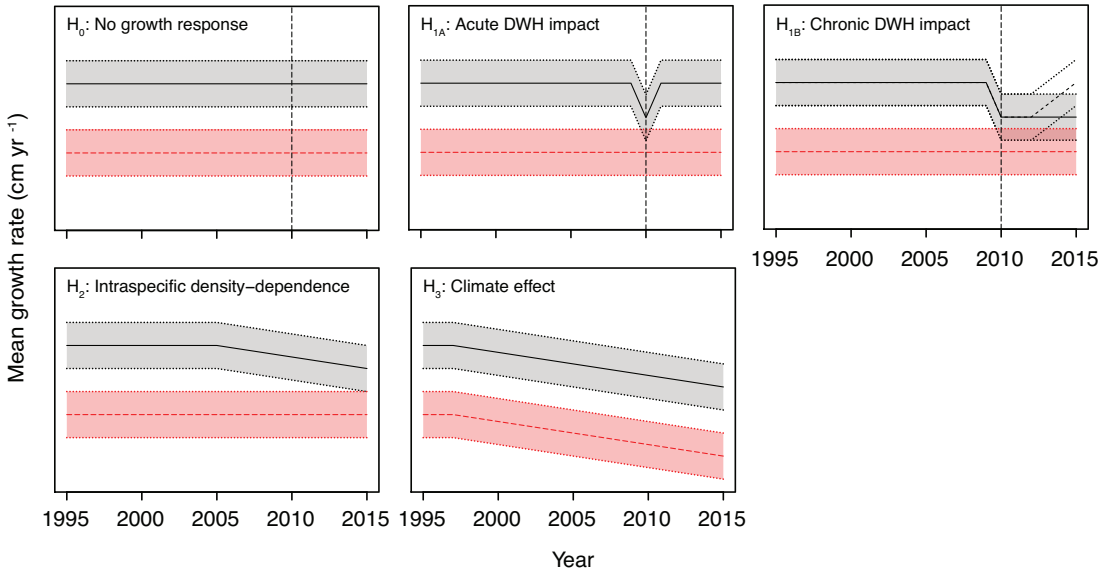

Figure 2.1. Conceptual model of alternative hypotheses for the size-class-specific growth response of Kemp's ridley sea turtles to environmental factors. All Kemp's ridleys first reside in oceanic habitats in the central Gulf of Mexico (GoM) for 1–3 years then recruit to neritic habitats along either the GoM or U.S. Atlantic Coast. The shaded areas represent growth variation for GoM (black lines, grey shading) and Atlantic (red lines, red shading) life stages. Vertical dashed lines identify the year of the Deepwater Horizon (DWH) oil spill (2010). H0 = no growth response in turtles from either geographic region or life stage to any factor examined. H_1 = acute or chronic *DWH* oil spill-induced growth response for GoM life stages only (oceanic and neritic); no growth response in Atlantic neritic life stages due to geographic isolation from *DWH* oil spill, although Atlantic turtles may exhibit a past response during their oceanic life stage when they occupied GoM habitats. H_2 = density-dependent decline in somatic growth beginning in the mid-2000s during period of exponential population growth; effect in GoM turtles only as > 80 % of the population is thought to reside in the GoM annually (Putman et al. 2013, NMFS & USFWS 2015). H_3 = declining growth beginning in the late 1990s in response to climate-driven ecological regime shift.

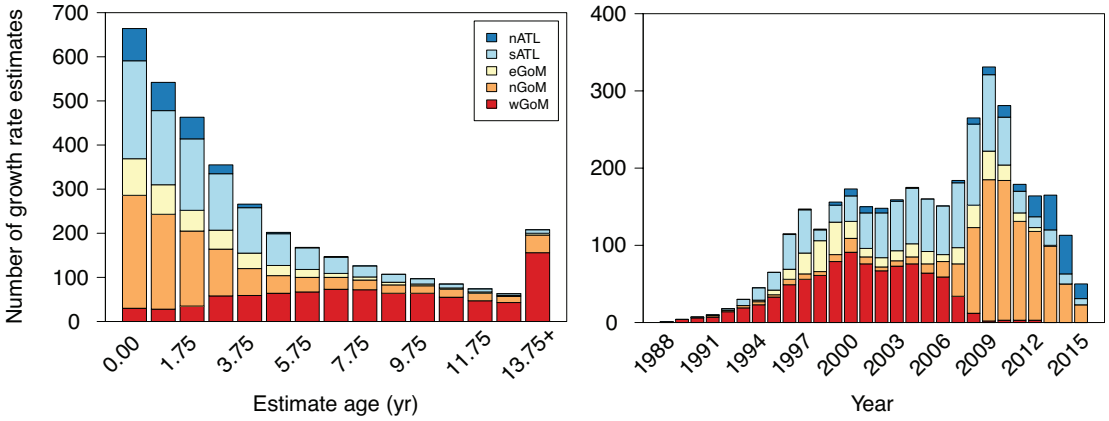

Figure 2.2. Frequency histograms of Kemp's ridley sea turtle back-calculated somatic growth rates by stranding location, age, and year. nATL = northern Atlantic (DE, NJ, NY, MA), sATL = southern Atlantic (eastern FL, GA, SC, NC, VA), eGoM = eastern Gulf of Mexico (western FL), nGoM = northern Gulf of Mexico (LA, MS, AL), wGoM = western Gulf of Mexico (TX).

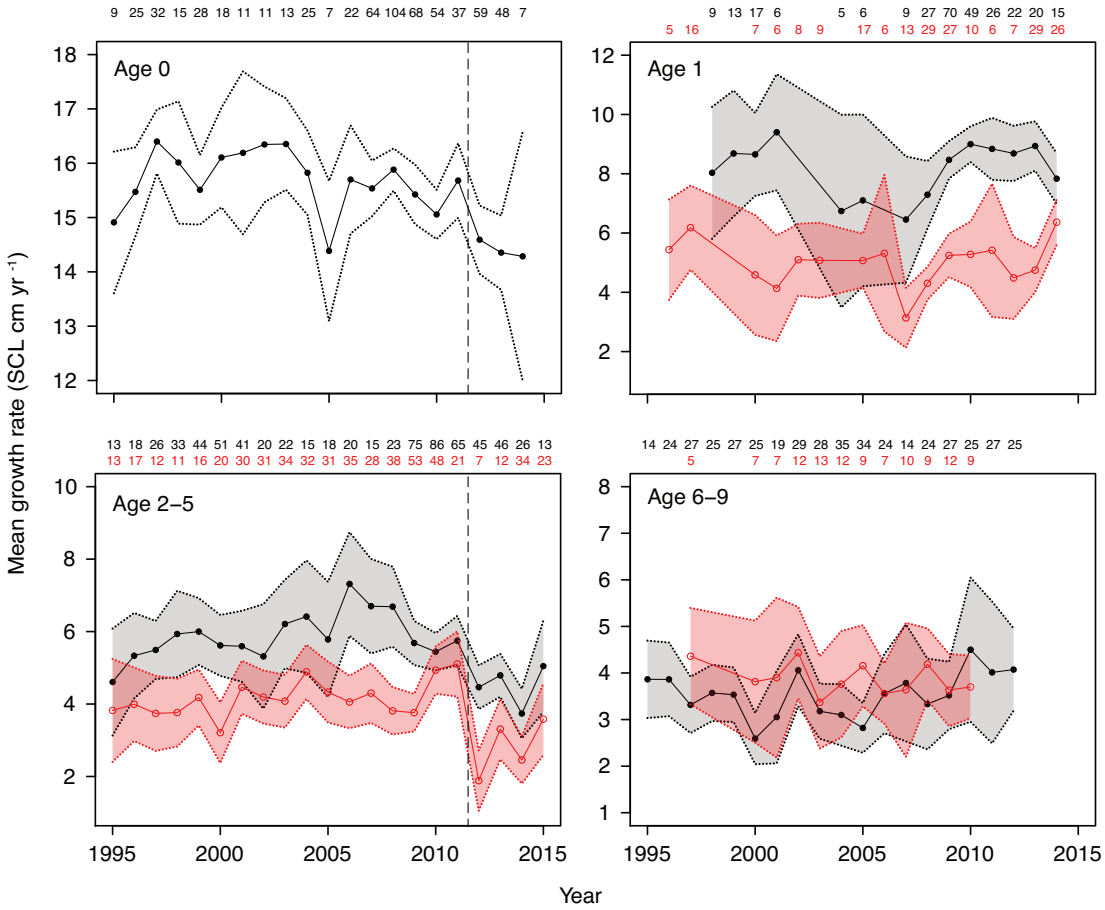

Figure 2.3. Time series of mean Kemp's ridley sea turtle growth rate by age class. Dotted lines bound 95% confidence intervals. Age 0 is data from both Gulf of Mexico (GoM) and Atlantic turtle given that they share oceanic habitats in the central GoM during this life stage and growth rates did not differ by stranding location for this age class. For all other age classes, data were analyzed separately due to regional differences in growth rates (black shaded area = Gulf of Mexico stranded turtles; red shaded area = Atlantic stranded turtles). Number of observations are presented above each plot. Vertical dashed lines identify significant breakpoints in each time series where there was concordance among statistical methods evaluated (see Table 2.3). Analyses excluded years with $N < 5$. SCL = straightline carapace length.

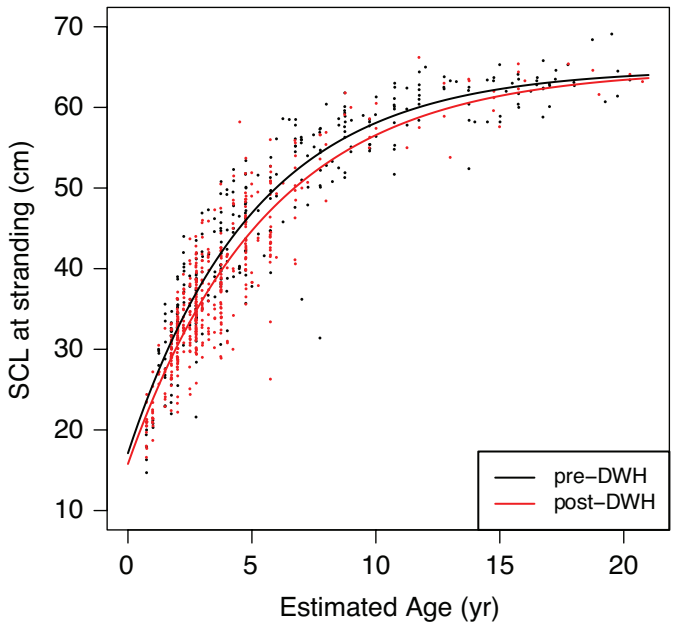

Figure 2.4. Von Bertalanffy growth functions estimated for Kemp's ridley sea turtles stranded in the Gulf of Mexico before (1993–2009, n = 309) and after (2010–2016, n = 459) the *Deepwater Horizon* oil spill. VBGFs estimated based on measured straightline carapace length (SCL) and estimated age at stranding. Parameter estimates for the best model were L_∞ = 64.79, t_0 = 1.56, K (pre–*DWH*) = 0.20, and K (post–*DWH*) = 0.18.

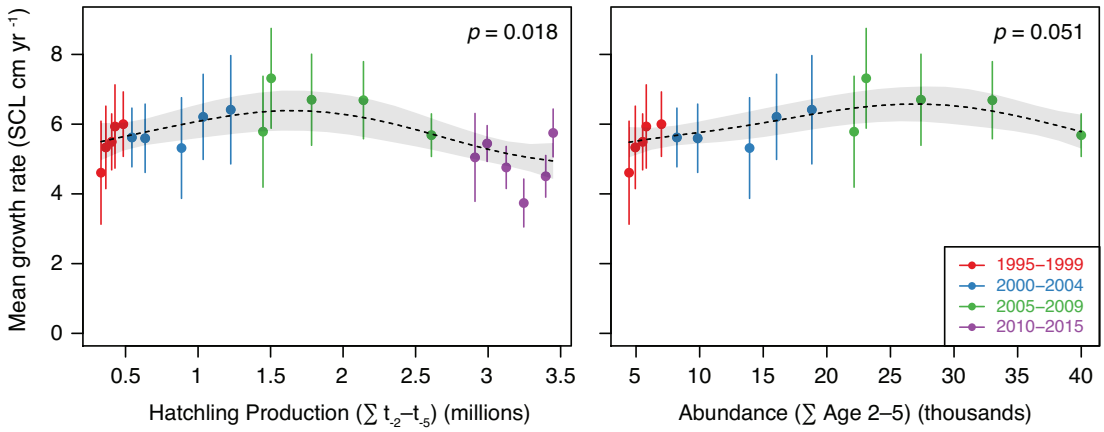

Figure 2.5. Relationship between mean back–calculated growth rate and population density metrics for Age 2–5 Kemp's ridley sea turtles stranded in the Gulf of Mexico. Dashed lines and grey ribbons are predicted values and 95% CI from GAM models with either cumulative hatchling production (left panels) or population abundance (right panels) included as a smoother term (see Table A4). Points are means ± 95% CI. SCL = straightline carapace length. See Figures A2–A4 for Age 0, Age 1, and Age 6–9 figures.

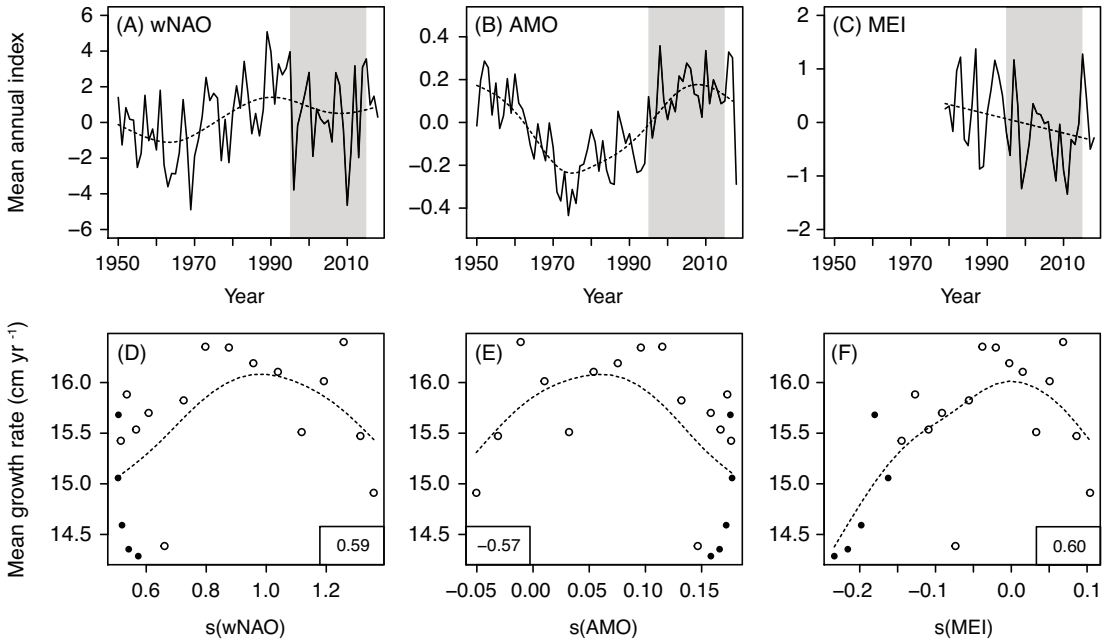

Figure 2.6. Relationships between (**A**-**C**) climate indices and year and (**D**-**F**) mean Age 0 growth rates and annualized climate indices (2-yr lag). Dashed lines are the GAM trends. (**A**-**C**) Shaded area identifies study period. (**D**-**F**) Cross-correlation values are presented in boxes within each plot. Open circles are years 1995–2009, whereas filled circles are year 2010–2015. wNAO: Winter North Atlantic Oscillation. AMO: Atlantic Multidecadal Oscillation. MEI: Multivariate El Niño Southern Oscillation Index.

CHAPTER 3: ELUCIDATING INTRA-POPULATION DIET VARIATION AND POTENTIAL INFLUENCE ON SOMATIC GROWTH IN THE KEMP'S RIDLEY SEA TURTLE (*LEPIDOCHELYS KEMPII*) THROUGH COMPLEMENTARY SKELETOCHRONOLOGICAL AND STABLE ISOTOPE ANALYSES

Matthew D. Ramirez, Larisa Avens, Lisa R. Goshe, Melissa L. Snover, Melissa Cook, and Selina S. Heppell

In preparation for submission to Frontiers in Marine Science

Abstract

Reptile growth is influenced by a suite of ecological processes that can cumulatively lead to divergent somatic growth rates within spatially structured populations. As somatic growth variation can strongly influence a species' population dynamics, identifying proximate drivers can be critical to the conservation and management of protected species. Kemp's ridley sea turtles (*Lepidochelys kempii*) exhibit spatial variation in both diet composition and growth, but whether components of this variation are linked has not been evaluated. Through an integration of skeletochronological and stable isotope analyses of stranded turtle humerus bones we characterized regional variation in Kemp's ridley diet composition and potential relationships with somatic growth rates. Turtles were divided into one of five regions within the U.S. Gulf of Mexico (GoM) and Atlantic Coast based on location of stranding, and humerus bones were sampled for stable carbon ($\delta^{13}C$) and nitrogen ($\delta^{15}N$) isotope ratios. These data were combined with region-specific prey stable isotope data sourced from the primary literature into a Bayesian stable isotope mixing model (MixSIAR) to estimate the proportional contribution of five prey groups (crustaceans, bivalves, gastropods, fish, macroalgae/seagrass) to Kemp's ridley diets. Our analysis revealed strong regional differences in mixing model-derived diet composition estimates that closely tracked published records of Kemp's ridley diet. Invertebrates generally comprised the largest proportion (43.5–97.7 %) of turtle diets. However, we also observed high proportional contributions of fish (42.6–43.1 %) to western GoM turtle diets and macroalgae/seagrass (42.4–47.8 %)—or

isotopically similar prey groups (e.g., tunicates)—to eastern GoM turtle diets. Growth rates were poorly correlated with $\delta^{15}N$ values and diet composition estimates, suggesting that diet composition alone may not explain the regional differences in somatic growth observed in this species. This study highlights the value of complementary skeletal and isotopic analyses to understanding regional diet variation in sea turtles as well as the importance of continued collection of isotopic data from both sea turtles and their prey. These results also help fill critical knowledge gaps in our understanding of the relationship between sea turtle foraging ecology and somatic growth dynamics, a topic of high importance to sea turtle conservation and management.

Introduction

Somatic growth variation in reptiles manifests from the cumulative effects of biological, ecological, and environmental processes (Congdon 1989, Stearns 1992). Environmental effects on growth rates are particularly strong in ectothermic reptiles, such as sea turtles, where resource quality and availability interact with temperature to influence somatic growth (Gibbons 1967, Dunham et al. 1989). Intra-specific differences in growth and size-at-age can have profound effects on individual fitness and population dynamics through influences on key life history features such as time to maturity (Frazer et al. 1993, Bjorndal et al. 2013a), size-dependent mortality (Werner & Gilliam 1984, O'Brien et al. 2005), and fecundity (Berry & Shine 1980, Frazer & Richardson 1986). Sea turtle somatic growth rates are highly variable within

and among species and life stages but disentangling the myriad potential drivers of this variation is challenging given the logistical limitations associated with studying highly migratory species (Omeyer et al. 2017). As the population dynamics of slow-growing, long-lived species such as sea turtles are sensitive to changes in demographic rates (Crouse et al. 1987, Gerber & Heppell 2004), identifying the proximate drivers of somatic growth variation is of high importance to sea turtle conservation and management.

Correlations between intra-specific variability in resource utilization and somatic growth have been documented across a wide range of marine species (Dunham 1978, Iraeta et al. 2006). For example, it is well-established that fish growth and population dynamics are strongly influenced by zooplankton composition, abundance, and distribution (Cushing 1990, Brodeur & Ware 1992, Durant et al. 2007). Similarly, variation in multiple seabird demographic rates, including growth, have been linked to differences in prey availability, composition, and energy density (Cairns 1988, Abraham & Sydeman 2004, Hennicke & Culik 2005, Piatt et al. 2007). In loggerhead sea turtles (*Caretta caretta*), geographic variation in resource availability and distribution is thought to underpin differences in somatic growth rates between oceanic and neritic life stages in the western North Atlantic (Bjorndal et al. 2003) and between loggerhead turtles of Mediterranean and Atlantic origin in the Mediterranean Sea (Piovano et al. 2011). These differences may relate to divergent prey energy densities or geographic differences in primary productivity (Bosc et al. 2004, Peckham et al. 2011). Observations of compensatory and density-dependent

growth in loggerhead and green sea turtles (*Chelonia mydas*) provide further support for the importance of resource use in shaping sea turtle growth rates (Bjorndal et al. 2000, 2003). Within the Gulf of Mexico, factors that affect foraging resources for sea turtles include fisheries (Robinson et al. 2015), seasonal hypoxic zones (Craig et al. 2001), oil spills (Wallace et al. 2017b), red tides (Dupont et al. 2010), hurricane activity (Engle et al. 2009), and climate change (Sanchez-Rubio et al. 2011), among others.

Kemp's ridley sea turtles (*Lepidochelys kempii*) display distinct regional differences in somatic growth rates that may be linked to differences in diet. During neritic life stages, this species occupies nearshore marine habitats throughout the Gulf of Mexico (GoM) and U.S. Atlantic (NMFS & USFWS 2015). Comparative studies prior to 2000 suggest juvenile Atlantic Kemp's ridley sea turtles exhibit slower grow rates than conspecifics in the GoM (Caillouet et al. 1995, Zug et al. 1997, NMFS & USFWS 2015, Avens et al. 2017). Similarly, although crabs are generally thought to constitute the bulk of their diet across their range, regional differences in Kemp's ridley foraging patterns have been observed that may influence their somatic growth rates (Shaver 1991, Burke et al. 1993, 1994, Seney & Musick 2005, Schmid & Tucker 2018). Diets are particularly variable among Kemp's ridleys that inhabit the GoM. For example, tunicates are an apparent common prey item for turtles in southwest Florida (Witzell & Schmid 2005), whereas fish— likely sourced as discards from shrimp fisheries—are often consumed by turtles in the northern and western GoM (Werner 1994, Cannon 1998, Stacy 2015). Shrimp fisheries are the

overwhelmingly dominant source of fish discards throughout the Kemp's ridleys' range (Harrington et al. 2005a), and shrimp fishing effort and thereby fish discards is an order of magnitude higher in the western and northern GoM than in the eastern GOM and U.S. Atlantic (Diamond 2004, Harrington et al. 2005a, Scott-Denton et al. 2012). In contrast to their GoM counterparts, Atlantic Kemp's ridleys appear less likely to deviate from the traditional diet of crabs and molluscs (Burke et al. 1993, 1994, Frick & Mason 1998, Seney & Musick 2005). Ultimately, whether this spatial variability in diet correlates with regional differences in growth rates has yet to be evaluated.

As the isotopic composition of consumer tissues closely tracks that of their assimilated diet, stable isotope analysis provides a mechanism to characterize intra-population variation in diet composition over space and time (Newsome et al. 2007, Katzenberg 2008). Importantly, the relative contribution of different resources to a consumer's diet can be quantified using mass-balance stable isotope mixing models when isotopic data are available for both consumers and potential prey (Phillips 2001). Additionally, while many environmental and physiological processes can influence stable isotope deposition rates into consumer tissues, the latest generation of mixing models allows for incorporation of various sources of uncertainty through Bayesian inference to improve estimations of diet composition (Phillips & Koch 2002, Semmens et al. 2009, Parnell et al. 2010, Stock & Semmens 2016). This approach in turn yields source contribution estimates that are accompanied by probability distributions that more accurately reflect model uncertainties. Kemp's

ridley humerus bones contain annual records of somatic growth that can be revealed through histological processing and analysis (Snover & Hohn 2004, Avens et al. 2017). Combining skeletochronological and stable isotope analyses within a mixing model framework may thus provide a means of investigating the influence of diet composition on sea turtle growth rates across multiple spatiotemporal scales. The integration of these tools has already shed valuable insight into sea turtle ontogenetic growth dynamics and resource shifts (Snover et al. 2010, Avens et al. 2013, Ramirez et al. 2017, Turner Tomaszewicz et al. 2017a, Ramirez et al. 2019).

In this study we integrated skeletochronological and stable isotope analyses of Kemp's ridley humerus bones to (1) characterize regional variation in diet composition and (2) quantify the relationship between diet composition and somatic growth rates. To reduce biases associated with translating isotopic data to diet composition estimates for a highly mobile species, our analysis assesses diet composition at higher taxonomic levels (e.g., % fish, % invertebrate, % macroalgae/seagrass) than is typical for stable isotope mixing models. We specifically investigated if turtles inhabiting areas where fish discards are prevalent (western and northern GoM) showed evidence of consuming greater proportions of fish relative to turtles from other regions (eastern GoM and U.S. Atlantic). Because the energy density of fish is generally higher than that of crustaceans (Doyle et al. 2007, Peckham et al. 2011, Schaafsma et al. 2018), we also investigated if fish subsidies to turtle diets may enhance somatic growth rates, thereby contributing to

regional differences in somatic growth. This investigation presents one of the first studies explicitly linking sea turtle foraging ecology to somatic growth dynamics.

Materials and Methods

Geographic Breakpoints

Variation in Kemp's ridley diet composition and growth was evaluated by dividing turtle and prey data among five geographic regions within the species' range (Figure 3.1): (1) western Gulf of Mexico (wGOM, n = 44 turtles; Texas/Mexico border to Vermillion Bay, LA), (2) northern Gulf of Mexico (nGOM, n = 28 turtles; Vermillion Bay, LA, to Mobile Bay, AL), (3) eastern Gulf of Mexico (eGOM, n = 24 turtles; Apalachicola Bay to Florida Bay, FL), (4) North Carolina (NC, n = 32 turtles; Long Bay to Albemarle Sound, NC), and (5) Virginia (VA, n = 25 turtles; North Carolina/Virginia border to lower Chesapeake Bay). These breakpoints were primarily determined based on known spatial variation in ocean chemistry. We explored using smaller geographic areas to more closely link turtle and prey stable isotope data in space. However, there was generally insufficient prey data for one or more prey groups to use smaller regional units for this analysis (see below).

Within the GoM, the West Florida Shelf is characterized by relatively low stable nitrogen isotope ratios ($\delta^{15}N$) due to the presence of *Trichodesmium* (Lenes et al. 2001, Mulholland et al. 2006, Vander Zanden et al. 2015), a N_2-fixing cyanobacteria; N_2-fixation reduces $\delta^{15}N$ values (Montoya et al. 2002). Marine organisms occupying the West Florida Shelf thereby may have lower $\delta^{15}N$ values

than conspecifics elsewhere due to chemical differences at the base of the food web. In contrast, the nGoM and Virginia may have relatively high $\delta^{15}N$ values and low stable carbon isotope ($\delta^{13}C$) values than adjacent regions due to high nitrogen loading from agricultural runoff (i.e., high nitrogen content; Black et al., 2017; Fritts et al., 2017) and freshwater influences, respectively—freshwater systems have distinctly lower $\delta^{13}C$ values than marine systems (Fry & Sherr 1989).

Prey Stable Isotope Ratios

Kemp's ridley sea turtles are generalist carnivores, consuming primarily invertebrates (crustaceans, gastropods, bivalves, tunicates) but also variable amounts of fish, macroalgae, and seagrasses (Shaver 1991, Seney & Musick 2005, Witzell & Schmid 2005). Although regional differences in foraging patterns have been observed for this species, such as increased consumption of fish in turtles from Louisiana and Texas (Werner 1994, Cannon 1998, Stacy 2015) and tunicates in turtles from Southwest Florida (Witzell & Schmid 2005), crabs have generally constituted > 75 % of observed diet (Shaver 1991, Burke et al. 1993, 1994, Seney & Musick 2005, Schmid & Tucker 2018). Given the spatiotemporal extent and retrospective nature of this study, we relied on the primary literature to source stable isotope data of representative prey species for our mixing model.

We first performed a structured literature search in Web of Science and Google Scholar using the following Boolean search terms: stable isotope, crustacean, crab, shrimp, mollusc, arthropod, gastropod, sea snail, bivalve, clam, oyster, mussel,

fish, tunicate, seagrass, and macroalgae. We then performed an unstructured literature search using the reference lists of relevant publications found in the structured search. Following exclusion of studies performed outside the geographic areas of interest, the literature search yielded 86 studies from which stable carbon and nitrogen isotope ratios were collated. If studies reported multiple stable isotope values for a single species, a weighted mean and pooled standard deviation (SD) were calculated to collapse the reported data into one estimate per species per study. Tunicates, though potentially an important Kemp's ridley prey group, were excluded from our analysis given their poor representation in the literature (n = 2 studies) and overlap in isotopic values with macroalgae and seagrass. The final prey stable isotope dataset was comprised of 552 isotopic records (see Table 3.1 for summary and Table B1 for full dataset). Original collection dates spanned 1975 to 2016, but primarily encompassed the years 1990 to 2016—pre-1990 data were included in some instances to fill in important data gaps for poorly represented taxa within each region (e.g., bivalves and gastropods).

Prey stable isotope data were grouped into five primary prey groups (crustaceans, bivalves, gastropods, fish, macroalgae/seagrass) within each of the five geographic regions (Figures B1, B2). For all animal prey groups, a simple mean and pooled SD were calculated for each region using the 552 isotopic values from the published literature. Although isotopically distinct, macroalgae and seagrass were grouped to reduce the number of sources in the mixing model. As with the other prey groups, we first calculated a simple mean and pooled SD for macroalgae and seagrass

separately and then calculated a simple mean of these estimates to yield final estimates for the macroalgae/seagrass prey group, thereby weighting each prey type equally in the models. Final means and SDs for all prey groups used in the mixing model are presented in Table 3.2. We assume that the published literature accurately captures the means and variances of these prey groups.

Given uncertainties in the types of fish consumed by sea turtles, potential fish prey for our analysis included species previously observed in Kemp's ridley gut and fecal contents (e.g., mullet, croaker, weakfish, menhaden, sea catfish, flatfish, lizardfish; see Cannon, 1998; Seney, 2016; Shaver, 1991; Stacy, 2015; Werner, 1994; Witzell and Schmid, 2005) as well as ecologically similar species abundant as shrimp fishery discards (e.g., porgy, pinfish, herring, searobin; Harrington et al., 2005b; Benaka et al., 2019). When possible, fish isotopic data were restricted to specimens < 30 cm in length to align with those likely to be consumed by Kemp's ridleys (E. Seney *pers. comm.*). However, only 45% of studies reported fish lengths, so this was not always possible. Fish stable isotope data were initially grouped based on feeding mode (e.g., piscivorous, benthophagous, planktivorous) to evaluate trophic differences. However, isotopic data for these three fish groups tended to overlap extensively in isospace within each region and were thus collapsed to reduce the number of sources in the mixing model.

Sea Turtle Stable Isotope Ratios

Kemp's ridley humerus bones utilized in this study were originally collected as whole front flippers from 153 turtles stranded dead along the U.S. Gulf and Atlantic Coasts between 1993 and 2015 by participants of the Sea Turtle Stranding and Salvage Network. At time of stranding, carapace length (notch to tip), calendar date, and stranding location (state, latitude, longitude) were recorded for each turtle. Body size way typically measured as straightline carapace length (SCL), but in cases where only curved carapace length was recorded measurements were converted to SCL following Avens et al. (2017). Prior to sampling, each humerus bone was cleaned of soft tissue using a knife and then boiled. To perform complementary growth and stable isotope analyses, two sequential 2–3 mm thick cross-sections were cut from each humerus bone distal to the site of the deltopectoral muscle insertion scar using a low-speed isomet saw (Buehler). One section was histologically processed using standard methods to reveal the annual growth layers contained within each bone and estimate sea turtle growth rates (see below), whereas the second was reserved for complementary stable isotope analysis.

Methods for histologically processing sea turtle bones are detailed in Avens and Snover (2013) but are briefly outlined here. First, humerus bone sections were decalcified over multiple days using a fixative/decalcifier (Cal-Ex II or RDO). Then, bone sections were thin sectioned using a freezing-stage microtome or cryostat, stained using Ehrlich's hematoxylin, and finally mounted onto microscope slides and digitally imaged. Two or three independent readers (among L. Avens, L. Goshe, M. Ramirez, and M. Snover) then analyzed the bone images to determine the number and

placement of lines of arrested growth (LAGs), which delimit the outer edges of each skeletal growth mark.

To characterize resource use, ~1.5 mg of bone dust was milled from the most recently deposited growth layer of each sea turtle bone cross-section reserved for stable isotope analysis (ESI New Wave Research MicroMill). This time period represents the geochemical history within one year of death, dependent on individual stranding date. A 0.3 mm diameter carbide drill bit (Brasseler) was used in conjunction with transparencies of the digital skeletochronology images to guide precision drilling to a depth of ≤ 1.0 mm for each sample. Bulk bone dust samples were analyzed for $\delta^{13}C$ and $\delta^{15}N$ values via continuous-flow isotope-ratio mass spectrometry at the Oregon State University Stable Isotope Lab (Corvallis, OR). The system consists of a Carlo Erba NA1500 elemental analyzer interfaced with a DeltaPlusXL isotope-ratio mass spectrometer (Finnigan MAT, Bremen, Germany). The standards used for $\delta^{13}C$ and $\delta^{15}N$ were Vienna Pee Dee Belemnite (VPDB) and atmospheric N_2, respectively. The internal standard IAEA-600 (Caffeine; isotopic composition of $\delta^{15}N$ = 1.00 ‰) was calibrated at regular intervals and used to correct for instrument drift and linearity. Analytical precision was 0.08 ‰ for $\delta^{13}C$ and 0.05 ‰ $\delta^{15}N$. In addition to stable isotope ratios, %N and %C were calculated using mass 28 and mass 44 peak areas, respectively, with a precision of 0.55 % for %N and 0.28 % for %C. C:N ratios (%C divided by %N) were below 3.5, characteristic of unaltered protein with low lipid content (Post et al. 2007). Following stable isotope analysis, bulk bone $\delta^{13}C$ values were mathematically corrected to account for

carbonate-derived carbon as recommended by Turner Tomaszewicz et al. (2015). Using their approach, we developed a $\delta^{13}C$ conversion equation ($\delta^{13}C_{collagen} = 0.975 * \delta^{13}C_{bulk} - 1.126$, $F_{1,42} = 550.1$, $p < 0.001$, adjusted $R^2 = 0.93$) that was used to mathematically correct bulk bone $\delta^{13}C$ values (see Appendix B for details).

We assumed that stranding location was reflective of recent foraging location based on two lines of evidence. First, while we did not know precise locations of death for turtles herein, conditions were likely favorable for short carcass drift distances. The majority of turtles included in our study stranded in the spring, summer, and fall when SSTs, and thereby decomposition rates, would have been relatively high (Higgins et al. 2007). Therefore, in order for stranding to occur before carcasses dissociated due to decomposition, drifts times and distances would have been necessarily low (~2–5 days, 15–30 km) (Nero et al. 2013, Santos et al. 2018). Second, Kemp's ridleys display relatively high intra- and inter-annual site fidelity to nearshore, shallow (< 50 m depth) foraging areas (generally <1000 km^2) that are well constrained spatially within our defined geographic regions (Renaud & Williams 2005, Schmid & Witzell 2006, Shaver & Rubio 2008, Seney & Landry Jr 2011, Coleman et al. 2017). Therefore, turtles that stranded within each geographic area are likely to have been foraging within the same geographic area prior to death. As Kemp's ridleys have been occasionally documented migrating >1000 km in a single year (Renaud & Williams 2005), we acknowledge that some of our turtles may be misclassified geographically, particularly those that stranded near the edges of our pre-defined geographic areas.

Stable Isotope Mixing Model

We implemented a Bayesian hierarchical mixing model using the *MixSIAR* package (v 3.1.10, Stock et al., 2018) in R (v 3.5.3, R Core Team, 2019) to estimate the proportional contribution of five prey groups (crustaceans, bivalves, gastropods, fish, macroalgae/seagrass) to Kemp's ridley diets. MixSIAR uses Markov chain Monte Carlo (MCMC) procedures to estimate posterior probability distributions of plausible proportional contributions of prey groups to consumer diets (Moore & Semmens 2008), while accounting for uncertainty associated with trophic discrimination factors (Parnell et al. 2010), concentration dependence (Phillips & Koch 2002), fixed and random effects (Semmens et al. 2009), and variability in the predation process (i.e., error structure) (Parnell et al. 2010, Stock & Semmens 2016). Initial investigations using a hierarchical structure that nested *individuals* within *regions* in a single modeling framework failed to converge after running for multiple days due to model complexity and size. Therefore, we implemented separate mixing models for each region.

To characterize inter- and intra-regional differences in diet composition, we implemented four mixing models for each region in a 2 x 2 factorial design that included one of two prior distributions (uninformative vs. informative prior; Figure B4) for each prey group and one of two model configurations (null model vs. individual random effect model). We first ran the models using uninformative priors that assumed a generalist diet and weighted prey groups equally (α = 1, 1, 1, 1, 1).

We then ran the model using an informative/specialist prior that weighted the prey group prior distributions using published diet composition data. Taking a weighted average of taxon-specific diet composition estimates from six Kemp's ridley diet studies (Appendix B, Table B2), we constructed the informative priors assuming diet compositions (by mass) of 76.7% for crustaceans, 2.1% for bivalves, 2.1% for gastropods, 6.0% for fish, and 2.1% for macroalgae/seagrass. As recommended by Stock et al. (2018), the hyperparameters (α) for the informative priors were scaled to have a total weight equal to the number of sources (α = 4.31, 0.12, 0.12, 0.34, 0.12). Inter-regional diet variation was assessed using null models, whereas intra-regional diet variation was assessed using models that included *individual* as a random effect. In all models, the invertebrate prey groups were aggregated *a posteriori* (Phillips et al. 2005). All models included multiplicative error (process x residual error) and were run using the "extreme" MCMC settings (chain length = 3,000,000 iterations; burn-in = 1,500,000; posterior thinning = 500; 3 chains). Convergence was assessed using Gelman-Rubin (R_c < 1.01) and Geweke diagnostics (Geweke 1992, Gelman & Rubin 1992). Most models that included an informative prior and individual random effects failed to converge with these settings. Convergence was achieved after re-running them using a chain length of 6,000,000 and burn-in of 3,000,000.

Prior to model implementation all source and consumer $\delta^{13}C$ values were corrected for the Suess Effect, the global decrease in atmospheric $\delta^{13}C$ values driven by the combustion of fossil fuels over the past 150 years (Keeling et al. 1979, Francey et al. 1999). We followed Chamberlain et al. (2005) and Fox-Dobbs et al. (2007) in

applying a linear correction to standardize our data. To develop a $\delta^{13}C$ correction factor we analyzed the atmospheric $\delta^{13}C$ data for Maua Loa and La Jolla available on the Scripps CO_2 Program website (http://scrippsco2.ucsd.edu) (Keeling et al. 2001), which indicated that atmospheric $\delta^{13}C$ values declined by ~0.025 ‰ per year since 1978. We used this rate of $\delta^{13}C$ change to correct turtle and prey $\delta^{13}C$ values to modern values (modern = 2016; i.e. $\delta^{13}C$ data were lowered by 0.025 ‰ in 2015, 0.050 ‰ in 2014, etc.). Concentrations of carbon and nitrogen for each prey group, derived from the literature (Appendix B, Table B3), were also included in the models to account for taxon-specific differences in digestibility (Phillips & Koch 2002).

Stable isotope mixing models require estimates of tissue-diet trophic discrimination factors (TDFs; Δ)—the difference in isotopic ratios between consumers and their diet—to estimate the proportional contribution of different prey groups to consumer diets. As bone-diet TDFs have not been quantified for Kemp's ridleys or other primarily carnivorous sea turtles, we used bone-diet TDFs estimated from dead, captive, juvenile green sea turtles (*Chelonia mydas*) ($\Delta^{13}C = 2.1 \pm 0.6$, $\Delta^{15}N = 5.1 \pm 1.1$) (Turner Tomaszewicz et al. 2017b). Although these turtles were maintained on omnivorous diets composed of ~56% animal matter (squid, shrimp, fish) and ~43% plant matter (lettuce) by weight, percent digestible N and C from animal protein was estimated to be 96.8% and 81.9%, respectively. Even though Bayesian stable isotope mixing models account for uncertainty in TDFs, their outputs are still highly sensitive to variation in TDFs (Bond & Diamond 2011). Given uncertainty in the bone-diet TDFs for sea turtles, we used a sensitivity analysis to

characterize the influence of varying TDFs on diet composition estimates that encompass the range of bone-diet TDFs reported for sea turtles and other animal species maintained on carnivorous diets (~2–6 ‰; e.g., Ambrose and DeNiro, 1986; Borrell et al., 2012; Cloyed et al., 2015; Fox-Dobbs et al., 2007; Hobson and Clark, 1992; Kim et al., 2012; Matsubayashi et al., 2017; Webb et al., 2016).

Somatic Growth Rates

To examine the influence of sea turtle trophic ecology on somatic growth rates, we compared complementary diet composition data generated from the stable isotope mixed models with annual somatic growth rate data generated through skeletochronology for each stranded turtle. The somatic growth rate data presented herein are a combination of newly collected (n = 58 turtles stranded 2010–2015) and previously collected data (n = 95 turtles stranded 1993–2009) originally presented in Snover et al. (2007) and Avens et al. (2017). We followed Avens et al. (2017) to calculate growth rates for the newly processed turtles.

First, for each histologically prepared bone cross-section, the diameter of each LAG and humerus section (HSD) were measured using image analysis software (Olympus Microsuite and cellSens). The body proportional hypothesis back-calculation technique (BPH; Francis 1990) was then used to estimate SCL for every measurable LAG, adjusted for turtle–specific SCL and HSD at death (Snover & Hohn 2004, Avens et al. 2017). Annual somatic growth rates were calculated by taking the difference between SCL estimates of successive LAGs. However, given LAGs are

deposited in the spring and we sampled turtles that died throughout the year, only 73/153 turtles had true annual growth rate estimates.

To extend the growth dataset we calculated marginal growth rates for the 36 turtles that stranded between November and March by taking the difference between SCL at stranding and the SCL estimate of the most external LAG. While these marginal growth rates are necessarily minimum estimates of annual somatic growth, Kemp's ridleys likely grow little during the boreal winter when temperatures are cooler and sea turtle metabolic rates and activity patterns are reduced (Balazs & Chaloupka 2004, Hochscheid et al. 2007, McMichael et al. 2008). Indeed, skeletal growth asymptotes in November (Snover & Hohn 2004). The 44 turtles that stranded between June and October were excluded from the growth analysis, highlighting a potential disconnect in data availability for linking sea turtle growth and diet that could be overcome in future analyses through targeted sampling of only turtles that stranded in the spring.

To examine the influence of sea turtle trophic ecology on somatic growth rates, we implemented a series of Generalized Linear Models (GLMs) that included somatic growth as the response variable, age as a fixed effect, and either $\delta^{15}N$ value or estimated diet composition as a fixed effect. Separate GLMs that included $\delta^{15}N$ values as a fixed effect were implemented for each region, whereas GLMs that included estimated diet composition as a fixed effect were only implemented for regions with considerable intra-population variation in diet composition. Age was included in the model to account for ontogenetic effects on growth and diet. Age was

chosen over body size to account for ontogenetic effects as models that included age had consistently lower AIC values than models that included body size. All GLMs included a Gamma distribution and were implemented in R (version 3.5.3) using the *mgcv* package (Wood 2006, R Core Team 2019).

Results

Prey and Sea Turtle Stable Isotope Ratios

Prey $\delta^{13}C$ and $\delta^{15}N$ values were significantly different both within and among regions (Kruskal-Wallis rank sum tests: $p < 0.05$; see Table B4). *Gastropod* was the only prey group that did not exhibit significant regional differences in both stable isotopes examined, although differences in $\delta^{13}C$ were evident. Despite this regional variation in isotopic composition within prey groups, the relative positioning of prey groups in bivariate isospace was similar for most groups (Figure 3.2). As expected, fish $\delta^{15}N$ values were greater than the other prey groups in all cases, with mean values ranging between 10.64 and 14.63 ‰ (Table 3.2). Similarly, the macroalgae/seagrass group exhibited the lowest $\delta^{15}N$ values (mean range 4.44 to 7.86 ‰) and highest $\delta^{13}C$ values of all prey groups (mean range −15.31 to −13.59 ‰), reflective of their position at the base of the food web. Bivalves, which tended to be sampled in closest proximity to coastlines and freshwater inputs, had the lowest $\delta^{13}C$ values (mean range −23.63 to −19.59 ‰). Crabs and gastropods displayed the greatest variability in isospace positioning of the five prey groups but generally fell within the polygon formed by macroalgae/seagrass, bivalves, and fish

(Figure 3.2). Within regions, fish, crustaceans, bivalves, and macroalgae/seagrass differed statistically for at least one stable isotope (Wilcoxon rank sum tests: $p < 0.05$; see Table B5). However, gastropods tended to share isospace with at least one other prey group in each region, likely due in part to small sample sizes—gastropod stable isotope values are poorly represented in the primary literature (see Figure B1).

Kemp's ridley bone stable isotope values were generally constrained by the prey stable isotope data (Figure 3.2). Summary characteristics of bone growth layers sampled for stable isotope ratios are presented in Table 3.3. An analysis of variance on these data showed there was significant variation among regions for both $\delta^{13}C$ ($F_{4,148} = 11.68$, $P < 0.001$) and $\delta^{15}N$ ($F_{4,148} = 129.19$, $P < 0.001$) values. A post hoc Tukey test determined that turtle bone $\delta^{13}C$ values were significantly lower in turtles stranded in the nGoM relative to all other regions ($P < 0.05$; Table B6), possibly a result of influences of the Mississippi River, as freshwater systems generally have distinctly lower $\delta^{13}C$ values than marine systems (Fry & Sherr 1989). In addition, $\delta^{15}N$ values were significantly higher in turtles from the wGoM and lower in turtles from the eGoM relative to all other regions ($P < 0.05$). Differences in $\delta^{15}N$ values between turtles in the eGoM and other regions may be driven by regional differences in nitrogen cycling or trophic ecology. The West Florida Shelf is an area of high N_2-fixation due to the presence of the cyanobacteria *Trichodesmium* (Lenes et al. 2001, Mulholland et al. 2006, Vander Zanden et al. 2015), which reduces $\delta^{15}N$ values (Montoya et al. 2002). Similarly, Kemp's ridleys in southwest Florida are known to eat tunicates, a low trophic level marine species with characteristically low $\delta^{15}N$

values (Williams et al. 2014). Along the U.S. Atlantic Coast, $\delta^{15}N$ values were significantly higher and less variable in turtles from Virginia relative to turtles in North Carolina, tracking differences in prey isotopic composition, which is possibly due to nutrient loading by anthropogenic activities in the Chesapeake Bay.

Regional Variation in Diet Composition

We observed distinct regional differences in diet composition (% fish vs. % invertebrate vs. % macroalgae/seagrass) for Kemp's ridleys (Figure 3.3, Table 3.4). Diet proportion estimates derived from mixing models that included both uninformative and informative priors indicated that Kemp's ridley diets were dominated by invertebrates in the nGoM, North Carolina, and Virginia (65.6–97.7%). In contrast, diets in the wGoM and eGoM were more evenly divided between invertebrates (43.6–54.5 %) and fish (42.6–43.1 %) or invertebrates (43.5–53.6 %) and macroalgae/seagrass (42.4–47.8 %), respectively. As it is unlikely that Kemp's ridleys would consume such high proportions of macroalgae/seagrass, the eGoM results likely reflect consumption of an isotopically similar basal resources, such as tunicates (~5.5 ‰; Williams et al., 2014), or reflect incorrect parameterization of the model. Within the wGoM and eGoM regions, individual variation in turtle diets was high for wGoM turtles but low for eGoM turtles. The proportional contribution of fish and invertebrates to individual wGoM turtle diets ranged between 12 and 60 % and 36 and 85 %, respectively, whereas the proportional contribution of

macroalgae/seagrass and invertebrates to individual eGoM turtle diets ranged between 32 and 48 % and 49 and 63 %.

In most cases, models that included uninformative priors estimated slightly greater contribution of fish and macroalgae/seagrass prey groups to Kemp's ridley diets relative to models with informative priors. However, posterior distributions and 95% credible intervals overlapped extensively between each set of models (Figures 3.3, B5). Larger differences between these model sets were evident in the pre-aggregated invertebrate data, where mixing models with uninformative priors estimated more even contribution of crustaceans, bivalves, and gastropods to Kemp's ridley diets relative to models with the informative priors (Figure B6).

As expected for Bayesian stable isotope mixing models (Bond & Diamond 2011), sensitivity analyses performed on the null mixing model with informative priors for wGoM turtles showed that changes in diet-bone TDFs affected estimated contribution of prey groups to Kemp's ridley diets (Figure B6). Specifically, the median estimated proportional contribution of fish and invertebrate prey to wGoM turtle diets was highly sensitive to changes in $\Delta^{15}N$ but less sensitive to changes in $\Delta^{13}C$, unsurprising given that these prey groups primarily differ in $\delta^{15}N$ values (Figure 3.2). Diet estimates within one standard deviation of the $\Delta^{15}N$ mean ranged between 7.9 and 66.9 % for fish and 30.7 and 79.2 % for invertebrates, whereas estimates within one standard deviation of the $\Delta^{13}C$ mean ranged between 35.7.and 45.4 % for fish and 41.7 and 62.6 % for invertebrates. Mixing model estimates for proportional contribution of individual invertebrate groups to turtle diets displayed

greater sensitivity to changes in $\Delta^{13}C$ values. Bivalve and gastropod estimates were in fact more sensitive to changes in $\Delta^{13}C$ than $\Delta^{15}N$, although their relative contribution to turtle diets remained low within one standard deviation of the mean $\Delta^{13}C$ value (0–7.4 % for bivalve, 0–11.9 % for gastropod). Crustacean estimates were equally sensitive to both changes in $\Delta^{13}C$ and $\Delta^{15}N$ values, with bivariate changes in both TDFs resulting in estimates ranging from 19.5 to 90.7 %.

Diet Composition and Somatic Growth Rates

After controlling for the influence of age on somatic growth rates, our GLMs revealed no significant relationships between $\delta^{15}N$ values and somatic growth rates across most regions (Table 3.5, Figure 3.4). The only exception was for nGoM turtles, where there was a weakly negative relationship between $\delta^{15}N$ values and somatic growth rates ($P = 0.07$). This negative trend was still evident when marginal growth rates were excluded from the analysis, but the relationship became non-significant ($P = 0.11$). When marginal growth rates were excluded, trends across the other regions remained the same, exhibiting a shallow, non-significant decline in somatic growth rates with increasing $\delta^{15}N$ values. These patterns were counter to our expectation of higher growth rate with diets of higher $\delta^{15}N$ (i.e., foraging higher in food web), and could indicate that turtles consume proportional higher amount of fish bycatch might actually have lower growth rates than those feeding primarily on invertebrates, or that physiological processes related to changes in size/age are influencing $\delta^{15}N$ values. In nGoM and VA turtles, $\delta^{15}N$ values and age exhibit a weakly positive relationship

(Figure 3.4). However, across all regions, turtles with the highest $\delta^{15}N$ values tended to span a wide range of ages, suggesting that larger/older turtles are generally not any more likely than smaller/younger turtles to feed higher in the food web.

Given the low intra-regional variation in diet composition for most regions, we only examined relationships between estimated diet composition and growth rates for turtles from the wGoM (Figure 3.5). For these turtles, growth rates were not strongly related to the proportion of fish in turtle diets (P = 0.20). Again, a shallow, non-significant, negative trend was evident in this relationship that did not change following exclusion of marginal growth rates from the analysis. Similar to covariate relationships with $\delta^{15}N$ values, the proportional contribution of fish was not strongly related to age (Figure 3.5).

Discussion

Our findings provide important novel insights into within population diet and growth variation for Kemp's ridley sea turtles. Through an integration of multiple skeletal analyses, we provide the first population-level evaluation of Kemp's ridley diet composition and investigation into the relationship between individual foraging ecology and somatic growth. Our stable isotope mixing model revealed strong regional differences in the proportional contribution of prey to turtle diets that generally supported findings based on published gut and fecal content studies. We specifically observed greater contribution of fish to turtle diets in the western GoM and greater contribution of macroalgae/seagrass—or other isotopically similar basal

resources—to turtle diets in the eastern GoM, whereas invertebrates dominated turtle diets in other regions. Through comparative analyses of somatic growth, stable isotope, and mixing model-derived diet composition estimates, we found that individual Kemp's ridley somatic growth rates were generally poorly correlated with stable isotope-based evidence of turtle trophic ecology within regions. Turtles that foraged higher in the food web did not grow faster and were not older/larger than conspecifics foraging lower in the food web. Interestingly, we observed declines in Kemp's ridley growth rates with increasing $\delta^{15}N$ values, a common measure of foraging trophic level, that were independent of ontogenetic growth effects, with the strongest evidence of this trend in turtles that stranded in the northern GoM.

Regional Diet Variation

Kemp's ridleys are opportunistic foragers, naturally feeding on a wide range of invertebrate species (Shaver 1991). A variety of crab species generally constitute > 75 % of total dietary dry mass, whereas molluscs and vegetation generally make up < 5–10 % (Shaver 1991, Burke et al. 1993, 1994, Seney & Musick 2005, Servis et al. 2015, Schmid & Tucker 2018). In the western and northern GoM, significant contributions of shrimp and fish to Kemp's ridley diets have also been observed, with fish comprising up to 13.7% of total diet dry mass (Werner 1994) and reported in 40.1 to 76.1% of stranded turtle gastrointestinal tracts in the western GoM (Cannon 1998, Stacy 2015). Fish prey are most likely obtained as discarded bycatch or bait from fisheries given that Kemp's ridleys are thought to lack the speed to catch these

species live (Shoop & Ruckdeschel 1982, National Research Council 1990). This conclusion is supported by the co-occurrence of *Nassarius* species—molluscs that scavenge dead animal tissues—in turtle stomachs that also contain fish (Shaver 1991, Bjorndal 1997). In contrast, fish are an uncommon prey item for Kemp's ridleys along the U.S. Atlantic Coast, occurring in only 16.7% of sampled turtles from Virginia and in none of the sampled turtles from New York (Burke et al. 1993, 1994, Seney & Musick 2005).

Results of our Bayesian isotope mixing model largely follow these patterns, with invertebrates comprising 68.5–97.7 % of turtle diets along the U.S. Atlantic Coast but smaller and more variable proportions within the GoM. In the western GoM, where shrimp fishing effort is relatively high (Scott-Denton et al. 2012), we estimated the population-level contribution of fish to turtle diets was 42.6–43.1 %. The similarity in posterior distribution estimates for models with informative and uninformative priors suggests our stable isotope data were highly informative and that these estimates are relatively robust (Moore & Semmens 2008). Kemp's ridleys display remarkable plasticity in diet that appears largely driven by local availability rather than preferences for specific prey species (Bjorndal 1997). Importantly, even with the implementation of bycatch reduction devices, shrimp fishery discards are high in the GoM, accounting for ~50 % of total U.S. fishery discards (Diamond 2004, Harrington et al. 2005a, Scott et al. 2012). It is thus probable that consumption of fish bycatch discarded by shrimp trawlers is a facultative response to local availability in addition to ease of acquisition.

Diet estimates for turtles in the northern GoM were similar to those for turtles along the U.S. Atlantic Coast, with estimated contributions of invertebrates to diets ranging between 65.6 and 94.2 %. These results were unexpected given our hypothesis regarding the spatial relationship between shrimp trawl activity and fish consumption, and contrast with recent necropsy results for the region (Stacy 2015). This may be due to spatial differences in prey availability. For example, blue crab landings in Louisiana represent > 75 % of all landings in the Gulf of Mexico, whereas those in Texas comprise only 7 % (GSFMC 2015). Therefore, even if substantial fish discards are present, availability of natural resources may be sufficient to support Kemp's ridleys in the northern GoM. In addition, non-shrimp crustaceans and invertebrates constitute ~10 % of bycatch in GoM shrimp trawl fisheries and thus may be selectively consumed by turtles (Scott-Denton et al. 2012). The negligible estimated contribution of fish to northern GoM turtle diets may also be due to the close proximity of fish and crustaceans in isospace for this region (Figure 3.2). Mixing models require sources to be sufficiently separated in order for the model to be able to differentiate them (Parnell et al. 2013). It is thus possible that fish do contribute more to Kemp's ridley diets than our mixing models indicate for this region. Further refinement of the prey stable isotope data to more accurately reflect both fish (species and size) and invertebrate species consumed by Kemp's ridley may improve mixing model-derived diet estimations for this and other regions.

Within the eastern GoM, we estimated Kemp's ridley diets primarily comprise invertebrates (43.5–53.6 %) and macroalgae/seagrass (42.4–47.8 %). These results do not align with the current understanding of Kemp's ridley diet composition and are likely due to two factors. First, the invertebrate prey groups in the eastern GoM are the most clustered in isospace relative to other regions, with $\delta^{13}C$ values for crustaceans and gastropods being particularly low (Figure 3.2). This, combined with slightly higher turtle $\delta^{13}C$ values in this region, resulted in the largest isotopic mismatch between invertebrates and turtles of all regions after accounting for trophic enrichment. It is possible that the prey data included in our mixing model did not accurately reflect those prey groups or turtle diets in this region. Such a $\delta^{13}C$ mismatch could arise if the eastern GoM crustaceans and gastropods included in our study derived a greater proportion of their carbon from terrestrial sources relative to the other regions (Michener & Schell 1994). Second, it is also possible that our mixing model is missing a key prey source. Notably, tunicates are thought to be an important prey source for Kemp's ridleys in southwest Florida, occurring in 83.3 % of fecal samples and constituting 38.6 % of fecal dry mass (n = 64 turtles; Witzell and Schmid, 2005). A dearth of tunicate stable isotope data prevented their inclusion in our mixing models. However, two tunicates sampled in Saint Joseph's Bay, Florida, had observed $\delta^{15}N$ values of 5.51 and 5.56 ‰ and $\delta^{13}C$ values of −12.72 and −12.78 ‰ (Williams et al. 2014), which fall within the range of seagrass and macroalgae stable isotope values included in our study. Therefore, our results may in

fact reflect consumption of this or another similar live bottom resource rather than macroalgae/seagrass.

These results illustrate important limitations of Bayesian stable isotope mixing models. Because dietary proportions must sum to one, uncertainty in stable isotope estimates for a single source can bias dietary proportion estimates for all sources (Parnell et al. 2013, Phillips et al. 2014). Such issues are compounded if source diet estimates are highly correlated, an unavoidable and common problem for stable isotope mixing models (Parnell et al. 2013, Chiaradia et al. 2014, deVries et al. 2016). Indeed, we observed high negative correlations between posterior proportion estimates of fish and crustaceans (−0.94) in the western GoM and between crustaceans and macroalgae/seagrass (−0.79) in the eastern GoM for the models that included informative priors, indicating that it was difficult for the model to differentiate between these pairs of sources due to their inverse relationship (Parnell et al. 2010). Nevertheless, concordance between estimated dietary proportions between the models with the informative and uninformative priors, the latter of which had much lower source correlations (−0.23, −0.25) for these pairs of sources, may indicate these estimates are well-supported, given the available data. Future analyses that compare gut content data and estimated diet composition from stable isotope mixing models for individual stranded turtles would aid interpretation of stable isotope data and our understanding of Kemp's ridley diet variation.

While isotopic mixing models have greatly advanced our abilities to discern diets from isotopic data, their utility and accuracy still rely on substantial ecological

knowledge for proper parameterization—these models will always attempt to fit the data, even if the consumers fall outside the mixing space (Phillips & Koch 2002, Parnell et al. 2010). Given the spatiotemporal scale of this study it was necessary to rely on prey isotopic data from the primary literature, which may have inserted certain biases into the analysis. We ameliorated temporal effects to the best of our abilities by using time-corrected $\delta^{13}C$ values. However, it was not possible to overcome spatial biases in sample collection and as a result these may represent the greatest source of bias in our analysis. Kemp's ridley sea turtles forage in a wide range of shallow, benthic marine habitats, including a substantial part of the continental shelf (Shaver et al. 2013, Hart et al. 2018a). Unfortunately, few studies have characterized invertebrate stable isotope values for continental shelf habitats resulting in greater prevalence of estuarine and coastal organisms in our prey isotopic dataset. Given the growing application of stable isotopes to the study of sea turtle foraging and spatial ecology (Pearson et al. 2017, Figgener et al. 2019), quantifying means and variances in known prey stable isotope values across sea turtle ranges should be a high-priority research area. Future analyses using compound-specific isotope analysis of amino acids, which can more accurately estimate consumer trophic position, may also greatly aid in understanding diet variation in sea turtles (Evershed et al. 2007, McMahon & Newsome 2018).

Trophic Ecology and Somatic Growth Dynamics

The lack of strong relationships between bone $\delta^{15}N$ values, mixing model-derived diet composition estimates, and somatic growth rates suggests that within-population variation in diet composition may not be a primary determinant of Kemp's ridley somatic growth variation, and that diet composition may not be a strong driver of the regional (Atlantic vs. GoM) somatic growth differences observed in this species. A suite of environmental factors has been suggested to explain variance in sea turtle somatic rates, including temperature (Bjorndal et al. 2003, Balazs & Chaloupka 2004), density-dependence (Bjorndal et al. 2000, Balazs & Chaloupka 2004), prey dynamics (Balazs 1982, Chaloupka et al. 2004), diet quality (McDermid et al. 2007, Peckham et al. 2011), and individual behavior (Wallace et al. 2009, Hatase et al. 2010). However, investigations into relationships between sea turtle trophic ecology and growth have largely been correlative given the highly migratory life history and conservation status of sea turtles. Wallace et al. (2009) provides the only other comparison of sea turtle trophic ecology and somatic growth where they compared blood plasma $\delta^{15}N$ and $\delta^{13}C$ values with growth rates of recaptured loggerhead turtles from North Carolina, USA. They found no strong relationships between these covariates, theorizing intra-population growth variation may instead be due to alternative habitat use (coastal vs. oceanic habitat) (McClellan & Read 2007). However, recent research suggests $\delta^{15}N$ values can be used to distinguish between these alternative foraging strategies (McClellan et al. 2010, Snover et al. 2010, Avens et al. 2013, Goodman Hall et al. 2015, Ramirez et al. 2015), suggesting that perhaps other factors underlie the observed variability in growth.

Surprisingly, our results suggest that turtles foraging at higher trophic levels may in fact exhibit lower growth rates than conspecifics foraging at lower trophic levels. Given that fish generally have higher energy densities than invertebrates (Doyle et al. 2007, Peckham et al. 2011, Schaafsma et al. 2018), these findings may indicate that energy expended to search for and consume fish (discards) exceeds energy gains of utilizing this resource or that Kemp's ridley sea turtles are not well adapted to consume fish. Although previous studies suggest fish and crabs have similar digestibilites (e.g., feeding experiments in fish species; Tibbetts et al., 2006; Williams et al., 2014), our understanding of sea turtle food digestion is poor for omnivorous species (Bjorndal 1997). As fish are not considered to be a natural prey item for sea turtles, it is plausible that fish may be less digestible than crabs due to evolutionary constraints. Similarly, our analysis does not shed light on the total amount of prey consumed, only relative contributions of different prey groups. Therefore, turtles consuming proportionally greater amounts of fish, but lower amounts of food overall may have relatively low growth rates but high $\delta^{15}N$ values.

However, it is also possible that the conditions that cause Kemp's ridleys to consume fish also contribute to reduced growth rates. If Kemp's ridleys consume fish due to low natural prey availability or poor condition, turtles may be nutritionally stressed which would lead to reduced growth rates. What's more, nutritionally stressed animals tend to have higher $\delta^{15}N$ tissue values because they catabolize their own tissues for energy. Given the retrospective nature of our study, we were not able to evaluate the nutritional condition at stranding for the turtles we sampled. However,

necropsies of Kemp's ridleys stranded in the northern GoM (Louisiana, Mississippi, Alabama) between 2010 and 2014 suggest there was a decline in stranded turtle nutritional condition during this period (Stacy 2015). As all but one of the northern GoM humerus bones we sampled were from turtles stranded between 2010 and 2014, the apparent decline in growth rates with increasing $\delta^{15}N$ values for this region may relate to a decline in nutritional condition. Future studies combining stranded turtle nutritional assays, skeletochronology, and stable isotope analyses would greatly aid in identifying factors underpinning the observed growth patterns. Additionally, applications of stable isotope mixing models to Kemp's ridleys at smaller spatial scales using greater taxonomic specificity for prey groupings would also be informative (e.g., Goodman Hall et al., 2015; Lemons et al., 2011; Wallace et al., 2009).

An important source of uncertainty in our growth analysis is the potential influence of growth rates on isotopic signatures and TDFs. For juvenile loggerhead sea turtles (*Caretta caretta*), somatic growth can explain up to half of the total rate of isotopic incorporation into blood, skin, and scute tissues, and likely explains age-related differences in nitrogen TDFs (Reich et al. 2008). Indeed, multiple studies have demonstrated that faster growth can reduce $\Delta^{15}N$ values because nitrogen input greatly exceeds nitrogen loss—more ^{14}N is retained in the body which lowers $\delta^{15}N$ values and reduces isotopic differences between consumers and their prey (Fuller et al. 2004, Martinez del Rio & Wolf 2005, Reich et al. 2008, Kurle et al. 2014). Such physiological effects, if not accounted for in stable isotope-based studies, can lead to

spurious conclusions, particularly in species with distinct ontogenetic changes in size and growth (Villamarín et al. 2018). For our study, a growth-induced decline in $\Delta^{15}N$ values may have caused us to underestimate the proportional contribution of fish to turtle diets for faster growing individuals. In contrast, diets high in animal-derived proteins typically lead to higher $\Delta^{15}N$ values for consumers (Vander Zanden et al. 2012, Kurle et al. 2014, Turner Tomaszewicz et al. 2017b). A diet-induced increase in $\Delta^{15}N$ would therefore potentially have the opposite effect as growth on TDFs, causing an overestimation of the proportional contribution of fish to turtle diets for individuals that forage higher in the food web. Given the sensitivity of our results to changes in $\Delta^{15}N$ values, more studies are needed that characterize isotopic routing in sea turtles and effects of diet type and physiology on TDFs.

Conclusions

The integration of skeletal growth and stable isotope analysis provides a powerful tool to reconstruct sea turtle trophic ecology while simultaneously investigating relationships between diet and somatic growth. Using this approach, we elucidated substantial regional variation in Kemp's ridley diet composition that largely follows the combined results of the myriad of site-specific studies on Kemp's ridley foraging ecology. This study also provides one of the few quantitative assessments of the relationship between sea turtle trophic ecology and somatic growth. Our analysis further highlights the unique importance of salvaged turtles to investigating intractable questions in sea turtle ecology.

Acknowledgements

We thank all past and present participants of the Sea Turtle Stranding and Salvage Network whose dedicated work made this study possible. We also thank K. Magnusson for providing lab space and equipment for skeletochronological analysis and J. McKay for assistance with stable isotope analyses. Thank you to J. Cordeiro, M. Davis, H. Hagler, K. McNeely, N. Owen, and M. VanBemmel for assistance with laboratory analyses. Thank you to B. Stacy and J. Keene (NOAA) for collection of humeri associated with the DWH Natural Resource Damage Assessment, and to J. Miller, A. Shiel, J. McKay, H. Haas and two anonymous reviewers for comments on this manuscript. Research was conducted under USFWS permit number TE-676379-5 issued to the NMFS Southeast Fisheries Science Center.

Table 3.1. Summary of literature review for Kemp's ridley sea turtle prey species included in the mixing model. See Table B1 for full dataset.

Prey groups	Taxonomic family (Common name, *n*[*])	Counts[*] by region				
		Gulf of Mexico			Atlantic	
		W	N	E	S	N
Crustacean/ Chelicerate		28	48	26	15	10
Horseshoe crab	Limulidae (horseshoe crabs, 4)	0	1	0	2	1
Crab	Portunidae (swimming crabs, 43), Panopeidae (mud crabs, 14), Epialtidae (spider crabs, 5), Menippidae (stone crabs, 4), Diogenidae (hermit crabs, 3), Aethridae (box crabs, 1), Paguridae (hermit crabs, 1), Multiple[**] (1)	13	26	17	9	7
Shrimp	Penaeidae (Penaeid shrimp, 48), Squillidae (Mantis shrimp, 3)	15	21	9	4	2
Bivalve	Ostreidae (Eastern oyster, 29), Mytilidae (mussels, 23), Veneridae (venus clams, 7), Mactridae (Atlantic rangia, 5), Tellinidae (tellin clams, 4), Arcidae (ark clam, 2), Pectinidae (scallops, 2)	15	27	12	13	5
Gastropod	Littorinidae (periwinkles, 18), Melongenidae (Crown conch, 3), Muricidae (murix snails, 3), Nassariidae (Nass mud snails, 3), Naticidae (Atlantic moon snail, 3), Busyconidae (whelks, 2), Calyptraeidae (slipper snail, 2), Cerithiidae (ceriths, 2), Columbellidae (dove snails, 2), Buccinidae (Tinted cantharus, 1), Neritidae (Olive nerite, 1), Potamididae (Ladder horn snail, 1), Turbinidae (West Indian starsnail, 1)	3	19	6	12	2
Fish	Sciaenidae (croaker and weakfish, 75), Sparidae (porgy and pinfish, 29), Engraulidae (anchovy, 23), Mugilidae (mullet, 20), Clupeidae (menhaden and herring, 18), Ariidae (sea catfish, 17), Paralichthyidae (flounder, 17), Haemulidae (grunt, 4), Phycidae (spotted hake, 3), Synodontidae (inshore lizardfish, 3), Achiridae (sole, 2), Pomatomidae (bluefish, 2), Triglidae (searobins, 2), Carangidae (round scad, 1)	42	52	86	20	16
Macroalgae/ Seagrass		25	11	35	11	13
Seagrass	Cymodoceaceae (shoal and manatee grass, 20), Hydrocharitaceae (turtlegrass, 18), Zosteraceae (Common eelgrass, 5), Multiple[**] (4), Unidentified (1)	14	3	25	3	3
Macroalgae	Ulvaceae (Sea lettuce, 13), Unidentified (8), Gracilariaceae (red algae, 6), Multiple[**] (5), Cladophoraceae (green algae, 2), Codiaceae (Green sea fingers, 2), Dictyotaceae (brown algae, 2), Gelidiaceae (red algae, 2), Solieriaceae (red algae, 2), Ceramiaceae (red algae, 1), Ectocarpaceae (brown algae, 1), Fucaceae (bladder wrack, 1), Halymeniaceae (red algae, 1), Wrangeliaceae (red algae, 1)	11	8	10	8	10

[*]*Number of species-specific isotopic values identified in the primary literature.* [**]*Mean composite of samples from multiple families.*

Table 3.2. Mean ± SD $\delta^{13}C$ and $\delta^{15}N$ values for potential prey groups by geographic region.

Prey Group	$\delta^{13}C$ (‰)			$\delta^{15}N$ (‰)		
	n_{means}	n_{total}	Mean ± SD	n_{means}	n_{total}	Mean ± SD
western GoM						
Crustacean	28	318	−18.37 ± 1.32	27	317	9.68 ± 1.33
Bivalve	14	165	−22.74 ± 1.70	15	262	9.65 ± 1.13
Gastropod	3	11	−14.81 ± 0.78	2	6	8.95 ± 0.35
Fish	42	311	−17.40 ± 1.44	33	274	12.64 ± 1.42
Macroalgae/Seagrass	25	153	−14.56 ± 2.11	24	93	6.43 ± 1.84
northern GoM						
Crustacean	48	1545	−18.67 ± 1.59	44	1517	10.89 ± 1.14
Bivalve	25	247	−23.63 ± 0.92	18	242	7.75 ± 0.66
Gastropod	19	478	−18.00 ± 0.74	15	461	9.36 ± 0.26
Fish	52	1334	−19.84 ± 1.13	52	1295	11.93 ± 0.79
Macroalgae/Seagrass	11	57	−15.31 ± 1.18	11	57	6.94 ± 0.94
eastern GoM						
Crustacean	26	570	−19.58 ± 1.92	22	544	6.88 ± 0.97
Bivalve	12	301	−22.40 ± 0.75	7	258	6.51 ± 0.36
Gastropod	6	30	−19.24 ± 1.94	5	29	6.49 ± 0.83
Fish	86	1679	−17.91 ± 1.22	65	1571	10.64 ± 1.09
Macroalgae/Seagrass	29	243	−14.57 ± 2.18	30	779	4.44 ± 1.37
North Carolina						
Crustacean	15	141	−17.68 ± 0.96	15	141	10.00 ± 0.85
Bivalve	13	45	−19.98 ± 0.35	6	35	7.62 ± 0.25
Gastropod	12	40	−16.81 ± 1.25	6	23	6.32 ± 0.61
Fish	17	206	−18.33 ± 0.98	17	208	11.98 ± 0.91
Macroalgae/Seagrass	11	35	−14.70 ± 0.61	5	14	4.81 ± 1.32
Virginia						
Crustacean	10	62	−16.43 ± 0.63	8	50	11.34 ± 0.98
Bivalve	5	97	−19.59 ± 0.98	5	97	9.84 ± 0.78
Gastropod	2	6	−16.21 ± 0.64	2	6	9.83 ± 0.54
Fish	16	318	−18.42 ± 1.33	11	258	14.63 ± 0.89
Macroalgae/Seagrass	13	94	−13.59 ± 1.51	13	94	7.86 ± 1.13

Mean ± SD is the simple mean and pooled SD of species-specific isotopic values collated from referenced studies. n_{means} is the number of mean values included in each $\delta^{13}C$ and $\delta^{15}N$ estimates. n_{total} is total number of prey items sampled in referenced studies. Values are uncorrected for trophic discrimination factors. See Table B1 for source list and complete prey stable isotope dataset resulting from the literature review.

Table 3.3. Summary characteristics for Kemp's ridley sea turtle bone growth layers sampled for stable isotope analysis. Only the most recently deposited growth layer was sampled for each turtle bone.

Geographic region	*n*	SCL (cm)	Year range	$\delta^{13}C_{cor}$ (‰)	$\delta^{13}N$ (‰)	%C	%N
western GoM	44	41.5 ± 8.1 (27.8, 58.9)	1999, 2012	−15.6 ± 0.8 (−17.6, −13.7)	16.3 ± 2.0 (10.9, 19.8)	13.8 ± 0.8	4.5 ± 0.3
northern GoM	28	42.7 ± 8.6 (25.7, 61.8)	1992, 2014	−17.1 ± 1.0 (−19.3, −15.0)	14.8 ± 1.7 (11.4, 17.7)		
eastern GoM	24	43.3 ± 8.0 (26.5, 56.3)	1999, 2013	−15.1 ± 1.6 (−19.6, −12.3)	12.0 ± 1.1 (10.7, 14.4)		
North Carolina	32	40.0 ± 7.7 (27.5, 59.6)	1997, 2012	−16.2 ± 1.5 (−19.1, −13.4)	13.9 ± 1.7 (11.2, 17.8)		
Virginia	25	43.7 ± 5.9 (29.9, 53.1)	1998, 2012	−15.3 ± 1.2 (−17.5, −13.5)	15.7 ± 1.4 (11.2, 17.3)		

Values reported are mean ± SD (min, max). Only the most external growth layers were sampled for each turtle. SCL is straightline carapace length (notch to tip) at stranding. Year is calendar year at start of growth layer sampled. $\delta^{13}C_{cor}$ are corrected for carbonate carbon and the Suess effect. Reported %C and %N are for all sampled growth layers.

Table 3.4. Median (95% CI) posterior Bayesian mixing model estimates of diet proportion by geographic region for Kemp's ridley sea turtles (n = 153).

Geographic region	Informative prior			Uninformative prior		
	Invert (%)	Fish (%)	Macroalgae/ Seagrass (%)	Invert (%)	Fish (%)	Macroalgae/ Seagrass (%)
western GoM (n = 44)	54.5 (35.5, 76.6)	43.1 (21.2, 62.7)	0.1 (0.0, 15.7)	43.6 (23.7, 64.6)	42.6 (25.6, 61.5)	11.8 (0.7, 34.3)
northern GoM (n = 28)	94.2 (60.0, 100.0)	1.5 (0.0, 21.7)	0.5 (0.0, 32.3)	65.6 (34.9, 91.1)	16.0 (1.3, 35.6)	17.7 (1.1, 40.9)
eastern GoM (n = 24)	53.6 (36.5, 79.6)	3.0 (0.0, 13.3)	42.4 (16.7, 58.1)	43.5 (25.6, 68.4)	8.6 (1.5, 17.0)	47.8 (23.3, 64.8)
North Carolina (n = 32)	96.6 (73.6, 100.0)	1.3 (0.0, 17.4)	0.1 (00.0, 19.7)	68.5 (46.0, 91.0)	18.4 (2.1, 35.3)	12.1 (0.7, 31.0)
Virginia (n = 25)	97.7 (80.3, 100.0)	1.0 (0.0, 13.1)	0.0 (0.0, 14.7)	77.5 (52.3, 94.7)	9.5 (0.8, 22.3)	12.1 (0.6, 34.9)

The uninformative prior is constructed from the Dirichlet Bayesian prior whereas the informative prior is constructed from diet proportions published in the primary literature (see Table B2).

Table 3.5. Summary of statistical output for Generalized Linear Models used to evaluate the influence of diet on Kemp's ridley sea turtle annual growth rates. (A) Comparison of $\delta^{15}N$ values and growth rates across all regions. (B) Comparison of median percent of fish in diet (*p*Fish) on growth rates for western GoM turtles only.

Model	N	AIC	Var	Est	SE	t	Pr>|*t*|
(A) Growth ~ $\delta^{15}N$ + Age							
wGoM	38	186.11	$\delta^{15}N$	–0.03	0.03	–0.741	0.463
			Age	–0.11	0.03	–4.234	**<0.001**
nGoM	20	83.93	$\delta^{15}N$	–0.10	0.05	–1.902	0.074
			Age	–0.07	0.04	–1.753	0.098
eGoM	16	83.23	$\delta^{15}N$	0.00	0.12	0.038	0.971
			Age	–0.11	0.08	–1.397	0.186
NC	18	65.90	$\delta^{15}N$	–0.04	0.03	–1.273	0.222
			Age	–0.09	0.02	–4.410	**<0.001**
VA	17	59.31	$\delta^{15}N$	–0.06	0.04	–1.465	0.165
			Age	–0.04	0.04	–1.196	0.252
(A) Growth ~ *p*Fish + Age							
wGoM	38	185.04	*p*Fish	–0.68	0.53	–1.295	0.204
			Age	–0.11	0.03	–4.364	**<0.001**

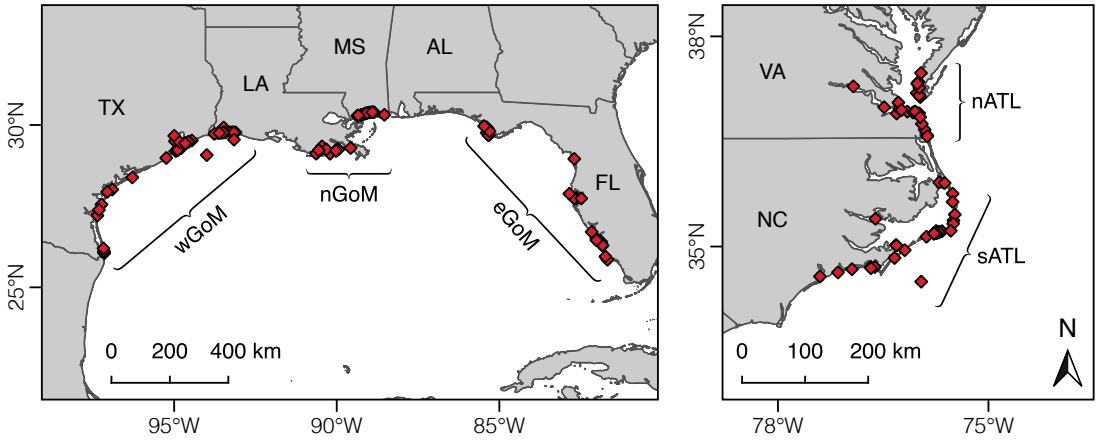

Figure 3.1. Map of Kemp's ridley sea turtle stranding locations for the humerus bones used in this study and geographic breakpoints used to cluster turtles and prey groups.

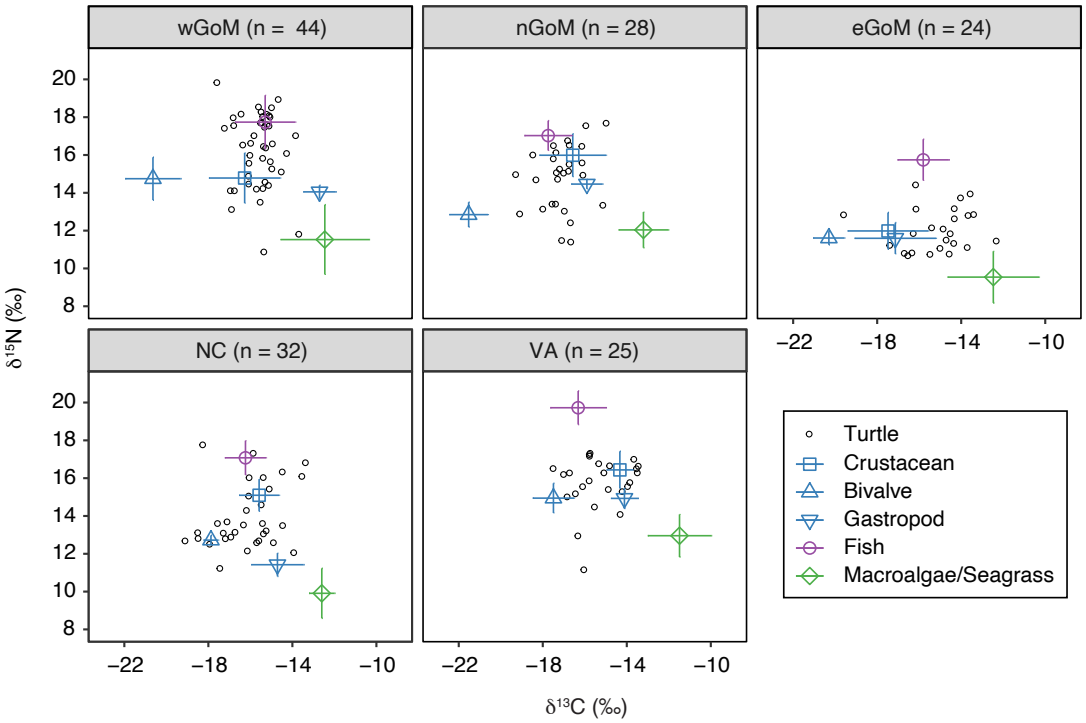

Figure 3.2. Biplots of $\delta^{13}C$ and $\delta^{15}N$ values for Kemp's ridley sea turtles (open circles) and their potential prey groups (mean ± SD) by geographic region. Turtle sample sizes are presented at the top of each plot. Data are for the most recently deposited growth layer prior to death only. Prey values are corrected for trophic discrimination factors ($\Delta^{13}C$ = 2.1 ‰, $\Delta^{15}N$ = 5.1 ‰; see Table 3.2 for uncorrected values).

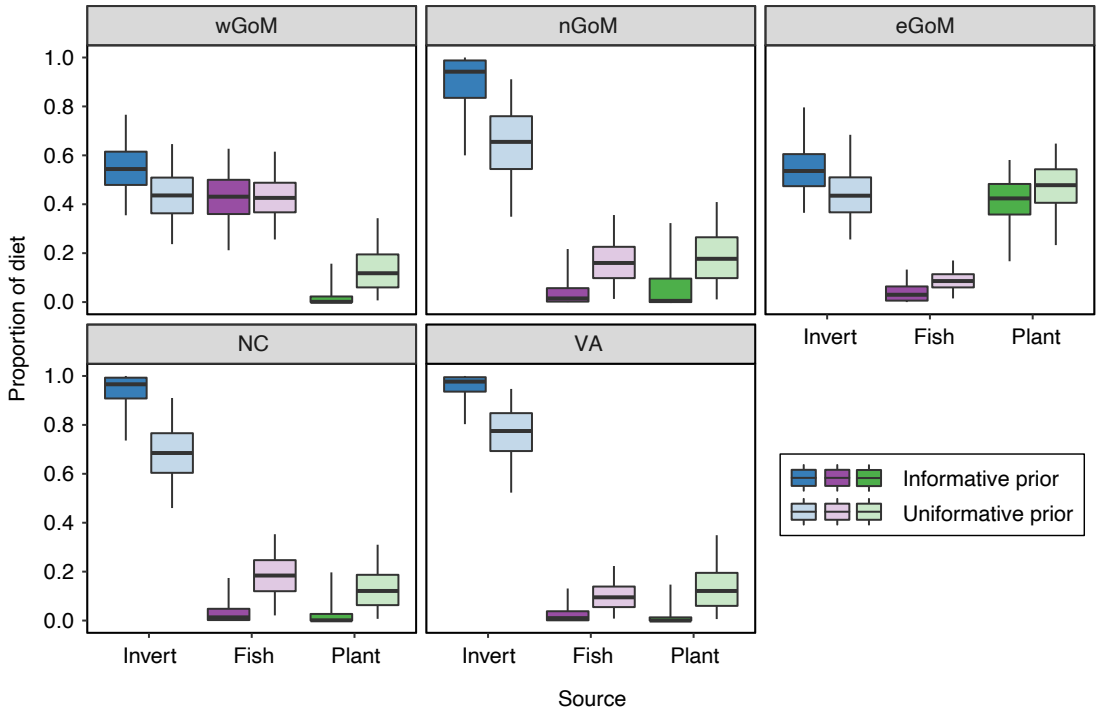

Figure 3.3. Proportional contribution of each prey group to Kemp's ridley sea turtle diets by geographic region based on MixSIAR models that included an informative prior constructed from published diet proportion data and an uninformative prior that assigned equal probability to all prey groups. Invertebrate prey groups (crustacean, bivalve, gastropod) were aggregated *a posteriori*. Lines in boxes are medians, boxes are 50% credible intervals, error bars are 95% credible intervals. See Table 3.4 for samples sizes, medians, and credible interval values.

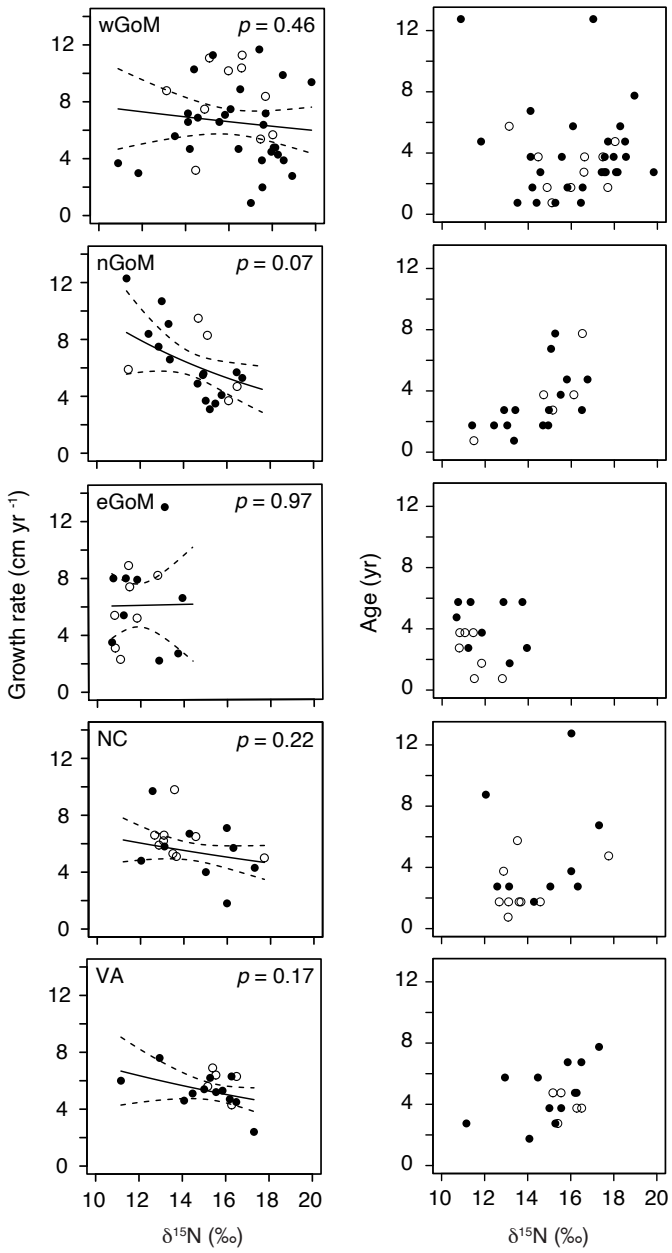

Figure 3.4. Generalized Linear Model results examining the relationships between annual Kemp's ridley sea turtle growth rates and $\delta^{15}N$ values, and age and $\delta^{15}N$ values, for individual turtles by geographic region. Data are for the most recently deposited growth layer prior to death only. Closed circles are true annual growth rates (i.e., turtle stranded in spring, yielding a complete growth interval). Open circles are estimated annual growth rates for turtles that stranded during the winter (Nov–Mar); we assumed that annual skeletal growth asymptotes in November (see *Somatic Growth and Diet Composition* in *Materials and Methods*).

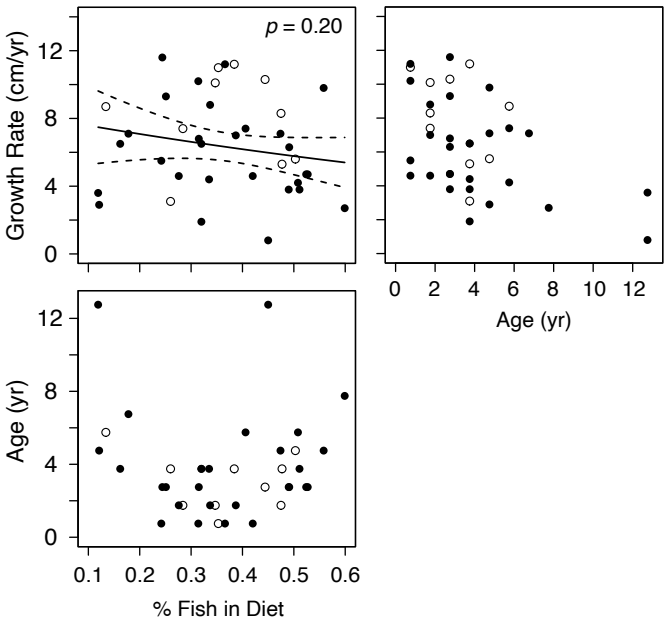

Figure 3.5. Generalized Linear Model results examining the relationship between annual Kemp's ridley sea turtle growth rates and proportional contribution of fish to western Gulf of Mexico turtle diets. Diet estimates are derived from a stable isotope mixing model that included informative priors. Data are for the most recently deposited growth layer prior to death only. Closed circles are true annual growth rates (i.e., turtle stranded in spring, yielding a complete growth interval). Open circles are estimated annual growth rates for turtles that stranded during the winter (Nov–Mar); we assumed that annual skeletal growth asymptotes in November (see *Somatic Growth and Diet Composition* in *Materials and Methods*).

CHAPTER 4: CLASSIFICATION OF KEMP'S RIDLEY SEA TURTLES TO MARINE ECOREGIONS THROUGH COMPLEMENTARY SKELETAL AND GEOCHEMICAL ANALYSES

Matthew D. Ramirez, Jessica A. Miller, Alyssa E. Shiel, Larisa Avens, Lisa R. Goshe, Melissa L. Snover, and Selina S. Heppell

In preparation for submission to Scientific Reports

Abstract

Understanding population structure and connectivity is central to effective conservation and management of mobile marine species. The critically endangered Kemp's ridley sea turtle (*Lepidochelys kempii*) inhabits multiple marine habitats throughout the western North Atlantic Ocean but is primarily distributed between Gulf of Mexico (GoM) and U.S. Atlantic Coast habitats during the juvenile and subadult life stages. Importantly, turtles rearing in these two areas have different vital rates—Kemp's ridleys residing in the Atlantic grow slower than conspecifics residing in the GoM. However, quantifying migratory connectivity between these two geographic areas has been challenging. Intrinsic geochemical markers (e.g., trace elements, stable isotopes) contained within animal tissues are natural recorders of habitat use and migrations over various spatial scales. Here we investigate the ability of complementary trace element, lead (Pb) stable isotope, and growth rate analyses to discriminate regional neritic habitat use of juvenile Kemp's ridleys using the humerus bones of dead stranded turtles (n = 83). Cross-validated quadratic discriminant analyses determined that somatic growth rates in conjunction with Sr:Ca, Cu:Ca, Ba:Ca, Mg:Ca, and Zn:Ca could classify stranded turtles to geographic region of stranding (Atlantic vs. Gulf of Mexico) with 79.5 % accuracy. Furthermore, quadratic discriminant analyses that included Pb isotopes showed that ^{208}Pb:^{206}Pb alone could accurately classify turtles with 94.1 % accuracy. These results suggest that Pb stable isotopes and somatic growth rates may provide a useful tool for assessing regional

habitat use and population connectivity in this and other sea turtle species within the western North Atlantic Ocean.

Introduction

Understanding when and where endangered species occur is fundamental to their protection as it allows for accurate risk assessment and effective conservation planning (Crooks & Sanjayan 2006). This is particularly true for highly migratory, widely dispersed species such as sea turtles (Martin et al. 2007, Runge et al. 2014), which are vulnerable to multiple natural and anthropogenic threats that can vary across space and time (Crouse et al. 1987, Lewison et al. 2014). As differential environmental stressors can ultimately manifest in distinct regional vital rates and population growth trajectories (Atkinson et al. 2008, Baker et al. 2011), elucidating population structure and connectivity can be integral to developing population assessments and evaluating conservation strategies and extinction risk (Heppell et al. 2003a). The integration of biogeographic and demographic information into threat evaluation can also aid prioritization of recovery actions (Bolten et al. 2011). Unfortunately, assessments of population connectivity for most mobile marine species, including sea turtles, is difficult due to their inaccessibility and cryptic nature and more tools are needed to characterize the dynamics of spatially structured populations.

Multiple geochemical markers, such as stable isotopes and trace elements, are now routinely used as natural tags of population structure and connectivity in marine

systems. Their utility is derived from the predictability with which elements and isotopes fractionate (or do not) within food webs (e.g., Ault et al., 1970; Peek and Clementz, 2012; Post, 2002), where the physico-chemical conditions unique to given habitats translate to distinct geochemical compositions in animal tissues. For example, elemental ratios deposited in fish otoliths, calcium carbonate accretionary structures located in a fish's head, can sometimes be used to discriminate populations due to the proportional uptake of certain metals relative to ambient water concentrations (e.g., Walther and Thorrold, 2006). However, both environmental (e.g., temperature, salinity) and physiological (e.g., age, growth, reproduction) factors can influence elemental uptake and incorporation rates into different body pools (Campana 1999, Elsdon & Gillanders 2002, Walther et al. 2010, Sturrock et al. 2015), and lack of chemical heterogeneity in marine systems can hinder the application of certain elements for stock discrimination (Peek & Clementz 2012, Sturrock et al. 2012, Tanner et al. 2015). Trace elements that substitute for calcium ions—strontium (Sr), magnesium (Mg), barium (Ba)—or are present in relatively high abundances in calcified structures—manganese (Mn), copper (Cu)—have proven particularly useful to stock discrimination in multi-variate analyses (Thresher 1999, Campana et al. 2000, Chang & Geffen 2013, Thomas et al. 2017, McMillan et al. 2017). For sea turtles, previous studies have demonstrated that Sr:Ca and Ba:Ca can identify oceanic vs. neritic habitat use in loggerhead (*Caretta caretta*) and Kemp's ridley (*Lepidochelys kempii*) sea turtles (Ramirez et al. 2019), whereas barium, chromium,

zirconium, and titanium can discriminate among green turtle (*Chelonia mydas*) oceanic foraging habitats (López-Castro et al. 2013).

While less commonly applied in ecological studies, lead (Pb) stable isotope ratios provide an additional tool to potentially distinguish animal populations that can overcome many of the limitations associated with trace element and light stable isotope analyses. First, lead exhibits negligible fractionation during metabolic processing due to the small fractional mass differences between their stable isotopes (^{204}Pb, ^{206}Pb, ^{207}Pb, ^{208}Pb; Ault et al., 1970; Rabinowitz and Wetherill, 1972), and can thereby more reliably transfer regional isotopic differences up food webs. Second, lead isotope ratios are highly heterogeneous in the environment (Sangster et al. 2000), with variation driven primarily by patterns of anthropogenic lead contamination but also local geology (Weiss et al. 2003, Boyle et al. 2014). Notably, human activities have reshaped global patterns of lead isotope composition since the Industrial Revolution as a result of fuel combustion (e.g., gasoline, coal) and high-temperature industrial processes (e.g., smelting) and the subsequent atmospheric transport of emissions across land and water masses (Weiss et al. 1999). As different ores have unique isotopic compositions based on their geological age and initial isotopic composition (Stacey & Kramers 1975, Sangster et al. 2000), region- or country-specific lead production and utilization patterns can yield unique environmental fingerprints. For example, lead ores utilized in North America, Europe (sourced from Australia), and North Africa have distinct ^{206}Pb/ ^{207}Pb and ^{208}Pb/ ^{206}Pb ratios—North American sources have higher ratios (i.e.., they have more ^{206}Pb and ^{208}Pb,

respectively)—that have transferred to neighboring water masses via prevailing winds (Weiss et al. 2003). Such geochemical variation has allowed for discrimination of fish nursery grounds in the central Pacific (Spencer et al. 2000), stock discrimination of Atlantic walruses (*Odobenus rosmarus rosmarus*) in the Canadian Arctic (Outridge & Stewart 1999, Stern et al. 1999, Stewart et al. 2003) and minke whales (*Balaenoptera acutorostrata*) in the North Atlantic (Born et al. 2003), and identification of oceanic foraging grounds for green turtles (*Chelonia mydas*) in the Atlantic Ocean (López-Castro et al. 2014).

The critically endangered Kemp's ridley sea turtle is distributed throughout the western North Atlantic Ocean and is primarily segregated between coastal habitats of the Gulf of Mexico and U.S. Atlantic Ocean (NMFS et al. 2011). The majority of the species resides in the GoM throughout life, while a small fraction (0–30% annually; Putman et al., 2013) of the population is passively transported to the U.S. Atlantic Coast between the ages of 1 and 3 via the Loop Current and Gulf Stream, where they reside for an unknown amount of time. It was thought that these Atlantic turtles might be lost to the breeding population (Ogren 1989), but recent observations of tagged Atlantic turtles nesting in Texas and Mexico suggest some of these turtles migrate to the GoM prior to maturity (Schmid 1995, Chaloupka & Zug 1997, Schmid & Witzell 1997, Turtle Expert Working Group 1998, NMFS et al. 2011, NMFS & USFWS 2015). Likewise, few adult-sized Kemp's ridleys strand in the Atlantic (see Chapter 5). Nevertheless, our understanding of the connectivity of these populations is poor. We do not know when this Atlantic-to-GoM ontogenetic

shift occurs, and our estimates of the proportion of each hatchling cohort that enter GoM vs. Atlantic ecoregions is based on analysis of prevailing ocean currents as opposed to marked individuals (Putman et al. 2013). Because somatic growth rates differ between these subgroups (Caillouet et al. 1995, Zug et al. 1997, NMFS & USFWS 2015, Avens et al. 2017), identifying geochemical fingerprints that can discriminate regional habitat use and be used to assess population connectivity will greatly aid population assessments for conservation planning.

In this study, we sampled the outer growth layers of humerus bones collected from Kemp's ridley sea turtles stranded along the U.S. GoM and Atlantic Coast for trace element concentrations and lead isotope ratios to determine whether intrinsic geochemical markers can discriminate between individuals resident in these distinct marine ecoregions. Given the regional differences in somatic growth evident in this species, we also evaluated the strength of somatic growth rate as a stock discriminator. Sea turtle humerus bones are a useful tool for geochemical studies as they contain continuously deposited, metabolically inert cortical bone tissue that maintains stable geochemical records over several years until they are resorbed into the metabolically active core of the bone (Zug et al. 1986, Snover & Hohn 2004, Koch 2007, Snover et al. 2010, Ramirez et al. 2015). Furthermore, the annual nature of bone deposition combined with external deposition of new bone tissue allows for targeted sampling of specific time intervals prior to death (i.e., ≤ 1 year) and estimation of annual growth rates. Lastly, as sea turtles are mobile predators, the

geochemical composition of their tissues will reflect broadscale patterns and sources of variance within regional food webs.

Materials and Methods

Sample Collection and Processing

Humerus bones were collected from stranded Kemp's ridleys through the National Sea Turtle Stranding and Salvage Network. Turtles stranded dead on U.S. beaches from Texas to Virginia between 1998 and 2014 (n = 82; Figure 4.1). Upon stranding, straightline carapace length (SCL, notch to tip), calendar date, and location (state, latitude, longitude) were recorded for each turtle. In some cases, only curved carapace length was recorded, which was later converted to SCL following Avens et al. (2017). Stranding location was used to categorize turtle bones into one of two geographic regions (Atlantic = Florida Atlantic Coast through Virginia; Gulf of Mexico = Texas through Florida Gulf Coast).

Humerus bones were extracted from whole flippers and then two 2–3 mm thick cross-sections were cut from each bone at the site of the deltopectoral muscle insertion scar using a low-speed isomet saw (Buehler). One section was reserved for geochemical analysis, whereas the other was histologically processed as described by Avens and Snover (2013) and Avens et al. (2017) to reveal annual bone growth layers (Snover & Hohn 2004, Avens et al. 2017). Digital images of the stained bone sections were used to identify, count, and measure each line of arrested growth (LAG) within each bone. These data were then used in conjunction with the body proportional

hypothesis back-calculation technique (BPH; Francis 1990) to estimate SCL for every measurable LAG, adjusted for turtle-specific SCL and humerus section diameter (HSD) at death (Snover & Hohn 2004, Avens et al. 2017).

Given that LAG deposition is annual for Kemp's ridleys (Snover & Hohn 2004, Avens et al. 2017), age at stranding was also estimated for each turtle based on LAG counts and date of stranding. For turtles with a visible first-year growth mark, or "annulus" (Snover & Hohn 2004), an initial age estimate was determined directly from LAG counts. For turtles without a visible first-year growth mark (i.e., due to bone resorption; Zug et al., 1986), an initial age estimate was determined by counting the number of visible LAGs and adding the estimated number of LAGs lost to resorption (Parham & Zug 1997). A final age estimate for each turtle was made by adjusting initial age estimates to the nearest 0.25 years based on the mean hatch date for the population (June) and individual stranding date. Final age estimates were used to back-assign age estimates to individual LAGs. The estimated age at the beginning of bone growth layers geochemically sampled in this study ranged between 1.75 and 12.75 yrs.

Bone Geochemical Analyses

To identify regional neritic habitat use, we employed two geochemical approaches—trace element and lead (Pb) isotope analysis—applied to the most recently deposited humerus bone growth layer of stranded Kemp's ridley turtles. This time period represented each turtles geochemical history within one year of death,

dependent on individual stranding date. Prior to geochemical sampling, the stable nitrogen isotope ($\delta^{15}N$) data for each turtle generated in Chapter 3 were examined to ensure the sampled growth layers were reflective of the neritic life stage (generally $\delta^{15}N$ values above 10.30 ‰, age ≥ 1.75)—bone $\delta^{15}N$ values can be used to identify oceanic-neritic ontogenetic shifts in this species (Ramirez et al. 2019).

Trace element ratios were collected via laser ablation-inductively coupled plasma-mass spectrometry (LA-ICP-MS) as described in Ramirez et al. (2019). Briefly, 'geochemical' bone cross-sections (n = 73) were polished, ultrasonically cleaned, and mounted onto glass slides using thermoplastic resin. Counts of ^{25}Mg, ^{43}Ca, ^{51}V, ^{55}Mn, ^{59}Co, ^{60}Ni, ^{65}Cu, ^{66}Zn, ^{86}Sr, ^{112}Cd, ^{138}Ba, and ^{208}Pb were then quantified as transects perpendicular to the bone growth layers using a Thermo Elemental X-Series II ICP-MS coupled with a Photon Machines Analyte G2 excimer laser ablation system at the OSU Keck Collaboratory for Plasma Spectrometry. The laser was set at a pulse rate of 5 Hz with a spot size of 85 µm and a travel rate of 15 µm s^{-1}. All transects were pre-ablated at a pulse rate of 2 Hz with a spot size of 110 µm and a travel rate of 50 µm s^{-1} to remove surface contamination. Count rates for each analyte were normalized to ^{43}Ca using standard procedures to yield bone metal-to-calcium (Me:Ca; mg g^{-1}) ratios (Kent & Ungerer 2006, Miller 2007). Standard reference materials NIST 612 and USGS MACS-1 were measured after every 4–6 samples and used to quantify instrument precision and accuracy, respectively (Table 4.1). Limits of detection (LOD) were calculated as three standard deviations of background values (ppm), adjusted for isotope mass abundance. Counts of ^{59}Co and

^{60}Ni regularly fell below study wide and transect-specific LODs and were thus excluded from further analysis. As in Ramirez et al. (2019), digital post-ablation images for each bone were used in conjunction with complementary 'skeletochronology' images to assign segments of the ablation transect data to individual bone growth layers, after which mean elemental ratios were calculated for the most external growth layer.

Bone dust for lead isotope analysis (^{206}Pb/^{204}Pb, ^{207}Pb/^{204}Pb, ^{208}Pb/^{204}Pb, ^{206}Pb/^{207}Pb, ^{208}Pb/^{206}Pb) was collected from bone cross-sections for 17 turtles using a computer-guided micro mill (ESI New Wave Research) in conjunction with transparencies of complementary digital 'skeletochronology' images to guide precision drilling to a depth of ≤ 1.0 mm. Carbide drill bits (1.0 mm diameter, Brasseler) were used to mill ~20 mg of bone dust from individual bone growth layers for Pb isotope analysis. Bone dust was collected under a laminar flow fume hood. Because we limited our analysis to the most external bone growth layer, which is often too narrow to produce sufficient bone dust for this Pb isotope analyses (see Table 4.2 for sampling summary), not all bones sampled for trace element concentrations were sampled for Pb isotope ratios.

All experimental work for Pb isotope analysis was conducted in a metal-free Class 1000 clean laboratory in the Oregon State University (OSU) Keck Collaboratory for Plasma Spectrometry (Corvallis, OR). All reagents used in this study were purified in-house using sub-boiled concentrated reagent grade acids and ultra-pure water (≥ 18 MΩ cm). Pb for isotope analysis was isolated by anion

exchange chromatography and analyzed via multi-collector inductively coupled plasma mass spectrometry (MC-ICP-MS) as previously described by Weis et al. (2006) and Shiel et al. (2010). First, 15–25 mg of turtle bone dust was weighed into 7 mL Savillex® PFA vials and digested overnight on a hot plate using 2 mL HNO_3. Samples were then re-suspended in 1.8 mL 0.5 M HBr and Pb was isolated via anion exchange chromatography using a 0.2 mL column of AG-1-X8 (200-400 mesh size, chloride form) resin. The resin was first cleaned in the column using two cycles of 18 MΩ water, 0.5 M HBr, and 6 M HCl and then conditioned with 18 MΩ water and 0.5 M HBr. Each sample was then loaded into the column and bulk elements were eluted with three successive washed of 0.5 M HBr—Pb absorbs to the resin. Pb was then eluted using 6 M HCl, collected in Savillex vials, and dried down. Fresh resin was used for each sample.

Prior to Pb isotope analysis, samples were brought up in 1 mL 3 % HNO_3 and spiked with thallium. Isotope ratios were then measured on a Nu Plasma 3D MC-ICP-MS (Nu Instruments, UK) using a DSN-100 (Nu Instruments, UK) membrane desolvator for sample introduction. Ion signal intensities were measured for masses 202–208 (isotopes of Pb, Tl, Hg). The internal standard NIST SRM 981 was measured after every two samples and used to correct for instrument drift and linearity (Galer & Abouchami 1998). In addition, a Tl standard was used to correct for instrumental mass fractionation and ^{204}Pb was corrected for isobaric ^{202}Hg interference. Measured, instrumental mass bias corrected Pb isotope ratios were normalized to the NIST SRM 981 values reported in Galer and Abouchami (1998)

[$^{208}Pb/^{204}Pb$ = 36.7219 ± 0.0044 (2σ), $^{207}Pb/^{204}Pb$ = 15.4963 ± 0.0016 (2σ), $^{206}Pb/^{204}Pb$ = 16.9405 ± 0.0015 (2σ)] using the sample-standard bracketing method (Albarède & Beard 2004). Ion signal intensity for ^{208}Pb was between 0.48 and 1.33 V and for ^{205}Tl was between 0.28 and 0.54 V. All Pb isotope data are presented as means ± 2 standard error (SE; internal precision).

Somatic Growth Rates

As somatic growth rates differ between Kemp's ridleys resident to the U.S. Atlantic and Gulf of Mexico (Avens et al. 2017) (Chapter 2), we included somatic growth as a variable in our models in addition to the geochemical data to differentiate Atlantic versus GoM habitat use. Following standard methods (Avens & Snover 2013), annual somatic growth rates for individual turtles were calculated by taking the difference between SCL estimates of successive LAGs. Our analysis focused exclusively on growth rate data for the most recently deposited growth layer prior to death (i.e., growth layers geochemically sampled). However, as LAGs are deposited in the spring (Snover & Hohn 2004) and we sampled turtles that died throughout the year, true annual growth rate estimates were only available for the 44 (of 82) turtles that stranded in the spring. To generate growth rate estimates for the remaining turtles in our study where only a partial growth rate was available, we employed one of two approaches based on date of stranding (outlined in Figure C1).

For turtles that stranded from November to March (14/82 turtles), we calculated a marginal growth rate by taking the difference between SCL at stranding

and the SCL estimate of the most external LAG. While these marginal growth rates are minimum estimates of somatic growth, we assume that Kemp's ridleys experience relatively little growth during the boreal winter when temperatures are cooler and sea turtle metabolic rates and activity patterns are reduced (Balazs & Chaloupka 2004, Hochscheid et al. 2007, McMichael et al. 2008). In an analysis of marginal Kemp's ridley bone growth layers, Snover & Hohn (2004) demonstrated that annual growth in this species plateaus in late October/early November.

Turtles stranded from May to October (24/82 turtles) would have been actively growing at time of death, with turtles stranding earlier in the calendar year missing a larger proportion of their potential terminal bone growth layer than turtles stranding later in the year. Given that we do not know how much more these turtles would have grown past death we compared each turtles' marginal growth rate (as calculated above) to the mean age-specific growth rate for each region. We assumed that the higher estimate of the two was closer to the hypothetical annual growth rate that would have been achieved had the turtle survived. and used it in our analysis; marginal growth was higher in 12/82 turtles, whereas mean age-specific growth was higher in 12/82 turtles. Mean age- and region-specific growth rates were calculated using all of the Kemp's ridley growth rate data generated via skeletochronology in Chapter 2 for the growth years 1988 to 2011—growth rate data for 2012 to 2015 were excluded from this analysis given the temporal shift in growth evident in those years (see Chapter 2).

Kemp's ridleys display distinct ontogenetic changes in growth (Chapter 2, Avens et al. 2017). As the turtles sampled in our study spanned a wide range of ages (1.75 to 12.75 yrs), it was necessary to standardize the somatic growth rate data to account for this variation in our analysis. To do so we used two approaches: weighting by age and feature scaling. For the first approach (hereafter 'weighted' growth rate; Figure C1), we estimated a weighting factor for each age class within each region. This weighting factor was calculated as the ratio of mean growth rate in age *x* divided by mean growth rate in age 1.75 for a given region—age 1.75 had highest growth rates in our study. Each of the 82 turtle growth estimates calculated previously was then transformed by dividing by this weighting factor. When applied, these weighting factors have the effect of giving all ages the same mean growth rate within a given region. For the GoM turtle aged 12.75, this approach produced an anomalously high weighted growth rate estimate of 33.5 cm yr^{-1}—all other estimates fell between 3.3 and 13.8 cm yr^{-1}. We therefore calculated the mean weighted growth rate estimate for all other GoM turtles and used this mean value for this individual.

For the second approach (hereafter 'scaled' growth rate), we transformed all growth rate estimates to be between 0 and 1 using feature scaling. First, all age-specific growth rate data presented in Chapter 1 were transformed using the following equation:

$$X_{new} = \frac{X - X_{min}}{X_{max} - X_{min}}$$

where X_{new} is the rescaled growth rate estimate, X is the true growth rate estimate for an individual within an age class, and X_{min} and X_{max} are the minimum and maximum growth rate estimates for a specific age class. This approach maintains the shape of each age-specific growth rate distribution but forces them to share the same scale (0 to 1). A linear regression model was then fit to the rescaled (response) and true (predictor) growth rate data for each age to generate linear equations that were used to estimate a scaled growth rate estimate from the growth rate estimates for each of the sampled turtles included in this study.

Statistical Analyses

Prior to statistical analyses, Me:Ca and Pb isotope data were checked for normality and homogeneity of variances using Shapiro-Wilk and Levene's tests, respectively. Zn:Ca, Sr:Ca, and all Pb isotope ratios met normality assumptions. All remaining elemental data were subsequently $\log_{10}$-transformed, after which Mg:Ca, Mn:Ca, Cd:Ca, and Pb:Ca met parametric assumptions. V:Ca, Cu:Ca, and Ba:Ca were approximately normal but continued to exhibit a slight right skew. Given the range of ages (1.75–12.75) and years (1998–2014) sampled, relationships between the geochemical data and these covariates were first examined using analysis of covariance (ANCOVA). Then, univariate and multivariate analysis of variance (ANOVA, MANOVA) were used to test for differences in individual and multi-geochemical fingerprints between geographic regions, accounting for age or year effects where appropriate (i.e., ANCOVA, MANOVA).

Quadratic discriminant function analysis (QDA) was used to quantify classification probabilities of Kemp's ridleys to geographic regions based on estimated growth rate (weighted and scaled), trace element concentrations, and Pb isotope ratios. QDA was chosen over linear discriminant analysis as it is less sensitive to heteroscedasticity, improving classification accuracy. Given variable sample size, separate QDAs were implemented for the trace element and Pb isotope datasets—both included either weighted or scaled growth rate estimates. A backward stepwise QDA was then performed with 73-fold cross-validation using the *stepclass* function from the *klaR* package in R to identify covariates that best separated GoM and Atlantic turtles within each model (Weihs et al. 2005). This approach begins with a model that includes all variables (i.e., full model) then generates new models by excluding single variables (i.e., reduced models) for comparison. Model performance of each reduced model is compared to the previous model, and if performance is improved the variable is excluded. This procedure is repeated until subsequent models no longer improve classification performance by more than 1%.

Covariates most influential to separating turtles by region were then used to implement final QDAs (i.e., reduced models). Final classification success rates were quantified using leave-one-out cross-validation and the overall significance of final models was evaluated by using Wilk's λ tests, or ANOVA in the case of models with only a single variable. QDAs were implemented in R using the *MASS* package (Venables & Ripley 2002, R Core Team 2019). A secondary stepwise variable selection procedure was also performed on the reduced variable dataset using a

minimization of Wilks' lambda (λ) criterion to quantify the importance of each variable to regional assignment (*greedy.wilks* function, *klaR* package). The significance level was set to 1 to allow for full reporting of results.

Results

Regional Variation in Geochemical Markers

Elemental concentrations and Pb isotope ratios differed between turtles that stranded on U.S. GoM and Atlantic beaches (trace element MANOVA $F_{1,71} = 3.11$, $P = 0.001$; Pb isotope MANOVA $F_{1,15} = 3.10$, $P = 0.055$; Figure 4.2). ANCOVAs showed significant effects of year on log(Mg:Ca), log(Cd:Ca), log(Ba:Ca), and all Pb isotope ratios ($P \leq 0.05$), and a weak effect of age on log(Ba:Ca). In all cases the relationship between elemental or isotopic ratios and year and age were non-linear, driven by sharp changes in values for certain years or ages, which prevented the removal of their effect through detrending. Final AN(C)OVAs that accounted for year or age effects, where necessary, indicated that there were significant differences between GoM and Atlantic stranded turtles for log(V:Ca), Zn:Ca, Sr:Ca, log(Ba:Ca), and all Pb isotope ratios (Table 4.3). Log(V:Ca), Zn:Ca, Sr:Ca, and ^{208}Pb:^{206}Pb were generally higher in Atlantic Kemp's ridleys, whereas log(Ba:Ca), ^{208}Pb:^{204}Pb, ^{207}Pb:^{204}Pb, ^{206}Pb:^{204}Pb, and ^{206}Pb:^{207}Pb were generally higher in GoM Kemp's ridleys (Figure 4.2).

Trace Element Discriminant Analysis

Backward stepwise trace element QDAs that included scaled growth rate estimates identified the same elemental ratios as important to regional classifications as models that included weighted growth rate estimates but had classification success rates that were 3.1–12.3 % lower (Table C1). Therefore, subsequent analyses focused on weighted growth rates.

The backward stepwise trace element QDA indicated that weighted growth rate, Sr:Ca, log(Cu:Ca), log(Ba:Ca), log(Mg:Ca), Zn:Ca, log(V:Ca), and log(Pb:Ca) contributed significantly to discrimination of turtles between regions. The cross-validated QDA performed on this reduced dataset found an overall classification success rate of 79.5 %, higher than the overall classification success rate of 75.3 % for the full dataset (Table 4.4). Atlantic Kemp's ridleys had a higher classification success rate in both models (reduced model = 87.8 %, full model = 80.4 %) than GoM conspecifics (68.7 % in both models). Although Atlantic Kemp's ridleys had higher classification success rates, they exhibited more variable and less certain posterior probabilities than the GoM turtles (Figure 4.3). Mis-classified Atlantic and GoM turtles tended to have higher and lower estimated growth rates, respectively, relative to conspecifics within each region. Otherwise mis-classifications were distributed across regions (TX = 4, MS = 3, FL Gulf = 3, FL Atlantic = 1, NC = 4) and ages (1.75 yr = 4, 2.75 yr = 3, 3.75 yr = 2, 4.75 yr = 1 , 5.75 yr = 1, 8.75 yr = 2, 9.75 yr = 1, 11.75 yr = 1) of turtles.

Based on minimization of the Wilk's λ criterion, weighted growth rate most separated turtles by region within the reduced trace element QDA (Table 4.5), with

modest improvement in classification observed following inclusion of Sr:Ca, log(Cu:Ca), log(Ba:Ca), log(Mg:Ca), and Zn:Ca. Wilk's λ changed little following addition of log(V:Ca) and log(Pb:Ca) to the model. These patterns were confirmed through the implementation of a QDA that included only weighted growth rate, which had a classification success rate of 75.4 %. (Table 4.4). The inclusion of the trace element data only increased classification success by 4.1 %. Classification borders and apparent error rates for all combinations of weighted growth rate and the other trace element ratios in the reduced QDA are presented in Figure 4.4.

Lead Isotope Discriminant Analysis

Results of the backward stepwise Pb isotope QDA identified ^{208}Pb:^{206}Pb as the only variable that contributed to discrimination of turtles between regions. A cross-validated QDA performed using this single stable isotope ratio had an overall classification success rate of 94.1 % (Table 4.4), with only one Atlantic Kemp's ridley mis-classified to the GoM region—all GoM turtle were correctly classified. The mis-classified Atlantic Kemp's ridley had the lowest ^{208}Pb:^{206}Pb and highest ^{206}Pb:^{207}Pb of sampled turtles within the region and was thereby closest geochemically to GoM turtles (Figure 4.5). This turtle otherwise had no anomalous characteristics relative to other stranded Atlantic turtles; it stranded in the Outer Banks of North Carolina at the age of 3.75 yr and had completed the oceanic-to-neritic ontogenetic shift 2 years prior to stranding (i.e., age 1.75 growth layer as based on bone stable nitrogen isotope ratios).

Notably, the reduced Pb isotope QDA performed significantly better than the full Pb isotope QDA, which classified all turtles to the GoM region and had a classification success rate of only 64.7 % (Table 4.4). Much like the reduced trace element QDA, the posterior probabilities resulting from the reduced Pb isotope QDA were more variable and less certain for Atlantic Kemp's ridley than their GoM conspecifics (Figure 4.3).

Discussion

We investigated the ability of trace element concentrations, lead isotope ratios, and somatic growth rates to discriminate regional habitat use of Kemp's ridley sea turtles throughout their range. While several elemental ratios could be combined with growth rates to distinguish Atlantic vs. GoM residency for Kemp's ridley sea turtles, lead isotope ratios (particularly $^{208}Pb/^{206}Pb$) could accurately assign turtles to stranding region in all but one case (94.1 % accuracy) and are the most promising indicator of regional habitat use. Quadratic discriminant analyses also revealed that estimated somatic growth rates in combination with a suite of trace element concentrations (Sr, Cu, Ba, Mg, Zn) could classify turtles to stranding region (U.S. GoM vs. Atlantic) with 79.5% accuracy. Within these latter models, somatic growth was the most important covariate to regional assignments, perhaps unsurprising given the well-documented differences in Atlantic and GoM Kemp's ridley growth rates (Avens et al., 2017, Chapter 2). Small samples sizes for complementary lead isotope and trace element data prevented implementation of models that included all three

classes of covariates. Nevertheless, our results suggest that $^{208}Pb/^{206}Pb$ and somatic growth rates may be useful indicators of regional Kemp's ridley habitat use that would allow for future investigations into population connectivity in this at other migratory species in the western North Atlantic Ocean (e.g., assessment of timing of Atlantic to GoM habitat shifts).

Pb Isotopes as Stock Discriminators

Despite strong environmental heterogeneity (Weiss et al. 2003), applications of Pb stable isotope analyses to ecological studies are uncommon relative to light stable isotopes (e.g., hydrogen, carbon, nitrogen). This is particularly true for the Gulf of Mexico, where few studies exist for which we can compare our results within the study period; environmental Pb isotope ratios evolve through time based on patterns of anthropogenic Pb utilization, although the rate of change has slowed in recent decades (Kelly et al. 2009, Boyle et al. 2014). Nevertheless, the patterns of Pb isotope ratios observed herein align with those of Shiel et al. (2012), who sampled bivalve tissues along the U.S. East Coast (Maine to South Carolina) and GoM (Alabama) in 2005 and 2006—the mean age of our Pb isotope data herein is 2007 (range: 2002 – 2014). Shiel et al. (2012) found that Eastern oysters (*Crassostrea virginica*) in Mobile Bay, Alabama, had lower $^{208}Pb/^{206}Pb$ (2.03564) and higher $^{206}Pb/^{207}Pb$ (1.21783) than oysters sampled at all sites along the U.S. East Coast (South Carolina to Maine; $^{208}Pb/^{206}Pb$ = 2.04734 – 2.07269; $^{206}Pb/^{207}Pb$ = 1.17949 – 1.20976). We similarly observed lower $^{208}Pb/^{206}Pb$ and higher $^{206}Pb/^{207}Pb$ in GoM Kemp's ridleys relative to

Atlantic Kemp's ridleys, with no overlap in $^{208}Pb/^{206}Pb$ between turtles stranded in each region. In contrast, our results differ with those of López-Castro et al. (2014), who found no differences in scute Pb isotope ratios between green turtles sampled from the East and West Coasts of Florida. This divergence is likely due to the fact that López-Castro et al. (2014) sampled scute growth layers reflective of the oceanic life stage and 33.4 % of West Florida and 66.7 % of East Florida turtles were assigned to oceanic foraging sites outside of North America (e.g., Sargasso Sea, Azores, Africa).

Although the history of lead pollution in the GoM is poorly studied relative to the western North Atlantic Ocean (Shen & Boyle 1987, Kelly et al. 2009, Horta-Puga & Carriquiry 2014), comparisons of turtle bone Pb isotope signatures with those of known anthropogenic sources suggest multiple possible drivers of the geographic Pb isotope patterns observed herein (Figure 4.5). First, Mexican coal is more radiogenic (lower $^{208}Pb/^{206}Pb$, higher $^{206}Pb/^{207}Pb$) than U.S. coal and thereby may contribute to the Pb isotope signatures observed in GoM turtles through atmospheric transport of pollutants across the GoM (Díaz-Somoano et al. 2009). Indeed, Atlantic Kemp's ridley Pb isotope signatures fall within the range of U.S. coals, whereas those for GoM turtles are closer to the Mexican coal signature or are intermediate between the two, possibly consistent with mixing of U.S. and Mexican coal sources in the GoM. Coal was likely a major source of Pb in the eastern U.S. into the early 2000s (Díaz-Somoano et al. 2009). This, combined with the possible transport of Mexican emissions across the GoM via the North American Westerlies (Weiss et al. 2003),

may explain the more radiogenic Pb isotope signatures observed in GoM turtles relative to conspecifics in the U.S. Atlantic.

The radiogenic GoM Kemp's ridley signatures may also be reflective of the influence of natural oil and gas seeps in the GoM. As ^{206}Pb, ^{207}Pb, and ^{208}Pb are final products of the radioactive decay of uranium and thorium (^{238}U, ^{235}U, ^{232}Th), the isotopic composition of a Pb ore deposit is primarily a function of its initial chemical composition (Pb, U, Th) and age, with younger ores generally being more radiogenic than older ores (Sangster et al. 2000). For example, Mexican coals are significantly younger (65 – 142 Ma) than U.S. coals (290 – 354 Ma), which may partly explain why Mexican coals have more radiogenic Pb isotope signatures (Díaz-Somoano et al. 2009). Importantly, the GoM contains hundreds of oil deposits similar in geological age to Mexican coals that have leaked into the GoM through natural seeps over thousands of years (Kennicutt 2017). U.S. Atlantic waters, by contrast, lack any major oil reserves or seeps (National Research Council 2003). While isotopic characterizations of GoM oil deposits are lacking, Pb and other light and heavy metals are abundant in crude oil (Osuji & Onojake 2004). Therefore, it is possible that these Pb sources are relatively radiogenic based on their geological age, leading to a more radiogenic geochemical fingerprint in the GoM. Further characterization of the Pb isotope composition of Mexican coal and Gulf of Mexico crude oil is needed to test these hypotheses.

Regional Somatic Growth Variation

Outside stable Pb isotopes, somatic growth was the next single best discriminator of regional habitat use in this species. These results add to the growing body of evidence that Atlantic and GoM Kemp's ridleys have different growth trajectories of ecological importance (Avens et al., 2017; Caillouet et al., 1995; NMFS and USFWS, 2015; Zug et al., 1997; Chapter 2), with Atlantic Kemp's ridleys growing slower than conspecifics in the GoM. In the most comprehensive analysis of regional Kemp's ridley somatic growth variation to date, Avens et al. (2017) demonstrated that these differences manifest early in life—within the 20–29.9 cm SCL size class (~2–5 yrs old)—but dissipate at larger sizes. Results from Chapter 2 follow these patterns, with this divergence in growth rates evident as early as the second year of life, following recruitment from oceanic to neritic habitats. Importantly, this interruption in growth seems to put Atlantic turtles on a new, lower growth trajectory (Avens et al. 2017). Whether these turtles ultimately achieve similar asymptotic sizes as their GoM conspecifics is currently unknown but is likely an important consideration for understanding nesting patterns and the species' population dynamics. Compensatory growth—catch-up growth following a period of delayed development resulting from nutrient limitation—has been documented in loggerhead turtles (Bjorndal et al. 2003) and could serve as a mechanism for Atlantic turtles to achieve similar size-at-age as GoM Kemp's ridleys. However, Snover et al. (2007) did not find evidence for compensatory growth in Atlantic Kemp's ridleys when applying the methods used by Bjorndal et al. (2003). Nevertheless, compensatory growth would only aid Atlantic Kemp's ridleys if they migrated from

Atlantic to GoM habitats during the juvenile life stage, years prior to sexual maturity (9–17 yrs; Avens et al., 2017), as somatic growth is negligible once sea turtles mature (Omeyer et al. 2017).

The utility of somatic growth for discriminating regional habitat use is to some extent limited by inherent variability in sea turtle growth rates within and among age classes. We corrected for ontogenetic growth effects to the best of our ability through scaling or weighting of age-specific somatic growth rates but there were nevertheless some Atlantic turtles that grew as fast as GoM conspecifics, and some GoM turtles that grew as slow as Atlantic conspecifics. A number of these turtles were ultimately mis-classified because of this. It is also entirely possible that some of these GoM turtles perceived to be mis-classified are of Atlantic origin because turtles resident in the GoM are ultimately a mix of life-long GoM residents and an unknown proportion of Atlantic migrants. Sampling of all visible growth layers for these misclassified turtles would aid in testing this hypothesis as would study of turtles with known migration histories in the year prior to death.

Our study illustrates the sensitivity of methodological decisions to classification success rates in discriminant analyses. As sea turtle growth rates decline non-monotonically with increasing age/size, we sought to correct our growth rate data to remove the potential influence of ontogeny. To this end we employed two methods to either scale or weight individual turtle growth rate estimates by age class and implemented separate models that used data derived from either approach. Classification success rates ultimately differed by up to 12.3 % dependent on which

growth dataset was used, suggesting that our results are highly sensitive to how growth rates are estimated. Furthermore, additional biases may have been inserted into our analyses through the use of marginal and mean age-specific growth rates where true annual growth rate estimates were lacking. To reduce these potential sources of bias, future extensions of our approach to study sea turtle population connectivity should focus analyses solely on bone growth layers with true growth rate estimates (i.e., turtles that died in the spring) and, if possible, should only focus on sampling turtles of specific ages or age classes.

Trace Elements and Habitat Use

The inclusion of a suite of trace element ratios into the quadratic discriminant analysis increased classification rates, albeit only marginally (4–5 %). Our results show that Sr:Ca, Cu:Ca, Ba:Ca, Mg:Ca, and Zn:Ca (in decreasing importance) may aid in assigning Kemp's ridleys to Atlantic versus GoM neritic habitats, regardless of the underlying mechanisms governing their deposition into sea turtle tissues (Ramirez et al. 2019). Although Sr and Mg are generally homogeneous in fully marine systems due to their long residence times (de Villiers 1999, Foster et al. 2010), multiple studies have demonstrated they can be useful discriminators of fish stocks as a result of environmental or physiological effects on incorporation rates (e.g., Humphreys et al., 2005; Rooker et al., 2001; Warner et al., 2005). In contrast, Ba, Cu, and Zn display greater horizontal and vertical variability in the ocean due to relatively short residence times (Peek & Clementz 2012, Sturrock et al. 2012), differences that

transfer to consumers and aid stock discrimination (e.g., Ashford et al., 2005; Baumann et al., 2015; Hamilton and Warner, 2009). Along the U.S. GoM and Atlantic Coast, water concentrations for these elements are largely derived from sediments, river effluents, and anthropogenic pollution, all of which can vary spatiotemporally and complicate their utility for stock discrimination (Gillanders 2002). Importantly, marine habitats near the Chesapeake Bay and mouth of Mississippi River, the largest drainage basin in the United States, may have unique geochemical compositions because of these sources that may be transferred up the food web to sea turtles. Our decision to pool samples across wide ocean regions and time periods (16 years) may have obscured such differences, and more fine scale spatiotemporal analyses may reveal greater heterogeneity.

Nevertheless, trace element concentrations of sea turtle tissues may not necessarily reflect water concentrations for some trace elements given that they ultimately derive elements from their diet (Schroeder et al. 1972), and multiple environmental and physiological factors may influence deposition rates into calcified tissues (Campana 1999, McMillan et al. 2017). For example, Sr, Ba, and Pb are known to biopurify as they move through food webs, decreasing in abundance in animal tissues relative to calcium with each trophic transfer (Elias et al. 1982, Burton et al. 1999, Peek & Clementz 2012). Diet, which varies spatially in this species (Chapter 3), may thus be an important determinant of certain trace element concentration. Similarly, temperature and growth, which are confounded in sea turtles, can significantly alter elemental uptake, with their effects varying across

species and elements (Friedland et al. 1998, Fowler et al. 2005, Chang & Geffen 2013, Sturrock et al. 2015). As growth and region are inherently confounded in Kemp's ridleys, apparent regional differences in elemental concentrations may simply be an artifact of strong physiological regulation (e.g., growth effects) which may be homogenizing elemental bone composition within each region.

While there is the potential for growth effects on elemental deposition rates, particularly in comparisons of fast-growing GoM and slow-growing Atlantic Kemp's ridleys, bivariate partition plots (Figure 4.4) suggest there are no strong relationships between growth rates and any elemental ratio measured herein at the population level. This conclusion is preliminary as this study was designed to address a broad spatial question, not investigate physiological effects on elemental incorporation rates in bone, and therefore growth, age, geography, and time are all necessarily confounded in our analysis. As experimental studies are infeasible for sea turtles because of their conservation status and life history, future bone studies narrowed to specific locations, years, and ages may allow for more robust investigations into the effect of growth on bone elemental incorporation rates.

Implications for Sea Turtle Assessment and Conservation

Understanding population structure and connectivity is of critical importance to the conservation and management of highly migratory species such as sea turtles (Webster et al. 2002, Crooks & Sanjayan 2006). Recent decades have seen a rapid increase in the number of studies characterizing sea turtle spatial ecology and

metapopulation dynamics largely due to advances in molecular techniques and electronic tagging systems (Avise 1998, Cooke 2008, Godley et al. 2010). While these techniques have greatly expanded our understanding of life stage transitions, life history variation, natal philopatry, and phylogeography (Jensen et al. 2013), they are constrained in their temporal and numerical application (e.g., satellite tags). Geochemical markers contained within inert tissues (e.g., turtle cortical bone), by contrast, provide a means of reconstructing habitat use over multiple years for many individuals at a reduced cost (Ramirez et al. 2015, 2019, Turner Tomaszewicz et al. 2017a). Importantly, identification of geochemical markers within turtle bones—a tissue that contains complementary information on annual size, age, and growth—that are unique to particular habitats as demonstrated herein for $^{208}Pb/^{206}Pb$ provides a means of not only studying movement and habitat use but also the timing of difficult to observe habitat shifts with respect to size and age. For Kemp's ridleys, this approach may ultimately provide a means of quantifying the proportion of turtles that reside in the U.S. Atlantic versus GoM as well as the contribution of Atlantic turtles to population growth and resilience, pressing questions for their conservation and management (NMFS & USFWS 2015).

Acknowledgements

We first thank the many participants of the Sea Turtle Stranding and Salvage Network for their dedicated work. We also thank C. Russo and N. Olsen for assistance with laser ablation-inductively coupled plasma-mass spectrometry; B.

Rutila, K. Melby, and C. Murphy for assistance with Pb isotope analyses; and, M. VanBemmel, J. Hart, K. McNeely, and N. Owens for assistance with bone imaging. Research was conducted under USFWS permit number TE-676379-5 issued to the NMFS Southeast Fisheries Science Center. Funding for this project was provided by National Oceanic and Atmospheric Administration National Marine Fisheries Service (NOAA-NMFS) and PADI Foundation (award # 28838). MDR was supported by the NSF Graduate Research Fellowship Program and the NOAA Office of Education Educational Partnership Program (award # NA16SEC4810007). This publications content is solely the responsibility of the award recipient and do not necessarily represent the official views of the U.S. Department of Commerce, National Oceanic and Atmospheric Administration.

Table 4.1. Estimated accuracy [relative standard deviations (RSD)], precision (percent difference from MACS-1 known values; mean ± SD), and limits of detection (LOD; mean ± SD) for trace element data collected via laser ablation-inductively coupled plasma-mass spectrometry.

Analyte*	NIST 612 RSD (%)	MACS-1** (% diff)	LOD (ppm)
^{24}Mg	15.20	—	1.344 ± 0.399
^{51}V	5.71	—	0.090 ± 0.034
^{55}Mn	6.96	4.9 ± 5.4	0.906 ± 0.133
^{65}Cu	11.46	20.9 ± 6.7	0.073 ± 0.015
^{66}Zn	19.43	21.0 ± 7.7	0.062 ± 0.016
^{86}Sr	4.32	16.0 ± 4.7	1.324 ± 0.249
^{112}Cd	22.44	52.4 ± 4.5	0.022 ± 0.006
^{138}Ba	5.90	24.0 ± 9.9	0.087 ± 0.037
^{208}Pb	30.02	26.9 ± 5.9	0.008 ± 0.003

* Me:Ca for precision estimate (MACS-1).
** Mg:Ca and V:Ca are not homogeneous in MACS-1 and were therefore not evaluated.

Table 4.2. Summary information [mean ± SD (range)] for Kemp's ridley bone growth layers sampled for trace element concentrations (mg g^{-1}, *μg g^{-1}) and lead isotope ratios by stranding region. Data presented are untransformed.

Analyte*	n	Atlantic	n	Gulf of Mexico
Year	47	2007 (1998–2011)	35	2007 (1999–2014)
Estimated age (yr)	47	5.15 (1.75–11.75)	35	4.06 (1.75–12.75)
Estimated growth rate (cm yr^{-1})	47	5.28 (1.80–9.80)	35	6.25 (1.50–12.20)
Mg:Ca	41	30.86 (21.43–42.28)	32	32.60 (0.17–1.51)
V:Ca*	41	0.57 (0.17–1.51)	32	0.52 (0.16–3.23)
Mn:Ca	41	0.05 (0.02–0.19)	32	0.07 (0.01–0.14)
Cu:Ca*	41	5.42 (0.42–51.66)	32	2.85 (0.44–12.66)
Zn:Ca	41	0.19 (0.13–0.24)	32	0.17 (0.09–0.28)
Sr:Ca	41	8.51 (4.71–10.11)	32	7.78 (5.26–9.72)
Cd:Ca*	41	0.29 (0.12–0.55)	32	0.25 (0.14–0.42)
Ba:Ca	41	0.09 (0.03–0.25)	32	0.17 (0.03–0.56)
Pb:Ca*	41	1.39 (0.49–4.90)	32	1.39 (0.33–7.37)
$^{208}Pb/^{204}Pb$	6	38.605 (38.509–38.700)	11	38.783 (38.486–39.062)
$^{207}Pb/^{204}Pb$	6	15.663 (15.654–15.679)	11	15.682 (15.661–15.702)
$^{206}Pb/^{204}Pb$	6	18.825 (18.728–18.918)	11	19.080 (18.826–19.304)
$^{208}Pb/^{206}Pb$	6	2.051 (2.046—2.056)	11	2.033 (2.015–2.044)
$^{206}Pb/^{207}Pb$	6	1.202 (1.196–1.207)	11	1.217 (1.202–1.230)

Table 4.3. Results of one-way AN(C)OVA comparing elemental concentrations among regions after controlling for age and year effects, where needed.

Trace element concentrations					Pb isotope ratios				
Analyte	df	MS	*F*	*P*	Analyte	df	MS	*F*	*P*
log(Mg:Ca)					**^{208}Pb/^{204}Pb**				
Region	1	0.008	1.61	0.209	Region	1	0.123	7.10	**0.019**
Year	1	0.021	4.07	**0.048**	Year	1	0.229	13.24	**0.003**
Error	70	0.005			Error	14	0.017		
log(V:Ca)					**^{207}Pb/^{204}Pb**				
Region	1	0.233	3.87	**0.053**	Region	1	0.001	8.76	**0.010**
Error	71	<0.060			Year	1	<0.001	1.12	0.309
					Error	14	<0.001		
log(Mn:Ca)					**^{206}Pb/^{204}Pb**				
Region	1	0.059	1.22	0.273	Region	1	0.251	10.47	**0.006**
Error	71	0.049			Year	1	0.033	1.37	0.262
					Error	14	0.024		
log(Cu:Ca)					**^{208}Pb/^{206}Pb**				
Region	1	0.399	2.45	0.122	Region	1	0.001	21.27	**<0.001**
Error	71	0.163			Year	1	<0.001	4.76	**0.047**
					Error	14	<0.001		
Zn:Ca					**^{206}Pb/^{207}Pb**				
Region	1	0.006	4.72	**0.033**	Region	1	<0.001	16.46	**0.001**
Error	71	0.001			Year	1	<0.001	11.01	**0.005**
					Error	14	<0.001		
Sr:Ca									
Region	1	9.560	7.69	**0.007**					
Error	71	1.243							
log(Cd:Ca)									
Region	1	0.040	2.13	0.149					
Year	1	0.085	4.49	**0.038**					
Error	70	0.019							
log(Ba:Ca)									
Region	1	0.579	7.12	**0.009**					
Year	1	1.316	16.19	**<0.001**					
Age	1	0.249	3.07	0.084					
Error	69								
log(Pb:Ca)									
Region	1	0.030	0.44	0.508					
Error	71	0.067							

Table 4.4. Predicted regional assignment of Kemp's ridley sea turtles based on cross-validated quadratic discriminant function analysis (QDA). Models included (A) trace element QDA_{full} (weighted growth rate + 9 trace element concentrations), (B) trace element $QDA_{reduced}$ (weighted growth rate + 7 trace element concentrations), (C) trace element QDA_{growth} (weighted growth rate only), (D) Pb isotope QDA_{full} (weighted growth rate + 5 Pb isotope ratios), and (E) Pb isotope $QDA_{reduced}$ (^{208}Pb:^{206}Pb only). Correct classifications are in **bold**. The most successful model is highlighted in grey. Final models were evaluated via (M)ANOVA. Atlantic (ATL) = Florida Atlantic Coast through Virginia, Gulf of Mexico (GoM) = Texas through Florida Gulf Coast.

		Predicted			
Model	Actual	ATL	GoM	% Correct	Model Evaluation
Weighted growth + trace element QDAs					
(A) trace element QDA_{full}	ATL	**33**	8	80.4	Wilk's $\lambda = 0.57$
	GoM	10	**22**	68.7	$F_{10,62} = 4.74$
	Total	43	30	75.3	$P < 0.001$
(B) trace element $QDA_{reduced}$	ATL	**36**	5	87.9	Wilk's $\lambda = 0.59$
	GoM	10	**22**	68.7	$F_{8,64} = 5.60$
	Total	46	27	79.5	$P < 0.001$
(C) trace element QDA_{growth}	ATL	**38**	3	92.7	ANOVA
	GoM	15	**17**	53.2	$F_{1,71} = 25.19$
	Total	53	20	75.4	$P < 0.001$
Weighted growth + Pb isotope QDAs					
(D) Pb isotope QDA_{full}	ATL	**0**	6	0.00	Wilk's $\lambda = 0.27$
	GoM	0	**11**	1.00	$F_{6,10} = 4.53$
	Total	0	17	64.7	$P = 0.018$
(E) Pb isotope $QDA_{reduced}$	ATL	**5**	1	83.3	ANOVA
	GoM	0	**11**	100	$F_{1,17} = 17.01$
	Total	5	12	94.1	$P < 0.001$

Table 4.5. Results of stepwise variable selection using the Wilk's λ criterion.

Variable	Wilks' λ	$F_{overall}$	$P_{overall}$	F_{diff}	P_{diff}
Weighted growth rate	0.738	25.19	<0.001	25.19	<0.001
+ Sr:Ca	0.705	14.64	<0.001	3.28	0.074
+ log(Cu:Ca)	0.681	10.77	<0.001	2.42	0.124
+ log(Ba:Ca)	0.643	9.41	<0.001	3.96	0.051
+ log(Mg:Ca)	0.618	8.30	<0.001	2.83	0.097
+ Zn:Ca	0.592	8.00	<0.001	2.89	0.093
+ log(V:Ca)	0.590	6.45	<0.001	0.17	0.684
+ log(Pb:Ca)	0.588	5.60	<0.001	0.22	0.642

F_{diff} and P_{diff} are the approximated F-statistic and P-value of the partial Wilks' λ for comparing the model with the new variable to the previous model. The model is initiated with the variable that most separates turtle by regions.

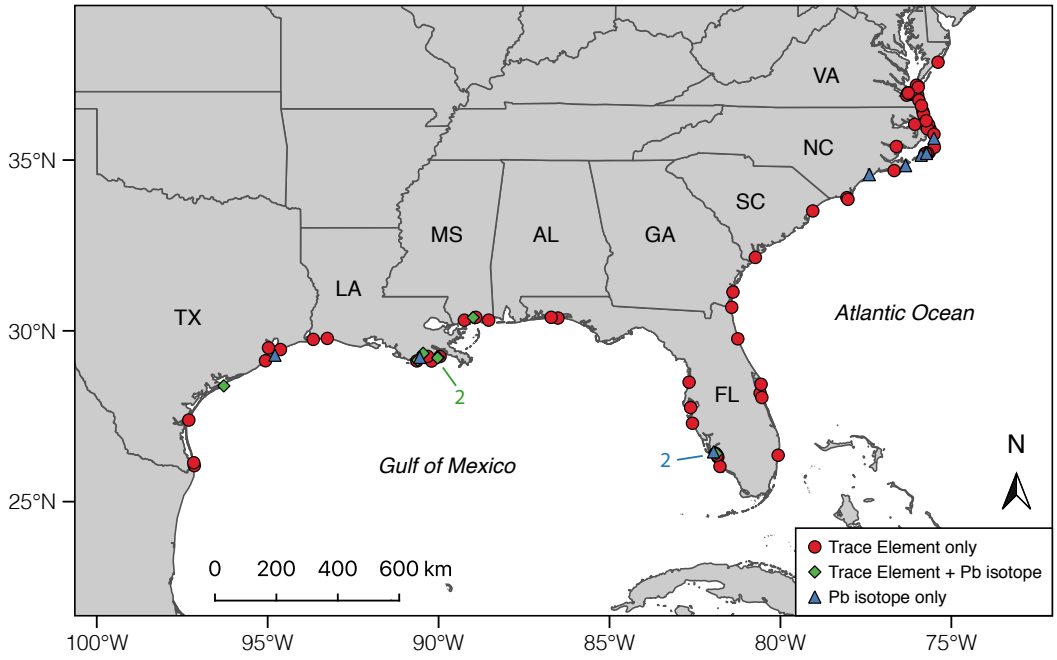

Figure 4.1. Stranding locations for Kemp's ridley sea turtles (n = 82) analyzed for trace element concentrations (n = 73) and Pb isotope ratios (n = 17).
Eight turtles were sampled for both geochemical markers.

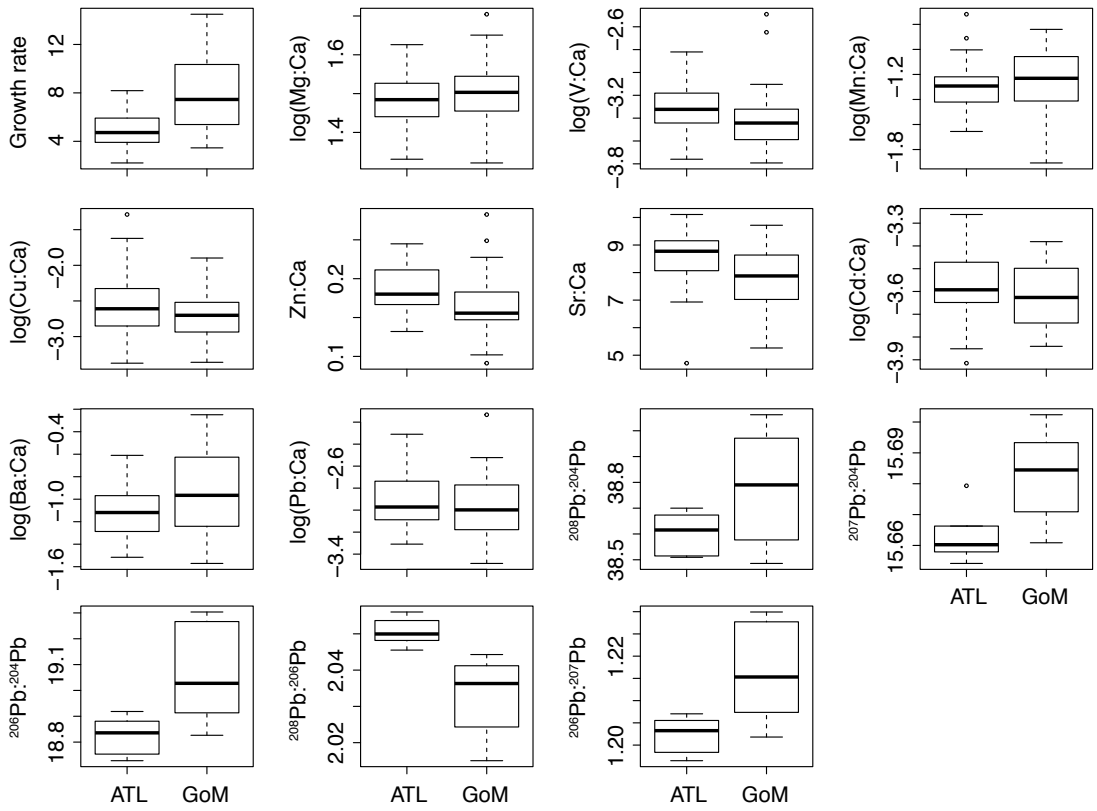

Figure 4.2. Boxplots of weighted annual growth rates (cm yr^{-1}; n = 73), trace element ratios (mg g^{-1} ; n = 73), and lead isotope ratios (n = 17) for Kemp's ridley sea turtles by stranding region (ATL, Atlantic = Florida Atlantic Coast to Virginia; GoM, Gulf of Mexico = Texas to Florida Gulf Coast). Data are for the most recently deposited humerus bone growth layer.

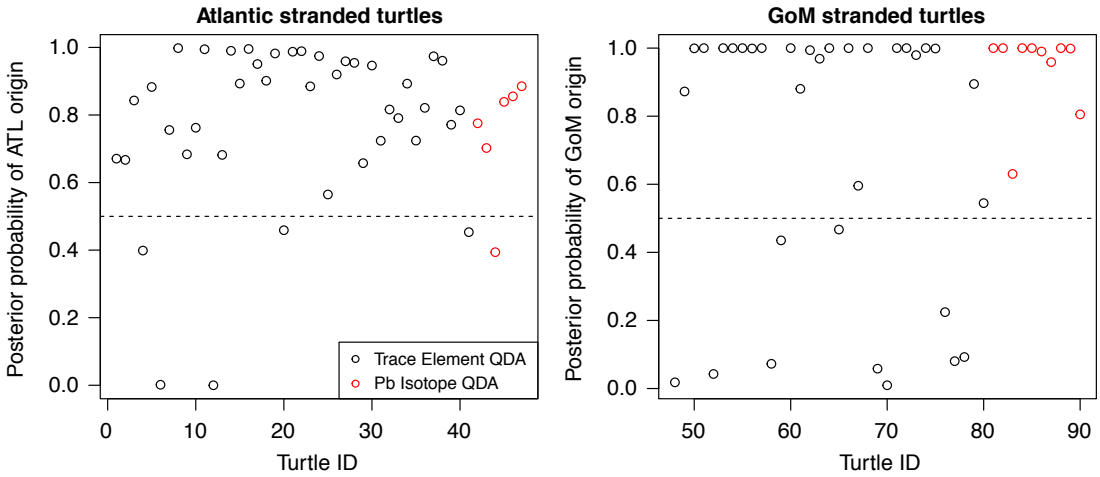

Figure 4.3. Posterior probabilities for regional assignments resulting from the reduced quadratic discriminant function models (black points = trace element $QDA_{reduced}$, red points = lead isotope $QDA_{reduced}$). Points that fall below the dashed line were mis-classified to the opposite region.

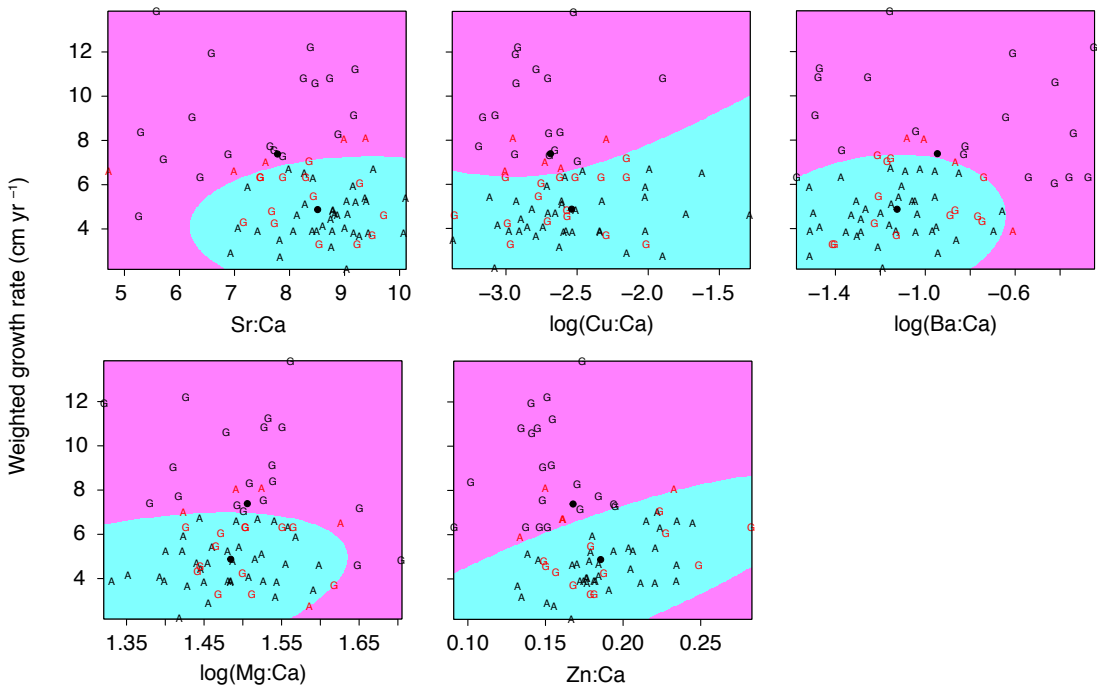

Figure 4.4. Partition plots showing the classifications of turtles to regions based on the reduced trace element QDA. Only variable combinations that include weighted growth rate, the variable that bests separated turtles by region, are displayed. Shaded regions delineate each classification area determined by the QDA (blue = Atlantic classification, pink = GoM classification). Letters indicate true region of stranding (A = Atlantic, G = GoM). Red font indicates incorrect classifications, black font indicates correct classifications.

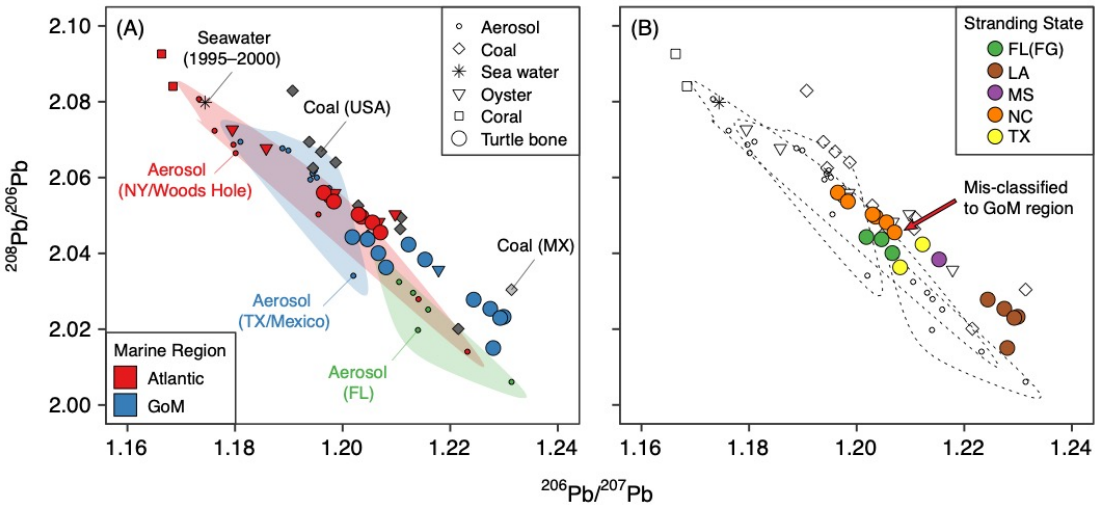

Figure 4.5. Biplots of $^{208}Pb/^{206}Pb$ and $^{206}Pb/^{207}Pb$ for Kemp's ridley sea turtles, potential Pb sources (aerosols, coal), and other animals (oyster, coral) sampled for Pb isotopes within the western North Atlantic Ocean and Gulf of Mexico (GoM). **(A)** Animal data by geographic region (Red = Atlantic, Blue = GoM). **(B)** Presented Kemp's ridley data by stranding state. Data sources: aerosols (shaded polygons; Bollhöfer & Rosman 2001, 2002, Soto-Jiménez et al. 2006), coal (Díaz-Somoano et al. 2009), seawater (Bermuda, 1995–2000; Kelly et al. 2009), Scleractinian coral (Kelly et al. 2009), Eastern oyster (Shiel et al. 2012).

CHAPTER 5: KEMP'S RIDLEY SEA TURTLE LIFE HISTORY VARIATION: DO ATLANTIC TURTLES MATTER?

Matthew D. Ramirez, Larisa Avens, Melissa Cook, Donna J. Shaver, and Selina S. Heppell

In preparation for submission to Endangered Species Research

Abstract

Intrapopulation variation in demographic rates strongly influence a species' population dynamics. These effects can be magnified in species with patchy distributions where overall population dynamics may be linked to variation in local processes. While the nesting distribution of Kemp's ridley sea turtles (*Lepidochelys kempii*) is restricted to the western Gulf of Mexico, juvenile life stages are geographically separated between Gulf of Mexico (GoM) and U.S. Atlantic Coast habitats. These subgroups are known to have different somatic growth rates, and habitat and fisheries impacts are thought to be very different between the two geographic areas. However, this life history complexity has yet to be integrated into population models. In this study, we use a spatially explicit, age-structured matrix population model to evaluate the relative contribution of Atlantic Kemp's ridley sea turtles to population growth and recovery during a period of rapid population growth (1990–2009). To parameterize this model, we performed novel analyses of sea turtle stranding data and growth rates estimated from stranded turtle humerus bones. We then evaluated the sensitivity of population growth and recovery time to changes in key transition probabilities that describe the movement of turtles among habitats and life stages within the western North Atlantic Ocean. GoM life stages had the highest elasticity values, indicating they had the strongest proportional contribution to population growth rates. Indeed, estimated population growth and recovery times were relatively insensitive to changes in the proportion of turtles entering Atlantic turtle life stages and the timing of Atlantic turtle recruitment to the GoM over the

period evaluated. Across all model simulations, population growth (measured as change in nest counts) differed by <1 % and recovery times (based on nesting female recovery criteria) varied by only four years. These models suggest Atlantic turtles make up < 5% of first-time nesters (neophytes) annually, even if the proportion of juveniles inhabiting the U.S. eastern seaboard is relatively large (e.g., 35%). Taken together, our results suggest that Atlantic turtles may not have strongly contributed to Kemp's ridley population growth during their recovery, even under the most extreme scenarios evaluated. However, the contribution of Atlantic Kemp's ridleys to population growth may be higher when population growth slows (i.e., since 2010) or when the population reaches carrying capacity. These results, if confirmed through additional independent analyses, may be important to future conservation and management planning for this critically endangered species.

Introduction

Accurate knowledge of demographic rates and the factors that influence them over appropriate spatiotemporal scales is central to the effective conservation and management of threatened and endangered species. Knowledge of intra-specific variability in demographic rates is particularly important for species with wide or patchy distributions where local effects have the potential to fundamentally alter a species' population trajectory or status depending on the structuring and connectivity of population subgroups (Runge et al. 2014). Such considerations are highly relevant for sea turtles, where individuals often display remarkable interannual fidelity to

specific foraging grounds and migratory routes despite having population-level distributions that span whole continental shelves or ocean basins (Avens et al. 2003, Broderick et al. 2007, Shaver et al. 2013, Tucker et al. 2014). Such life history variation has been linked to differences in a suite of demographics rates (e.g., growth, clutch size, remigration interval, etc.) in multiple sea turtle populations and species (e.g., Hawkes et al. 2006, Caut et al. 2008, Zbinden et al. 2011, Hatase et al. 2013). Integrating this life history variation into sea turtle demographic models to evaluate the relative contribution of geographically segregated population subgroups may be of high importance to conservation planning and risk assessments but is often hampered by insufficient habitat-specific vital rate data (Heppell et al. 2003b, National Research Council 2010).

Considering the effect of life history variation on population dynamics is particularly pertinent to the conservation of the critically endangered Kemp's ridley sea turtle (*Lepidochelys kempii*), whose juvenile population is segregated into Gulf of Mexico and U.S. Atlantic Coast subgroups that have different growth rates (NMFS et al. 2011, Avens et al. 2017). Following hatching from their primary nesting beaches in the western Gulf of Mexico, Kemp's ridleys enter a 1- to 3-year oceanic life stage before recruiting to neritic habitats in the GoM and U.S. Atlantic (Turtle Expert Working Group 2000). The precise number of Kemp's ridleys that inhabit the U.S. Atlantic Coast remains largely unknown but particle simulations suggest ocean currents may carry up to 30% of oceanic stage turtles to the U.S. Atlantic Coast annually (Putman et al. 2013). Importantly, multiple growth studies involving data

prior to the year 2000 have indicated that Atlantic Kemp's ridleys grow slower than GoM conspecifics (Caillouet et al. 1995, Zug et al. 1997, NMFS & USFWS 2015, Avens et al. 2017), with an interruption of growth occurring within the first 1–2 years of life (Chapter 2). Some Atlantic ridleys ultimately return to the GoM prior to maturation (reviewed in NMFS et al. 2011), but their contribution to population growth has yet to be evaluated.

The combination of a unique conservation history and certain life history features have led to the development of multiple Kemp's ridley population models over the past two decades (e.g., Heppell et al. 2004, NMFS & USFWS 2015, Gallaway et al. 2016, Kocmoud et al. 2019). Once comprising a population of over 40,000 nesting females in 1947 (>120,000 nests annually) (Carr 1963, Bevan et al. 2016), the population experienced a 99% decline throughout the 20th century to a low of ~300 nesting females in 1985 (702 nests) due to human activities (e.g., direct harvest of eggs and nesting females, poaching, fisheries activities; Turtle Expert Working Group 1998). The implementation of conservation measures to protect nests and increase in-water survival resulted in exponential population growth in the 1990s and 2000s before nest production began to fluctuate unpredictably beginning in 2010 (NMFS & USFWS 2015). The reasons for this change in population growth are not well understood but two primary hypotheses are negative impacts of the 2010 *Deepwater Horizon* oil spill on survival and/or density-dependent effects on demographic rates (NMFS & USFWS 2015, Shaver et al. 2016, Caillouet et al. 2018). As at least 85 % of annual nest production for the entire species occurs on only a ~60

km stretch of beach in Mexico (NMFS et al. 2011), nest protection has been a vital part of this species' conservation since 1966. In fact, from 1978 onwards, nearly all nests have been protected in a fenced corral or monitored *in-situ*, yielding an unprecedented record of nest and hatchling production for nearly an entire species that have served as vital input for population assessments.

Although multiple population models have been developed to evaluate Kemp's ridley population dynamics and predict time to recovery, none have included separate Atlantic and GoM life stages nor considered the importance of Atlantic ridleys to overall species population dynamics due to a lack of subgroup-specific vital rates. Survival rate estimates for juveniles have been based on a catch curve analysis of GoM strandings only (Turtle Expert Working Group 2000). The primary model used for Kemp's ridley status assessment is a deterministic age-structured matrix model fit to observed nests that was originally developed by Turtle Expert Working Group (1998) and subsequently updated with new hatchling production data to estimate time to recovery thresholds (Turtle Expert Working Group 2000, Heppell et al. 2004, NMFS et al. 2011, NMFS & USFWS 2015). Since 2010, additional models have been developed to identify possible impacts of the 2010 *Deepwater Horizon* oil spill and explore cause and effect scenarios to explain post-2009 fluctuations in nest counts (Crowder & Heppell 2011, Gallaway et al. 2016a b, Kocmoud et al. 2019). Given that a potentially significant portion of the Kemp's ridley population resides in habitats with divergent demographic rates, there is a need to evaluate the relative contribution of these subgroups to population growth and recovery.

Importantly, new sources of data allow for estimation of growth and transition probabilities for juveniles in both ocean regions, as well as new survival rate estimates using the large data set of stranded turtles from 1980 to 2016. Detailed ocean circulation models provide the first estimations of the proportion of turtles that recruit from oceanic to GoM vs. Atlantic neritic life stages (Putman et al. 2013). Similarly, stable isotope analyses of stranded turtle humerus bones can now be used to elucidate the timing of oceanic-to-neritic ontogenetic shifts (i.e., size, age) (Snover 2002, Ramirez et al. 2019). Recent skeletochronological analyses of turtle humeri also provide new data on age-specific maturation probabilities (Chapter 2, Avens et al. *in prep.*). Lastly, decades of stranding data collected through the Sea Turtle Stranding and Salvage Network (STSSN) provide a means of estimating Atlantic (and GoM) turtles survival rates over the past 20 years as well as transition probabilities for Atlantic turtles recruiting to the GoM through comparisons of size and age distributions.

The primary objective of this study was to evaluate the relative contribution of Atlantic Kemp's ridleys to overall species population growth rate during the species' pre-2010 recovery, measured as the deterministic growth rate of a spatially explicit, age-structured matrix population model. The model was parameterized to match the exponentially increasing index of nest counts from index beaches prior to 2009. To inform Atlantic Kemp's ridley parameters for this model we performed novel analyses of the STSSN dataset as well as new stable isotope analyses of humerus bones collected from dead stranded turtles in both the U.S. Atlantic and GoM. We

specifically evaluated the sensitivity of population growth and time to recovery to changes in transition probabilities for turtles into and out of U.S. Atlantic life stages. Given uncertainties in the mechanisms driving nest count fluctuations since 2010, and our objective of quantifying the relative rather than absolute contribution of Atlantic turtles to population growth, our analysis focuses on the time period 1966–2009.

Materials and Methods

Model Structure

Our spatially-explicit matrix population model extended the model used for the species' most recent population assessment to include separate Atlantic and GoM juvenile life stages with unique demographic rates and transition probabilities (Figure 5.1; NMFS & USFWS 2015). As in previous forms of this model, the Kemp's ridley life cycle was split into five life stages—oceanic juvenile, small neritic juvenile (Atlantic/GoM), large neritic juvenile (Atlantic/GoM), neophyte (first time nesting adult), adult—with separate survival rates applied to each age class and region derived from catch curve analyses and maximum likelihood estimation. The female only model uses annual time steps and is initiated each year (1966–2009) by the number of female hatchlings released from the species' primary nesting beaches in Mexico, which accounts for at least 85% of total hatchling production for the species (NMFS & USFWS 2015). Female hatchling numbers are based on fixed sex ratios of 0.76 for nests protected in corrals and 0.64 for the varying number of nests left *in-situ* annually on the nesting beach beginning in 2004 when corral capacity was reached

(NMFS et al. 2011). We assume an initial age distribution of 4800 adults and no juveniles based on observation of ~6000 nests in 1966 and intensive egg harvest through the 1950s and 1960s (Heppell et al. 2004); recorded hatchling production from 1966 to 2009 serves as annual cohort strength moving forward. The model uses maximum likelihood estimation to predict the number of nests laid by Kemp's ridley sea turtles on the index nesting beaches (Rancho Nuevo, Tepehuajes, Playa Dos) in Mexico from 1978 to 2009.

Within the model, turtles spend 1–2 years in the oceanic life stage before recruiting to the small neritic juvenile life stage in either the Atlantic or GoM compartments of the model. Transition probabilities from oceanic to small neritic juvenile life stages were derived from bone stable isotope analyses (% shift at age to Atlantic vs. GoM) and published estimates based on particle tracking experiments (total % to Atlantic vs. GoM) (see Ontogenetic Shift: Oceanic-to-Neritic Life Stages below). The small neritic juvenile life stage extends through age 5 and 7 for GoM and Atlantic turtles, respectively. These age classes were based on age- and size-specific shifts in mortality rates. The Atlantic small neritic juvenile life stage extends two years longer than the GoM small neritic juvenile life stage because Atlantic Kemp's ridleys require approximately two additional years to reach similar sizes as GoM conspecifics as a result of delayed growth early in life (L. Avens *in prep.*). Turtles then enter the large neritic juvenile life stages where they remain until maturity, which occurs at variable ages as described by maturation schedules generated from skeletochronological analyses (Avens et al. 2017). We explore multiple scenarios

regarding the recruitment of Atlantic turtles to the GoM (Ontogenetic Shift: Atlantic-to-GoM Neritic Life Stages below) but generally assume that Atlantic turtles recruit to the GoM prior to or at maturation and subsequently remain in the GoM for the remainder of their life. Reproductive rates remained the same as those used in the most recent population assessment and are summarized in Table 5.1 (NMFS & USFWS 2015).

Model Parameterization

Age at Maturation

Given variable growth rates among turtles (Snover et al. 2007b, Avens et al. 2017), age at maturation was represented by a logistic curve that allowed for variable maturation among individuals. Specifically, we used the logistic cumulative probability distribution function presented by Avens et al. (2017) derived from skeletochronological analyses of stranded Kemp's ridley humeri that predicted 50 % of GoM Kemp's ridleys matured by age 13.3 yr (α_{gom}). A similar maturation schedule is lacking for Atlantic Kemp's ridleys, but a growth curve fit to length at age estimates suggest that Atlantic turtles would reach a typical size at maturation about 2 years later than juveniles growing in the Gulf of Mexico (Avens et al. *in prep.*). Therefore, we applied the same logistic function used for GoM turtles to Atlantic turtles but shifted the distribution backwards by two years (i.e., α_{atl} = 50% mature at age 15.3 yr). This function predicts GoM turtles mature between age 6 and 21 and Atlantic turtles mature between age 8 and 23 (Equation 1).

$$Proportion\ mature\ = \frac{1}{1+\ e^{-0.64(age-\alpha)}} \quad (1)$$

Ontogenetic Shift: Oceanic-to-Neritic Life Stages

In order to separate Atlantic and GoM juvenile life stages it was necessary to estimate the proportion of turtles that ultimately recruit to either the U.S. Atlantic or GoM and as well as the ages at which this ontogenetic shift occurs. Using particle tracking experiments in combination with an ocean circulation model, Putman et al. (2013) predicted that between 0 and 28.4 % (mean = 14.78 %) of particles were transported East of the Florida Peninsula after two years. We therefore used 15 % as our base scenario for the proportion of oceanic stage turtles that recruit to Atlantic (15 %) versus GoM (85 %) small neritic juvenile life stages.

All Kemp's ridley population models to date have assumed a fixed, 2-year oceanic stage duration (Heppell et al. 2004, Gallaway et al. 2016a, Kocmoud et al. 2019). However, the Kemp's ridley oceanic life stage can last between 1 and 3 years (Zug et al. 1997, Turtle Expert Working Group 2000). Given this variability we sought to empirically estimate the proportion of turtles that complete this ontogenetic shift at a given age to introduce greater biological realism to our model. To this end we expanded the work of Ramirez et al. (2019) to sequentially sample the humerus bone growth layers of a total of 91 Kemp's ridleys that stranded along the U.S. Atlantic (n = 43) and Gulf (n = 48) Coasts for stable nitrogen isotope ($\delta^{15}N$) ratios. $\delta^{15}N$ values differ between oceanic and neritic habitats occupied by this species and

can thereby be used to identify the age at which turtles migrate between these areas through sequential sampling of humerus bone growth layers (Snover 2002, Ramirez et al. 2019, Bean & Logan 2019) (see Chapter 3 for full methodological details).

This analysis revealed that the timing of the oceanic-to-neritic ontogenetic shift differed for turtles that stranded in the GoM versus Atlantic (Table 5.2). For GoM stranded turtles, 74% of turtles recruited to neritic habitats at age 1, whereas 22% recruited at age 2—three turtles recruited to neritic habitats at age 3. In contrast, 40 % of Atlantic stranded turtles recruited to neritic habitats at age 1, 46 % at age 2, and 13 % at age 3. Based on these results, for our model we assumed that 75 % of GoM turtles transitioned to the small neritic juvenile life stage at age 1 and 15 % at age 2. For Atlantic turtles, we assumed 50 % of turtles transitioned to the small neritic juvenile life stage at age 1 and 50 % at age 2.

Ontogenetic Shift: Atlantic-to-GoM Neritic Life Stages

Although tagging studies have revealed that Atlantic Kemp's ridleys return to the GoM to reproduce (Schmid 1995, Chaloupka & Zug 1997, Schmid & Witzell 1997, Turtle Expert Working Group 1998, NMFS et al. 2011), our understanding of this transition is poor. To evaluate the potential timing of this transition we analyzed and compared the length frequency distributions of Kemp's ridleys stranded in the Atlantic and GoM obtained through the Sea Turtle Stranding and Salvage Network between 1980 and 2016. We also compared stranding age distributions by converting

stranding size to age using habitat-specific von Bertalanffy growth functions (Avens et al. *in prep.*).

Examination of these distributions revealed strong differences in the size and age structure between Atlantic and GoM Kemp's ridleys (Figure 5.2). Specifically, turtles tended to accumulate in the larger size classes (> 50 cm straightline carapace length, SCL) and older age classes (> 6 yr) in the GoM resulting in a distinct hump in the size distribution centered at ~60 cm SCL, near the mean size at sexual maturity for this species (61–65 cm SCL; Avens et al. 2017). This accumulation is consistent with the slowing and cessation of growth as turtles approach maturation as a larger range of ages will be reflected in a smaller range of sizes, leading to a distinct hump in the size distribution. In contrast, counts of Atlantic turtles declined continuously from a peak at ~30 cm SCL. The lack of a similar a hump in the Atlantic Kemp's ridley size distribution suggests that these turtles are either dying off before maturation, are leaving the U.S. Atlantic Coast, or both. Given the observation of tagged Atlantic turtles in the GoM as mature adults we assume Atlantic Kemp's ridleys ultimately recruit back to the GoM prior to maturation. As the divergences in the Atlantic and GoM size and age distribution begin at ~ 6 years of age (Figure 5.2), for our model we assume that Atlantic Kemp's ridleys begin to transition to GoM habitats at age 7. Interestingly, this estimate aligns with the hypothesis of Chaloupka & Zug (1997) that a growth spurt at ~8 years of age was indicative of an ontogenetic shift from Atlantic to GoM foraging habitats.

As the specific rate at which Atlantic Kemp's ridleys recruit to the GoM is unknown, we implemented two models that relied on different cumulative probability distribution functions (CDF; Figure D1) to describe this ontogenetic shift as well as a third model that assumes that no Atlantic turtles recruit back to the GoM.

Model 1 (base model; maturation transition): Atlantic Kemp's ridleys transition to the GoM at maturation following the logistic maturation schedule (Equation 1) which assumes 50 % of Atlantic turtles mature at 15.3 yrs old (tails range from 8 to 23 yrs).

Model 2 (pre-maturation transition): Atlantic Kemp's ridleys transition to the GoM at age 7 with the proportion migrating to the GoM increasing exponentially until age 23, after which all Atlantic turtles mature as dictated by the maturation ogive. When turtles recruit to the GoM they assume GoM survival rates but retain the Atlantic turtle maturation schedule. The shape of this distribution was determined by fitting an exponential model to the declining side of the Atlantic Kemp's ridley age distribution beginning at age 7 (Figure 5.2; Equation 2).

$$Proportion\ to\ GoM = 1 - e^{-0.29(age-6)} \tag{2}$$

Model 3 (no transition): Atlantic Kemp's ridleys do not recruit back to the GoM. This model was implemented to compare our results against historical assumptions that Atlantic turtles are lost to the breeding population.

Juvenile Survival Rates

Survival rates for all juvenile life stages were estimated either empirically using catch curve analyses of stranding data or through maximum likelihood estimation. When data on age-specific abundance is available, such as fish catch or sea turtle strandings, mortality rates can be estimated from the sequential decline in counts by age. Given that juvenile survival rates have not been measured for Kemp's ridley sea turtles, we used stranding length frequency data collected through the Sea Turtle Stranding and Salvage Network since 1980 to estimate survival rates for small neritic (GoM, Atlantic) and large neritic (GoM) juvenile life stages. Catch curve analyses assume constant recruitment and mortality through time. As these assumptions are violated for Kemp's ridleys due to increasing nest counts through time and the implementation of turtle excluder devices (TED) in trawl fisheries in the 1980s and 1990s (Turtle Expert Working Group 2000, Heppell et al. 2007), we used a cohort-based approach to generate our catch curves.

Following Turtle Expert Working Group (2000), we first re-indexed stranding data from calendar year (January 1 year i to December 31 year i) to ridley year (July 1 year i to June 30 year $i+1$). We then used habitat-specific growth curves to estimate an age and cohort for each turtle. To account for variable effort, a weighting factor was estimated for each year as the ratio of stranding counts in year x divided by stranding counts in 1991, the year with the lowest strandings. Each stranding observation was then transformed by dividing by this weighting factor (i.e., individual turtles stranding in years other than 1991were reflected as numbers less than 1).

Separate weighting factors were generated for turtles that stranded in the GoM and Atlantic, and stranding data from Mississippi and Alabama were excluded from this analysis given that stranding response effort in these states was not standardized until 2010 (Figure D2).

A catch curve was then generated for each cohort by summing weighted observations for each age, log transforming these values, and fitting a regression line through ages 2–5 and 6–9 for GoM turtles and ages 2–7 for Atlantic turtles. Catch curves were not implemented for age 0–1 and 8+ (for Atlantic turtles) because they were not fully represented in the stranding dataset. Cohort-specific estimates of instantaneous mortality (Z) and annual mortality ($A = 1 - e^{-Z}$) were then estimated from the slopes of the regression lines and then visually examined to identify temporal trends (Figure D3).

Within the GoM, mortality rates shown by the Z slopes were higher for the 1980 to 1988 cohorts than those in subsequent cohorts (Figure D3). We therefore combined weighted observations across all cohorts within each of these time periods (1980–1988, 1992+) and re-ran the catch curve analyses to generate final mortality and survival rate ($S = 1 - A$) estimates for small (2–5) and large (6–9) neritic juveniles in the GoM (Figure 5.3). Our pre-1990 annual Z estimates (0.3–1.2) are higher than those reported by NMFS et al. (2011) (0.3–0.6) because our catch curves include ages 2–5 rather than 2–6, but separate catch curves on the age 2–6 data yielded a similar range to previous analyses of these data (0.3–0.9). In the Atlantic, mortality rates were variable but showed no distinct trends through time. We therefore collapsed

weighted observations across all cohorts (1980–2010) to generate a final survival rate estimate for small neritic juveniles (2–7) in the Atlantic.

Survival rates for oceanic juveniles, large neritic juveniles (Atlantic), and adults were estimated using negative log-likelihood estimation (Equation 3):

$$NLL = \ln(\sigma) + \Sigma \frac{(obs-pred)^2}{2\sigma^2} \quad (3)$$

where *obs* and *pred* are the observed and predicted number of nests for each year beginning in 1978 when nest counts were standardized. Fitted parameters were bounded between 0.1 and 0.6 for oceanic juveniles and 0.65 and 0.95 for large neritic juveniles and adults as in NMFS et al. (2015). We included two additional constraints in our model fitting: (1) within each life stage, survival rates cannot decrease through time (i.e., 1966–1988 ≤ 1989–2004 ≤ 2005–2009); and, (2) within each time period, survival rates cannot decrease with age (i.e., small juvenile ≤ large juvenile ≤ adult). This model fitting procedure was implemented separately for each of the three models.

Previous population models for this species have required one or more shifts in mortality in 1989/1990 and the late 1990s to achieve reasonable fits to the nesting data (Heppell et al. 2004, NMFS et al. 2011, Gallaway et al. 2016a, Kocmoud et al. 2019). We evaluated model fit across a range of mortality shift scenarios and the best fit (lowest NLL) was achieved with mortality shifts in 1989 and 2005 for neritic life stages—oceanic juvenile survival was assumed to remain constant through time.

These breakpoints were optimal in all three models evaluated and align with known shifts in anthropogenic mortality rates, which are overwhelmingly driven by interactions with shrimp trawl fisheries (Finkbeiner et al. 2011). Specifically, the federal requirement of turtle excluder devices (TEDs) in U.S. trawl fisheries came into effect in 1989 and a sharp reduction in shrimp fishing effort occurred within the GoM in the early 2000s (Jenkins 2012, Gallaway et al. 2016b). There was additionally an acceleration in nest production around 2005 (NMFS & USFWS 2015).

Model Implementation, Evaluation, and Projection

Elasticity analysis was used to evaluate the sensitivity of asymptotic population growth rate (λ) of each model to proportional changes in habitat-specific survival and fertility (reproductive output). Elasticity is also a measure of the relative contribution of different life stages and vital rates to λ (Heppell 1998, Caswell 2001). Elasticities were summed across relevant ages for each life stage to generate cumulative elasticities (e.g., GoM small neritic juvenile survival elasticity = sum age 2–5 elasticity values). We also evaluated the sensitivity of population growth rate (as reflected by predicted nest count; λ_{nest}) to changes in the proportion of turtles that recruit from oceanic to GoM vs. Atlantic neritic habitats annually. Separate analyses were performed for each model, which included different functions describing the recruitment of neritic Atlantic turtles to neritic GoM habitats. For each sensitivity

analysis, the proportion of oceanic turtles recruiting to Atlantic habitats annually was varied from 5 to 35 %, with 15% representing the base scenario.

To illustrate the sensitivity of long-term recovery to varying assumptions regarding the recruitment of Kemp's ridleys among oceanic and neritic habitats, we used each of the three models evaluated to project the Kemp's ridley population forward in time from 2009 to 2030 and estimate recovery times based on the pre-2010 demographic rates. I specifically estimated time to reaching annual nesting female count criteria using the scenarios assessed in the sensitivity analyses. Downlisting criteria under the Endangered Species Act are 10,000 nesting females per season at the index nesting beaches (Rancho Nuevo, Tepehuajes, Playa Dos) in Mexico and de-listing criteria are a 6-year average of 40,000 nesting females per season across all nesting beaches (NMFS et al. 2011). This exercise was not intended to quantitively forecast population growth and recovery as my projections specifically assumed that demographic rates from 2005 to 2009 remain constant through 2030, with the exception of total egg survival and hatchling sex ratios. As in NMFS et al. (2011), corral capacity was set at 14,500 nests. Given that corral and *in-situ* nests have unique demographic rates, effective egg survival and hatchling sex ratios will vary as the proportion of nests left *in-situ* on the nesting beaches increase through time (Heppell et al. 2004).

Results

Juvenile Survival Rates

Using cohort-specific catch curve analyses (Figure 5.3), we estimated annual survival rates were 0.522 and 0.669 for GoM small neritic juveniles (ages 2–5) for the 1980–1988 and 1992–2011 cohorts, respectively, which were subsequently applied to the 1996–1989 and 1990–2009 time periods in all models. The survival rate estimated and applied for GoM large neritic juveniles (ages 6+) for the 1990–2009 time period was 0.669—insufficient data allowed for derivation of estimates for the 1966–1989 time period. For Atlantic small neritic juveniles (age 2–7), we estimated a constant annual survival rate of 0.651. Given the lack of distinct temporal shifts in mortality this estimate was applied to all time periods (Figure D3).

Best fit survival rate estimates for all remaining life stages—oceanic juvenile (ages 0–1), large neritic juvenile (1966–1988), and adult—are presented in Table 5.3. Estimates were relatively invariant among the three models evaluated, with estimated oceanic juvenile survival ranging between 0.318 and 0.325 and GoM large neritic juvenile survival (1966–1988) ranging between 0.774 and 0.788. Patterns of adult mortality were identical across all three models. Within the best fit models, Atlantic large neritic juvenile survival was estimated to equal small neritic juvenile survival rates (0.651) in all cases but Model 1 where during the 2005–2009 time period they were estimated to equal adult survival rates.

Elasticity and Sensitivity Analyses

Elasticity analyses revealed that GoM small neritic juvenile survival had the largest proportional effect on asymptotic population growth followed by large neritic

juvenile survival, adult survival, and fertility (Figure 5.4A). GoM neritic juvenile survival elasticities remained relatively high until age 7 when they began to decline until maturity. Relative to the survival rates of the more abundant GoM turtles, Atlantic and oceanic juvenile survival rates had little influence on population growth rate (Figure 5.4A). The lower Atlantic turtle elasticities are likely due to the fact that few Atlantic Kemp's ridleys are ultimately predicted to survive to maturity and join the reproductive population (Figure 5.5). For example, Models 1 (maturation transition) and 2 (pre-maturation transition) predict that only 3–4% of all neophytes in 2009 once inhabited the U.S. Atlantic Coast under the base scenario of 15 % of oceanic juvenile recruiting to the Atlantic annually. This is likely driven by the reduced survivorship to maturity for Atlantic turtles in our models (Table 5.3). Indeed, even if 35 % of oceanic juveniles recruited to the Atlantic annually, our models predict they would contribute only 7–10% of new nesters.

Sensitivity analyses revealed little effect of the proportion of turtles entering or leaving the Atlantic on population growth rates (λ_{nest}), as expected given the results of the elasticity analyses. Although the absolute percent change in nest count increased or decreased by ~10 % with every 10% change in the proportion of oceanic turtles that recruit to the Atlantic (Figure 5.6), there was ultimately less than a 1% change in rate of nest production through time (Figure 5.7). These patterns were consistent across all models that included different Atlantic-to-GoM transition probabilities (Figures 5.6, D4). For models that varied the proportion of turtles that entered the Atlantic from 5 to 35 % annually, the average 2005–2009 rate of nest

count increase ranged between 20.42 and 21.26 % (Model 1: maturation transition), 19.93 and 20.25 % (Model 2: pre-maturation transition), and 20.33 and 20.34 % (Model 3: no transition).

Population Projections

Given the minimal effect of variable ontogenetic shifts on population growth, estimated recovery times varied little among the scenarios evaluated (Figure 5.8.). For both Model 1 and 2, which assume some Atlantic ridleys recruit to the GoM prior to or at maturation, increasing the proportion of turtles recruiting to the Atlantic from 5 to 35 % annually resulted in only a one year delay in reaching the annual nesting female downlisting threshold (2011 to 2012) and a two (2021 to 2023) or three year (2021 to 2024) delay in reaching the delisting threshold under the pre-2010 scenario of exponentially increasing nest numbers. Results for Model 3, which assumed no Atlantic turtles return to the GoM, were largely the same with the changes in the proportion of turtles recruiting to the Atlantic resulting in a three year delay in reaching both the annual nesting female downlisting (2010 to 2013) and delisting criteria (2021 to 2024).

Discussion

Using a spatially explicit, age-structured matrix population model, we present the first quantitative assessment of the contribution of Atlantic Kemp's ridleys to species population growth. This simulation model was developed to explore multiple

ecological scenarios and their potential effect on population growth and recovery time during a period of exponential population growth (1990–2009) and was not intended to accurately predict or project true population size. We therefore recommend caution when interpreting our results as baseline demographic rates, particularly model-derived survival rates, should not be assumed to be accurate. Nevertheless, our analysis suggests that Atlantic turtles may not have contributed substantially to Kemp's ridley population growth during the pre-2010 population recovery, when the population growth rate was the highest. In this model, the proportional contribution of Atlantic juveniles is much lower than GoM juveniles, even if Atlantic turtles return to the GoM as large juveniles, well in advance of maturity, or if upwards of a third of the population recruits to U.S. Atlantic Coast habitats following the oceanic life stage. However, these dynamics may change under different scenarios, particularly when population growth rates stabilize or are substantially lower than the near exponential growth occurring in the early 2000s. Importantly, this analysis indicates that small changes in the survival of GoM turtles is likely to have a much greater effect on population growth than a similar change in Atlantic turtles (Heppell 1998).

We performed multiple simulations to examine the sensitivity of population growth rate and recovery time to the proportion and timing of turtles entering and leaving the U.S. Atlantic annually. Our results suggest that even under the most extreme scenarios, few Atlantic Kemp's ridleys (<5 %) ultimately survive and return to the GoM to join the reproductive population and thereby contribute little to population growth relative to those growing up in the GoM. This largely aligns with

the long-standing presumption that females nesting in the western GoM are almost entirely composed of turtles that did not spend time in the Atlantic (Caillouet et al. 2015). Indeed, given the low elasticities for Atlantic turtle life stages, population growth in our models is driven almost entirely by GoM turtle dynamics. This is particularly evident in comparisons of oceanic and GoM life stage survival rates estimated through model fitting, which vary little among the three fitted models evaluate (i.e., large changes in the Atlantic-to-GoM recruitment function can be compensated by very small changes in GoM survival rates). As a result, estimated time to meeting nesting female recovery criteria, based on population projections from 2009 onwards (i.e., excluding post-2010 effects), vary by a maximum of four years among all models evaluated (downlisting: 2010–2013; delisting: 2021–2024). These results match anticipated recovery times prior to the post-2010 nesting setback, which expected Kemp's ridleys would meet downlisting criteria by 2011 and delisting criteria by 2024 (NMFS et al. 2011).

Although our models suggest Kemp's ridley population growth is relatively insensitive to Atlantic turtle demographic rates, this conclusion is entirely predicated on our model configuration being an accurate representation of true population dynamics during the period of population recovery, from the mid 1990s through 2009. As with all previous Kemp's ridley population models, key uncertainties remain regarding many of the demographic rates included herein. Critical uncertainties also persist regarding Atlantic Kemp's ridley ontogenetic shifts and maturation. We provide new estimates of Kemp's ridley oceanic-to-neritic transition

probabilities and shed additional light on the value of particle tracking within ocean circulation models for sea turtle conservation and management. However, given the apparent variability in recruitment of Kemp's ridleys to the U.S. Atlantic (Putman et al. 2013), additional research is needed to more precisely estimate the proportion of turtles recruiting to U.S. Atlantic habitats over inter-annual time scales and to validate results of these particle simulation models. Additional description of the Atlantic-to-GoM ontogenetic shift would also improve future population models and may be possible with future research on isotope signatures in bone growth layers (Chapter 4).

While characterizing these transitions will be no small task given the apparent low number of turtles that return to the GoM, new insights may be attained through the implementation of largescale, collaborative tagging studies or geochemical analyses of stranded turtle bone tissue in the GoM (i.e., extend Chapter 4 analyses). Such studies would also be key to quantifying size and age at maturation for Atlantic Kemp's ridleys, which is currently unknown. We assumed that Atlantic Kemp's ridleys matured at similar sizes as GoM Kemp's ridleys and did not exhibit compensatory growth (Snover et al. 2007b). However, recent studies suggest sea turtle size at sexual maturity is not genetically fixed and that intrapopulation variation in these parameters is primarily driven by individual somatic growth rates and not post-maturation growth (Bjorndal et al. 2013a, 2014, Omeyer et al. 2018). It is thus conceivable that Atlantic Kemp's ridleys simply mature at smaller size or ages than GoM conspecifics.

In-water survival rates have been and continue to be the most pressing data needed to inform sea turtle demographic models (Heppell et al. 2004, National Research Council 2010). We provide novel analyses of stranding data that add important new survival rate information for GoM and Atlantic small neritic juvenile and GoM large juvenile life stages. However, these data are imperfect as sea turtle strandings are influenced by many environmental (e.g., temperature, wind, currents, distance to coastline) and anthropogenic (e.g., fishing effort, TED compliance) factors that vary across space and time (Epperly et al. 1996, Hart et al. 2006, Nero et al. 2013, Santos et al. 2018). Better survival rate data are particularly needed for large neritic Atlantic Kemp's ridley juveniles as best fit estimates herein for this life stage tended to settle on the bounds we placed on this parameter. Given the low elasticity for Atlantic turtle survival rates, any number of parameter combinations generated through model fitting could ultimately yield reasonable fits to the nesting data. Therefore, our study further highlights the need for additional research on sea turtle survival rates (Pfaller et al. 2018), but particularly for Kemp's ridley sea turtles.

Given the conservation status of this species there is considerable interest in understanding mechanisms underpinning the nesting changes that have occurred since 2010 and most recent population models have been narrowly focused on this topic (Crowder & Heppell 2011, NMFS & USFWS 2015, Gallaway et al. 2016b, Kocmoud et al. 2019). These models are in agreement that a significant mortality event must have occurred in 2010, possibly linked to the *Deepwater Horizon* (DWH*)* oil spill. However, the population has not rebounded as expected under "pulse" perturbation

scenarios prompting speculation that DWH effects may persist (i.e., “press” perturbation; Crowder & Heppell 2011) or that a combination of factors may be influencing demographic rates (e.g., shift in age structure, Caillouet 2014; density dependent changes in remigration interval, Gallaway et al. 2016b, Shaver et al. 2016, Kocmoud et al. 2019; decline in GoM carrying capacity, Caillouet et al. 2018). While our model was not designed to examine this issue, it does suggest that Atlantic Kemp’s ridleys are likely not currently an important part of this story and would not be able to “rescue” the population from extinction should deleterious effects in the GoM persist or worsen (Hufbauer et al. 2015).

As Atlantic and GoM Kemp’s ridleys face distinct threats and stressors (Lewison et al. 2014, Hart et al. 2018a), future investigations into the role of Atlantic turtles in shaping the species’ population dynamics would benefit from additional study of regional difference in demographic rates. For example, we know that somatic growth rates differ between these population subgroups (Caillouet et al. 1995, Zug et al. 1997, NMFS & USFWS 2015, Avens et al. 2017, Chapter 2), but casual factors and their potential effect on other demographic rates remain unknown. Additionally, it has been hypothesized that the carrying capacity of the GoM has been reached and that density-dependent factors may be affecting adult female re-nesting intervals (Gallaway et al. 2016b, Caillouet et al. 2018, Kocmoud et al. 2019). However, density dependent effects would be expected to vary spatiotemporally and manifest in other demographics rates (e.g., growth, survival, clutch frequency, etc.; Chapter 2). Notably, Atlantic Kemp’s ridleys co-occur with a large loggerhead turtle (*Caretta*

caretta) population. Although limited tracking data suggests loggerheads and Kemp's ridleys may partition habitats in the Chesapeake Bay (Byles 1988), much still remains unknown regarding the extent to which they compete for resources. Enhanced inter-specific competition, combined with more variable environmental conditions (e.g., water temperature) and interactions with regionally variable fisheries, could lead to divergent demographic rates.

Understanding how life history variation influences demographic rates and population dynamics is critical to conserving highly mobile, patchily distributed species (Runge et al. 2014), especially critically endangered species such as the Kemp's ridley sea turtle (Wibbels & Bevan 2019). Through the development of a spatially explicit, age-structured matrix population model, we simulated regional Kemp's ridley population dynamics during the species' pre-2010 population recovery. Our results suggest Atlantic turtles contributed little to overall population growth and recovery during this time period. Nevertheless, many uncertainties in key demographic rates prevent precise estimation of current and future population size, so our results only outline the potential relative contribution of Atlantic versus GoM turtles to population growth. While primarily qualitative, these results may be important to the development of future conservation and management plans for this species, which faces a suite of threats that vary spatiotemporally that continue to threaten their recovery (Bjorndal et al. 2011).

Acknowledgements

This publication was made possible by the National Oceanic and Atmospheric Administration, Office of Education Educational Partnership Program award number (NA16SEC4810007). Its contents are solely the responsibility of the award recipient and do not necessarily represent the official views of the U.S. Department of Commerce, National Oceanic and Atmospheric Administration. We thank the participants of the Sea Turtle Stranding and Salvage Network (STSSN) whose tireless work over the past 40 years allowed for parameterization of key components of this model. We also that the state and federal coordinators of the STSSN for their permission to use the stranding data in this analysis. We also extend special thanks to J. Moore, K. A. Curtis, T. Eguchi, and J. Seminoff for their input during the development of this model, and J. Miller, A. Shiel, and J. McKay for input on this manuscript.

Table 5.1. Summary of input parameter used across all models.

Parameter	Value	Source
Reproduction		
Clutch frequency	2.5 nests/yr	NMFS et al. (2011)
Clutch size	97 eggs	NMFS et al. (2011)
Sex ratio (corral)	0.76	NMFS et al. (2011)
Sex ratio (*in-situ*)	0.64	NMFS et al. (2011)
Egg survival (corral)	0.678	NMFS et al. (2011)
Egg survival (*in-situ*)	0.50	NMFS et al. (2011)
Breeding probability	0.50	NMFS et al. (2011)
Corral capacity	14500 nests	NMFS et al. (2011)
Maturation		
GoM age at 50% maturity (min, max)	13.3 yr (6 – 21)	Avens et al. (2017)
ATL age at 50% maturity (min, max)	15.3 yr (8 – 23)	This study*
Ontogenetic Shifts		
Proportion to GoM	0.85	Putman et al. (2013)
Proportion to ATL	0.15	Putman et al. (2013)
Proportion to GoM at age 1	0.80	This study
Proportion to GoM at age 2	0.20	This study
Proportion to ATL at age 1	0.50	This study
Proportion to ATL at age 2	0.50	This study

*Assumes 2 years delay in maturation relative to GoM Kemp's ridleys given differences in growth patterns between regions.

Table 5.2. Age at oceanic-to-neritic habitat shift by stranding region based on bone $\delta^{15}N$ values (‰) [mean ± SD (sample size)].

Shift age	n	Pre-shift $\delta^{15}N$ (‰)	Post-shift $\delta^{15}N$ (‰)	Proportion of turtles (%)
Gulf of Mexico stranded turtles				
0.75	56	9.65 ± 0.58 (18)	12.93 ± 1.85 (56)	74
1.75	17	9.41 ± 0.57 (16)	12.66 ± 2.69 (12)	22
2.75	3	9.62 ± 0.48 (3)	14.61 ± 0.27 (2)	4
Atlantic stranded turtles				
0.75	21	9.42 ± 0.61 (12)	12.47 ± 1.84 (20)	40
1.75	24	9.64 ± 0.50 (25)	13.18 ± 1.57 (24)	46
2.75	7	9.14 ± 0.56 (5)	13.79 ± 1.91 (5)	13

Table 5.3. Summary of survival rate estimates generated through catch curve analyses of stranding data (non-bolded values) or maximum likelihood estimation (bolded values) for the three models evaluated. Model predicted nest counts were fit to observed nests on three index nesting beaches for the years 1966–2009.

	1966–1988	1989–2004	2005–2009
Model 1 (base model): Atlantic turtles shift to GoM at maturation (logistic function)			
Oceanic juv (ages 0–1)	**0.318**	**0.318**	**0.318**
GOM small neritic juv (ages 1–5)	0.522	0.669	0.669
GOM large neritic juv (ages 6+)	**0.780**	0.826	0.826
ATL small neritic juv (ages 1–7)	0.651	0.651	0.651
ATL large neritic juv (ages 8+)	**0.651**	**0.651**	**0.950**
Adult	**0.843**	**0.843**	**0.950**
NLL	–32.347		
CV	0.088		
Model 2: Atlantic turtles shift to GoM at age 7 (exponential function)			
Oceanic juv (ages 0–1)	**0.311**	**0.311**	**0.311**
GOM small neritic juv (ages 1–5)	0.522	0.669	0.669
GOM large neritic juv (ages 6+)	**0.774**	0.826	0.826
ATL small neritic juv (ages 1–7)	0.651	0.651	0.651
ATL large neritic juv (ages 8+)	**0.651**	**0.651**	**0.651**
Adult	**0.844**	**0.844**	**0.950**
NLL	–31.767		
CV	0.090		
Model 3: No Atlantic turtles shift to GoM			
Oceanic juv (ages 0–1)	**0.325**	**0.325**	**0.325**
GOM small neritic juv (ages 1–5)	0.522	0.669	0.669
GOM large neritic juv (ages 6+)	**0.788**	0.826	0.826
ATL small neritic juv (ages 1–7)	—	—	—
ATL large neritic juv (ages 8+)	—	—	—
Adult	**0.843**	**0.843**	**0.950**
NLL	–32.398		
CV	0.088		

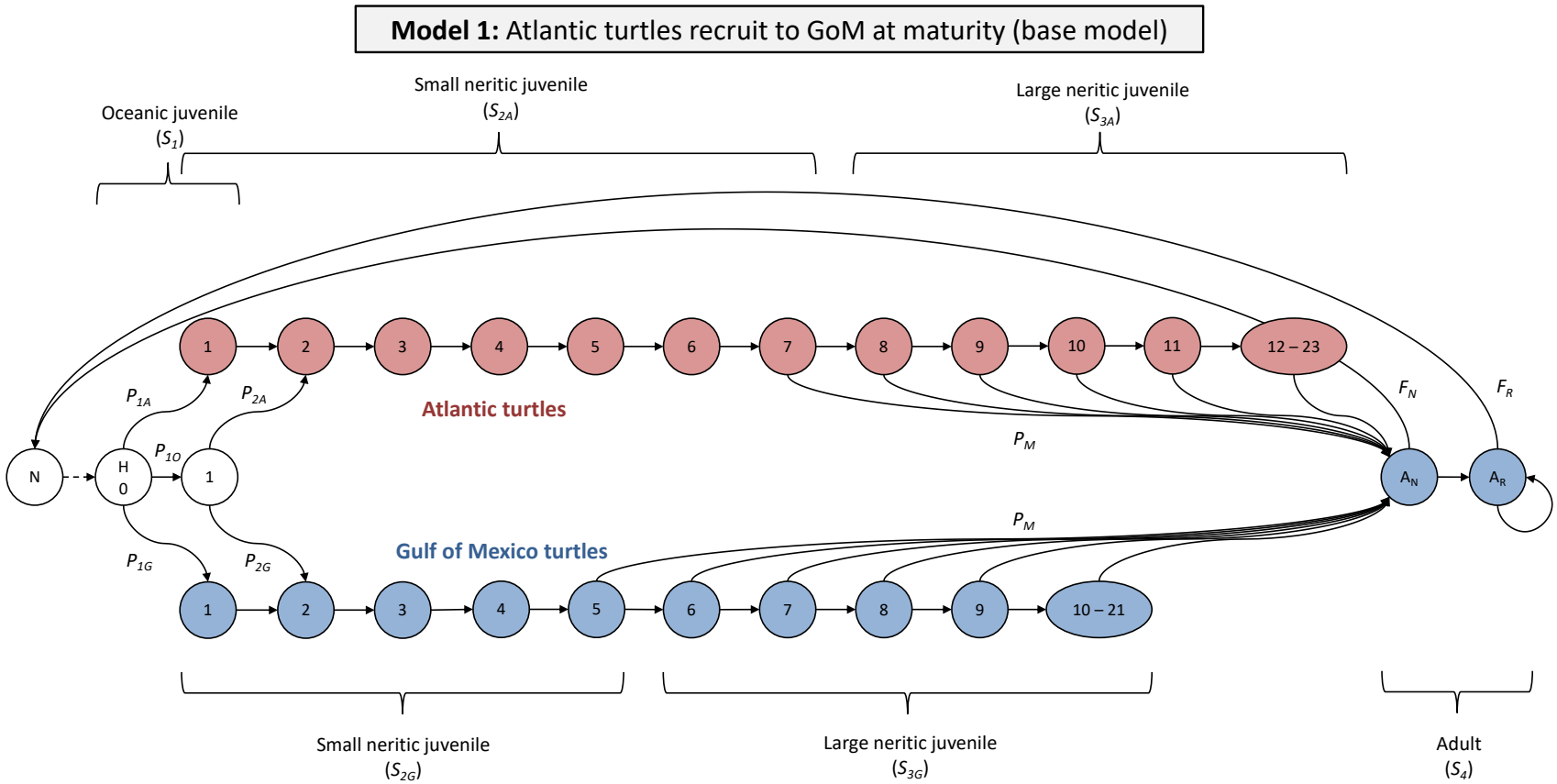

Figure 5.1. Conceptual diagram of base spatially explicit, age structured matrix population model.

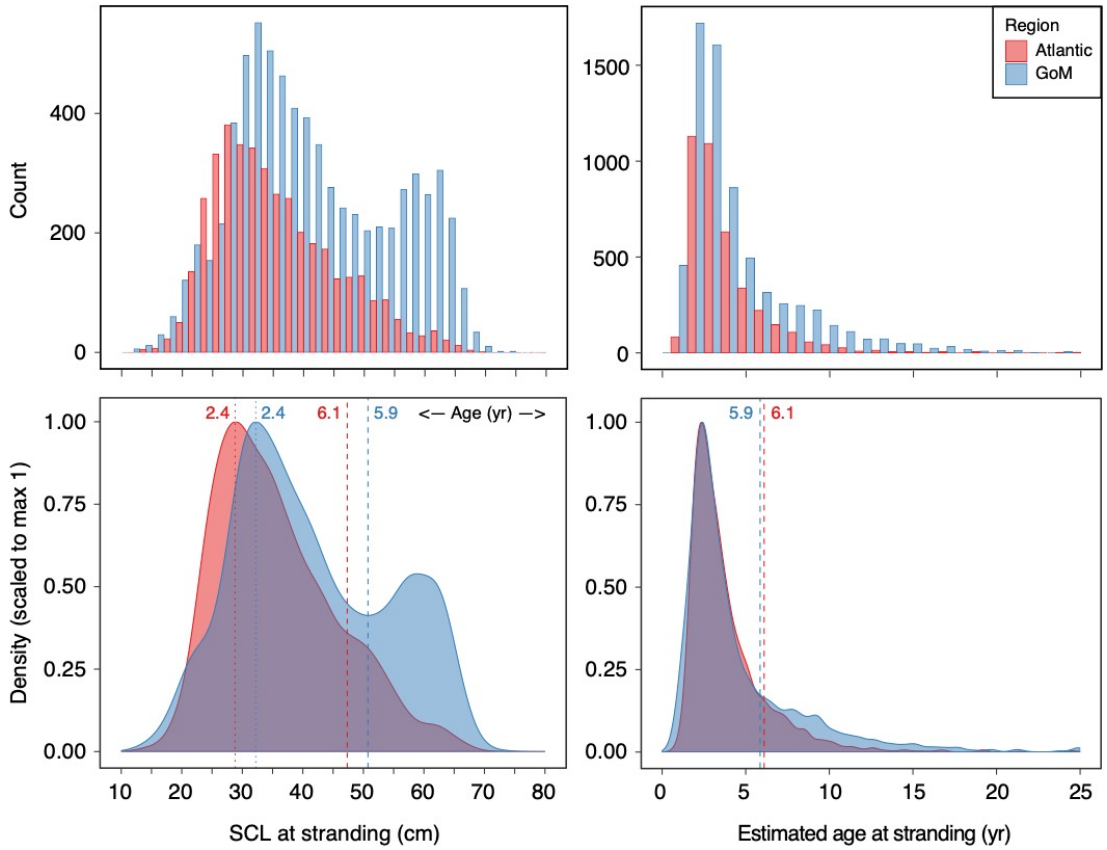

Figure 5.2. Summary of sizes (straightline carapace length, SCL) and ages of stranded Kemp's ridley sea turtles by region.

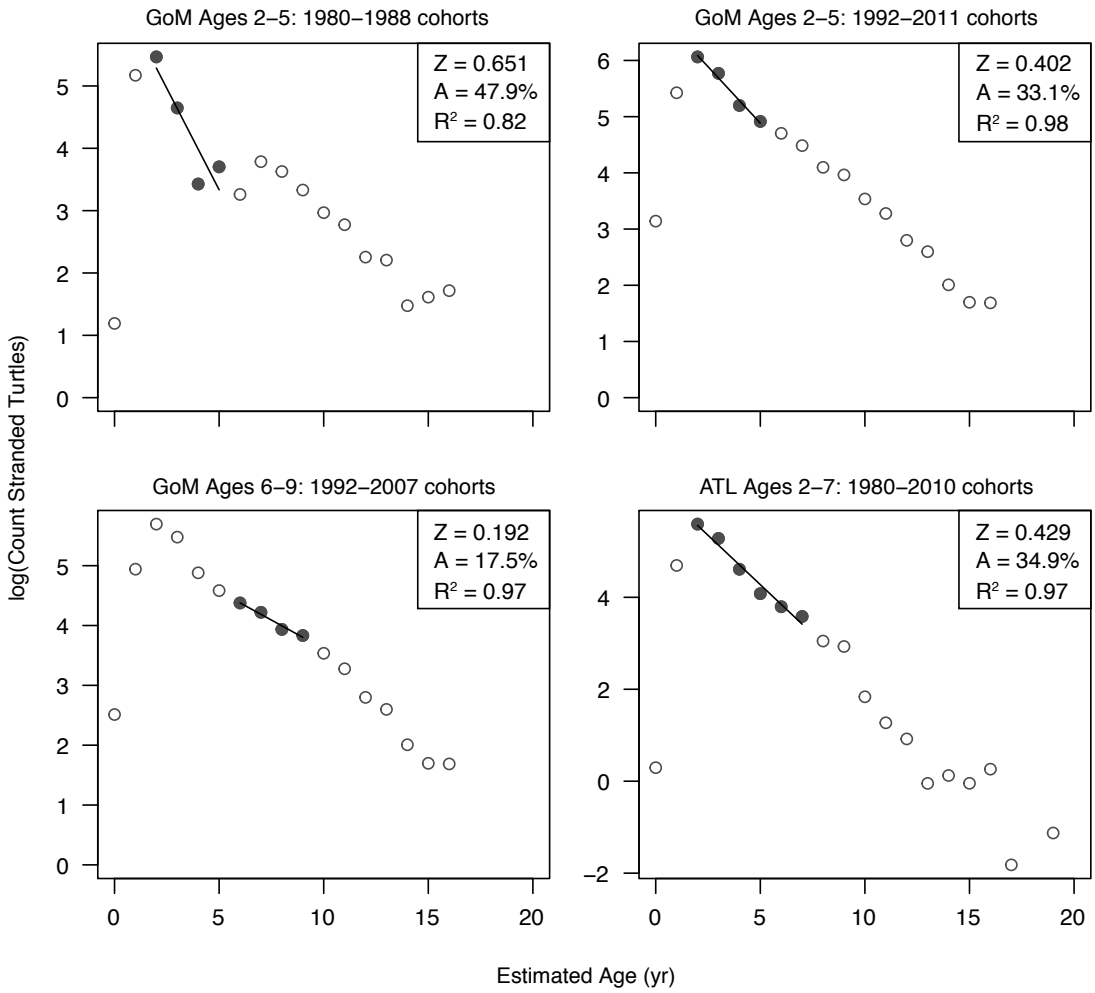

Figure 5.3. Results of region- and age-specific catch curve analyses for Kemp's ridley sea turtles. Data were binned across cohorts, including only cohorts fully represented for each age class within each time period. Z is the estimated instantaneous mortality rate, whereas A is the estimated annual mortality rate ($A = 1 - e^{-Z}$).

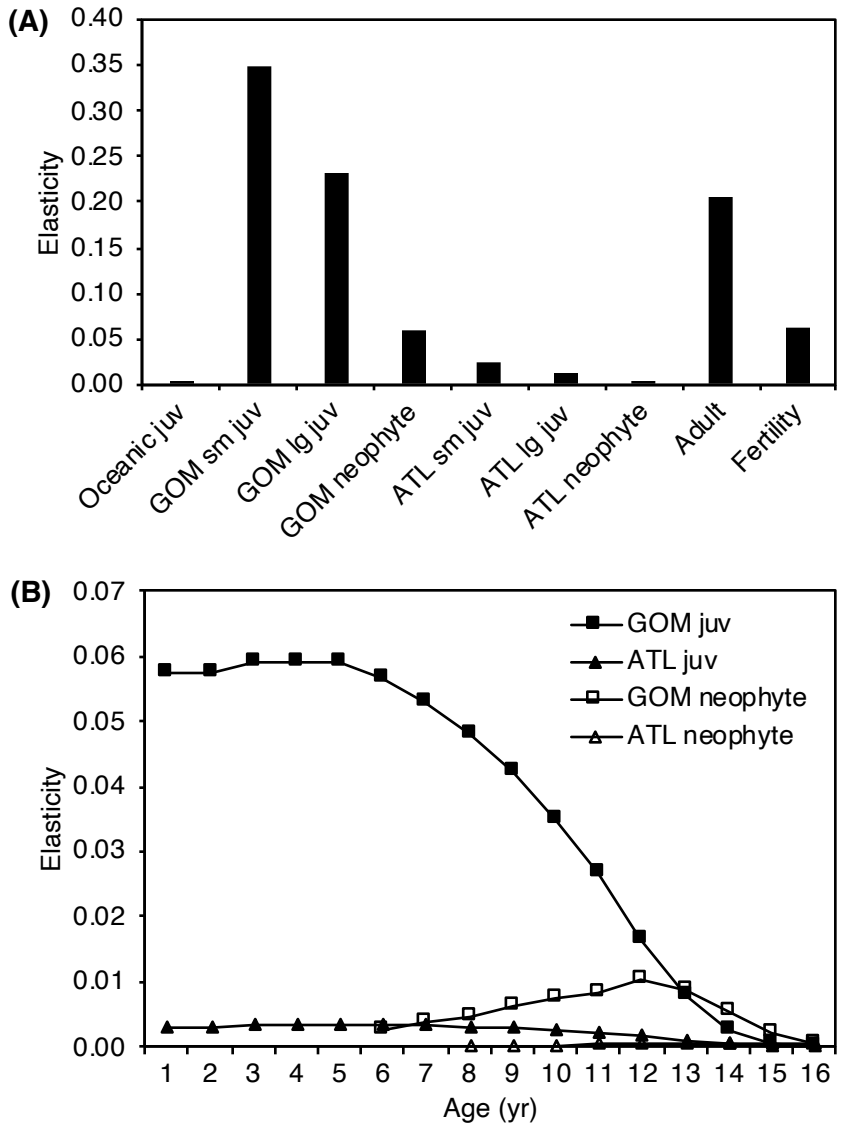

Figure 5.4. Habitat- and stage-specific survival and fertility elasticities for Kemp's ridley sea turtles (2005–2009). **(A)** Elasticities summed across life stages. **(B)** Age-specific survival elasticities.

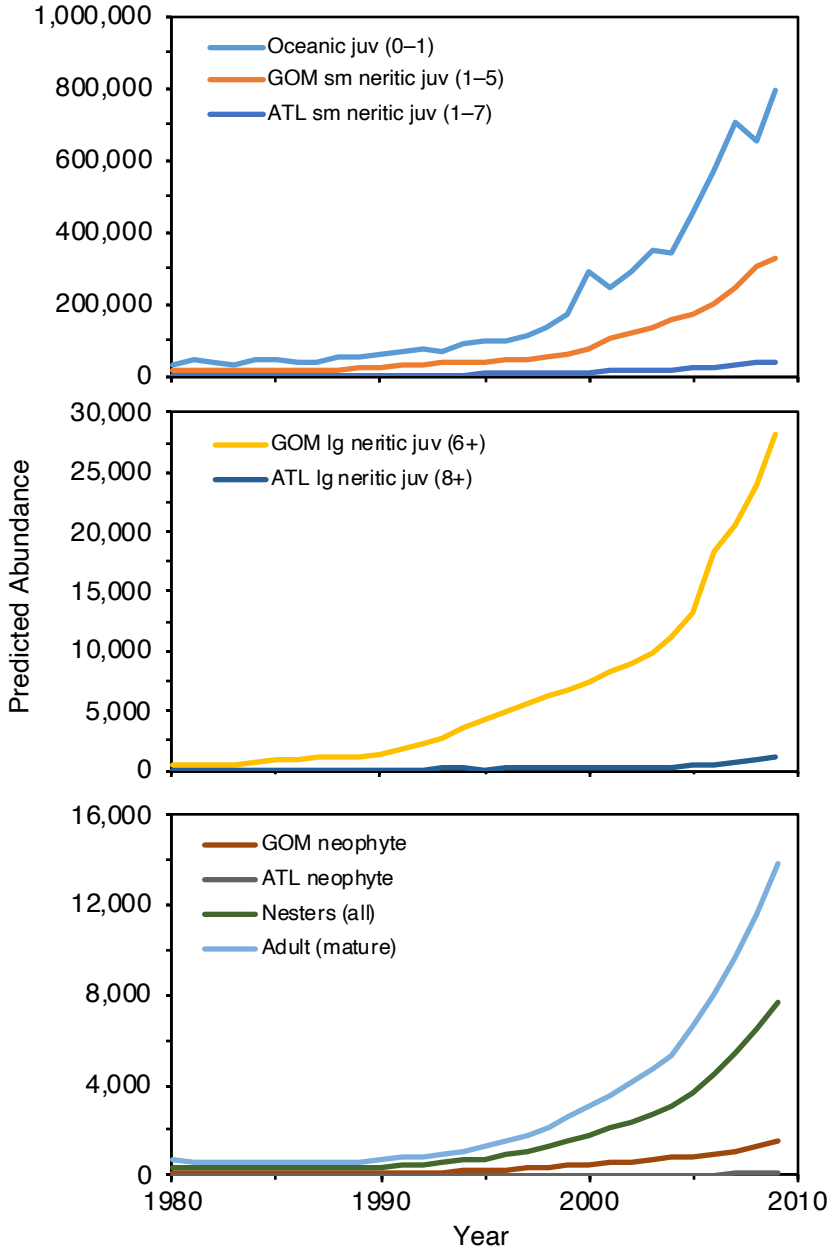

Figure 5.5. Estimated population size by life stage for the base model (Model 1: Atlantic turtles shift to GoM at maturation; base scenario = 15% to Atlantic, ATL, annually). Neophyte = first time nesting female. Age 1 turtles occur in both the oceanic and small neritic juvenile life stages due to variable recruitment between habitats.

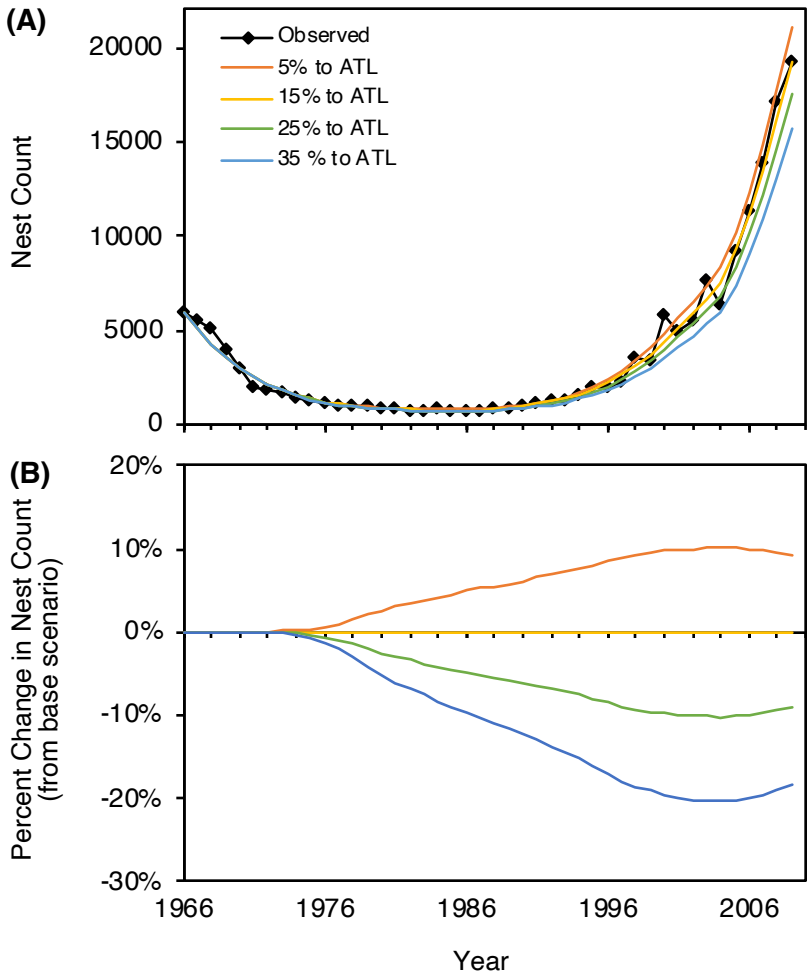

Figure 5.6. **(A)** Predicted nest counts for the base model (Model 1: Atlantic turtles shift to GoM at maturation) ran using varying proportions of turtles entering U.S. Atlantic life stages from the oceanic life stage. **(B)** Percent change in nests counts relative to the base scenario (base scenario = 15% to Atlantic, ATL, annually). Plots for Model 2 and 3 presented in Figure D4.

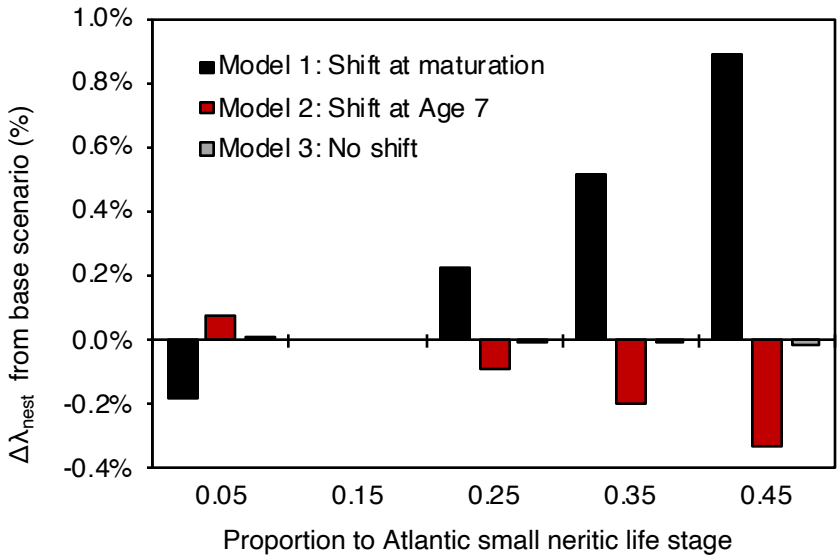

Figure 5.7. Sensitivity of population growth rate (percent change in λ_{nest} for period 2005–2009) to change in the proportion of turtles entering U.S. Atlantic life stages from the oceanic life stage (base scenario = 15% to Atlantic, ATL, annually) for each model evaluated. Model 1 (base model): Atlantic turtles shift to GoM at maturation (logistic function). Model 2: Atlantic turtles shift to GoM beginning at age 7 (exponential function). Model 3: No Atlantic turtles shift to GoM.

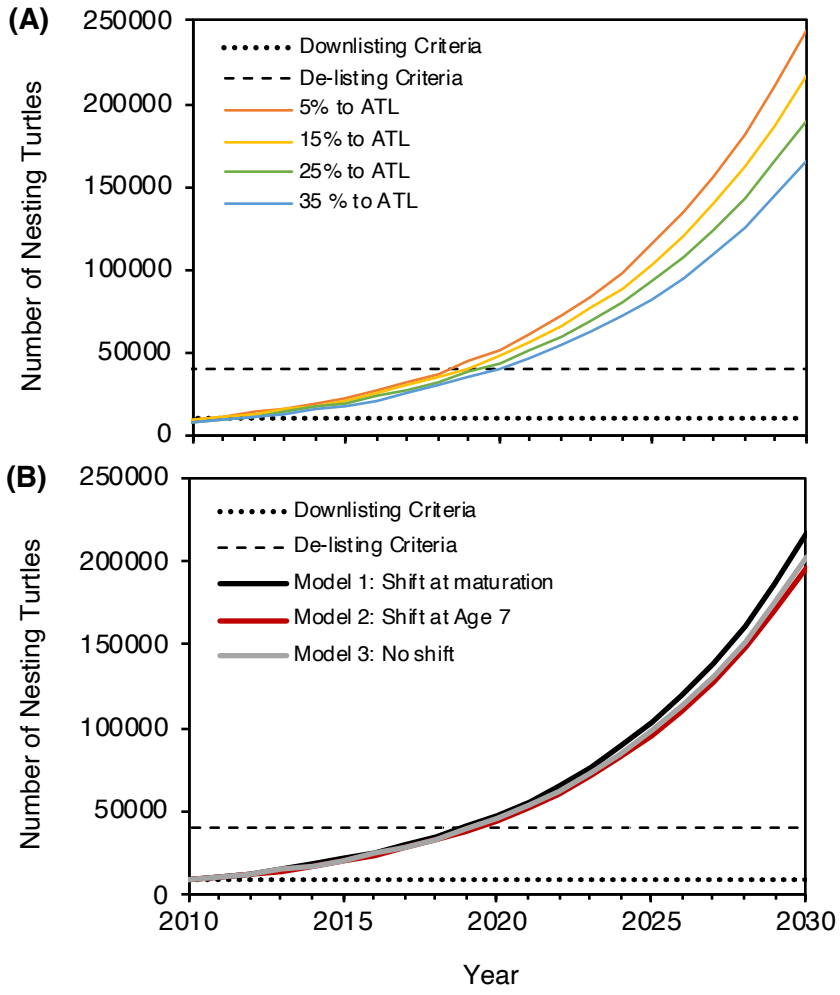

Figure 5.8. **(A)** Predicted number of nesting females per year based on projection of base model (Model 1: Atlantic turtles shift to GoM at maturation) and varying proportions of turtles entering U.S. Atlantic life stages from the oceanic life stage. **(B)** Projection for all three models evaluated using base scenario (15% to Atlantic annually). Endangered Species Act nesting female downlisting criteria are 10,000 nesting females per season at the index nesting beaches (Rancho Nuevo, Tepehuajes, Playa Dos) in Mexico; delisting criteria are a 6-year average of 40,000 nesting females per season across all nesting beaches (NMFS et al. 2011).

CHAPTER 6: GENERAL CONCLUSION

The goal of my dissertation was to evaluate how various environmental factors influence sea turtle growth rates and how somatic growth variation subsequently influences sea turtle population dynamics. To this end, Chapters 2 and 3 examined the influence of the 2010 *Deepwater Horizon* oil spill, climate change, changing population density, and regionally variable diet composition on Kemp's ridley sea turtle growth rates. Chapter 4 focused on the development of geochemical tools to characterize alternative habitat use that, in the future, may allow for quantification of Atlantic-to-Gulf of Mexico (GoM) transition probabilities critical to parameterization of spatially explicit population models. Lastly, Chapter 5 examined how life history variation, specifically regionally variable growth rates, influences Kemp's ridley population growth and recovery time. I focused my research on the critically endangered Kemp's ridley sea turtle due to the availability of a robust growth dataset and large tissue collection (i.e., humerus bones from dead stranded turtles), as well as the species' unique life history and distribution, which provided a means of testing multiple alternative hypotheses regarding the influence of environmental factors on somatic growth and population dynamics. Although this analysis focused on a single species, many of the results and methods employed may be applicable to other sea turtle and migratory marine megafauna in the western North Atlantic Ocean.

My research revealed that various environmental factors drive stage- and habitat-specific growth responses in Kemp's ridley sea turtles. Indeed, in Chapter 2 I

observed a simultaneous decline in somatic growth rates for oceanic (Age 0) and small neritic juveniles (Age 2–5) in both the GoM and Atlantic. Moreover, analyses indicated that drivers of this variation are likely regionally variable and additive. For example, while I hypothesized these simultaneous declines may ultimately be due in part to both direct and indirect effects of the *DWH* oil spill, Age 0 growth rates also appeared to be influenced by regionally variable climate and Age $2–5_{GoM}$ growth rates may be influenced by changing population density. Unfortunately, these results did not align with most of my *a priori* hypotheses related to environmental drivers of somatic growth variation in sea turtles. Also, my study design, which focused on broadscale patterns over multiple decades, prevented evaluation and exclusion of many competing hypotheses. Establishing direct links between sea turtle growth rates and the *DWH* oil spill exposure through geochemical analyses of bone tissue is perhaps the most important next step in evaluating *DWH* oil spill effects on sea turtles and disentangling the effects of multiple potential environmental drivers of somatic growth variation. Specifically, analyses of bone trace element and polycyclic aromatic hydrocarbon (PAH) concentrations may allow for the retrospective characterization of *DWH* oil spill exposure in sea turtles as there is some evidence that concentrations of these geochemicals increased in both the water column and animal tissues following the oil spill (Wise et al. 2014, López-Duarte et al. 2016, Romero et al. 2018). Importantly, these geochemicals would be expected to be retained unaltered in sea turtle cortical bone tissue.

Drivers of the post-2012 change in Age 2–5_{ATL} growth rates, along with those of large neritic and subadult juvenile growth variation, are poorly understood. The identification of a geochemical fingerprint of *DWH* oil spill exposure would allow for testing of our principal hypothesis that changes in Atlantic turtle somatic growth is related to carry over effects from *DWH* oil spill impacts on oceanic habitats and life stages. However, if *DWH* impacts on oceanic life stages were indirect then a *DWH* geochemical fingerprint would likely contribute little to investigating this hypothesis. Expanding our understanding of the dynamics of oceanic habitats occupied by Kemp's ridleys and the processes that govern the recruitment of oceanic turtles to neritic habitats and life stages in both the GoM and Atlantic may shed important light on factors that may explain this regionally variable growth response. Additionally, Atlantic Kemp's ridleys are poorly studied relative to their GoM counterparts, so additional study of Atlantic Kemp's ridley foraging ecology, migratory connectivity, and both inter-and intra-specific competitive interactions may provide important new insights into somatic growth dynamics. Lastly, low sample sizes and an incomplete growth time series prevented robust analysis of drivers of large neritic juvenile growth dynamics. Collection and analysis of humerus bones from additional large juvenile and adult Kemp's ridleys in the future will help fill this knowledge gap.

My decision to integrate bone stable isotope and growth analyses to examine the relationship between diet composition and growth represents a major advance in our ability to link these two major ecological factors but comes with certain limitations and data needs that presently limit the utility of this approach. The ideal

way of estimating dietary proportions using stable isotope mixing models is to simultaneously collect tissue samples of consumers—preferably tissues with rapid turnover rates (i.e., short time between food intake and assimilation of constituents into the body)—and all potential prey over a specific area and period of time (Phillips et al. 2014). Such an approach was not possible for our analysis given the spatial scale and retrospective nature of our study. Many factors are thus confounded in our analysis (e.g., time, space, data availability) that may have affected our ability to detect diet variation within and among regions and our ability to characterize relationships between diet composition and somatic growth rates. Nevertheless, we detected novel relationships between stable nitrogen isotope ratios, diet composition, and growth that may serve as the foundation for much additional research. Chapter 3 therefore represents but the first step in using sea turtle bones to study connections between diet and somatic growth variation. Future studies that narrow their spatiotemporal scope would go a long way in ameliorating some of these issues. Additionally, much greater effort is needed to characterize the means and variances of potential prey stable isotope ratios across all habitats utilized by sea turtles in order to improve these models and effectively expand their application.

Perhaps the most exciting finding from my research was the identification of a geochemical marker that allows us to differentiate GoM vs. Atlantic habitat use: Pb isotopes. Quantifying population connectivity is central to understanding the dynamics of patchily distributed species (Crooks & Sanjayan 2006, Runge et al. 2014), particularly those demonstrated to have regionally variable vital rates such as

the Kemp's ridley sea turtle (Avens et al. 2017). Nevertheless, we do not know the relative proportion of Kemp's ridleys that reside along the U.S. Atlantic Coast let alone the sizes/ages at which they migrate to GoM habitats. In Chapter 4, I demonstrated that Pb isotopes may be the key to answering such questions in future analyses. Specifically, a largescale extension of this research to large juvenile and adult Kemp's ridleys stranded in the GoM, which represent an unknown mix of life-long GoM residents and Atlantic migrants, may allow researchers to identify the timing of Atlantic-to-GoM ontogenetic shifts and quantify the proportion of turtles that ultimately occupy these disparate habitats. Such information could ultimately be included in spatially explicit population models to more accurately quantify the contribution of Atlantic vs. GoM Kemp's ridleys to population growth and develop region-specific management plants. Importantly, as Pb isotopes do not fractionate within foods (i.e., Pb isotope ratios in tissues directly track those in the environment) our results are likely applicable to the study of connectivity in many other migratory species in the western North Atlantic Ocean that occupy GoM and Atlantic habitats (e.g., other sea turtle species, marine mammals, sharks).

I originally had hoped to extend the Chapter 4 analysis to aid in parameterization of my Chapter 5 population model, but circumstances prevented this additional research from occurring. Part of this setback was due to the Burt Hall fire that compromised necessary analytical equipment. But methodological limitations also slowed progress on this research. Solutions-based analyses of Pb isotopes are very time-consuming and require a relatively large amount of sample. Indeed, the

average amount of bone dust that can be extracted from individual bone growth layers is near the minimum sample requirements for this approach. Trying to sample all of the growth layers for individual turtles would have in many cases been infeasible, not to mention cost prohibitive given the time it takes to analyze these samples once prepared. An exciting potential avenue for continuing this work in the future would be laser-ablation multi-collector inductively coupled plasma mass spectrometry (MC-ICP-MS), which combines the sensitivity of MC-ICP-MS with the flexibility of sampling via laser ablation to characterize Pb isotope ratios of solid materials (Ponting et al. 2003, Kent 2008). If this approach has great enough precision to detect the *very small* differences in Pb isotope ratios of turtles from the Atlantic and GoM, it might allow for the rapid sampling of hundreds of turtle bones in a matter of days at a significantly reduced cost relative to the solutions-based approach.

Variable growth has the potential to influence sea turtle population dynamics through effects on time to maturity and size-specific mortality. When regional differences in demographic rates exist for a species of conservation concern, it is pertinent to evaluate how this life history variation influences overall species population dynamics. In Chapter 5, I implemented a spatially explicit, age-structured matrix population model to evaluate how regionally variable growth rates influence Kemp's ridley population growth and recovery time. I specifically evaluated the relative importance of Atlantic Kemp's ridleys to population growth and found that they likely contributed little to the species' pre-2010 population recovery under a

range of scenarios. This represented the first population model for this species that included separate Atlantic life stages and demographic rates.

While my population model included many new sources of information related to Atlantic turtle vital rates and movement patterns, key uncertainties remain that constrain precise quantification of this species' population dynamics. As for most sea turtle species, in-water survival rate are the most pressing data need in order to more accurately estimate population sizes and trends (Crouse et al. 1987, Crowder et al. 1994, Heppell et al. 2004). However, given the logistical difficulties of conducting mark-recapture studies in highly mobile marine species, expanded study of sea turtle strandings may be a more feasible approach to quantifying sea turtle survival rates in the future. There is still much we do not know about the causes and patterns of sea turtle strandings that would aid interpretation of these data, although recent efforts are working to fill some of this knowledge gaps. For example, recent tagging studies of frozen sea turtle carcasses have greatly increased our understanding of the physical processes that govern sea turtle carcass movements and decomposition rates (Higgins et al. 2007, Nero et al. 2013, Santos et al. 2018). Nevertheless, we still do not know what proportion of strandings are associated with natural versus anthropogenic mortality nor what proportion of total mortality they represent. Maintaining consistent stranding response effort across space and time will be critical to reducing biases in the stranding dataset. Ameliorating these sources of uncertainty would greatly enhance the value of stranded turtles to survival rate estimation.

Highly migratory species pose unique challenges to studying somatic growth and potential drivers of growth variation. However, my research demonstrated the potentially transformative value of stranded sea turtle bones to addressing otherwise intractable questions in sea turtle ecology. While biologging technologies have greatly expanded the information we can obtain from individual animals (Wilmers et al. 2015), mark-recapture studies may never allow us to robustly evaluate drivers of somatic growth variation in sea turtles within reasonable time frames as tag returns are low and resulting growth intervals are inconsistent. Responding to stranded sea turtles is potentially less resource-intense than implementing large-scale mark-recapture studies, and routine collection of humerus bones from a subset of stranded turtles that are already being monitored through the Sea Turtle Stranding and Salvage Network may be a more feasible approach to rapidly censusing a populations' somatic growth rates and exploring drivers of somatic growth variation in real time (e.g., following an oil spill or red tide event). Importantly, such efforts can yield large, long-term datasets that are necessary for evaluating changes in demographic rates across space and time.

Taken together, this research has greatly expanded our understanding of the drivers of sea turtle somatic growth and population dynamics. Out of necessity, this research examined effects at broad spatial scales. Much knowledge may be gained by examining local effects on somatic growth rates through comparison of region- or state-specific growth rate data presented herein with local factors (e.g., temperature, prey availability, fishing pressure, salinity, etc.). At the individual turtle level,

comparing somatic growth rate data with other data obtained from necropsies, such as nutritional condition and stomach contents, may also provide novel insights into the drivers of somatic growth variation. Ultimately, my results provide important new information on Kemp's ridley sea turtle life history and population dynamics that may be important to future population assessments and development of conservation plans.

BIBLIOGRAPHY

Abraham CL, Sydeman WJ (2004) Ocean climate, euphausiids and auklet nesting: inter-annual trends and variation in phenology, diet and growth of a planktivorous seabird, *Ptychoramphus aleuticus*. Marine Ecology Progress Series 274:235–250.

Albarède F, Beard B (2004) Analytical methods for non-traditional isotopes. Reviews in Mineralogy and Geochemistry 55:113–152.

Albers PH (2006) Birds and polycyclic aromatic hydrocarbons. Avian and Poultry Biology Reviews 17:125–140.

Ambrose SH, DeNiro MJ (1986) The isotopic ecology of East African mammals. Oecologia 69:395–406.

Ashford JR, Jones CM, Hofmann E, Everson I, Moreno C, Duhamel G, Williams R (2005) Can otolith elemental signatures record the capture site of Patagonian toothfish (*Dissostichus eleginoides*), a fully marine fish in the Southern Ocean? Canadian Journal of Fisheries and Aquatic Sciences 62:2832–2840.

Atkinson D (1994) Temperature and organism size—a biological law for ectotherms. Advances in Ecological Research 25:1–58.

Atkinson S, Demaster DP, Calkins DG (2008) Anthropogenic causes of the western Steller sea lion *Eumetopias jubatus* population decline and their threat to recovery. Mammal Review 38:1–18.

Ault WA, Senechal RG, Erlebach WE (1970) Isotopic composition as a natural tracer of lead in the environment. Environmental Science & Technology 4:305–313.

Avens L, Braun-McNeill J, Epperly S, Lohmann KJ (2003) Site fidelity and homing behavior in juvenile loggerhead sea turtles (*Caretta caretta*). Marine Biology 143:211–220.

Avens L, Goshe LR, Coggins L, Shaver DJ, Higgins B, Landry AM, Bailey R (2017) Variability in age and size at maturation, reproductive longevity, and long-term growth dynamics for Kemp's ridley sea turtles in the Gulf of Mexico. PLoS ONE 12:e0173999.

Avens L, Goshe LR, Pajuelo M, Bjorndal KA, MacDonald BD, Lemons GE, Bolten AB, Seminoff JA (2013) Complementary skeletochronology and stable isotope analyses offer new insight into juvenile loggerhead sea turtle oceanic stage duration and growth dynamics. Marine Ecology Progress Series 491:235–251.

Avens L, Snover ML (2013) Age and age estimation in sea turtles. In: *The Biology of Sea Turtles*. Wyneken J, Lohmann KJ, Musick JA (eds) CRC Press, Boca Raton, FL, p 97–134

Avise JC (1998) Conservation genetics in the marine realm. Journal of Heredity 89:377–382.

Baker JD, Harting AL, Wurth TA, Johanos TC (2011) Dramatic shifts in Hawaiian monk seal distribution predicted from divergent regional trends. Marine Mammal Science 27:78–93.

Balazs GH (1982) Growth rates of immature green turtles in the Hawaiian Archipelago. In: *Biology and conservation of sea turtles*. Bjorndal KA (ed) Smithsonian Institution Press, Washington, D.C., p 117–125

Balazs GH, Chaloupka M (2004) Spatial and temporal variability in somatic growth of green sea turtles (*Chelonia mydas*) resident in the Hawaiian Archipelago. Marine Biology 145:1043–1059.

Baty F, Ritz C, Charles S, Brutsche M, Flandrois J-P, Delignette-Muller M-L (2015) A toolbox for nonlinear regression in *R*: the package nlstools. J Stat Soft 66.

Baumann H, Wells RJD, Rooker JR, Zhang S, Baumann Z, Madigan DJ, Dewar H, Snodgrass OE, Fisher NS (2015) Combining otolith microstructure and trace elemental analyses to infer the arrival of juvenile Pacific bluefin tuna in the California Current Ecosystem. ICES J Mar Sci 72:2128–2138.

Bean SB, Logan JM (2019) Stable isotope analyses of cold-stunned Kemp's ridley (*Lepidochelys kempii*) sea turtles at the northern extent of their coastal range. Marine Biology 166:64.

Beaugrand G, Conversi A, Chiba S, Edwards M, Fonda-UmanI S, Greene C, Mantua N, Otto SA, Reid PC, Stachura, Stemmann, Sugisaki H (2015) Synchronous marine pelagic regime shifts in the Northern Hemisphere. Philosophical Transactions of the Royal Society B: Biological Sciences 370:20130272.

Beaugrand G, McQuatters-Gollop A, Edwards M, Goberville E (2013) Long-term responses of North Atlantic calcifying plankton to climate change. Nature Clim Change 3:263–267.

Benaka L. R, Bullock D, Hoover AL, Olsen NA (2019) U.S. National Bycatch Report First Edition Update 3. U.S. Department of Commerce, Silver Spring, MD.

Berry JF, Shine R (1980) Sexual size dimorphism and sexual selection in turtles (order testudines). Oecologia 44:185–191.

Bertrand K, Hare L (2017) Evaluating benthic recovery decades after a major oil spill in the Laurentian Great Lakes. Environmental Science & Technology 51:9561–9568.

Beston JA (2011) Variation in life history and demography of the American black bear. The Journal of Wildlife Management 75:1588–1596.

Bevan E, Wibbels T, Najera BMZ, Sarti L, Martinez FI, Cuevas JM, Gallaway BJ, Pena LJ, Burchfield PM (2016) Estimating the historic size and current status of the Kemp's ridley sea turtle (*Lepidochelys kempii*) population. Ecosphere 7:e01244.

Beyer J, Trannum HC, Bakke T, Hodson PV, Collier TK (2016) Environmental effects of the Deepwater Horizon oil spill: A review. Marine Pollution Bulletin 110:28–51.

Bjorndal KA (1997) Foraging ecology and nutrition of sea turtles. In: *The Biology of Sea Turtles*. Lutz PL, Musick JA (eds) CRC Press, Boca Raton, FL, p 199–231

Bjorndal KA, Bolten AB, Chaloupka M, Saba VS, Bellini C, Marcovaldi MAG, Santos AJB, Bortolon LFW, Meylan AB, Meylan PA, Gray J, Hardy R, Brost B, Bresette M, Gorham JC, Connett S, Crouchley BVS, Dawson M, Hayes D,

Diez CE, van Dam RP, Willis S, Nava M, Hart KM, Cherkiss MS, Crowder AG, Pollock C, Hillis-Starr Z, Muñoz Tenería FA, Herrera-Pavón R, Labrada-Martagón V, Lorences A, Negrete-Philippe A, Lamont MM, Foley AM, Bailey R, Carthy RR, Scarpino R, McMichael E, Provancha JA, Brooks A, Jardim A, López-Mendilaharsu M, González-Paredes D, Estrades A, Fallabrino A, Martínez-Souza G, Vélez-Rubio GM, Boulon RH, Collazo JA, Wershoven R, Hernández VG, Stringell TB, Sanghera A, Richardson PB, Broderick AC, Phillips Q, Calosso M, Claydon JAB, Metz TL, Gordon AL, Landry AM, Shaver DJ, Blumenthal J, Collyer L, Godley BJ, McGowan A, Witt MJ, Campbell CL, Lagueux CJ, Bethel TL, Kenyon L (2017) Ecological regime shift drives declining growth rates of sea turtles throughout the West Atlantic. Glob Change Biol:4556–4568.

Bjorndal KA, Bolten AB, Chaloupka MY (2000) Green turtle somatic growth model: evidence for density dependence. Ecological Applications 10:269–282.

Bjorndal KA, Bolten AB, Dellinger T, Delgado C, Martins HR (2003) Compensatory growth in oceanic loggerhead sea turtles: response to a stochastic environment. Ecology 84:1237–1249.

Bjorndal KA, Bowen BW, Chaloupka M, Crowder LB, Heppell SS, Jones CM, Lutcavage ME, Policansky D, Solow AR, Witherington BE (2011) Better science needed for restoration in the Gulf of Mexico. Science 331:537–538.

Bjorndal KA, Chaloupka M, Saba VS, Diez CE, van Dam RP, Krueger BH, Horrocks JA, Santos AJB, Bellini C, Marcovaldi MAG, Nava M, Willis S, Godley BJ, Gore S, Hawkes LA, McGowan A, Witt MJ, Stringell TB, Sanghera A, Richardson PB, Broderick AC, Phillips Q, Calosso MC, Claydon JAB, Blumenthal J, Moncada F, Nodarse G, Medina Y, Dunbar SG, Wood LD, Lagueux CJ, Campbell CL, Meylan AB, Meylan PA, Burns Perez VR, Coleman RA, Strindberg S, Guzmán-H. V, Hart KM, Cherkiss MS, Hillis-Starr Z, Lundgren IF, Boulon RH, Connett S, Outerbridge ME, Bolten AB (2016) Somatic growth dynamics of West Atlantic hawksbill sea turtles: a spatio-temporal perspective. Ecosphere 7:e01279.

Bjorndal KA, Parsons J, Mustin W, Bolten AB (2013a) Threshold to maturity in a long-lived reptile: interactions of age, size, and growth. Mar Biol 160:607–616.

Bjorndal KA, Parsons J, Mustin W, Bolten AB (2014) Variation in age and size at sexual maturity in Kemp's ridley sea turtles. Endang Species Res 25:57–67.

Bjorndal KA, Schroeder BA, Foley AM, Witherington BE, Bresette M, Clark D, Herren RM, Arendt MD, Schmid JR, Meylan AB, Meylan PA, Provancha JA, Hart KM, Lamont MM, Carthy RR, Bolten AB (2013b) Temporal, spatial, and body size effects on growth rates of loggerhead sea turtles (*Caretta caretta*) in the Northwest Atlantic. Marine Biology 160:2711–2721.

Black HD, Andrus CFT, Lambert WJ, Rick TC, Gillikin DP (2017) Δ15N values in *Crassostrea virginica* shells provides early direct evidence for nitrogen loading to Chesapeake Bay. Sci Rep 7:44241.

Bollhöfer A, Rosman KJR (2001) Isotopic source signatures for atmospheric lead: the Northern Hemisphere. Geochimica et Cosmochimica Acta 65:1727–1740.

Bollhöfer A, Rosman KJR (2002) The temporal stability in lead isotopic signatures at selected sites in the Southern and Northern Hemispheres. Geochimica et Cosmochimica Acta 66:1375–1386.

Bolten AB (2003) Variation in sea turtle life history patterns: neritic vs. oceanic developmental stages. In: *The Biology of Sea Turtles*. Lutz PL, Musick JA, Wyneken J (eds) CRC Press, Boca Raton, FL, p 243–273

Bolten AB, Crowder LB, Dodd MG, MacPherson SL, Musick JA, Schroeder BA, Witherington BE, Long KJ, Snover ML (2011) Quantifying multiple threats to endangered species: an example from loggerhead sea turtles. Frontiers in Ecology and the Environment 9:295–301.

Bond AL, Diamond AW (2011) Recent Bayesian stable-isotope mixing models are highly sensitive to variation in discrimination factors. Ecological Applications 21:1017–1023.

Born EW, Outridge P, Riget FF, Hobson KA, Dietz R, Øien N, Haug T (2003) Population substructure of North Atlantic minke whales (*Balaenoptera acutorostrata*) inferred from regional variation of elemental and stable isotopic signatures in tissues. Journal of Marine Systems 43:1–17.

Borrell A, Abad-Oliva N, Gómez-Campos E, Giménez J, Aguilar A (2012) Discrimination of stable isotopes in fin whale tissues and application to diet assessment in cetaceans. Rapid Communications in Mass Spectrometry 26:1596–1602.

Bosc E, Bricaud A, Antoine D (2004) Seasonal and interannual variability in algal biomass and primary production in the Mediterranean Sea, as derived from 4 years of SeaWiFS observations. Global Biogeochemical Cycles 18.

Boyle E, Lee J-M, Echegoyen Y, Noble A, Moos S, Carrasco G, Zhao N, Kayser R, Zhang J, Gamo T, Obata H, Norisuye K (2014) Anthropogenic lead emissions in the ocean: the evolving global experiment. Oceanography 27:69–75.

Broderick AC, Coyne MS, Fuller WJ, Glen F, Godley BJ (2007) Fidelity and over-wintering of sea turtles. Proc R Soc B 274:1533–1539.

Brodeur RD, Ware DM (1992) Long-term variability in zooplankton biomass in the subarctic Pacific Ocean. Fisheries Oceanography 1:32–38.

Brown-Peterson NJ, Krasnec MO, Lay CR, Morris JM, Griffitt RJ (2016) Responses of juvenile southern flounder exposed to Deepwater Horizon oil-contaminated sediments. Environ Toxicol Chem:1–10.

Burke VJ, Morreale SJ, Standora EA (1994) Diet of the Kemp's ridley sea turtle, *Lepidochelys kempii*, in New York waters. Fishery Bulletin 92:26–32.

Burke VJ, Standora EA, Morreale SJ (1993) Diet of juvenile Kemp's ridley and loggerhead sea turtles from Long Island, New York. Copeia 1993:1176–1180.

Burnham KP, Anderson DR (2002) Model selection and multimodel inference: a practical information-theoretic approach, 2nd ed. Springer, New York.

Burton JH, Price TD, Middleton WD (1999) Correlation of bone Ba/Ca and Sr/Ca due to biological purification of calcium. Journal of Archaeological Science 26:609–616.

Byles RA (1988) Behavior and ecology of sea turtles from Chesapeake Bay, Virginia. Doctoral Dissertation, The College of William & Mary, Williamsburg, VA

Caillouet CW (2019) Excessive annual numbers of neritic immature kemp's ridleys may prevent population recovery. Marine Turtle Newsletter 158:1–9.

Caillouet CW (2014) Interruption of the Kemp's ridley population's pre-2010 exponential growth in the Gulf of Mexico and its aftermath: one hypothesis. Marine Turtle Newsletter 143:1–7.

Caillouet CW, Fontaine CT, Manzella-Tirpak SA, Williams TD (1995) Growth of head-started Kemp's ridley sea turtles (*Lepidochelys kempii*) following release. Chelonian Conservation and Biology 1:231–234.

Caillouet CW, Gallaway BJ, Putman NF (2016) Kemp's ridley sea turtle saga and setback: novel analyses of cumulative hatchlings released and time-lagged annual nests in Tamaulipas, Mexico. Chelonian Conservation and Biology 15:115–131.

Caillouet CW, Raborn SW, Shaver DJ, Putman NF, Gallaway BJ, Mansfield KL (2018) Did declining carrying capacity for the Kemp's Ridley sea turtle population within the Gulf of Mexico contribute to the nesting setback in 2010−2017? Chelonian Conservation and Biology 17:123–133.

Caillouet CW, Shaver DJ, Landry Jr AM (2015) Kemp's ridley sea turtle (*Lepidochelys kempii*) head-start and reintroduction to Padre Island National Seashore, Texas. Herpetological Conservation and Biology 10:309–377.

Cairns DK (1988) Seabirds as indicators of marine food supplies. Biological Oceanography 5:261–271.

Campana SE (1999) Chemistry and composition of fish otoliths: pathways, mechanisms and applications. Marine Ecology Progress Series 188:263–297.

Campana SE, Chouinard GA, Hanson JM, Fréchet A, Brattey J (2000) Otolith elemental fingerprints as biological tracers of fish stocks. Fisheries Research 46:343–357.

Cannon AC (1998) Gross necropsy results of sea turtles stranded on the upper Texas and western Louisiana coasts, 1 January-31 December 1994. U.S. Department of Commerce.

Carr A (1963) Panspecific reproductive convergence in *Lepidochelys kempii*. Ergebnisse der Biologie 26:298–303.

Caswell H (2001) Matrix Population Models, 2nd ed. Sinauer Associates, Inc. Publishers, Sunderland, MA.

Caswell H (1983) Phenotypic plasticity in life-history traits: demographic effects and evolutionary consequences. American Zoologist 23:35–46.

Caut S, Guirlet E, Angulo E, Das K, Girondot M (2008) Isotope analysis reveals foraging area dichotomy for Atlantic leatherback turtles. PLoS ONE 3:e1845.

Chaloupka M, Kamezaki N, Limpus C (2008) Is climate change affecting the population dynamics of the endangered Pacific loggerhead sea turtle? Journal of Experimental Marine Biology and Ecology 356:136–143.

Chaloupka M, Limpus C, Miller J (2004) Green turtle somatic growth dynamics in a spatially disjunct Great Barrier Reef metapopulation. Coral Reefs 23:325–335.

Chaloupka M, Zug G (1997) A polyphasic growth function for the endangered Kemp's ridley sea turtle, *Lepidochelys kempii*. Fishery Bulletin 95:849–856.

Chamberlain CP, Waldbauer JR, Fox-Dobbs K, Newsome SD, Koch PL, Smith DR, Church ME, Chamberlain SD, Sorenson KJ, Risebrough R (2005) Pleistocene to recent dietary shifts in California condors. PNAS 102:16707–16711.

Chang M-Y, Geffen AJ (2013) Taxonomic and geographic influences on fish otolith microchemistry. Fish Fish 14:458–492.

Chiaradia A, Forero MG, McInnes JC, Ramírez F (2014) Searching for the true diet of marine predators: incorporating Bayesian priors into stable isotope mixing models. PLOS ONE 9:e92665.

Cloyed CS, Newsome SD, Eason PK (2015) Trophic discrimination factors and incorporation rates of carbon- and nitrogen-stable isotopes in adult green frogs, *Lithobates clamitans*. Physiological and Biochemical Zoology 88:576–585.

Coleman AT, Pitchford JL, Bailey H, Solangi M (2017) Seasonal movements of immature Kemp's ridley sea turtles (*Lepidochelys kempii* in the northern Gulf of Mexico. Aquatic Conserv: Mar Freshw Ecosyst 27:253–267.

Coleman AT, Pulis EE, Pitchford JL, Crocker K, Heaton AJ, Carron AM, Hatchett W, Shannon D, Austin F, Dalton M, others (2016) Population ecology and rehabilitation of incidentally captured Kemp's ridley sea turtles (*Lepidochelys kempii*) in the Mississippi Sound, USA. Herpetological Conservation and Biology 11:253–264.

Congdon JD (1989) Proximate and evolutionary constraints on energy relations of reptiles. Physiological Zoology 62:356–373.

Cooke S (2008) Biotelemetry and biologging in endangered species research and animal conservation: relevance to regional, national, and IUCN Red List threat assessments. Endang Species Res 4:165–185.

Craig JK, Crowder LB, Gray CD, McDaniel CJ, Kenwood TA, Hanifen JG (2001) Ecological effects of hypoxia on fish, sea turtles, and marine mammals in the northwestern Gulf of Mexico. In: *Coastal and Estuarine Studies*. Rabalais NN, Turner RE (eds) American Geophysical Union, Washington, D. C., p 269–291

Crain CM, Kroeker K, Halpern BS (2008) Interactive and cumulative effects of multiple human stressors in marine systems. Ecology Letters 11:1304–1315.

Crooks KR, Sanjayan M (eds) (2006) Connectivity conservation: maintaining connections for nature. Cambridge University Press, Cambridge.

Crouse DT, Crowder LB, Caswell H (1987) A stage-based population model for loggerhead sea turtles and implications for conservation. Ecology 68:1412–1423.

Crowder LB, Crouse DT, Heppell SS, Martin TH (1994) Predicting the impact of turtle excluder devices on Loggerhead sea turtle populations. Ecological Applications 4:437–445.

Crowder LB, Heppell SS (2011) The decline and rise of a sea turtle: How Kemp's ridleys are recovering in the Gulf of Mexico. Solutions 2:67–73.

Curtis KA, Moore JE (2013) Calculating reference points for anthropogenic mortality of marine turtles. Aquatic Conserv: Mar Freshw Ecosyst 23:441–459.

Cushing DH (1990) Plankton production and year-class strength in fish populations: an update of the match/mismatch hypothesis. In: *Advances in Marine Biology*. Blaxter JHS, Southward AJ (eds) Academic Press, p 249–293

deVries MS, Stock BC, Christy JH, Goldsmith GR, Dawson TE (2016) Specialized morphology corresponds to a generalist diet: linking form and function in smashing mantis shrimp crustaceans. Oecologia 182:429-.

deYoung B, Barange M, Beaugrand G, Harris R, Perry RI, Scheffer M, Werner F (2008) Regime shifts in marine ecosystems: detection, prediction and management. Trends in Ecology & Evolution 23:402–409.

Diamond SL (2004) Bycatch quotas in the Gulf of Mexico shrimp trawl fishery: can they work? Rev Fish Biol Fisheries 14:207–237.

Díaz-Somoano M, Kylander ME, López-Antón MA, Suárez-Ruiz I, Martínez-Tarazona MR, Ferrat M, Kober B, Weiss DJ (2009) Stable lead isotope compositions in selected coals from around the world and implications for present day aerosol source tracing. Environ Sci Technol 43:1078–1085.

Dmitriew CM (2011) The evolution of growth trajectories: what limits growth rate? Biological Reviews 86:97–116.

Doyle TK, Houghton JDR, McDevitt R, Davenport J, Hays GC (2007) The energy density of jellyfish: Estimates from bomb-calorimetry and proximate-composition. Journal of Experimental Marine Biology and Ecology 343:239–252.

Drinkwater KF, Belgrano A, Borja A, Conversi A, Edwards M, Greene CH, Ottersen G, Pershing AJ, Walker H (2003) The response of marine ecosystems to climate variability associated with the North Atlantic Oscillation. In: *Geophysical Monograph Series*. Hurrell JW, Kushnir Y, Ottersen G, Visbeck M (eds) American Geophysical Union, Washington, D. C., p 211–234

Dunham AE (1978) Food availability as a proximate factor influencing individual growth rates in the iguanid lizard *Sceloporus merriami*. Ecology 59:770–778.

Dunham AE, Grant BW, Overall KL (1989) Interfaces between biophysical and physiological ecology and the population ecology of terrestrial vertebrate ectotherms. Physiological Zoology 62:335–355.

Dupont J, Hallock P, Jaap W (2010) Ecological impacts of the 2005 red tide on artificial reef epibenthic macroinvertebrate and fish communities in the eastern Gulf of Mexico. Mar Ecol Prog Ser 415:189–200.

Durant J, Hjermann D, Ottersen G, Stenseth N (2007) Climate and the match or mismatch between predator requirements and resource availability. Clim Res 33:271–283.

DWH NRDA Trustees (2016) Deepwater Horizon Oil Spill: Final Programmatic Damage Assessment and Restoration Plan and Final Programmatic Environmental Impact Statement. Department of Commerce and National Oceanic and Atmospheric Administration.

Edwards M, Beaugrand G, Helaouët P, Alheit J, Coombs S (2013) Marine ecosystem response to the Atlantic Multidecadal Oscillation. PLoS ONE 8:e57212.

Elias R W, Hirao, Y., Patterson, C. C. (1982) The circumvention of the natural biopurification of calcium along nutrient pathways by atmospheric inputs of industrial lead. Geochimica et Cosmochimica Acta 46:2561–2580.

Elsdon TS, Gillanders BM (2002) Interactive effects of temperature and salinity on otolith chemistry: challenges for determining environmental histories of fish. Canadian Journal of Fisheries & Aquatic Sciences 59:1796–1808.

Engle VD, Hyland JL, Cooksey C (2009) Effects of Hurricane Katrina on benthic macroinvertebrate communities along the northern Gulf of Mexico coast. Environ Monit Assess 150:193–209.

Epperly SP, Braun J, Chester AJ, Cross FA, Merriner JV, Tester PA, Churchill JH (1996) Beach strandings as an indicator of at-sea mortality of sea turtles. Bulletin of Marine Science 59:289–297.

Evershed RP, Bull ID, Corr LT, Crossman ZM, van Dongen BE, Evans CJ, Jim S, Mottram HR, Mukherjee AJ, Pancost RD (2007) Compound-specific stable isotope analysis in ecology and paleoecology. In: *Stable Isotopes in Ecology and Environmental Science*. Michener RH, Lajtha K (eds) Blackwell Publishing, Malden, MA, p 480–540

Figgener C, Bernardo J, Plotkin PT (2019) Beyond trophic morphology: stable isotopes reveal ubiquitous versatility in marine turtle trophic ecology. Biol Rev:brv.12543.

Finkbeiner EM, Wallace BP, Moore JE, Lewison RL, Crowder LB, Read AJ (2011) Cumulative estimates of sea turtle bycatch and mortality in USA fisheries between 1990 and 2007. Biological Conservation 144:2719–2727.

Foster GL, Pogge von Strandmann P a. E, Rae JWB (2010) Boron and magnesium isotopic composition of seawater. Geochem Geophys Geosyst 11:Q08015.

Fowler AJ, Gillanders BM, Hall, K. C. (2005) Relationship between elemental concentration and age from otoliths of adult snapper (*Pagrus auratus*, Sparidae): implications for movement and stock structure. Marine and Freshwater Research 56:661–676.

Fox-Dobbs K, Bump JK, Peterson RO, Fox DL, Koch PL (2007) Carnivore-specific stable isotope variables and variation in the foraging ecology of modern and ancient wolf populations: case studies from Isle Royale, Minnesota, and La Brea. Can J Zool 85:458–471.

Francey RJ, Allison CE, Etheridge DM, Trudinger CM, Enting IG, Leuenberger M, Langenfelds RL, Michel E, Steele LP (1999) A 1000-year high precision record of $\delta^{13}C$ in atmospheric CO_2. Tellus B: Chemical and Physical Meteorology 51:170–193.

Francis R (1990) Back-calculation of fish length: a critical review. Journal of Fish Biology 36:883–902.

Frazer NB, Greene JL, Gibbons JW (1993) Temporal variation in growth rate and age at maturity of male painted turtles, *Chrysemys picta*. The American Midland Naturalist 130:314–324.

Frazer NB, Richardson JI (1986) The relationship of clutch size and frequency to body size in loggerhead turtles, *Caretta caretta*. Journal of Herpetology 20:81–84.

Frick MG, Mason PA (1998) *Lepidochelys kempi* (Kemp's ridley sea turtle) diet. Herpetological Review 29:166–168.

Friedland KD, Reddin DG, Shimizu N, Haas RE, Youngson AF (1998) Strontium:calcium ratios in Atlantic salmon (*Salmo salar*) otoliths and observations on growth and maturation. Can J Fish Aquat Sci 55:1158–1168.

Fritts AK, Fritts MW, Haag WR, DeBoer JA, Casper AF (2017) Freshwater mussel shells (Unionidae) chronicle changes in a North American river over the past 1000 years. Science of The Total Environment 575:199–206.

Fry B, Sherr EB (1989) 13C measurements as indicators of carbon flow in marine and frehswater ecosystems. In: *Stable Isotopes in Ecological Research*. Rundel PW, Ehleringer JR, Nagy KA (eds) Springer New York, New York, NY, p 196–229

Fuller BT, Fuller JL, Sage NE, Harris DA, O'Connell TC, Hedges REM (2004) Nitrogen balance and $\delta^{15}N$: why you're not what you eat during pregnancy. Rapid Communications in Mass Spectrometry 18:2889–2896.

Gaillard J-M, Loison A, ToÏgo C, Delorme D, Laere GV (2003) Cohort effects and deer population dynamics. Écoscience 10:412–420.

Galer SJG, Abouchami W (1998) Practical application of lead triple spiking for correction of instrumental mass discrimination. Mineral Mag A 62:491–492.

Gallaway BJ, Gazey WJ, Caillouet CW, Plotkin PT, Abreu Grobois FA, Amos AF, Burchfield PM, Carthy RR, Castro Martinez MA, Cole JG, Coleman AT, Cooke M, DiMarco S, Epperly SP, Fujiwara M, Gomez Gamez D, Graham GL, Griffin WL (2016a) Development of a Kemp's ridley sea turtles stock assessment model. Gulf of Mexico Science 33:138–157.

Gallaway BJ, Gazey WJ, Wibbels T, Bevan E, Shaver DJ, George J (2016b) Evaluation of the status of the Kemp's ridley sea turtle after the 2010 Deepwater Horizon oil spill. Gulf of Mexico Science 33:192–205.

Gelman A, Rubin DB (1992) Inference from iterative simulation using multiple sequences. Statist Sci 7:457–472.

Gerber LR, Heppell SS (2004) The use of demographic sensitivity analysis in marine species conservation planning. Biological Conservation 120:121–128.

Geweke J (1992) Evaluating the accuracy of sampling-based approaches to the calculation of posterior moments.Bernardo JM, Berger JO, Dawid AP, Smith AFM (eds) Claredon Press, Oxford, U.K.

Giannini A, Chiang JCH, Cane MA, Kushnir Y, Seager R (2001) The ENSO Teleconnection to the tropical Atlantic Ocean: contributions of the remote and

local SSTs to rainfall variability in the topical Americas. Journal of Climate 14:4530–4544.

Gibbons JW (1967) Variation in growth rates in three populations of the painted turtle, *Chrysemys picta*. Herpetologica 23:296–303.

Gillanders BM (2002) Temporal and spatial variability in elemental composition of otoliths: implications for determining stock identify and connectivity of populations. Canadian Journal of Fisheries and Aquatic Sciences 59:669–679.

Godley BJ, Barbosa C, Bruford M, Broderick AC, Catry P, Coyne MS, Formia A, Hays GC, Witt MJ (2010) Unravelling migratory connectivity in marine turtles using multiple methods: migratory connectivity in marine turtles. Journal of Applied Ecology 47:769–778.

Goodman Hall AG, Avens L, McNeill JB, Wallace B, Goshe LR (2015) Inferring long-term foraging trends of individual juvenile loggerhead sea turtles using stable isotopes. Mar Ecol Prog Ser 537:265–276.

Gower J, Young E, King S (2013) Satellite images suggest a new Sargassum source region in 2011. Remote Sensing Letters 4:764–773.

Greene CH, Meyer-Gutbrod E, Monger BC, McGarry LP, Pershing AJ, Belkin IM, Fratantoni PS, Mountain DG, Pickart RS, Proshutinsky A, Ji R, Bisagni JJ, Hakkinen SMA, Haidvogel DB, Wang J, Head E, Smith P, Reid PC, Conversi A (2013) Remote climate forcing of decadal-scale regime shifts in Northwest Atlantic shelf ecosystems. Limnology and Oceanography 58:803–816.

GSFMC (2015) The blue crab fishery of the Gulf of Mexico: a regional management plan. Gulf State Marine Fisheries Commission, Ocean Springs, MS.

Hall RJ, Belisle AA, Sileo L (1983) Residues of petroleum hydrocarbons in tissues of sea turtles exposed to the Ixtoc I oil spill. Journal of Wildlife Diseases 19:106–109.

Halpern BS, Walbridge S, Selkoe KA, Kappel CV, Micheli F, D'Agrosa C, Bruno JF, Casey KS, Ebert C, Fox HE, Fujita R, Heinemann D, Lenihan HS, Madin EMP, Perry MT, Selig ER, Spalding M, Steneck R, Watson R (2008) A global map of human impact on marine ecosystems. Science 319:948–952.

Hamann M, Godfrey M, Seminoff J, Arthur K, Barata P, Bjorndal K, Bolten A, Broderick A, Campbell L, Carreras C, Casale P, Chaloupka M, Chan S, Coyne M, Crowder L, Diez C, Dutton P, Epperly S, FitzSimmons N, Formia A, Girondot M, Hays G, Cheng I, Kaska Y, Lewison R, Mortimer J, Nichols W, Reina R, Shanker K, Spotila J, Tomás J, Wallace B, Work T, Zbinden J, Godley B (2010) Global research priorities for sea turtles: informing management and conservation in the 21st century. Endangered Species Research 11:245–269.

Hamilton SL, Warner RR (2009) Otolith barium profiles verify the timing of settlement in a coral reef fish. Marine Ecology Progress Series 385:237–244.

Hammill MO, Sauvé C (2017) Growth and condition in harp seals: evidence of density-dependent and density-independent influences. ICES J Mar Sci 74:1395–1407.

Harrington JM, Myers RA, Rosenberg AA (2005a) Wasted fishery resources: discarded by-catch in the USA. Fish and Fisheries 6:350–361.

Harrington JM, Myers RA, Rosenberg AA (2005b) Wasted resources: bycatch and discards in U. S. Fisheries. Oceana, Washington, D.C.

Hart KM, Iverson AR, Fujisaki I, Lamont MM, Bucklin D, Shaver DJ (2018a) Marine threats overlap key foraging habitat for two imperiled sea turtle species in the Gulf of Mexico. Front Mar Sci 5.

Hart KM, Iverson AR, Fujisaki I, Lamont MM, Bucklin D, Shaver DJ (2018b) Sympatry or syntopy? Investigating drivers of distribution and co-occurrence for two imperiled sea turtle species in Gulf of Mexico neritic waters. Ecol Evol 8:12656–12669.

Hart KM, Lamont MM, Sartain AR, Fujisaki I (2014) Migration, foraging, and residency patterns for northern Gulf loggerheads: implications of local threats and international movements. PLOS ONE 9:e103453.

Hart KM, Mooreside P, Crowder LB (2006) Interpreting the spatio-temporal patterns of sea turtle strandings: going with the flow. Biological Conservation 129:283–290.

Hatase H, Omuta K, Tsukamoto K (2013) A mechanism that maintains alternative life histories in a loggerhead sea turtle population. Ecology 94:2583–2594.

Hatase H, Omuta K, Tsukamoto K (2010) Oceanic residents, neritic migrants: a possible mechanism underlying foraging dichotomy in adult female loggerhead turtles (*Caretta caretta*). Marine Biology 157:1337–1342.

Hawkes LA, Broderick AC, Coyne MS, Godfrey MH, Lopez-Jurado L-F, Lopez-Suarez P, Merino SE, Varo-Cruz N, Godley BJ (2006) Phenotypically linked dichotomy in sea turtle foraging requires multiple conservation approaches. Current Biology 16:990–995.

Hennicke JC, Culik BM (2005) Foraging performance and reproductive success of Humboldt penguins in relation to prey availability. Marine Ecology Progress Series 296:173–181.

Heppell SS (1998) Application of life history theory and population model analysis. Copeia 1998:367–375.

Heppell SS, Burchfield PM, Pena LJ (2007) Kemp's ridley recovery: how far have we come, and where are we headed? In: *Biology and Conservation of Ridley Sea Turtles*. Plotkin PT (ed) Johns Hopkins University Press, Baltimore, M.D., p 325–335

Heppell SS, Caswell H, Crowder LB (2000) Life histories and elasticity patterns: perturbation analysis for species with minimal demographic data. Ecology 81:654.

Heppell SS, Crouse DT, Crowder LB, Epperly SP, Gabriel W, Henwood T, Marquez R, Thompson NB (2004) A population model to estimate recovery time, population size and management impacts on Kemp's ridley sea turtles. Chelonian Conservation and Biology 4:765–771.

Heppell SS, Crowder LB, Crouse DT, Epperly SP, Frazer NB (2003a) Population models for Atlantic loggerheads: past, present and future. In: *Loggerhead Sea*

Turtles. Bolten AB, Witherington BE (eds) Smithsonian Institution Press, Washington, D.C., p 255–273

Heppell SS, Snover ML, Crowder LB (2003b) Sea turtle population ecology. In: *The Biology of Sea Turtles*. Lutz PL, Musick JA, Wyneken J (eds) CRC Press, Boca Raton, FL, p 275–306

Herdter ES, Chambers DP, Stallings CD, Murawski SA (2017) Did the *Deepwater Horizon* oil spill affect growth of Red Snapper in the Gulf of Mexico? Fisheries Research 191:60–68.

Higgins B, Cannon A, Gitschlag G (2007) Sea turtle decomposition study. Galveston, TX.

Hobson KA, Clark RG (1992) Assessing avian diets using stable isotopes II: factors influencing diet-tissue fractionation. The Condor 94:189–197.

Hochscheid S, Bentivegna F, Bradai M, Hays G (2007) Overwintering behaviour in sea turtles: dormancy is optional. Mar Ecol Prog Ser 340:287–298.

Horta-Puga G, Carriquiry JD (2014) The last two centuries of lead pollution in the Southern Gulf of Mexico recorded in the annual bands of the scleractinian coral *Orbicella faveolata*. Bulletin of Environmental Contamination and Toxicology 92:567–573.

Hothorn T, Hornik K, van de Wiel MA, Zeileis A (2006) Coin: conditional inference procedures in a permutation test framework. R package version 04-5.

Hothorn T, Lausen B (2003) On the exact distribution of maximally selected rank statistics. Computational Statistics & Data Analysis 43:121–137.

Hufbauer RA, Szűcs M, Kasyon E, Youngberg C, Koontz MJ, Richards C, Tuff T, Melbourne BA (2015) Three types of rescue can avert extinction in a changing environment. Proc Natl Acad Sci USA 112:10557–10562.

Humphreys RL, Campana SE, DeMartini EE (2005) Otolith elemental fingerprints of juvenile Pacific swordfish *Xiphias gladius*. Journal of Fish Biology 66:1660–1670.

Iraeta P, Monasterio C, Salvador A, Díaz JA (2006) Mediterranean hatchling lizards grow faster at higher altitude: a reciprocal transplant experiment. Functional Ecology 20:865–872.

Jansen T, Burns F (2015) Density dependent growth changes through juvenile and early adult life of North East Atlantic Mackerel (*Scomber scombrus*). Fisheries Research 169:37–44.

Jenkins LD (2012) Reducing sea turtle bycatch in trawl nets: A history of NMFS turtle excluder device (TED) research. Marine Fisheries Review 74:26–4419.

Jensen M. P, FitzSimmons NN, Dutton PH (2013) Molecular genetics of sea turtles. In: *The Biology of Sea Turtles*. Wyneken J, Lohmann KJ, Musick JA (eds) CRC Press, Boca Raton, FL, p 135–161

Karnauskas M, Schirripa MJ, Craig JK, Cook GS, Kelble CR, Agar JJ, Black BA, Enfield DB, Lindo-Atichati D, Muhling BA, Purcell KM, Richards PM, Wang C (2015) Evidence of climate-driven ecosystem reorganization in the Gulf of Mexico. Global Change Biology 21:2554–2568.

Katzenberg MA (2008) Stable isotope analysis: a tool for studying past diet, demography, and life history. In: *Biological Anthropology of the Human Skeleton*, 2nd ed. Katzenberg MA, Saunders SR (eds) John Wiley & Sons, Inc., Hoboken, NJ, p 413–441

Keeling CD, Mook WG, Tans PP (1979) Recent trends in the $^{13}C/^{12}C$ ratio of atmospheric carbon dioxide. Nature 277:121–122.

Keeling CD, Piper SC, Bacastow RB, Wahlen M, Whorf TP, Heimann M, Meijer HA (2001) Exchanges of atmospheric CO2 and $^{13}CO_2$ with the terrestrial biosphere and oceans from 1978 to 2000. I. Global aspects. SIO Reference Series, No 01-06, Scripps Institution of Oceanography, San Diego:88 pages.

Kellar NM, Speakman TR, Smith CR, Lane SM, Balmer BC, Trego ML, Catelani KN, Robbins MN, Allen CD, Wells RS, Zolman ES, Rowles TK, Schwacke LH (2017) Low reproductive success rates of common bottlenose dolphins *Tursiops truncatus* in the northern Gulf of Mexico following the Deepwater Horizon disaster (2010-2015). Endangered Species Research 33:143–158.

Kelly AE, Reuer MK, Goodkin NF, Boyle EA (2009) Lead concentrations and isotopes in corals and water near Bermuda, 1780–2000. Earth and Planetary Science Letters 283:93–100.

Kennicutt MC (2017) Oil and gas seeps in the Gulf of Mexico. In: *Habitats and Biota of the Gulf of Mexico: Before the Deepwater Horizon Oil Spill*. Ward CH (ed) Springer New York, New York, NY, p 275–358

Kent AJR (2008) In-situ analysis of Pb isotope ratios using laser ablation MC-ICP-MS: Controls on precision and accuracy and comparison between Faraday cup and ion counting systems. J Anal At Spectrom 23:968.

Kent AJR, Ungerer CA (2006) Analysis of light lithophile elements (Li, Be, B) by laser ablation ICP-MS: comparison between magnetic sector and quadrupole ICP-MS. American Mineralogist 91:1401–1411.

Kim SL, Tinker MT, Estes JA, Koch PL (2012) Ontogenetic and among-individual variation in foraging strategies of Northeast Pacific White sharks based on stable isotope analysis. PLoS ONE 7:e45068.

Koch PL (2007) Isotopic study of the biology of modern and fossil vertebrates. In: *Stable Isotopes in Ecology and Environmental Science*. Michener R, Lajtha K (eds) Blackwell Publishing, Malden, MA, p 99–154

Kocmoud AR, Wang H-H, Grant WE, Gallaway BJ (2019) Population dynamics of the endangered Kemp's ridley sea turtle following the 2010 oil spill in the Gulf of Mexico: Simulation of potential cause-effect relationships. Ecological Modelling 392:159–178.

Kurle CM, Koch PL, Tershy BR, Croll DA (2014) The effects of sex, tissue type, and dietary components on stable isotope discrimination factors ($\Delta^{13}C$ and $\Delta^{15}N$) in mammalian omnivores. Isotopes in Environmental and Health Studies 50:307–321.

Lamont MM, Fujisaki I (2014) Effects of ocean temperature on nesting phenology and fecundity of the loggerhead sea turtle (*Caretta caretta*). Journal of Herpetology 48:98–102.

Lane SM, Smith CR, Mitchell J, Balmer BC, Barry KP, McDonald T, Mori CS, Rosel PE, Rowles TK, Speakman TR, Townsend FI, Tumlin MC, Wells RS, Zolman ES, Schwacke LH (2015) Reproductive outcome and survival of common bottlenose dolphins sampled in Barataria Bay, Louisiana, USA, following the *Deepwater Horizon* oil spill. Proc R Soc B 282:20151944.

Larsson K, Forslund P (1991) Environmentally induced morphological variation in the Barnacle Goose, Branta leucopsis. Journal of Evolutionary Biology 4:619–636.

Lemons G, Lewison R, Komoroske L, Gaos A, Lai C-T, Dutton P, Eguchi T, LeRoux R, Seminoff JA (2011) Trophic ecology of green sea turtles in a highly urbanized bay: Insights from stable isotopes and mixing models. Journal of Experimental Marine Biology and Ecology 405:25–32.

Lenes JM, Darrow BP, Cattrall C, Heil CA, Callahan M, Vargo GA, Byrne RH, Prospero JM, Bates DE, Fanning KA, Walsh JJ (2001) Iron fertilization and the *Trichodesmium* response on the West Florida shelf. Limnology and Oceanography 46:1261–1277.

Lewison RL, Crowder LB, Wallace BP, Moore JE, Cox T, Zydelis R, McDonald S, DiMatteo A, Dunn DC, Kot CY, Bjorkland R, Kelez S, Soykan C, Stewart KR, Sims M, Boustany A, Read AJ, Halpin P, Nichols WJ, Safina C (2014) Global patterns of marine mammal, seabird, and sea turtle bycatch reveal taxa-specific and cumulative megafauna hotspots. Proceedings of the National Academy of Sciences 111:5271–5276.

López-Castro M, Bjorndal K, Kamenov G, Zenil-Ferguson R, Bolten A (2013) Sea turtle population structure and connections between oceanic and neritic foraging areas in the Atlantic revealed through trace elements. Marine Ecology Progress Series 490:233–246.

López-Castro MC, Bjorndal KA, Kamenov GD, Bolten AB (2014) Identifying oceanic foraging grounds of sea turtles in the Atlantic using lead isotopes. Marine Biology 161:2269–2278.

López-Duarte PC, Fodrie FJ, Jensen OP, Whitehead A, Galvez F, Dubansky B, Able KW (2016) Is exposure to Macondo oil reflected in the otolith chemistry of marsh-resident fish? PLOS ONE 11:e0162699.

Lorenzen K, Enberg K (2002) Density-dependent growth as a key mechanism in the regulation of fish populations: evidence from among-population comparisons. Proceedings of the Royal Society of London B: Biological Sciences 269:49–54.

Luczak C., Beaugrand G., Jaffré M., Lenoir S. (2011) Climate change impact on Balearic shearwater through a trophic cascade. Biology Letters 7:702–705.

MacArthur L, Phillips D, Hyndes G, Hanson C, Vanderklift M (2011) Habitat surrounding patch reefs influences the diet and nutrition of the western rock lobster. Mar Ecol Prog Ser 436:191–205.

Madsen T, Shine R (2000) Silver spoons and snake body sizes: prey availability early in life influences long-term growth rates of free-ranging pythons. Journal of Animal Ecology 69:952–958.

Martin TG, Chasdès I, Arcese P, Marra PP, Possingham HP, Norris DR (2007) Optimal conservation of migratory species. PLoS ONE:e751.

Martinez del Rio C, Wolf BO (2005) Mass-balance models for animal isotopic ecology. In: *Physiological and ecological adaptations to feeding in vertebrates*. Starck JM, Wang T (eds) Science Publishers, Enfield, New Hampshire, p 141–174

Matsubayashi J, Saitoh Y, Osada Y, Uehara Y, Habu J, Sasaki T, Tayasu I (2017) Incremental analysis of vertebral centra can reconstruct the stable isotope chronology of teleost fishes. Methods in Ecology and Evolution 8:1755–1763.

Mazaris AD, Kallimanis AS, Sgardelis SP, Pantis JD (2008) Do long-term changes in sea surface temperature at the breeding areas affect the breeding dates and reproduction performance of Mediterranean loggerhead turtles? Implications for climate change. Journal of Experimental Marine Biology and Ecology 367:219–226.

McAdam AG, Boutin S (2003) Effects of food abundance on genetic and maternal variation in the growth rate of juvenile red squirrels. Journal of Evolutionary Biology 16:1249–1256.

McCauley DJ, Pinsky ML, Palumbi SR, Estes JA, Joyce FH, Warner RR (2015) Marine defaunation: Animal loss in the global ocean. Science 347:1255641–1255641.

McClellan CM, Braun-McNeill J, Avens L, Wallace BP, Read AJ (2010) Stable isotopes confirm a foraging dichotomy in juvenile loggerhead sea turtles. Journal of Experimental Marine Biology and Ecology 387:44–51.

McClellan CM, Read AJ (2007) Complexity and variation in loggerhead sea turtle life history. Biology Letters 3:592–594.

McDermid KJ, Stuercke B, Balazs GH (2007) Nutritional composition of marine plants in the diet of the green sea turtle (Chelonia mydas) in the Hawaiian Islands. BULLETIN OF MARINE SCIENCE 81:17.

McDonald T, Schroeder B, Stacy B, Wallace B, Starcevich L, Gorham J, Tumlin M, Cacela D, Rissing M, McLamb D, Ruder E, Witherington B (2017) Density and exposure of surface-pelagic juvenile sea turtles to *Deepwater Horizon* oil. Endangered Species Research 33:69–82.

McMahon KW, Newsome SD (2018) Amino acid isotope analysis: a new frontier in studies of animal migration and foraging ecology. In: *Tracking Animal Migration with Stable Isotopes*, 2nd ed. Hobson KA, Wassenaar LI (eds) Academic Press, London, UK, p 173–190

McMichael E, Seminoff J, Carthy R (2008) Growth rates of wild green turtles, *Chelonia mydas*, at a temperate foraging habitat in the northern Gulf of Mexico: assessing short-term effects of cold-stunning on growth. Journal of Natural History 42:2793–2807.

McMillan MN, Izzo C, Junge C, Albert OT, Jung A, Gillanders BM (2017) Analysis of vertebral chemistry to assess stock structure in a deep-sea shark, *Etmopterus spinax*. ICES J Mar Sci 74:793–803.

Meador JP, Sommers FC, Ylitalo GM, Sloan CA (2006) Altered growth and related physiological responses in juvenile Chinook salmon (*Oncorhynchus tshawytscha*) from dietary exposure to polycyclic aromatic hydrocarbons (PAHs). Can J Fish Aquat Sci 63:2364–2376.

Mendelssohn IA, Andersen GL, Baltz DM, Caffey RH, Carman KR, Fleeger JW, Joye SB, Lin Q, Maltby E, Overton EB, Rozas LP (2012) Oil impacts on coastal wetlands: implications for the Mississippi River Delta ecosystem after the *Deepwater Horizon* oil spill. BioScience 62:562–574.

Michener RH, Schell DM (1994) Stable isotope ratios as tracers in marine aquatic food webs. In: *Stable Isotopes in Ecology and Environmental Science*. Lajtha K, Michener RH (eds) Blackwell, Oxford, p 138–157

Miller JA (2007) Scales of variation in otolith elemental chemistry of juvenile staghorn sculpin (*Leptocottus armatus*) in three Pacific Northwest estuaries. Marine Biology 151:483–494.

Mitchelmore C, Bishop C, Collier T (2017) Toxicological estimation of mortality of oceanic sea turtles oiled during the *Deepwater Horizon* oil spill. Endangered Species Research 33:39–50.

del Monte-Luna P, Guzmán-Hernández V, Cuevas EA, Arreguín-Sánchez F, Lluch-Belda D (2012) Effect of North Atlantic climate variability on hawksbill turtles in the Southern Gulf of Mexico. Journal of Experimental Marine Biology and Ecology 412:103–109.

Montoya JP, Carpenter EJ, Capone DG (2002) Nitrogen fixation and nitrogen isotope abundances in zooplankton of the oligotrophic North Atlantic. Limnology and Oceanography 47:1617–1628.

Moore JW, Semmens BX (2008) Incorporating uncertainty and prior information into stable isotope mixing models. Ecology Letters 11:470–480.

Morreale SJ, Plotkin PT, Shaver DJ, Kalb HJ (2007) Adult migration and habitat utilization: ridley turtles in their element. In: *Biology and Conservation of Ridley Sea Turtles*. Johns Hopkins University Press, Baltimore, M.D., p 213–229

Mulholland MR, Bernhardt PW, Heil CA, Bronk DA, O'Neil JM (2006) Nitrogen fixation and release of fixed nitrogen by *Trichodesmium* spp. in the Gulf of Mexico. Limnology and Oceanography 51:1762–1776.

Müller J, Hothorn T (2004) Maximally selected two-sample statistics as a new tool for the identification and assessment of habitat factors with an application to breeding-bird communities in oak forests. European Journal of Forest Research 123:219–228.

Murawski S, Fleeger J, Patterson III W, Hu C, Daly K, Romero I, Toro-Farmer G (2016) How did the Deepwater Horizon oil spill affect coastal and continental shelf ecosystems of the Gulf of Mexico? Oceanog 29:160–173.

Musick JA, Limpus CJ (1997) Habitat utilization and migration in juvenile sea turtles. In: *The Biology of Sea Turtles*. Lutz PL, Musick JA (eds) CRC Press, Boca Raton, FL, p 137–164

Myers RA, Worm B (2003) Rapid worldwide depletion of predatory fish communities. Nature 423:280–283.

National Research Council (2010) Assessment of sea-turtle status and trends: integrating demography and abundance. The National Academies Press, Washington, D.C.

National Research Council (ed) (1990) Decline of the sea turtles: causes and prevention. National Academy Press, Washington, D.C.

National Research Council (2003) Oil in the sea III: Inputs, fates, and effects. The National Academies Press, Washington, D.C.

Nero R, Cook M, Coleman A, Solangi M, Hardy R (2013) Using an ocean model to predict likely drift tracks of sea turtle carcasses in the north central Gulf of Mexico. Endang Species Res 21:191–203.

Newsome SD, Martinez del Rio C, Bearhop S, Phillips DL (2007) A niche for isotopic ecology. Frontiers in Ecology and the Environment 5:429–436.

NMFS, USFWS (2015) Kemp's ridley sea turtle (*Lepidochelys kempii*) 5-year review: summary and evaluation. National Marine Fisheries Service, Silver Spring, MD.

NMFS, USFWS, SEMARNAT (2011) Bi-national recovery plan for the Kemp's Ridley sea turtle (*Lepidochelys kempii*), Second Revision. National Marine Fisheries Service, Silver Spring, MD.

O'Brien S, Robert B, Tiandray H (2005) Hatch size, somatic growth rate and size-dependent survival in the endangered ploughshare tortoise. Biological Conservation 126:141–145.

Ogle DH, Wheeler P, Dinno A (2018) FSA: fisheries stock analysis. R package version 0822.

Ogren LH (1989) Distribution of juvenile and subadult Kemp's ridley turtles: Preliminary results from the 1984-1987 surveys. In: *Proceedings from the 1st Symposium on Kemp's ridley Sea Turtle Biology, Conservation, and Management. Sea Grant College Program, Galveston, TX*.

Omeyer L, Godley B, Broderick A (2017) Growth rates of adult sea turtles. Endangered Species Research 34:357–371.

Omeyer LCM, Fuller WJ, Godley BJ, Snape RTE, Broderick AC (2018) Determinate or indeterminate growth? Revisiting the growth strategy of sea turtles. Marine Ecology Progress Series 596:199–211.

Osuji L, Onojake C (2004) Trace heavy metals associated with crude oil: a case study of Ebocha-8 oil-spill-polluted site in Niger Delta, Nigeria. C&B 1:1708–1715.

Outridge PM, Stewart RE (1999) Stock discrimination of Atlantic walrus (*Odobenus rosmarus rosmarus*) in the eastern Canadian Arctic using lead isotope and element signatures in teeth. Can J Fish Aquat Sci 56:105–112.

Parham JF, Zug GR (1997) Age and growth of loggerhead sea turtles (*Caretta caretta*) of coastal Georgia: an assessment of skeletochronological age-estimates. Bulletin of Marine Science 61:287–304.

Parnell AC, Inger R, Bearhop S, Jackson AL (2010) Source partitioning using stable isotopes: coping with too much variation. PLoS ONE 5:e9672.

Parnell AC, Phillips DL, Bearhop S, Semmens BX, Ward EJ, Moore JW, Jackson AL, Grey J, Kelly DJ, Inger R (2013) Bayesian stable isotope mixing models. Environmetrics:n/a-n/a.

Pearson R, van de Merwe J, Limpus C, Connolly R (2017) Realignment of sea turtle isotope studies needed to match conservation priorities. Marine Ecology Progress Series 583:259–271.

Peckham SH, Maldonado Diaz D, Tremblay Y, Ochoa R, Polovina J, Balazs G, Dutton PH, Nichols WJ (2011) Demographic implications of alternative foraging strategies in juvenile loggerhead turtles *Caretta caretta* of the North Pacific Ocean. Marine Ecology Progress Series 425:269–280.

Peek S, Clementz MT (2012) Sr/Ca and Ba/Ca variations in environmental and biological sources: a survey of marine and terrestrial systems. Geochimica et Cosmochimica Acta 95:36–52.

Perez CR, Moye JK, Cacela D, Dean KM, Pritsos CA (2017) Body mass change in flying homing pigeons externally exposed to *Deepwater Horizon* crude oil. Ecotoxicology and Environmental Safety 146:104–110.

Peterson CH, Rice SD, Short JW, Esler D, Bodkin JL, Ballachey BE, Irons DB (2003) Long-term ecosystem response to the Exxon Valdez oil spill. Science 302:2082–2086.

Pfaller JB, Chaloupka M, Bolten AB, Bjorndal KA (2018) Phylogeny, biogeography and methodology: a meta-analytic perspective on heterogeneity in adult marine turtle survival rates. Scientific Reports 8.

Phillips DL (2001) Mixing models in analyses of diet using multiple stable isotopes: a critique. Oecologia 127:166–170.

Phillips DL, Inger R, Bearhop S, Jackson AL, Moore JW, Parnell AC, Semmens BX, Ward EJ (2014) Best practices for use of stable isotope mixing models in food-web studies. Canadian Journal of Zoology 92:823–835.

Phillips DL, Koch PL (2002) Incorporating concentration dependence in stable isotope mixing models. Oecologia 130:114–125.

Phillips DL, Newsome SD, Gregg JW (2005) Combining sources in stable isotope mixing models: alternative methods. Oecologia 144:520–527.

Piatt JF, Harding AMA, Shultz M, Speckman SG, Pelt TI van, Drew GS, Kettle AB (2007) Seabirds as indicators of marine food supplies: Cairns revisited. Marine Ecology Progress Series 352:221–234.

Piovano S, Clusa M, Carreras C, Giacoma C, Pascual M, Cardona L (2011) Different growth rates between loggerhead sea turtles (*Caretta caretta*) of Mediterranean and Atlantic origin in the Mediterranean Sea. Marine Biology 158:2577–2587.

Ponting M, Evans JA, Pashley V (2003) Fingerprinting of roman mints using laser-ablation MC-ICP-MS lead isotope analysis. Archaeometry 45:591–597.

Post DM (2002) Using stable isotopes to estimate trophic position: Models, methods, and assumptions. Ecology 83:703–718.

Post DM, Layman CA, Arrington DA, Takimoto G, Quattrochi J, Montaña CG (2007) Getting to the fat of the matter: models, methods and assumptions for dealing with lipids in stable isotope analyses. Oecologia 152:179–189.

Powers SP, Hernandez FJ, Condon RH, Drymon JM, Free CM (2013) Novel pathways for injury from offshore oil spills: direct, sublethal and indirect effects of the *Deepwater Horizon* oil spill on pelagic *Sargassum* communities. PLOS ONE 8:e74802.

Putman NF, Abreu-Grobois FA, Iturbe-Darkistade I, Putman EM, Richards PM, Verley P (2015) Deepwater Horizon oil spill impacts on sea turtles could span the Atlantic. Biology Letters 11:20150596.

Putman NF, Mansfield KL, He R, Shaver DJ, Verley P (2013) Predicting the distribution of oceanic-stage Kemp's ridley sea turtles. Biol Lett 9:20130345.

R Core Team (2019) R: A language and environment for statistical computing. R Foundation for Statistical Computing, Vienna, Austria.

Rabinowitz M. B, Wetherill G (1972) Identifying sources of lead contamination by stable isotope techniques. Environmental Science & Technology 6.

Ramirez M, Miller J, Parks E, Avens L, Goshe L, Seminoff J, Snover M, Heppell S (2019) Reconstructing sea turtle ontogenetic habitat shifts through trace element analysis of bone tissue. Marine Ecology Progress Series 608:247–262.

Ramirez MD, Avens L, Seminoff JA, Goshe LR, Heppell SS (2017) Growth dynamics of juvenile loggerhead sea turtles undergoing an ontogenetic habitat shift. Oecologia 183:1087–1099.

Ramirez MD, Avens L, Seminoff JA, Goshe LR, Heppell SS (2015) Patterns of loggerhead turtle ontogenetic shifts revealed through isotopic analysis of annual skeletal growth increments. Ecosphere 6:1–17.

Rees A, Alfaro-Shigueto J, Barata P, Bjorndal K, Bolten A, Bourjea J, Broderick A, Campbell L, Cardona L, Carreras C, Casale P, Ceriani S, Dutton P, Eguchi T, Formia A, Fuentes M, Fuller W, Girondot M, Godfrey M, Hamann M, Hart K, Hays G, Hochscheid S, Kaska Y, Jensen M, Mangel J, Mortimer J, Naro-Maciel E, Ng C, Nichols W, Phillott A, Reina R, Revuelta O, Schofield G, Seminoff J, Shanker K, Tomás J, van de Merwe J, Van Houtan K, Vander Zanden H, Wallace B, Wedemeyer-Strombel K, Work T, Godley B (2016) Are we working towards global research priorities for management and conservation of sea turtles? Endangered Species Research 31:337–382.

Reich KJ, Bjorndal KA, Martínez del Rio C (2008) Effects of growth and tissue type on the kinetics of ^{13}C and ^{15}N incorporation in a rapidly growing ectotherm. Oecologia 155:651–663.

Reich KJ, López-Castro MC, Shaver DJ, Iseton C, Hart KM, Hooper MJ, Schmitt CJ (2017) $\delta^{13}C$ and $\delta^{15}N$ in the endangered Kemp's ridley sea turtle *Lepidochelys kempii* after the *Deepwater Horizon* oil spill. Endangered Species Research 33:281–289.

Reid PC, Beaugrand G (2012) Global synchrony of an accelerating rise in sea surface temperature. Journal of the Marine Biological Association of the United Kingdom 92:1435–1450.

Renaud ML, Williams JA (2005) Kemp's ridley sea turtle movements and migrations. Chelonian Conservation and Biology 4:808–816.

Robinson KL, Ruzicka JJ, Hernandez FJ, Graham WM, Decker MB, Brodeur RD, Sutor M (2015) Evaluating energy flows through jellyfish and gulf menhaden (*Brevoortia patronus*) and the effects of fishing on the northern Gulf of Mexico ecosystem. ICES J Mar Sci 72:2301–2312.

Romero IC, Sutton T, Carr B, Quintana-Rizzo E, Ross SW, Hollander DJ, Torres JJ (2018) Decadal assessment of polycyclic aromatic hydrocarbons in mesopelagic fishes from the Gulf of Mexico reveals exposure to oil-derived sources. Environ Sci Technol 52:10985–10996.

Romero IC, Toro-Farmer G, Diercks A-R, Schwing P, Muller-Karger F, Murawski S, Hollander DJ (2017) Large-scale deposition of weathered oil in the Gulf of Mexico following a deep-water oil spill. Environmental Pollution 228:179–189.

Rooker JR, Secor DH, Zdanowicz VS, Itoh T (2001) Discrimination of northern bluefin tuna from nursery areas in the Pacific Ocean using otolith chemistry. Marine Ecology Progress Series 218:275–282.

Rouhani S, Baker MC, Steinhoff M, Zhang M, Oehrig J, Zelo IJ, Emsbo-Mattingly SD, Nixon Z, Willis JM, Hester MW (2017) Nearshore exposure to *Deepwater Horizon* oil. Marine Ecology Progress Series 576:111–124.

Rozas LP, Minello TJ, Miles MS (2014) Effect of Deepwater Horizon oil on growth rates of juvenile Penaeid shrimps. Estuaries and Coasts 37:1403–1414.

Rudloe A, Rudloe J (2005) Site specificity and the impact of recreational fishing activity on subadult endangered Kemp's ridley sea turtles in estuarine foraging habitats in the northeastern Gulf of Mexico. goms 23.

Runge CA, Martin TG, Possingham HP, Willis SG, Fuller RA (2014) Conserving mobile species. Frontiers in Ecology and the Environment 12:395–402.

Sæther B-E, Bakke Ø (2000) Avian life history variation and contribution of demographic traits to the population growth rate. Ecology 81:642–653.

Sanchez-Rubio G, Perry H, Franks JS, Johnson DR (2018) Occurrence of pelagic *Sargassum* in waters of the U.S. Gulf of Mexico in response to weather-related hydrographic regimes associated with decadal and interannual variability in global climate. Fishery Bulletin 116:93–106.

Sanchez-Rubio G, Perry HM, Biesiot PM, Johnson DR, Lipcius RN (2011) Climate-related hydrological regimes and their effects on abundance of juvenile blue crabs (*Callinectes sapidus*) in the northcentral Gulf of Mexico. Fishery Bulletin 109:139–146.

Sangster DF, Outridge PM, Davis WJ (2000) Stable lead isotope characteristics of lead ore deposits of environmental significance. Environmental Reviews 8:115–147.

Santos BS, Friedrichs MAM, Rose SA, Barco SG, Kaplan DM (2018) Likely locations of sea turtle stranding mortality using experimentally-calibrated, time and space-specific drift models. Biological Conservation 226:127–143.

Schaafsma FL, Cherel Y, Flores H, van Franeker JA, Lea M-A, Raymond B, van de Putte AP (2018) Review: the energetic value of zooplankton and nekton species of the Southern Ocean. Mar Biol 165:129.

Schmid JR (1995) Marine turtle populations on the east-central coast of Florida: results of tagging studies at Cape Canaveral, Florida, 1986-1991. Fishery Bulletin 93:139–151.

Schmid JR (1998) Marine turtle populations on the West-central coast of Florida: Results of tagging studies at the Cedar Keys, Florida, 1986-1995. Fishery Bulletin 96:589–602.

Schmid JR, Tucker AD (2018) Comparing diets of Kemp's ridley sea turtles (*Lepidochelys kempii*) in mangrove estuaries of Southwest Florida. Journal of Herpetology 52:252–258.

Schmid JR, Witzell WN (1997) Age and growth of wild Kemp's ridley turtles (*Lepidochelys kempi*): cumulative results of tagging studies in Florida. Chelonian Conservation and Biology 2:532–537.

Schmid JR, Witzell WN (2006) Seasonal migrations of immature Kemp's ridley turtles (*Lepidochelys kempii*) aling the West coast of Florida. Gulf of Mexico Science 24:28–40.

Schroeder HA, Tipton IH, Nason AP (1972) Trace metals in man: strontium and barium. Journal of Chronic Diseases 25:491–517.

Schwacke L, Thomas L, Wells R, McFee W, Hohn A, Mullin K, Zolman E, Quigley B, Rowles T, Schwacke J (2017) Quantifying injury to common bottlenose dolphins from the *Deepwater Horizon* oil spill using an age-, sex- and class-structured population model. Endangered Species Research 33:265–279.

Schwacke LH, Smith CR, Townsend FI, Wells RS, Hart LB, Balmer BC, Collier TK, De Guise S, Fry MM, Guillette LJ, Lamb SV, Lane SM, McFee WE, Place NJ, Tumlin MC, Ylitalo GM, Zolman ES, Rowles TK (2014) Health of Common Bottlenose Dolphins (*Tursiops truncatus*) in Barataria Bay, Louisiana, following the *Deepwater Horizon* oil spill. Environmental Science & Technology 48:93–103.

Scott R, Marsh R, Hays GC (2012) Life in the really slow lane: loggerhead sea turtles mature late relative to other reptiles. Functional Ecology 26:227–235.

Scott-Denton E, Cryer PF, Duffy MR, Gocke JP, Harrelson MR, Kinsella DL, Nance JM, Pulver JR, Smith RC, Williams JA (2012) Characterization of the U.S. Gulf of Mexico and South Atlantic Penaeid and Rock Shrimp Fisheries Based on Observer Data. Marine Fisheries Review 74:1–27.

Semmens BX, Ward EJ, Moore JW, Darimont CT (2009) Quantifying Inter- and Intra-Population Niche Variability Using Hierarchical Bayesian Stable Isotope Mixing Models. PLOS ONE 4:e6187.

Seney E, Landry Jr AM (2011) Movement patterns of immature and adult female Kemp's ridley sea turtles in the northwestern Gulf of Mexico. Marine Ecology Progress Series 440:241–254.

Seney EE (2016) Diet of Kemp's ridley sea turtles incidentally caught on recreational fishing gear in the Northwestern Gulf of Mexico. Chelonian Conservation and Biology 15:132–137.

Seney EE, Musick JA (2005) Diet analysis of Kemp's ridley sea turtles (*Lepidochelys kempii*) in Virginia. Chelonian Conservation and Biology 4:864–871.

Servis JA, Lovewell G, Tucker AD (2015) Diet analysis of subadult Kemp's ridley (*Lepidochelys kempii*) turtles from West-central Florida. Chelonian Conservation and Biology 14:173–181.

Shaver DJ (1991) Feeding ecology of wild and head-started Kemp's ridley sea turtles in South Texas waters. Journal of Herpetology 25:327.

Shaver DJ, Hart KM, Fujisaki I, Rubio C, Sartain AR, Peña J, Burchfield PM, Gamez DG, Ortiz J (2013) Foraging area fidelity for Kemp's ridleys in the Gulf of Mexico. Ecology and Evolution 3:2002–2012.

Shaver DJ, Rubio C (2008) Post-nesting movement of wild and head-started Kemp's ridley sea turtles *Lepidochelys kempii* in the Gulf of Mexico. Endangered Species Research 4:43–55.

Shaver DJ, Rubio C, Shelby Walker J, George J, Amos AF, Reich K, Jones C, Shearer T (2016) Kemp's ridley sea turtle (*Lepidochelys kempii*) nesting on the Texas coast: geographic, temporal, and demographic trends through 2014. Gulf of Mexico Science 33.

Shen GT, Boyle EA (1987) Lead in corals: reconstruction of historical industrial fluxes to the surface ocean. Earth and Planetary Science Letters 82:289–304.

Shiel AE, Weis D, Orians KJ (2010) Evaluation of zinc, cadmium and lead isotope fractionation during smelting and refining. Science of The Total Environment 408:2357–2368.

Shiel AE, Weis D, Orians KJ (2012) Tracing cadmium, zinc and lead sources in bivalves from the coasts of western Canada and the USA using isotopes. Geochimica et Cosmochimica Acta 76:175–190.

Shoop CR, Ruckdeschel C (1982) Increasing turtle strandings in the southeast United States: A complicating factor. Biological Conservation 23:213–215.

Snover ML (2002) Growth and ontogeny of sea turtles using skeletochronology: methods, validation and application to conservation. Duke University, Durham, NC

Snover ML, Avens L, Hohn AA (2007a) Back-calculating length from skeletal growth marks in loggerhead sea turtles *Caretta caretta*. Endangered Species Research 3:95–104.

Snover ML, Hohn AA (2004) Validation and interpretation of annual skeletal marks in loggerhead (*Caretta caretta*) and Kemp's ridley (*Lepidochelys kempii*) sea turtles. Fisheries Bulletin 102:682–692.

Snover ML, Hohn AA, Crowder LB, Heppell SS (2007b) Age and growth in Kemp's ridley sea turtles: evidence from mark-recapture and skeletochronology. In:

Biology and Conservation of Ridley Sea Turtles. Plotkin PT (ed) Johns Hopkins University Press, Baltimore, M.D., p 89–106

Snover ML, Hohn AA, Crowder LB, Macko SA (2010) Combining stable isotopes and skeletal growth marks to detect habitat shifts in juvenile loggerhead sea turtles *Caretta caretta*. Endangered Species Research 13:25–31.

Soto-Jiménez MF, Hibdon SA, Rankin CW, Aggarawal J, Ruiz-Fernández AC, Páez-Osuna F, Flegal AR (2006) Chronicling a century of lead pollution in Mexico: stable lead isotopic composiiton analyses of dated sediment cores. Environmental Science & Technology 40:764–770.

Spencer K, Shafer DJ, Gauldie RW, DeCarlo EH (2000) Stable lead isotope ratios from distinct anthropogenic sources in fish otoliths: a potential nursery ground stock marker. Comparative Biochemistry and Physiology Part A: Molecular & Integrative Physiology 127:273–284.

Stacey JS, Kramers JD (1975) Approximation of terrestrial lead isotope evolution by a two-stage model. Earth and Planetary Science Letters 26:207–221.

Stacy BA (2015) Summary of necropsy findings for non-visibly oiled sea turtles documented by stranding response in Alabama, Louisiana, and Mississippi 2010 through 2014.

Stacy N, Field C, Staggs L, MacLean R, Stacy B, Keene J, Cacela D, Pelton C, Cray C, Kelley M, Holmes S, Innis C (2017) Clinicopathological findings in sea turtles assessed during the Deepwater Horizon oil spill response. Endangered Species Research 33:25–37.

Stearns SC (1992) The evolution of life histories. Oxford University Press, Oxford, U.K.

Stern RA, Outridge PM, Davis WJ, Stewart REA (1999) Reconstructing lead isotope exposure histories preserved in the growth layers of walrus teeth using the SHRIMP II ion microprobe. Environmental Science & Technology 33:1771–1775.

Stewart RE, Outridge PM, Stern RA (2003) Walrus life-history movements reconstructed from lead isotopes in annual layers of teeth. Marine mammal science 19:806–818.

Stock BC, Jackson AL, Ward EJ, Parnell AC, Phillips DL, Semmens BX (2018) Analyzing mixing systems using a new generation of Bayesian tracer mixing models. PeerJ 6:e5096.

Stock BC, Semmens BX (2016) Unifying error structures in commonly used biotracer mixing models. Ecology 97:2562–2569.

Sturrock AM, Hunter E, Milton JA, EIMF, Johnson RC, Waring CP, Trueman CN (2015) Quantifying physiological influences on otolith microchemistry. Methods in Ecology and Evolution 6:806–816.

Sturrock AM, Trueman CN, Darnaude AM, Hunter E (2012) Can otolith elemental chemistry retrospectively track migrations in fully marine fishes? Journal of Fish Biology 81:766–795.

Tanner SE, Reis-Santos P, Cabral HN (2015) Otolith chemistry in stock delineation: A brief overview, current challenges and future prospects. Fisheries Research.

Thomas ORB, Ganio K, Roberts BR, Swearer SE (2017) Trace element–protein interactions in endolymph from the inner ear of fish: implications for environmental reconstructions using fish otolith chemistry. Metallomics 9:239–249.

Thresher RE (1999) Elemental composition of otoliths as a stock delineator in fishes. Fisheries Research 43:165–204.

Tibbetts SM, Milley JE, Lall SP (2006) Apparent protein and energy digestibility of common and alternative feed ingredients by Atlantic cod, *Gadus morhua* (Linnaeus, 1758). Aquaculture 261:1314–1327.

Tucker AD, MacDonald BD, Seminoff JA (2014) Foraging site fidelity and stable isotope values of loggerhead turtles tracked in the Gulf of Mexico and northwest Caribbean. Mar Ecol Prog Ser 502:267–279.

Turner Tomaszewicz CN, Seminoff JA, Peckham SH, Avens L, Kurle CM (2017a) Intrapopulation variability in the timing of ontogenetic habitat shifts in sea turtles revealed using δ15N values from bone growth rings. J Anim Ecol 86:694–704.

Turner Tomaszewicz CN, Seminoff JA, Price M, Kurle CM (2017b) Stable isotope discrimination factors and between-tissue isotope comparisons for bone and skin from captive and wild green sea turtles (*Chelonia mydas*). Rapid Commun Mass Spectrom 31:1903–1914.

Turner Tomaszewicz CN, Seminoff JA, Ramirez MD, Kurle CM (2015) Effects of demineralization on the stable isotope analysis of bone samples. Rapid Commun Mass Spectrom 29:1879–1888.

Turtle Expert Working Group (1998) An assessment of the Kemp's ridley (*Lepidochelys kempii*) and loggerhead (*Caretta caretta*) sea turtle populations in the western North Atlantic.

Turtle Expert Working Group (2000) Assessment update for the Kemp's ridley and loggerhead sea turtle populations in the western North Atlantic.

Van Houtan KS, Halley JM (2011) Long-term climate forcing in loggerhead sea turtle nesting. PLoS ONE 6:e19043.

Vander Zanden HB, Bjorndal KA, Mustin W, Ponciano JM, Bolten AB (2012) Inherent variation in stable isotope values and discrimination factors in two life stages of green turtles. Physiological and Biochemical Zoology 85:431–441.

Vander Zanden HB, Tucker AD, Hart KM, Lamont MM, Fujisaki I, Addison DS, Mansfield KL, Phillips KF, Wunder MB, Bowen GJ, Pajuelo M, Bolten AB, Bjorndal KA (2015) Determining origin in a migratory marine vertebrate: a novel method to integrate stable isotopes and satellite tracking. Ecological Applications 25:320–335.

VanderKooy S (2013) Stock assessment report GDAR 01: Gulf of Mexico blue crab. Ocean Springs, MS.

Venables WN, Ripley BD (2002) Modern Applied Statistics with S. Springer, New York.

Villamarín F, Jardine TD, Bunn SE, Marioni B, Magnusson WE (2018) Body size is more important than diet in determining stable-isotope estimates of trophic position in crocodilians. Sci Rep 8:2020.

de Villiers S (1999) Seawater strontium and Sr/Ca variability in the Atlantic and Pacific oceans. Earth and Planetary Science Letters 171:623–634.

Wallace B, Stacy B, Rissing M, Cacela D, Garrison L, Graettinger G, Holmes J, McDonald T, McLamb D, Schroeder B (2017a) Estimating sea turtle exposures to *Deepwater Horizon* oil. Endangered Species Research 33:51–67.

Wallace BP, Avens L, Braun-McNeill J, McClellan CM (2009) The diet composition of immature loggerheads: Insights on trophic niche, growth rates, and fisheries interactions. Journal of Experimental Marine Biology and Ecology 373:50–57.

Wallace BP, Brosnan T, McLamb D, Rowles T, Ruder E, Schroeder B, Schwacke L, Stacy B, Sullivan L, Takeshita R, Wehner D (2017b) Effects of the *Deepwater Horizon* oil spill on protected marine species. Endangered Species Research 33:1–7.

Walther BD, Kingsford MJ, O'Callaghan MD, McCulloch MT (2010) Interactive effects of ontogeny, food ration and temperature on elemental incorporation in otoliths of a coral reef fish. Environ Biol Fish 89:441–451.

Walther BD, Thorrold SR (2006) Water, not food, contributes the majority of strontium and barium deposited in the otoliths of a marine fish. Mar Ecol Prog Ser 311:125–130.

Warden ML, Haas HL, Rose KA, Richards PM (2015) A spatially explicit population model of simulated fisheries impact on loggerhead sea turtles (*Caretta caretta*) in the Northwest Atlantic Ocean. Ecological Modelling 299:23–39.

Warner RR, Swearer SE, Caselle JE, Sheehy M, Paradis G (2005) Natal trace-elemental signatures in the otoliths of an open-coast fish. Limnol Oceanogr 50:1529–1542.

Webb EC, Stewart A, Miller B, Tarlton J, Evershed RP (2016) Age effects and the influence of varying proportions of terrestrial and marine dietary protein on the stable nitrogen-isotope compositions of pig bone collagen and soft tissues from a controlled feeding experiment. STAR: Science & Technology of Archaeological Research 2:54–66.

Webster MS, Marra PP, Haig SM, Bensch S, Holmes RT (2002) Links between worlds: unraveling migratory connectivity. Trends in Ecology & Evolution 17:76–83.

Weihs C, Ligges U, Luebke K, Raabe N (2005) KlaR Analyzing German Business Cycles. In: *Data Analysis and Decision Support*. Baier D, Decker R, Schmidt-Thieme L (eds) Springer-Verlag, Berlin, p 3350343

Weis D, Kieffer B, Maerschalk C, Barling J, de Jong J, Williams GA, Hanano D, Pretorius W, Mattielli N, Scoates JS, Goolaerts A, Friedman RM, Mahoney JB (2006) High-precision isotopic characterization of USGS reference materials by TIMS and MC-ICP-MS. Geochemistry, Geophysics, Geosystems 7:n/a-n/a.

Weiss D, Boyle EA, Wu J, Chavagnac V, Michel A, Reuer MK (2003) Spatial and temporal evolution of lead isotope ratios in the North Atlantic Ocean between 1981 and 1989. Journal of Geophysical Research 108.

Weiss D, Shotyk W, Kempf MA (1999) Archives of atmospheric lead pollution. Naturwissenschaften 86:262–275.

Werner EE, Gilliam JF (1984) The ontogenetic niche and species interactions in size-structured populations. Annual Review of Ecology and Systematics 15:393–425.

Werner SA (1994) Feeding ecology of wild and head stared Kemp's ridley sea turtles. Master's Thesis, Texas A&M University, College Station, TX

Wibbels T, Bevan E (2019) *Lepidochelys kempii*. The IUCN Red List of Threatened Species e.T11533A142050590.

Williams NC, Bjorndal KA, Lamont MM, Carthy RR (2014) Winter diets of immature green turtles (*Chelonia mydas*) on a northern feeding ground: integrating stomach contents and stable isotope analyses. Estuaries and Coasts 37:986–994.

Wilmers CC, Nickel B, Bryce CM, Smith JA, Wheat RE, Yovovich V (2015) The golden age of bio-logging: how animal-borne sensors are advancing the frontiers of ecology. Ecology 96:1741–1753.

Wilson RM, Cherrier J, Sarkodee-Adoo J, Bosman S, Mickle A, Chanton JP (2015) Tracing the intrusion of fossil carbon into coastal Louisiana macrofauna using natural 14C and 13C abundances. Deep Sea Research Part II: Topical Studies in Oceanography.

Wise JP, Wise JTF, Wise CF, Wise SS, Gianios C, Xie H, Thompson WD, Perkins C, Falank C, Wise JP (2014) Concentrations of the genotoxic metals, Chromium and Nickel, in Whales, tar balls, oil slicks, and released oil from the Gulf of Mexico in the immediate aftermath of the Deepwater Horizon oil crisis: Is genotoxic metal exposure part of the Deepwater Horizon legacy? Environmental Science & Technology 48:2997–3006.

Witherington B (2002) Ecology of neonate loggerhead turtles inhabiting lines of downwelling near a Gulf Stream front. Marine Biology 140:843–853.

Witherington B, Hirama S, Hardy R (2012) Young sea turtles of the pelagic *Sargassum*-dominated drift community: habitat use, population density, and threats. Marine Ecology Progress Series 463:1–22.

Witzell WN, Schmid JR (2005) Diet of immature Kemp's ridley turtles (*Lepidochelys kempi*) from Gullivan Bay, Ten Thousand Islands, southwest Florida. Bulletin of Marine Science 77:191–200.

Witzell WN, Schmid JR (2004) Immature sea turtles in Gullivan Bay, Ten Thousand Islands, southwest Florida. goms 22.

Wood SN (2006) Generalized Additive Models: an introduction with R. Chapman and Hall/CRC, Boca Raton, FL.

Ylitalo G, Collier T, Anulacion B, Juaire K, Boyer R, da Silva D, Keene J, Stacy B (2017) Determining oil and dispersant exposure in sea turtles from the

northern Gulf of Mexico resulting from the *Deepwater Horizon* oil spill. Endangered Species Research 33:9–24.

Zbinden J, Bearhop S, Bradshaw P, Gill B, Margaritoulis D, Newton J, Godley B (2011) Migratory dichotomy and associated phenotypic variation in marine turtles revealed by satellite tracking and stable isotope analysis. Marine Ecology Progress Series 421:291–302.

Zeileis A, Kleiber C, Krämer W, Hornik K (2003) Testing and dating of structural changes in practice. Computational Statistics & Data Analysis 44:109–123.

Zeileis A, Leisch F, Hornik K, Kleiber C (2002) Strucchange: An R Package for Testing for Structural Change in Linear Regression Models. Journal of Statistical Software 7:1–38.

Zug GR, Kalb HJ, Luzar SJ (1997) Age and growth in wild Kemp's ridley sea turtles *Lepidochelys kempii* from skeletochronological data. Biological Conservation 80:261–268.

Zug GR, Wynn AH, Ruckdeschel C (1986) Age determination of loggerhead sea turtles, *Caretta caretta*, by incremental growth marks in the skeleton. Smithsonian Contributions to Zoology 427:1–44.

APPENDIX A: CHAPTER 2 SUPPLEMENTAL INFORMATION

Table A1. Summary characteristics for stranded Kemp's ridley sea turtles by stranding state.

Location	Stranding data				Growth rate data	
	n	SCL (cm) Mean ± SD (range)	Age (yr) Mean ± SD (range)	Year range	*n*	Year range
Texas	200	55.6 ± 10.9 (4.2 – 69.1)	11.87 ± 6.47 (1.00 – 30.25)	1997 – 2013	915	1988 – 2012
Louisiana	193	41.1 ± 12.1 (16.6 – 65.4)	4.82 ± 4.02 (0.75 – 20.25)	1999 – 2015	425	1998 – 2014
Mississippi	185	39.7 ± 10.7 (21.0 – 66.2)	5.10 ± 4.60 (0.75 – 20.75)	1993 – 2016	479	1990 – 2015
Alabama	61	38.1 ± 9.1 (23.4 – 65.4)	4.26 ± 4.68 (1.25 – 23.00)	1997 – 2014	151	1994 – 2013
Florida, Gulf	142	41.1 ± 11.0 (20.3 – 65.4)	4.62 ± 3.23 (1.00 – 15.75)	1998 – 2013	354	1994 – 2013
Florida, Atlantic	17	51.1 ± 9.7 (31.5 – 66.7)	9.70 ± 4.19 (2.50 – 18.75)	1998 – 2012	87	1995 – 2010
Georgia	15	37.4 ± 7.2 (28.5 – 50.8)	5.23 ± 2.28 (2.00 – 9.50)	2002 – 2011	51	1998 – 2010
South Carolina	6	40.2 ± 10.9 (25.1 – 55.9)	5.34 ± 3.09 (1.75 – 10.25)	2011 – 2012	23	2005 – 2011
North Carolina	255	35.1 ± 9.3 (19.3 – 64.4)	4.14 ± 2.65 (1.00 – 14.75)	1993 – 2016	602	1991 – 2015
Virginia	69	42.7 ± 9.1 (23.1 – 59.8)	6.28 ± 3.05 (1.25 – 16.00)	1998 – 2013	261	1994 – 2011
Delaware	1	23.2	1.00	2011	1	2010
New Jersey	4	28.4 ± 5.5 (23.3 – 36.0)	3.76 ± 1.35 (2.00 – 5.50)	2004 – 2012	13	2000 – 2011
New York	4	26.4 ± 2.1 (23.8 – 28.3)	2.75 ± 1.36 (1.25 – 4.50)	2001 – 2001	10	1996 – 2000
Massachusetts	68	28.1 ± 4.1 (19.3 – 40.0)	3.73 ± 1.38 (1.25 – 8.50)	2002 – 2017	195	1999 – 2015

*Stranding state unknown for 15 turtles (2 in Gulf of Mexico, 13 in Atlantic)

Table A2. Results of Reverse Helmert Coding schemes used to compare mean age class-specific growth rates of Kemp's ridley sea turtles before and after the Deepwater Horizon oil spill. Number of asterisks (*) indicates degree of significance based on p–values for Reverse Helmert Coding schemes (* = $p < 0.05$, ** = $p < 0.01$, *** = $p < 0.001$; empty cells mean no significant change in mean growth rate). Colors indicate direction of change in mean growth rate (**black** = increase, **red** = decrease). Shaded rows identify significant years where there was concordance complementary breakpoint and cutpoint analyses. Analyses excluded years with $N < 5$ (noted by dash).

Reverse Helmert comparison	Age class						
		Gulf of Mexico stranded turtles			Atlantic stranded turtles		
Comparison	0	1	2–5	6–9	1	2–5	6–9
2000 vs. 1995–1999				**			
2001 vs. 1995–2000							
2002 vs. 1995–2001		–					
2003 vs. 1995–2002		–					
2004 vs. 1995–2003					–	*	
2005 vs. 1995–2004				*			
2006 vs. 1995–2005		–	**				
2007 vs. 1995–2006					**		
2008 vs. 1995–2007							
2009 vs. 1995–2008							
2010 vs. 1995–2009		*				***	
2011 vs. 1995–2009						**	–
2012 vs. 1995–2009	**		*			*	–
2013 vs. 1995–2009	***		*	–			–
2014 vs. 1995–2009			***	–	**	***	–
2015 vs. 1995–2009	–	–		–	–		–

Table A3. Summary of statistical output for age class-specific Generalized Additive Models (GAMs) used to analyze the influence of population density metrics on mean back–calculated growth rates for Kemp's ridley sea turtles stranded in the U.S. Gulf of Mexico and Atlantic Coasts. *Abund* is cumulative oceanic or neritic juvenile turtle abundance in a given year estimated from a Kemp's ridley sea turtle population model (up to 2009; NMFS & USFWS 2015). *HatchProd* is cumulative hatchling production for years, t(x), prior to a given year. Dev = deviance explained by the model (data sourced from NMFS & USFWS 2015). The models exclude years with $N < 5$.

					Smooth term			
Model	*N*	Dev (%)	Adj. R^2	AIC	Variable	*Edf*	*F*	Prob(*F*)
(a) Model: growth rate ~ turtle abundance								
GAM_{Age0}	15	9.4	0.03	22.08	Abund (Σ Ages 0–1)	1.00	1.34	0.267
GAM_{Age1_GoM}	9	72.8	0.57	22.67	Abund (Σ Ages 0–1)	2.96	3.00	0.117
GAM_{Age1_Atl}	11	35.2	0.23	31.03	Abund (Σ Ages 0–1)	1.61	1.94	0.212
$GAM_{Age2–5_GoM}$	15	52.8	0.42	24.36	Abund (Σ Ages 2–5)	2.60	3.43	**0.051**
$GAM_{Age2–5_Atl}$	15	37.7	0.26	16.82	Abund (Σ Ages 2–5)	2.23	2.35	0.154
$GAM_{Age6–9_GoM}$	15	1.36	–0.06	22.70	Abund (Σ Ages 2–5)	1.00	0.18	0.679
$GAM_{Age6–9_Atl}$	11	5.70	5.16	13.34	Abund (Σ Ages 2–5)	1.00	0.54	0.479
Model: growth rate ~ prior hatchling production								
GAM_{Age0}	20	15.5	0.11	43.69	HatchProd (Σ t_0–t_{-1})	1.00	3.30	0.086
GAM_{Age1_GoM}	14	0.01	–0.08	39.04	HatchProd (Σ t_0–t_{-1})	1.00	0.00	0.979
GAM_{Age1_ATL}	16	60.2	0.46	40.43	HatchProd (Σ t_0–t_{-1})	4.00	2.65	0.071
$GAM_{Age2–5_GoM}$	21	48.5	0.41	43.82	HatchProd (Σ t_{-2}–t_{-5})	2.73	4.17	**0.018**
$GAM_{Age2–5_Atl}$	21	2.43	–0.03	51.09	HatchProd (Σ t_{-2}–t_{-5})	1.00	0.47	0.500
$GAM_{Age6–9_GoM}$	18	24.4	0.14	28.34	HatchProd (Σ t_{-2}–t_{-5})	1.84	1.82	0.197
$GAM_{Age6–9_Atl}$	12	7.34	–0.02	12.97	HatchProd (Σ t_{-2}–t_{-5})	1.00	0.79	0.394

Table A4. Cross-correlation coefficients for comparison of age class-specific mean growth rates and lagged climate indices (0- to 5-yr lags). Bold numbers identify correlation values ≥ 0.50. Colors and shading indicated direction and degree of correlations, respectively (blue = negative correlation, red = positive correlation).

	Lag year					
Age class	0	1	2	3	4	5
Winter North Atlantic Oscillation (wNAO) Index						
Age 0	0.22	0.46	**0.59**	**0.54**	**0.54**	**0.60**
Age 1_{GoM}	0.23	0.20	0.17	0.16	0.02	–0.13
Age $1_{Atlantic}$	0.30	0.26	0.15	–0.12	–0.17	–0.22
Age $2–5_{GoM}$	–0.27	–0.05	0.09	0.21	0.27	0.32
Age $2–5_{Atlantic}$	–0.09	–0.01	0.04	0.14	0.23	0.25
Age $6–9_{GoM}$	–0.06	–0.23	–0.42	–0.44	**–0.53**	**–0.59**
Age $6–9_{Atlantic}$	0.34	0.35	0.35	0.11	0.08	0.06
Atlantic Multidecadal Oscillation (AMO) Index						
Age 0	–0.17	–0.42	**–0.57**	**–0.52**	**–0.52**	**–0.60**
Age 1_{GoM}	–0.25	–0.22	–0.19	–0.20	–0.06	0.09
Age $1_{Atlantic}$	–0.31	–0.29	–0.18	0.10	0.16	0.21
Age $2–5_{GoM}$	0.31	0.08	–0.05	–0.17	–0.23	–0.28
Age $2–5_{Atlantic}$	0.11	0.04	–0.01	–0.11	–0.20	–0.22
Age $6–9_{GoM}$	0.01	0.19	0.39	0.42	**0.52**	**0.60**
Age $6–9_{Atlantic}$	–0.33	–0.35	–0.36	–0.11	–0.09	–0.07
Multivariate El Niño Southern Oscillation Index (MEI)						
Age 0	**0.51**	**0.59**	**0.60**	0.49	0.41	0.40
Age 1_{GoM}	–0.03	–0.03	–0.03	–0.01	–0.08	–0.15
Age $1_{Atlantic}$	0.03	0.03	–0.04	–0.21	–0.22	–0.23
Age $2–5_{GoM}$	0.21	0.32	0.36	0.39	0.37	0.34
Age $2–5_{Atlantic}$	0.24	0.25	0.24	0.26	0.28	0.25
Age $6–9_{GoM}$	–0.25	–0.32	–0.40	–0.36	–0.37	–0.38
Age $6–9_{Atlantic}$	0.27	0.25	0.23	0.03	0.01	–0.01

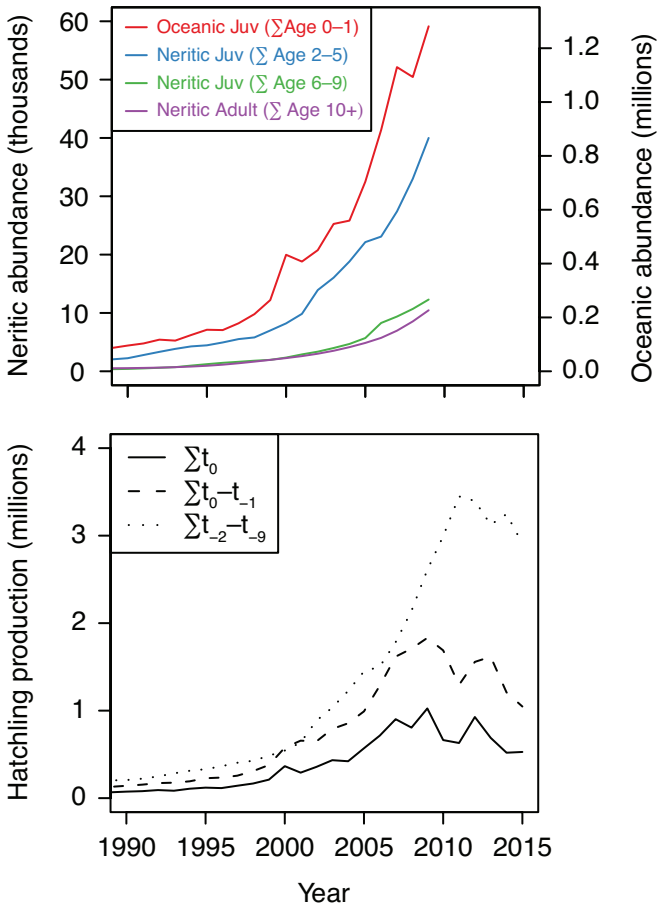

Figure A1. Time series of Kemp's ridley sea turtle abundance. Top panel: population–model derived estimates of annual number of turtles in each age class through 2009. Post–2010 abundances were excluded due to poor model fit (see NMFS and USFWS 2015). Bottom panel: cumulative hatchling production from the species' index nesting beach in Tamaulipas, Mexico (data sourced from NMFS & USFWS 2015).

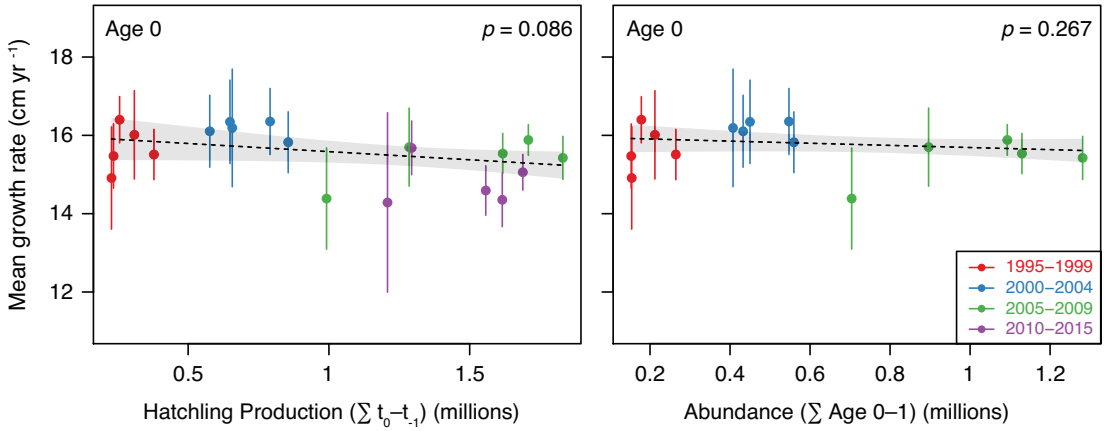

Figure A2. Relationship between mean back–calculated growth rate and population density metrics for Age 0 Kemp's ridley sea turtles stranded in the Gulf of Mexico and Atlantic Coast. Dashed lines and grey ribbons are predicted values and 95% CI from GAM models with either cumulative hatchling production (left panel) or population abundance (right panel) included as a smoother term (see Table A4). Points are means ± 95% CI.

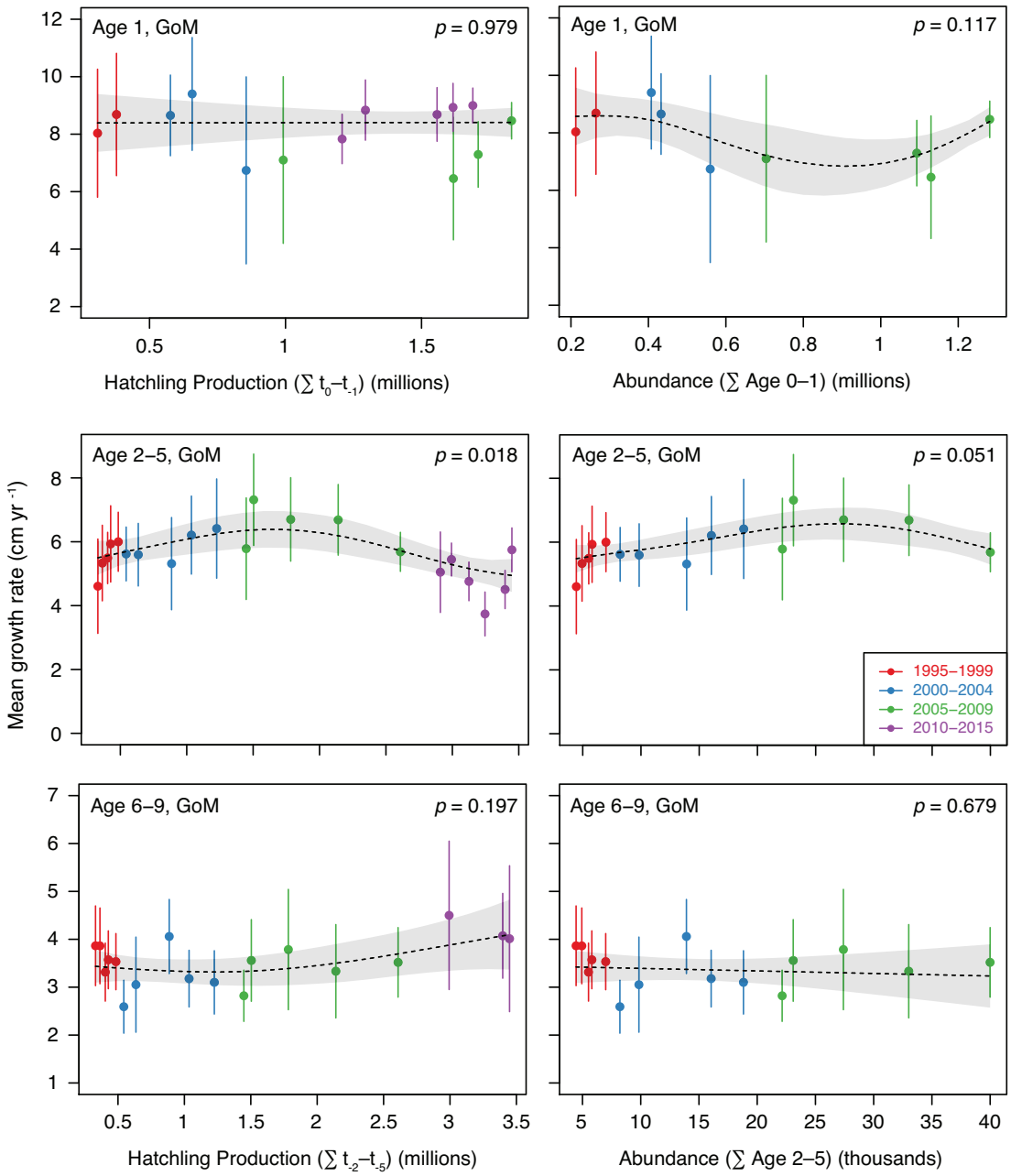

Figure A3. Relationship between mean back–calculated growth rate and population density metrics for Age 1, Age 2–5, and Age 6–9 Kemp's ridley sea turtles stranded in the Gulf of Mexico. Dashed lines and grey ribbons are predicted values and 95% CI from GAMs with either cumulative hatchling production (left panel) or population abundance (right panel) included as a smoother term (see Table A4). Points are means ± 95% CI.

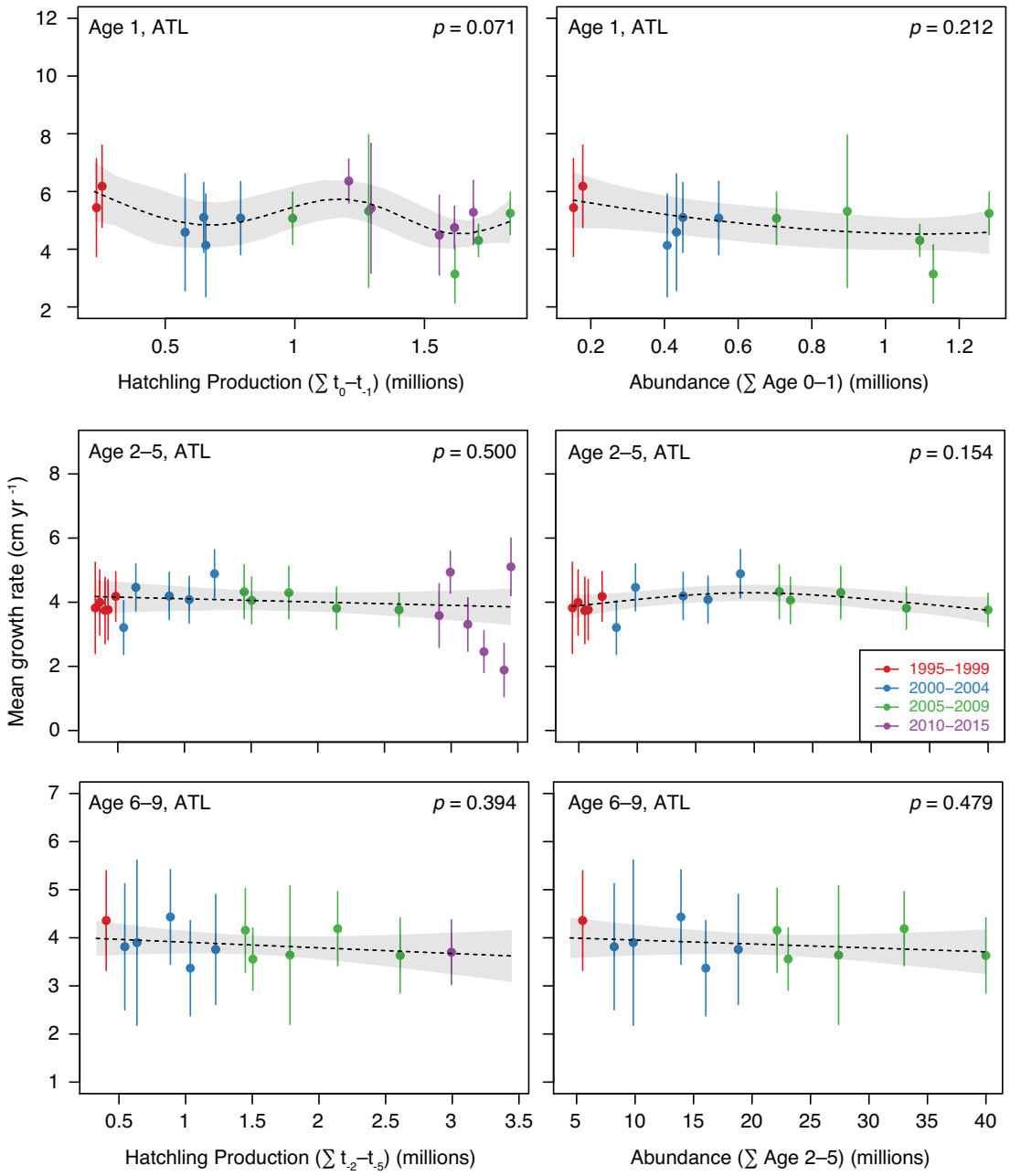

Figure A4. Relationship between mean back–calculated growth rate and population density metrics for Age 1, Age 2–5, and Age 6–9 Kemp's ridley sea turtles stranded along the Atlantic Coast. Dashed lines and grey ribbons are predicted values and 95% CI from GAM models with either cumulative hatchling production (left panel) or population abundance (right panel) included as a smoother term (see Table A4). Points are means ± 95% CI.

APPENDIX B: CHAPTER 3 SUPPLEMENTAL INFORMATION

Materials and Methods

Bulk sea turtle bone $\delta^{13}C$ carbonate carbon correction

Following stable isotope analysis, bulk bone $\delta^{13}C$ values were mathematically corrected to account for carbonate-derived carbon as recommended by Turner Tomaszewicz et al. (2015). Using their approach, we collected ~15 mg cortical bone dust from 43 Kemp's ridley sea turtle humeri using an ESI New Wave Research MicroMill, sampling only the central portion of the cortical bone. To generate sufficient bone dust for analysis, we sampled across multiple humerus bone growth layers. Approximately 1.5 mg of this bulk bone dust was then packaged into tin cups for each turtle for stable carbon and nitrogen isotope analysis (hereafter $\delta^{13}C_{bulk}$ and $\delta^{15}N_{bulk}$).

We then placed the remaining bone dust in individual 1.5 mL microcentrifuge tubes, added 0.5 mL of 0.25 M HCL, stirred the contents with a metal spatula, and refrigerated the bone-acid solution for 1–2 hours. We then centrifuged the samples for 2 minutes, rinsed the samples three times with nanopore water, and then pipetted down each solution to 0.25 mL. Each sample was then mixed, transferred into pre-weighed tin capsules, and dried for 48 hours. The isolated collagen samples were then analyzed for $\delta^{13}C$ and $\delta^{15}N$ values (hereafter $\delta^{13}C_{collagen}$ and $\delta^{15}N_{collagen}$).

Paired samples were then compared to assess effects of acidification on stable isotope values. As in Turner Tomaszewicz et al. (2015), bulk and collagen values did not differ for $\delta^{15}N$ (Wilcoxon signed rank test, $V = 527$, $p = 0.12$) but were significantly different for $\delta^{13}C$ (Wilcoxon signed rank test, $V = 941$, $p < 0.001$). The

relationship between $\delta^{13}C_{bulk}$ and $\delta^{13}C_{collagen}$ was well described by a simple linear model ($\delta^{13}C_{collagen} = 0.98 * \delta^{13}C_{bulk} - 1.13$, $F_{1,42} = 550.1$, $p < 0.001$, adjusted $R^2 = 0.93$). We applied this equation to our broader Kemp's ridley bone stable isotope dataset used in the mixing models to mathematically convert $\delta^{13}C_{bulk}$ values to $\delta^{13}C_{collagen}$ values. $\delta^{15}N_{bulk}$ data were left untransformed.

Informative Prior

We used published Kemp's ridley sea turtle diet composition data to serve as informative priors in our analyses. We identified seven studies that presented detailed diet composition data (% dry mass or % wet volume) for multiple turtles (Table B2). For each study, we aggregated data for each prey group utilized herein and then calculated a weighted mean across all studies based on the number of turtles sampled. Within these studies, bivalves and gastropods tended to be aggregated within a single mollusc group. We therefore calculated a weighted mean for molluscs and then split the weighted mean evenly to generate informative priors for bivalves and gastropods. Witzell and Schmid (2005) was excluded from this calculation given the abnormally high percentage of their Other/Unidentified category. Final diet composition estimates used as informative priors were 76.7% for crustaceans, 2.1% for bivalves, 2.1% for gastropods, 6.0% for fish, and 2.1% for seagrass/algae.

Concentration of carbon and nitrogen in prey sources

Mixing model derived estimates of diet composition can be strongly influenced by differences in elemental compositions about potential prey sources (Phillips & Koch 2002), particularly for omnivorous species (MacArthur et al. 2011). Given that our models include both plant and animal species, we sought to account for taxon-specific digestibility in our analyses. To this end we performed a literature review using Web of Science and Google Scholar for published carbon and nitrogen elemental concentrations of representative prey items.

Through this search we identified 44 research articles that reported carbon and nitrogen elemental concentrations of bivalves (n = 4), crustaceans (n = 5), fish (n = 9), gastropods (n = 3), macroalgae (n = 12), and seagrass (n = 11) from primarily the U.S. GoM and Atlantic (Table B2). These data were averaged within each taxonomic group to generate means used in our stable isotope mixed models. Only data for animal soft tissue were used in this analysis, whereas samples for macroalgae and seagrasses where whole samples. Mean %C and %N, respectively, were 44.46 and 12.19 % for bivalves; 39.27 and 11.42 % for crustaceans; 41.12 and 9.54 % for gastropods; 42.85 and 11.64 % for fish; 22.06 and 1.70 % for macroalgae; and, 36.37 and 2.03 % for seagrasses. As in the broader analysis, means for macroalgae and seagrasses were averaged to generate plant values of 29.22 % carbon and 1.87 % nitrogen used in the analysis.

Table B1. Stable carbon and nitrogen isotope values for potential Kemp's ridley sea turtle prey species included in the stable isotope mixing model. Data were summarized by prey group and region (see *Prey Stable Isotope Ratios* in *Materials and Methods* for full details).

Phylum	Family/Order	Prey Group	Common Name	Scientific Name	N	$\delta^{15}N$ (‰)	SD	N	$\delta^{13}C$ (‰)	SD	State	Sampling Year	Source
Mollusca	Arcidae	Bivalve	Clam	Arca ponderosa				1	-18.30		NC	1975	Thayer et al. 1978
Mollusca	Arcidae	Bivalve	Clam	Arca transversa				1	-18.90		NC	1975	Thayer et al. 1978
Mollusca	Mactridae	Bivalve	Atlantic rangia	*Rangia cuneata, Corbicula fluminea*	20	6.28	0.19	20	-22.67	0.37	NC	2002	Bucci et al. 2007b
Mollusca	Mactridae	Bivalve	Atlantic rangia	*Rangia cuneata, Corbicula fluminea*	5	9.26	0.25	5	-24.16	0.19	NC	2002	Bucci et al. 2007b
Mollusca	Mactridae	Bivalve	Atlantic rangia	*Rangia cuneata*	15	9.15	0.86				LA	2005	Fry 2008
Mollusca	Mactridae	Bivalve	Atlantic rangia	*Rangia cuneata*	1	6.80		1	-27.40		MS	2006	Rush et al. 2010
Mollusca	Mactridae	Bivalve	Atlantic rangia	*Rangia cuneata*	14	7.20	0.28	14	-26.30	0.59	MS	2006	Rush et al. 2010
Mollusca	Mytilidae	Bivalve	Ribbed mussel	*Geukensia demissa*	1	7.60		1	-25.30		MS	2008	Baker et al. 2013
Mollusca	Mytilidae	Bivalve	Ribbed mussel	*Geukensia demissa*	3	6.40	0.52	3	-18.30	0.35	NC	2008	Baker et al. 2013
Mollusca	Mytilidae	Bivalve	Ribbed mussel	*Geukensia demissa*	2	7.90	0.57	2	-19.10	0.35	NC	2008	Baker et al. 2013
Mollusca	Mytilidae	Bivalve	Ribbed mussel	*Geukensia demissa*	1	6.60		1	-20.20		TX	2008	Baker et al. 2013
Mollusca	Mytilidae	Bivalve	Hooked mussel	*Ischadium recurvum*	15	6.94	0.23	15	-24.83	0.58	LA	2010	Beck and La Peyre 2015
Mollusca	Mytilidae	Bivalve	Hooked mussel	*Ischadium recurvum*	15	8.99	0.35	15	-25.69	0.43	LA	2010	Beck and La Peyre 2015
Mollusca	Mytilidae	Bivalve	Hooked mussel	*Ischadium recurvum*	15	9.17	0.27	15	-23.97	0.31	LA	2010	Beck and La Peyre 2015
Mollusca	Mytilidae	Bivalve	Mussel	*Brachidontes spp*				3	-24.10		FL(FG)	1992	Chanton and Lewis 2002
Mollusca	Mytilidae	Bivalve	Hooked mussel	*Ischadium recurvum*	15	5.86	0.76	15	-24.90	1.04	MS	2006	Dillon et al. 2015
Mollusca	Mytilidae	Bivalve	Ribbed mussel	*Geukensia demissa*				12	-22.98		LA	2010	Fry and Anderson 2014
Mollusca	Mytilidae	Bivalve	Ribbed mussel	*Geukensia demissa*				12	-22.37		LA	2010	Fry and Anderson 2014

Mollusca	Mytilidae	Bivalve	Ribbed mussel	*Geukensia demissa*	6	8.20	0.73	6	-17.30	0.24	VA	1997	Knoff et al. 2001
Mollusca	Mytilidae	Bivalve	Mussel	*Unidentified*	55	7.43	0.47	55	-24.05	0.75	LA	2013	Olin et al. 2017
Mollusca	Mytilidae	Bivalve	Ribbed mussel	*Geukensia demissa*	2	6.20	0.57	2	-27.20	1.70	MS	2006	Rush et al. 2010
Mollusca	Mytilidae	Bivalve	Ribbed mussel	*Geukensia demissa*	8	6.70	0.54	8	-22.60	0.76	MS	2006	Rush et al. 2010
Mollusca	Mytilidae	Bivalve	Carolina marsh clam	*Polymesoda caroliniana*	1	8.50		1	-22.00		MS	1988	Sullivan and Moncreiff 1990
Mollusca	Mytilidae	Bivalve	Hooked mussel	*Ischadium recurvum*	4	6.60		6	-21.90		MS	1988	Sullivan and Moncreiff 1990
Mollusca	Mytilidae	Bivalve	Ribbed mussel	*Geukensia demissa*	2	7.30		2	-21.80		MS	1988	Sullivan and Moncreiff 1990
Mollusca	Mytilidae	Bivalve	Mussel	*Unidentified*				1	-21.10		AL	2010	Wilson et al. 2015
Mollusca	Mytilidae	Bivalve	Mussel	*Unidentified*				1	-22.10		FL(FG)	2010	Wilson et al. 2015
Mollusca	Mytilidae	Bivalve	Mussel	*Unidentified*				3	-24.20	0.60	LA	2010	Wilson et al. 2015
Mollusca	Mytilidae	Bivalve	Mussel	*Unidentified*				1	-27.10		MS	2010	Wilson et al. 2015
Mollusca	Mytilidae	Bivalve	Mussel	*Unidentified*	1	8.00		1	-22.20		TX	1999	Winemiller et al. 2007
Mollusca	Ostreidae	Bivalve	Eastern oyster	*Crassostrea virginica*	40	4.99	0.50	40	-22.56	0.93	FL(FG)	2008	Abeels et al. 2012
Mollusca	Ostreidae	Bivalve	Eastern oyster	*Crassostrea virginica*	2	7.80		2	-20.70		FL(FG)	2008	Baker et al. 2013
Mollusca	Ostreidae	Bivalve	Eastern oyster	*Crassostrea virginica*	5	9.30	0.22	5	-18.00	0.17	LA	2008	Baker et al. 2013
Mollusca	Ostreidae	Bivalve	Eastern oyster	*Crassostrea virginica*	1	6.80		1	-19.20		NC	2008	Baker et al. 2013
Mollusca	Ostreidae	Bivalve	Eastern oyster	*Crassostrea virginica*	3	8.90	0.35	3	-21.10	0.17	TX	2008	Baker et al. 2013
Mollusca	Ostreidae	Bivalve	Eastern oyster	*Crassostrea virginica*	1	8.90		1	-20.90		TX	2008	Baker et al. 2013
Mollusca	Ostreidae	Bivalve	Eastern oyster	*Crassostrea virginica*	15	9.36	0.23	15	-23.20	0.50	LA	2010	Beck and La Peyre 2015
Mollusca	Ostreidae	Bivalve	Eastern oyster	*Crassostrea virginica*	15	11.54	0.27	15	-23.70	0.46	LA	2010	Beck and La Peyre 2015
Mollusca	Ostreidae	Bivalve	Eastern oyster	*Crassostrea virginica*	15	11.64	0.77	15	-22.54	0.31	LA	2010	Beck and La Peyre 2015
Mollusca	Ostreidae	Bivalve	Eastern oyster	*Crassostrea virginica*	15	12.01	0.31	15	-20.49	0.31	LA	2010	Beck and La Peyre 2015
Mollusca	Ostreidae	Bivalve	Eastern oyster	*Crassostrea virginica*	27	8.48	1.16				AL	2007	Biancani et al. 2012
Mollusca	Ostreidae	Bivalve	Eastern oyster	*Crassostrea virginica*	41	13.34	2.22	40	-21.05	2.44	TX	2009	Bishop et al. 2017

Mollusca	Ostreidae	Bivalve	Eastern oyster	*Crassostrea virginica*	96	9.82	1.00				TX	2012	Blomberg et al. 2017
Mollusca	Ostreidae	Bivalve	Eastern oyster	*Crassostrea virginica*				28	-23.35		FL(FG)	1992	Chanton and Lewis 2002
Mollusca	Ostreidae	Bivalve	Eastern oyster	*Crassostrea virginica*	70	7.11	0.60	70	-24.01	1.31	MS	2006	Dillon et al. 2015
Mollusca	Ostreidae	Bivalve	Eastern oyster	*Crassostrea virginica*	33	9.50	0.57	33	-22.40	1.15	VA	2005	Fertig et al. 2014
Mollusca	Ostreidae	Bivalve	Eastern oyster	*Crassostrea virginica*	19	11.00	0.87	19	-20.50	0.87	VA	2005	Fertig et al. 2014
Mollusca	Ostreidae	Bivalve	Eastern oyster	*Crassostrea virginica*	36	5.57	0.38	36	-26.48	1.57	FL(FG)	2012	Loh et al. 2017
Mollusca	Ostreidae	Bivalve	Eastern oyster	*Crassostrea virginica*	10	9.29	0.76	10	-22.79	1.20	TX	2006	Oakley et al. 2014
Mollusca	Ostreidae	Bivalve	Eastern oyster	*Crassostrea virginica*	150	8.25	0.31	150	-21.68	0.40	FL(FG)	2006	Oczkowski et al. 2011
Mollusca	Ostreidae	Bivalve	Eastern oyster	*Crassostrea virginica*	6	5.75	0.55	6	-23.25	0.82	FL(FG)	2008	Olin et al. 2013
Mollusca	Ostreidae	Bivalve	Eastern oyster	*Crassostrea virginica*	16	8.80	0.40	16	-25.60	0.50	MS	2010	Olsen et al. 2014
Mollusca	Ostreidae	Bivalve	Eastern oyster	*Crassostrea virginica*	3	8.10		6	-21.40		MS	1988	Sullivan and Moncreiff 1990
Mollusca	Ostreidae	Bivalve	Oyster	*Unidentified*				2	-21.40	0.20	AL	2010	Wilson et al. 2015
Mollusca	Ostreidae	Bivalve	Oyster	*Unidentified*				10	-22.00	1.00	FL(FG)	2010	Wilson et al. 2015
Mollusca	Ostreidae	Bivalve	Oyster	*Unidentified*				2	-23.80	0.20	LA	2010	Wilson et al. 2015
Mollusca	Ostreidae	Bivalve	Oyster	*Unidentified*				7	-23.80	0.70	LA	2010	Wilson et al. 2015
Mollusca	Ostreidae	Bivalve	Oyster	*Unidentified*				2	-26.40	2.50	MS	2010	Wilson et al. 2015
Mollusca	Ostreidae	Bivalve	Oyster	*Unidentified*	4	10.20	1.30	4	-22.76	0.30	TX	1999	Winemiller et al. 2007
Mollusca	Pectinidae	Bivalve	Calico scallop	*Argopecten gibbus*	23	7.20	0.30	23	-17.60	0.50	FL(FG)	1998	Sulak et al. 2012
Mollusca	Pectinidae	Bivalve	Bay scallop	Argopecten irradians				4	-18.70	0.52	NC	1975	Thayer et al. 1978
Mollusca	Tellinidae	Bivalve	Tellin spp	*Tellina alternata*	1	7.50		1	-19.20		MS	1991	Moncreiff and Sullivan 2001
Mollusca	Tellinidae	Bivalve	Baltic macoma clam	Macoma balthica				1	-18.60		NC	1975	Thayer et al. 1978
Mollusca	Tellinidae	Bivalve	Narrowed macoma clam	Macoma tenta				1	-17.80		NC	1975	Thayer et al. 1978
Mollusca	Tellinidae	Bivalve	Tellin spp	*Tellina versicolor*				1	-17.30		NC	1975	Thayer et al. 1978
Mollusca	Veneridae	Bivalve	Northern quahog	*Mercenaria mercenaria*				1	-21.50		FL(FG)	1992	Chanton and Lewis 2002

Mollusca	Veneridae	Bivalve	Northern quahog	*Mercenaria mercenaria*	4	9.10	0.14	4	-19.47	0.00	NC	2007	Deehr et al. 2014
Mollusca	Veneridae	Bivalve	Marsh clam	*Unidentified*	1	6.00		1	-20.00		FL(FG)	2012	Denton et al. 2019
Mollusca	Veneridae	Bivalve	Northern quahog	*Mercenaria mercenaria*	35	11.72	0.81	35	-18.81	0.89	VA	2010	Hondula and Price 2014
Mollusca	Veneridae	Bivalve	Northern quahog	*Mercenaria mercenaria*	4	8.80	1.60	4	-17.40	1.40	VA	1997	Knoff et al. 2001
Mollusca	Veneridae	Bivalve	Southern quahog	*Mercenaria campechiensis*	2	10.80		2	-18.50		MS	1991	Moncreiff and Sullivan 2001
Mollusca	Veneridae	Bivalve	Clam	Chione cancellata				1	-18.70		NC	1975	Thayer et al. 1978
Arthropoda	Aethridae	Crab	Calico box crab	*Hepatus epheliticus*	2	14.10		2	-16.20		MS	1991	Moncreiff and Sullivan 2001
Arthropoda	Diogenidae	Crab	Striped hermit crab	*Clibanarius vittatus*	72	9.60		72	-15.10		MS	1991	Moncreiff and Sullivan 2001
Arthropoda	Diogenidae	Crab	Striped hermit crab	*Clibanarius vittatus*	8	11.65	0.37	8	-19.35	0.41	LA	2007	Simonsen 2008
Arthropoda	Diogenidae	Crab	Striped hermit crab	*Clibanarius vittatus*	1	9.40		2	-19.60		MS	1988	Sullivan and Moncreiff 1990
Arthropoda	Epialtidae	Crab	Spider crab	*Libinia spp*	3	3.27	0.87	3	-21.85	2.22	FL(FG)	2008	Abeels et al. 2012
Arthropoda	Epialtidae	Crab	Longnose spider crab	*Libinia dubia*	2	13.90		2	-17.20		MS	1991	Moncreiff and Sullivan 2001
Arthropoda	Epialtidae	Crab	Portly spider crab	*Libinia emarginata*	2	13.70		2	-17.30		MS	1991	Moncreiff and Sullivan 2001
Arthropoda	Epialtidae	Crab	Longnose spider crab	*Libinia dubia*	5	12.60	1.10	5	-17.00	1.60	NC	1997	Snover et al. 2010
Arthropoda	Epialtidae	Crab	Portly spider crab	*Libinia emarginata*	11	10.65	0.48	11	-17.92	1.33	NC	2007	Wallace et al. 2009
Arthropoda	Limulidae	Crab	Horseshoe crab	*Limulus polyphemus*	1	10.30		1	-13.20		VA	1997	Knoff et al. 2001
Arthropoda	Limulidae	Crab	Horseshoe crab	*Limulus polyphemus*	5	12.10		5	-15.70		MS	1991	Moncreiff and Sullivan 2001
Arthropoda	Limulidae	Crab	Horseshoe crab	*Limulus polyphemus*	9	13.30	0.90	9	-17.00	0.60	NC	1997	Snover et al. 2010
Arthropoda	Limulidae	Crab	Horseshoe crab	*Limulus polyphemus*	10	11.62	0.46	10	-16.97	1.31	NC	2007	Wallace et al. 2009
Arthropoda	Menippidae	Crab	Stone crab	*Menippe mercenaria*	11	5.02	0.09	11	-19.65	1.90	FL(FG)	2008	Abeels et al. 2012
Arthropoda	Menippidae	Crab	Stone crab	*Menippe mercenaria*	1	14.10		1	-16.50		MS	1991	Moncreiff and Sullivan 2001
Arthropoda	Menippidae	Crab	Gulf stone crab	*Menippe adina*	9	9.18	3.39	9	-17.55	2.43	TX	2006	Oakley et al. 2014
Arthropoda	Menippidae	Crab	Gulf stone crab	*Menippe adina*	36	13.63	0.64	36	-16.51	0.38	LA	2016	Reeves et al. 2019
Arthropoda	Multiple	Crab	Crab	*Unidentified*	5	11.17	1.37	5	-22.36	1.01	AL	2011	Kroetz et al. 2017

Arthropoda	Paguridae	Crab	Gray hermit crab	*Pagurus pollicaris*	25	11.60		25	-15.60		MS	1991	Moncreiff and Sullivan 2001
Arthropoda	Panopeidae	Crab	Flatback mud crab	*Eurypanopeus depressus*	40	4.05	0.67	40	-17.89	1.58	FL(FG)	2008	Abeels et al. 2012
Arthropoda	Panopeidae	Crab	Knot-fingered mud crab	*Panopeus lacustris*	1	5.88		1	-17.62		FL(FG)	2008	Abeels et al. 2012
Arthropoda	Panopeidae	Crab	Mud crab	*Panopeus spp*	4	4.41	1.00	4	-20.96	1.84	FL(FG)	2008	Abeels et al. 2012
Arthropoda	Panopeidae	Crab	Oystershell mud crab	*Panopeus simpsoni*	7	4.97	0.88	7	-19.46	1.08	FL(FG)	2008	Abeels et al. 2012
Arthropoda	Panopeidae	Crab	Flatback mud crab	*Eurypanopeus depressus*	15	8.92	0.62	15	-22.86	1.67	LA	2010	Beck and La Peyre 2015
Arthropoda	Panopeidae	Crab	Flatback mud crab	*Eurypanopeus depressus*	15	11.42	0.50	15	-21.61	1.94	LA	2010	Beck and La Peyre 2015
Arthropoda	Panopeidae	Crab	Flatback mud crab	*Eurypanopeus depressus*	15	11.60	1.16	15	-21.03	2.29	LA	2010	Beck and La Peyre 2015
Arthropoda	Panopeidae	Crab	Flatback mud crab	*Eurypanopeus depressus*	15	12.50	0.46	15	-20.66	1.16	LA	2010	Beck and La Peyre 2015
Arthropoda	Panopeidae	Crab	Black-fingered mud crab	*Panopeus herbstii*	15	6.20	1.20	15	-23.70	0.70	FL(FG)	2012	Denton et al. 2019
Arthropoda	Panopeidae	Crab	Oystershell mud crab	*Panopeus simpsoni*	28	6.67	1.04	28	-20.01	1.17	MS	2006	Dillon et al. 2015
Arthropoda	Panopeidae	Crab	Estuarine mud crab	*Rhithropanopeus harrisii*	1	7.60		1	-22.60		FL(FG)	1983	Harrigan et al. 1989
Arthropoda	Panopeidae	Crab	Black-fingered mud crab	*Panopeus herbstii*	3	11.40	0.35	3	-14.20	0.35	VA	1997	Knoff et al. 2001
Arthropoda	Panopeidae	Crab	Mud crab	*Panopeidae spp*				3	-14.68	0.46	VA	1999	Pruell et al. 2003
Arthropoda	Panopeidae	Crab	Mud crab	*Panopeidae spp*				1	-15.60		FL(FG)	2010	Wilson et al. 2015
Arthropoda	Portunidae	Crab	Blue crab	*Callinectes sapidus*	1	9.50		1	-17.50		FL(FG)	2008	Baker et al. 2013
Arthropoda	Portunidae	Crab	Blue crab	*Callinectes sapidus*	2	10.30	0.28	2	-17.20	2.69	LA	2008	Baker et al. 2013
Arthropoda	Portunidae	Crab	Blue crab	*Callinectes sapidus*	2	11.00	0.07	2	-16.60	0.14	LA	2008	Baker et al. 2013
Arthropoda	Portunidae	Crab	Blue crab	*Callinectes sapidus*	5	8.90	1.34	5	-15.20	1.12	NC	2008	Baker et al. 2013
Arthropoda	Portunidae	Crab	Blue crab	*Callinectes sapidus*	4	9.40	3.80	4	-17.10	0.60	NC	2008	Baker et al. 2013
Arthropoda	Portunidae	Crab	Blue crab	*Callinectes sapidus*	3	7.40	0.17	3	-15.30	0.69	TX	2008	Baker et al. 2013
Arthropoda	Portunidae	Crab	Blue crab	*Callinectes sapidus*	2	8.50	2.47	2	-19.20	1.41	TX	2008	Baker et al. 2013
Arthropoda	Portunidae	Crab	Blue crab	*Callinectes sapidus*	4	9.20	0.60	4	-16.50	2.66	TX	2008	Baker et al. 2013
Arthropoda	Portunidae	Crab	Blue crab	*Callinectes sapidus*	35	9.60	0.40	35	-23.40	0.80	NC	2002	Bucci et al. 2007b
Arthropoda	Portunidae	Crab	Blue crab	*Callinectes sapidus*	15	12.00	0.70	15	-21.50	1.10	NC	2002	Bucci et al. 2007b

Arthropoda	Portunidae	Crab	Blue crab	*Callinectes sapidus*				8	-21.90		FL(FG)	1992	Chanton and Lewis 2002
Arthropoda	Portunidae	Crab	Blue crab	*Callinectes sapidus*	16	9.54	0.41	16	-17.98	0.32	NC	2007	Deehr et al. 2014
Arthropoda	Portunidae	Crab	Blue crab	*Callinectes sapidus*	1	6.80		1	-21.90		FL(FG)	2012	Denton et al. 2019
Arthropoda	Portunidae	Crab	Blue crab	*Callinectes sapidus*	4	7.70	1.10	4	-17.70	1.20	FL(FG)	2012	Denton et al. 2019
Arthropoda	Portunidae	Crab	Blue crab	*Callinectes sapidus*	8	5.94	1.96	8	-19.13	1.10	MS	2006	Dillon et al. 2015
Arthropoda	Portunidae	Crab	Blue crab	*Callinectes sapidus*	11	11.41	0.34	11	-17.91	0.15	VA	2005	Douglass et al. 2011
Arthropoda	Portunidae	Crab	Swimming crab	*Callinectes spp*	3	12.30	0.77	3	-17.56	0.40	AL	2008	Drymon et al. 2012
Arthropoda	Portunidae	Crab	Blue crab	*Callinectes sapidus*	14	8.60	0.49	14	-19.60	0.56	LA	2000	Duque 2004
Arthropoda	Portunidae	Crab	Blue crab	*Callinectes sapidus*	137	10.60	1.53	137	-19.54	2.35	LA	2007	Gelpi et al. 2013
Arthropoda	Portunidae	Crab	Blue crab	*Callinectes sapidus*	92	12.75	1.59	92	-20.13	2.38	LA	2007	Gelpi et al. 2013
Arthropoda	Portunidae	Crab	Blue crab	*Callinectes sapidus*	1	8.70		1	-23.20		FL(FG)	1983	Harrigan et al. 1989
Arthropoda	Portunidae	Crab	Blue crab	*Callinectes sapidus*	22	9.41	0.94	22	-19.15	1.44	TX	2004	Hoeinghau and Davis 2007
Arthropoda	Portunidae	Crab	Blue crab	*Callinectes sapidus*	6	11.50	2.45	6	-14.60	0.49	VA	1997	Knoff et al. 2001
Arthropoda	Portunidae	Crab	Ocellate lady crab	*Ovalipes ocellatus*	1	11.00		1	-17.70		VA	1997	Knoff et al. 2001
Arthropoda	Portunidae	Crab	Speckled swimming crab	*Arenaeus cribrarius*	3	11.30	0.52	3	-17.30	0.17	VA	1997	Knoff et al. 2001
Arthropoda	Portunidae	Crab	Blue crab	*Callinectes sapidus*	11	13.10		11	-18.00		MS	1991	Moncreiff and Sullivan 2001
Arthropoda	Portunidae	Crab	Iridescent swimming crab	*Portunus gibbesii*	18	13.20		18	-17.30		MS	1991	Moncreiff and Sullivan 2001
Arthropoda	Portunidae	Crab	Blue crab	*Callinectes sapidus*	15	9.58	2.01	15	-17.32	2.52	TX	2006	Oakley et al. 2014
Arthropoda	Portunidae	Crab	Blue crab	*Callinectes sapidus*	9	10.23	1.48	9	-22.73	1.48	FL(FG)	2008	Olin et al. 2013
Arthropoda	Portunidae	Crab	Blue crab	*Callinectes sapidus*	15	9.26	2.19	15	-21.06	1.04	FL(FG)	2008	Olin et al. 2013
Arthropoda	Portunidae	Crab	Blue crab	*Callinectes sapidus*				9	-15.95	1.02	VA	1999	Pruell et al. 2003
Arthropoda	Portunidae	Crab	Blue crab	*Callinectes sapidus*	22	11.43	1.59	22	-17.20	1.31	TX	2014	Rezek et al. 2017
Arthropoda	Portunidae	Crab	Blue crab	*Callinectes sapidus*	3	5.60	0.07	3	-15.30	0.96	MS	2006	Rush et al. 2010
Arthropoda	Portunidae	Crab	Blue crab	*Callinectes sapidus*	3	6.30	0.76	3	-22.70	2.42	MS	2006	Rush et al. 2010
Arthropoda	Portunidae	Crab	Blue crab	*Callinectes sapidus*	7	11.20	0.90	7	-16.60	1.50	NC	1997	Snover et al. 2010
Arthropoda	Portunidae	Crab	Blue crab	*Callinectes sapidus*				1	-19.70		TX	1991	Street et al. 1997
Arthropoda	Portunidae	Crab	Blue crab	*Callinectes sapidus*	5	8.60		10	-19.60		MS	1988	Sullivan and Moncreiff 1990
Arthropoda	Portunidae	Crab	Blue crab	*Callinectes sapidus*	42	11.22	1.17	42	-20.57	2.22	AL	2010	Vedral 2012
Arthropoda	Portunidae	Crab	Blue crab	*Callinectes sapidus*	4	9.28	0.38	4	-16.26	1.65	NC	2007	Wallace et al. 2009
Arthropoda	Portunidae	Crab	Blue crab	*Callinectes sapidus*	13	12.00	0.70	6	-20.30	4.80	FL(FG)	1992	Wilson et al. 2009

Arthropoda	Portunidae	Crab	Blue crab	*Callinectes sapidus*				1	-16.40		AL	2010	Wilson et al. 2015
Arthropoda	Portunidae	Crab	Blue crab	*Callinectes sapidus*				1	-18.60		LA	2010	Wilson et al. 2015
Arthropoda	Portunidae	Crab	Blue crab	*Callinectes sapidus*	7	11.10	2.30	7	-19.30	2.30	TX	1999	Winemiller et al. 2007
Chordata	Achiridae	Fish	Lined sole	*Achirus lineatus*	1	8.02		1	-22.78		FL(FG)	2009	Abeels et al. 2012
Chordata	Achiridae	Fish	Hogchoker	*Trinectes maculatus*	6	10.30	0.71	6	-21.70	2.36	FL(FG)	2008	Olin et al. 2013
Chordata	Ariidae	Fish	Hardhead sea catfish	*Ariopsis felis*				10	-19.36		FL(FG)	1992	Chanton and Lewis 2002
Chordata	Ariidae	Fish	Hardhead sea catfish	*Ariopsis felis*	8	13.26	0.40	8	-18.96	1.05	AL	2008	Drymon et al. 2012
Chordata	Ariidae	Fish	Hardhead sea catfish	*Ariopsis felis*	16	13.40	1.20	16	-19.70	2.00	LA	2003	Fry and Chuchal 2012
Chordata	Ariidae	Fish	Hardhead sea catfish	*Ariopsis felis*	25	13.60		25	-17.00		MS	1991	Moncreiff and Sullivan 2001
Chordata	Ariidae	Fish	Gafftopsail sea catfish	*Bagre marinus*	21	15.53	1.05	21	-18.62	0.92	TX	2006	Oakley et al. 2014
Chordata	Ariidae	Fish	Hardhead sea catfish	*Ariopsis felis*	24	14.05	1.08	24	-19.23	1.81	TX	2006	Oakley et al. 2014
Chordata	Ariidae	Fish	Gafftopsail sea catfish	*Bagre marinus*	23	11.83	2.82	23	-19.89	2.82	FL(FG)	2006	Olin et al. 2012
Chordata	Ariidae	Fish	Gafftopsail sea catfish	*Bagre marinus*	16	11.10	1.20	16	-18.90	2.40	FL(FG)	2006	Olin et al. 2012
Chordata	Ariidae	Fish	Hardhead sea catfish	*Ariopsis felis*	40	12.01	1.45	40	-21.03	1.93	FL(FG)	2006	Olin et al. 2012
Chordata	Ariidae	Fish	Hardhead sea catfish	*Ariopsis felis*	23	10.72	1.75	23	-21.12	2.41	FL(FG)	2006	Olin et al. 2012
Chordata	Ariidae	Fish	Hardhead sea catfish	*Ariopsis felis*				7	-12.60		TX	1991	Street et al. 1997
Chordata	Ariidae	Fish	Gafftopsail sea catfish	*Bagre marinus*	16	12.10	1.10	16	-17.20	1.70	FL(FG)	1998	Sulak et al. 2012
Chordata	Ariidae	Fish	Hardhead sea catfish	*Ariopsis felis*	21	10.10	1.00	21	-19.70	1.60	FL(FG)	1998	Sulak et al. 2012
Chordata	Ariidae	Fish	Hardhead sea catfish	*Ariopsis felis*	7	11.50		11	-20.30		MS	1988	Sullivan and Moncreiff 1990
Chordata	Ariidae	Fish	Hardhead sea catfish	*Ariopsis felis*	12	14.50	0.70	8	-19.30	0.90	FL(FG)	1992	Wilson et al. 2009
Chordata	Ariidae	Fish	Hardhead sea catfish	*Ariopsis felis*				4	-17.10	0.50	FL(FG)	2010	Wilson et al. 2015
Chordata	Ariidae	Fish	Hardhead sea catfish	*Ariopsis felis*	6	13.70	1.00	6	-19.00	1.30	TX	1999	Winemiller et al. 2007
Chordata	Carangidae	Fish	Round scad	Decapterus punctatus	29	10.50	0.65	29	-17.30	0.54	NC	1990	Thomas and Cahoon 1993
Chordata	Clupeidae	Fish	Gulf menhaden	*Brevoortia patronus*				1	-20.70		FL(FG)	1992	Chanton and Lewis 2002

Chordata	Clupeidae	Fish	Atlantic menhaden	*Brevoortia tyrannus*	19	11.71	0.84	19	-18.99	0.25	NC	2007	Deehr et al. 2014
Chordata	Clupeidae	Fish	Gulf menhaden	*Brevoortia patronus*	24	12.20	1.47	24	-21.30	1.47	LA	2003	Fry and Chuchal 2012
Chordata	Clupeidae	Fish	Gulf menhaden	*Brevoortia patronus*	2	11.90		2	-19.60		MS	1991	Moncreiff and Sullivan 2001
Chordata	Clupeidae	Fish	Scaled herring	*Harengula jaguana*	220	13.10		220	-18.20		MS	1991	Moncreiff and Sullivan 2001
Chordata	Clupeidae	Fish	Gulf menhaden	*Brevoortia patronus*	36	13.47	1.26	36	-19.96	1.20	TX	2006	Oakley et al. 2014
Chordata	Clupeidae	Fish	Gulf menhaden	*Brevoortia patronus*	161	12.08	0.49	161	-20.81	1.38	MS	2010	Olsen et al. 2014
Chordata	Clupeidae	Fish	Atlantic menhaden	*Brevoortia tyrannus*				3	-19.41	0.63	VA	1999	Pruell et al. 2003
Chordata	Clupeidae	Fish	Scaled herring	*Harengula jaguana*	7	9.40	1.40	7	-16.20	2.20	FL(FG)	2009	Rossman et al. 2015
Chordata	Clupeidae	Fish	Threafin herring	*Opisthonema oglinum*	11	9.20	0.40	11	-17.50	1.70	FL(FG)	2009	Rossman et al. 2015
Chordata	Clupeidae	Fish	Gulf menhaden	*Brevoortia patronus*	9	10.80	0.80	9	-20.60	1.90	LA	2005	Senn et al. 2010
Chordata	Clupeidae	Fish	Gulf menhaden	*Brevoortia patronus*				10	-18.50		TX	1991	Street et al. 1997
Chordata	Clupeidae	Fish	Gulf menhaden	*Brevoortia patronus*	6	11.30		7	-21.30		MS	1988	Sullivan and Moncreiff 1990
Chordata	Clupeidae	Fish	Scaled herring	*Harengula jaguana*	1	12.10		1	-17.80		MS	1988	Sullivan and Moncreiff 1990
Chordata	Clupeidae	Fish	Gulf menhaden	*Brevoortia patronus*	2	12.00	0.30	2	-17.10	0.10	FL(FG)	2007	Wilson et al. 2013
Chordata	Clupeidae	Fish	Scaled herring	*Harengula jaguana*	2	11.70	0.60	2	-17.80	0.20	FL(FG)	2007	Wilson et al. 2013
Chordata	Clupeidae	Fish	Scaled herring	*Harengula jaguana*				4	-19.10	0.20	FL(FG)	2010	Wilson et al. 2015
Chordata	Clupeidae	Fish	Gulf menhaden	*Brevoortia patronus*	4	14.47	0.42	4	-20.50	1.60	TX	1999	Winemiller et al. 2007
Chordata	Engraulidae	Fish	Bay anchovy	*Anchoa mitchilli*	1	11.90		1	-21.20		FL(FG)	2008	Baker et al. 2013
Chordata	Engraulidae	Fish	Bay anchovy	*Anchoa mitchilli*	1	12.70		1	-20.50		LA	2008	Baker et al. 2013
Chordata	Engraulidae	Fish	Bay anchovy	*Anchoa mitchilli*	3	12.90	0.17	3	-20.60	0.52	LA	2008	Baker et al. 2013
Chordata	Engraulidae	Fish	Bay anchovy	*Anchoa mitchilli*	1	12.10		1	-21.30		NC	2008	Baker et al. 2013
Chordata	Engraulidae	Fish	Bay anchovy	*Anchoa mitchilli*	2	13.50	0.49	2	-18.40	0.14	TX	2008	Baker et al. 2013

Chordata	Engraulidae	Fish	Bay anchovy	*Anchoa mitchilli*	3	13.70	0.52	3	-21.60	1.04	TX	2008	Baker et al. 2013
Chordata	Engraulidae	Fish	Bay anchovy	*Anchoa mitchilli*	38	16.20	0.86	38	-19.40	0.74	VA	2006	Buchheister and Latour 2011
Chordata	Engraulidae	Fish	Bay anchovy	*Anchoa mitchilli*				23	-20.15		FL(FG)	1992	Chanton and Lewis 2002
Chordata	Engraulidae	Fish	Anchovy	*Anchoa mitchilli, Anchoa hespetus*	27	13.13	1.50	27	-19.81	0.13	NC	2007	Deehr et al. 2014
Chordata	Engraulidae	Fish	Anchovy	*Anchoa spp*	11	13.59	0.51	11	-21.96	1.36	AL	2008	Drymon et al. 2012
Chordata	Engraulidae	Fish	Bay anchovy	*Anchoa mitchilli*	19	12.70	1.05	19	-21.60	1.22	LA	2000	Duque 2004
Chordata	Engraulidae	Fish	Bay anchovy	*Anchoa mitchilli*	119	14.80		119	-19.10		MS	1991	Moncreiff and Sullivan 2001
Chordata	Engraulidae	Fish	Longnose anchovy	*Anchoa nasus*	24	14.30		24	-18.40		MS	1991	Moncreiff and Sullivan 2001
Chordata	Engraulidae	Fish	Bay anchovy	*Anchoa mitchilli*	10	13.43	1.14	10	-21.00	1.87	TX	2006	Oakley et al. 2014
Chordata	Engraulidae	Fish	Bay anchovy	*Anchoa mitchilli*	10	13.10	0.50	10	-21.30	0.60	MS	2010	Olsen et al. 2014
Chordata	Engraulidae	Fish	Bay anchovy	*Anchoa mitchilli*				18	-18.17	1.45	VA	1999	Pruell et al. 2003
Chordata	Engraulidae	Fish	Bay anchovy	*Anchoa mitchilli*	7	13.10	1.00	7	-19.00	2.20	LA	2005	Senn et al. 2010
Chordata	Engraulidae	Fish	Bay anchovy	*Anchoa mitchilli*	84	13.33	0.56	84	-21.34	1.59	LA	2005	Simonsen and Cowan 2013
Chordata	Engraulidae	Fish	Bay anchovy	*Anchoa mitchilli*	2	12.00		3	-20.60		MS	1988	Sullivan and Moncreiff 1990
Chordata	Engraulidae	Fish	Longnose anchovy	*Anchoa nasus*	1	12.40		1	-19.50		MS	1988	Sullivan and Moncreiff 1990
Chordata	Engraulidae	Fish	Bay anchovy	*Anchoa mitchilli*	26	14.30	0.80	21	-20.00	0.80	FL(FG)	1992	Wilson et al. 2009
Chordata	Engraulidae	Fish	Bay anchovy	*Anchoa mitchilli*				2	-17.90	0.20	FL(FG)	2010	Wilson et al. 2015
Chordata	Engraulidae	Fish	Bay anchovy	*Anchoa mitchilli*	9	12.80	0.85	9	-20.30	0.40	TX	1999	Winemiller et al. 2007
Chordata	Haemulidae	Fish	Tomtate grunt	*Haemulon aurolineatum*				10	-18.00	0.25	FL(FG)	2007	Nelson et al. 2012
Chordata	Haemulidae	Fish	Tomtate grunt	*Haemulon aurolineatum*	40	10.50	0.90	40	-16.60	0.70	FL(FG)	2010	Radabaugh and Peebles 2014
Chordata	Haemulidae	Fish	White grunt	*Haemulon plumierii*	36	10.50	0.40	36	-16.20	0.40	FL(FG)	2010	Radabaugh and Peebles 2014
Chordata	Haemulidae	Fish	Tomtate grunt	*Haemulon aurolineatum*	6	10.00	0.59	6	-15.90	0.49	NC	1990	Thomas and Cahoon 1993

Chordata	Mugilidae	Fish	Flathead grey mullet	*Mugil cephalus*	4	8.73	0.40	4	-15.88	1.26	FL(FG)	2008	Baker et al. 2013
Chordata	Mugilidae	Fish	Flathead grey mullet	*Mugil cephalus*	3	8.70	0.35	3	-15.20	0.17	LA	2008	Baker et al. 2013
Chordata	Mugilidae	Fish	Flathead grey mullet	*Mugil cephalus*	2	7.90	2.97	2	-19.30	1.63	MS	2008	Baker et al. 2013
Chordata	Mugilidae	Fish	Flathead grey mullet	*Mugil cephalus*	1	7.80		1	-15.20		TX	2008	Baker et al. 2013
Chordata	Mugilidae	Fish	Flathead grey mullet	*Mugil cephalus*	3	10.30	1.56	3	-18.80	0.35	TX	2008	Baker et al. 2013
Chordata	Mugilidae	Fish	White mullet	*Mugil curema*	3	6.30	0.17	3	-13.40	0.35	TX	2008	Baker et al. 2013
Chordata	Mugilidae	Fish	White mullet	*Mugil curema*	2	8.50		2	-14.90		TX	2008	Baker et al. 2013
Chordata	Mugilidae	Fish	Flathead grey mullet	*Mugil cephalus*	3	10.10	2.08	3	-18.00	0.69	LA	2003	Fry and Chuchal 2012
Chordata	Mugilidae	Fish	Flathead grey mullet	*Mugil cephalus*	3	9.20		3	-14.60		MS	1991	Moncreiff and Sullivan 2001
Chordata	Mugilidae	Fish	White mullet	*Mugil curema*	6	9.60		6	-15.70		MS	1991	Moncreiff and Sullivan 2001
Chordata	Mugilidae	Fish	Flathead grey mullet	*Mugil cephalus*	4	9.36	2.64	4	-16.14	1.88	TX	2006	Oakley et al. 2014
Chordata	Mugilidae	Fish	Flathead grey mullet	*Mugil cephalus*	11	8.58	0.58	11	-18.35	3.50	FL(FG)	2006	Olin et al. 2012
Chordata	Mugilidae	Fish	Flathead grey mullet	*Mugil cephalus*	1	5.74		1	-14.57		FL(FG)	2006	Olin et al. 2012
Chordata	Mugilidae	Fish	Flathead grey mullet, White mullet	*Mugil cephalus, Mugil curema*	5	5.99	0.83	5	-12.33	1.56	FL(FG)	2000	Reynolds et al. 2001
Chordata	Mugilidae	Fish	Mullet	*Mugil spp*	10	10.64	1.19	10	-15.41	2.73	TX	2014	Rezek et al. 2017
Chordata	Mugilidae	Fish	Flathead grey mullet	*Mugil cephalus*	15	9.90	4.00	15	-12.90	1.60	FL(FG)	2009	Rossman et al. 2015
Chordata	Mugilidae	Fish	Flathead grey mullet	*Mugil cephalus*				3	-13.50		TX	1991	Street et al. 1997
Chordata	Mugilidae	Fish	Flathead grey mullet	*Mugil cephalus*				2	-12.90		TX	1991	Street et al. 1997
Chordata	Mugilidae	Fish	Flathead grey mullet	*Mugil cephalus*	1	8.00		7	-18.90		MS	1988	Sullivan and Moncreiff 1990
Chordata	Mugilidae	Fish	Flathead grey mullet	*Mugil cephalus*	8	10.45	1.80	8	-17.40	0.90	TX	1999	Winemiller et al. 2007
Chordata	Paralichthyidae	Fish	Summer flounder	*Paralichthys dentatus*	1	15.16					NC	2002	Bucci et al. 2007a

Chordata	Paralichthyidae	Fish	Summer flounder	*Paralichthys dentatus*	43	15.95	0.95	43	-18.05	0.93	VA	2006	Buchheister and Latour 2011
Chordata	Paralichthyidae	Fish	Flounder	*Paralichthys spp*				4	-19.83		FL(FG)	1992	Chanton and Lewis 2002
Chordata	Paralichthyidae	Fish	Fringed flounder	*Etropus crossotus*				2	-19.75		FL(FG)	1992	Chanton and Lewis 2002
Chordata	Paralichthyidae	Fish	Flounder	*Paralichthys spp*	4	11.02	0.39	4	-17.36	0.61	NC	2007	Deehr et al. 2014
Chordata	Paralichthyidae	Fish	Gulf flounder	*Paralichthys albigutta*				5	-16.10	1.50	FL(FG)	2007	Nelson et al. 2012
Chordata	Paralichthyidae	Fish	Southern flounder	*Paralichthys lethostigma*	1	10.36		1	-16.54		TX	2006	Oakley et al. 2014
Chordata	Paralichthyidae	Fish	Dusky flounder	*Syacium papillosum*	324	9.10	0.90	324	-17.50	1.00	FL(FG)	2010	Radabaugh et al. 2013
Chordata	Paralichthyidae	Fish	Southern flounder	*Paralichthys lethostigma*	1	10.80		1	-19.90		LA	2005	Senn et al. 2010
Chordata	Paralichthyidae	Fish	Southern flounder	*Paralichthys lethostigma*	2	9.70		6	-20.00		MS	1988	Sullivan and Moncreiff 1990
Chordata	Paralichthyidae	Fish	Southern flounder	*Paralichthys lethostigma*	10	12.91	1.26	10	-18.47	3.23	NC	2007	Wallace et al. 2009
Chordata	Paralichthyidae	Fish	Flounder	*Paralichthys spp*	7	14.50	0.80	4	-20.00	0.90	FL(FG)	1992	Wilson et al. 2009
Chordata	Paralichthyidae	Fish	Gulf flounder	*Paralichthys albigutta*	9	6.20	2.10	9	-17.40	0.90	FL(FG)	2007	Wilson et al. 2013
Chordata	Paralichthyidae	Fish	Gulf flounder	*Paralichthys albigutta*	12	10.00	1.10	12	-15.00	1.20	FL(FG)	2007	Wilson et al. 2013
Chordata	Paralichthyidae	Fish	Gulf flounder	*Paralichthys albigutta*	2	12.40	1.40	2	-15.50	2.40	FL(FG)	2007	Wilson et al. 2013
Chordata	Paralichthyidae	Fish	Southern flounder	*Paralichthys lethostigma*	2	13.22	1.68	2	-18.50	0.10	TX	1999	Winemiller et al. 2007
Chordata	Paralichthyidae	Fish	Summer flounder/ Flathead catfish	*Paralichthys dentatus/ Pylodictis olivaris*	3	12.35	0.49				NC	2002	Bucci et al. 2007a
Chordata	Phycidae	Fish	Spotted hake	*Urophycis regia*	4	15.79	0.40	4	-18.83	0.14	VA	2006	Buchheister and Latour 2011
Chordata	Phycidae	Fish	Spotted hake	*Urophycis regia*				1	-17.80		NC	1975	Thayer et al. 1978
Chordata	Phycidae	Fish	Spotted hake	*Urophycis regia*				1	-18.20		NC	1975	Thayer et al. 1978
Chordata	Pomatomidae	Fish	Bluefish	*Pomatomus saltatrix*	5	14.30	0.80	5	-17.61	0.16	NC	2007	Deehr et al. 2014
Chordata	Pomatomidae	Fish	Bluefish	*Pomatomus saltatrix*	1	15.27		1	-17.23		TX	2006	Oakley et al. 2014
Chordata	Sciaenidae	Fish	Atlantic croaker	*Micropogonias undulatus*	14	15.58	1.26	14	-19.30	1.14	VA	2006	Buchheister and Latour 2011

Chordata	Sciaenidae	Fish	Spot croaker	*Leiostomus xanthurus*	22	14.85	1.26	22	-18.31	1.90	VA	2006	Buchheister and Latour 2011
Chordata	Sciaenidae	Fish	Weakfish	*Cynoscion regalis*	16	15.61	0.55	16	-18.92	0.47	VA	2006	Buchheister and Latour 2011
Chordata	Sciaenidae	Fish	American silver perch	*Bairdiella chrysoura*				12	-19.63		FL(FG)	1992	Chanton and Lewis 2002
Chordata	Sciaenidae	Fish	Atlantic croaker	*Micropogonias undulatus*				16	-19.65		FL(FG)	1992	Chanton and Lewis 2002
Chordata	Sciaenidae	Fish	Sand weakfish	*Cynoscion arenarius*				6	-20.05		FL(FG)	1992	Chanton and Lewis 2002
Chordata	Sciaenidae	Fish	Spot croaker	*Leiostomus xanthurus*				16	-19.19		FL(FG)	1992	Chanton and Lewis 2002
Chordata	Sciaenidae	Fish	Atlantic croaker	*Micropogonias undulatus*	2	12.27	0.04	2	-18.94	0.51	NC	2007	Deehr et al. 2014
Chordata	Sciaenidae	Fish	Southern kingcroacker	*Menticirrhus americanus*	1	12.30					NC	2007	Deehr et al. 2014
Chordata	Sciaenidae	Fish	Spot croaker	*Leiostomus xanthurus*	22	11.17	0.56	22	-16.53	0.19	NC	2007	Deehr et al. 2014
Chordata	Sciaenidae	Fish	Atlantic croaker	*Micropogonias undulatus*	69	12.57	0.71	69	-19.13	1.05	AL	2008	Drymon et al. 2012
Chordata	Sciaenidae	Fish	Atlantic croaker	*Micropogonias undulatus*	14	11.80	1.50	14	-21.10	1.87	LA	2003	Fry and Chuchal 2012
Chordata	Sciaenidae	Fish	Spot croaker	*Leiostomus xanthurus*	16	12.50	1.60	16	-21.10	2.40	LA	2003	Fry and Chuchal 2012
Chordata	Sciaenidae	Fish	Northern kingcroacker	*Menticirrhus saxatillis*	3	9.40	0.69	3	-14.30	0.35	VA	1997	Knoff et al. 2001
Chordata	Sciaenidae	Fish	Southern kingcroacker	*Menticirrhus americanus*	3	13.20	0.35	3	-17.80	0.35	VA	1997	Knoff et al. 2001
Chordata	Sciaenidae	Fish	Spot croaker	*Leiostomus xanthurus*	1	12.90		1	-12.50		VA	1997	Knoff et al. 2001
Chordata	Sciaenidae	Fish	Atlantic croaker	*Micropogonias undulatus*	5	13.40		5	-16.50		MS	1991	Moncreiff and Sullivan 2001
Chordata	Sciaenidae	Fish	Spot croaker	*Leiostomus xanthurus*	4	13.50		4	-17.40		MS	1991	Moncreiff and Sullivan 2001
Chordata	Sciaenidae	Fish	Spotted weakfish	*Cynoscion nebulosus*	3	14.60		3	-17.50		MS	1991	Moncreiff and Sullivan 2001
Chordata	Sciaenidae	Fish	American silver perch	*Bairdiella chrysoura*				5	-17.50	1.30	FL(FG)	2007	Nelson et al. 2012
Chordata	Sciaenidae	Fish	Atlantic croaker	*Micropogonias undulatus*				5	-17.30	1.30	FL(FG)	2007	Nelson et al. 2012
Chordata	Sciaenidae	Fish	Spot croaker	*Leiostomus xanthurus*				5	-15.90	0.90	FL(FG)	2007	Nelson et al. 2012

Chordata	Sciaenidae	Fish	Spotted weakfish	*Cynoscion nebulosus*				5	-16.60	0.70	FL(FG)	2007	Nelson et al. 2012
Chordata	Sciaenidae	Fish	American silver perch	*Bairdiella chrysoura*	5	16.16	2.48	5	-18.79	1.77	TX	2006	Oakley et al. 2014
Chordata	Sciaenidae	Fish	Atlantic croaker	*Micropogonias undulatus*	13	12.82	1.33	13	-17.37	1.69	TX	2006	Oakley et al. 2014
Chordata	Sciaenidae	Fish	Gulf kingcroacker	*Menticirrhus littoralis*	13	13.94	0.87	13	-17.08	1.26	TX	2006	Oakley et al. 2014
Chordata	Sciaenidae	Fish	Sand weakfish	*Cynoscion arenarius*	7	15.20	0.40	7	-18.12	0.74	TX	2006	Oakley et al. 2014
Chordata	Sciaenidae	Fish	Spot croaker	*Leiostomus xanthurus*	16	13.78	1.68	16	-19.36	2.12	TX	2006	Oakley et al. 2014
Chordata	Sciaenidae	Fish	Spotted weakfish	*Cynoscion nebulosus*	12	13.71	2.46	12	-17.45	2.39	TX	2006	Oakley et al. 2014
Chordata	Sciaenidae	Fish	Sand weakfish	*Cynoscion arenarius*	8	11.15	0.21	8	-22.53	0.42	FL(FG)	2008	Olin et al. 2013
Chordata	Sciaenidae	Fish	Southern kingcroacker	*Menticirrhus americanus*	8	10.31	0.44	8	-22.36	0.54	FL(FG)	2008	Olin et al. 2013
Chordata	Sciaenidae	Fish	Atlantic croaker	*Micropogonias undulatus*				10	-18.98	2.39	VA	1999	Pruell et al. 2003
Chordata	Sciaenidae	Fish	Spot croaker	*Leiostomus xanthurus*				12	-17.60	0.93	VA	1999	Pruell et al. 2003
Chordata	Sciaenidae	Fish	Weakfish	*Cynoscion regalis*				17	-17.90	1.91	VA	1999	Pruell et al. 2003
Chordata	Sciaenidae	Fish	Spot croaker	*Leiostomus xanthurus*	1	5.80		1	-11.98		FL(FG)	2000	Reynolds et al. 2001
Chordata	Sciaenidae	Fish	Atlantic croaker	*Micropogonias undulatus*	4	15.38	0.30	4	-17.05	0.80	TX	2014	Rezek et al. 2017
Chordata	Sciaenidae	Fish	Spot croaker	*Leiostomus xanthurus*	24	10.30	1.40	24	-16.70	2.10	FL(FG)	2009	Rossman et al. 2015
Chordata	Sciaenidae	Fish	Spotted weakfish	*Cynoscion nebulosus*	27	11.50	1.70	27	-14.30	1.70	FL(FG)	2009	Rossman et al. 2015
Chordata	Sciaenidae	Fish	Spotted weakfish	*Cynoscion nebulosus*	4	13.00	0.90	4	-19.10	1.50	LA	2005	Senn et al. 2010
Chordata	Sciaenidae	Fish	Atlantic croaker	*Micropogonias undulatus*	243	13.03	1.29	243	-18.50	1.52	LA	2005	Simonsen and Cowan 2013
Chordata	Sciaenidae	Fish	Spotted weakfish	*Cynoscion nebulosus*	89	14.17	0.86	89	-19.78	1.01	LA	2005	Simonsen and Cowan 2013
Chordata	Sciaenidae	Fish	American silver perch	*Bairdiella chrysoura*				1	-17.10		TX	1991	Street et al. 1997
Chordata	Sciaenidae	Fish	Spot croaker	*Leiostomus xanthurus*				4	-10.00		TX	1991	Street et al. 1997

Chordata	Sciaenidae	Fish	Spotted weakfish	*Cynoscion nebulosus*				6	-15.40		TX	1991	Street et al. 1997
Chordata	Sciaenidae	Fish	American silver perch	*Bairdiella chrysoura*	29	12.10	1.60	29	-18.00	1.70	FL(FG)	1998	Sulak et al. 2012
Chordata	Sciaenidae	Fish	Atlantic croaker	*Micropogonias undulatus*	4	14.10	0.30	4	-20.30	0.80	FL(FG)	1998	Sulak et al. 2012
Chordata	Sciaenidae	Fish	Spotted weakfish	*Cynoscion nebulosus*	19	12.40	1.80	19	-17.20	1.90	FL(FG)	1998	Sulak et al. 2012
Chordata	Sciaenidae	Fish	American silver perch	*Bairdiella chrysoura*	4	12.20		7	-19.40		MS	1988	Sullivan and Moncreiff 1990
Chordata	Sciaenidae	Fish	American star drum	*Stellifer lanceolatus*	1	10.20		1	-20.80		MS	1988	Sullivan and Moncreiff 1990
Chordata	Sciaenidae	Fish	Atlantic croaker	*Micropogonias undulatus*	6	10.20		13	-22.40		MS	1988	Sullivan and Moncreiff 1990
Chordata	Sciaenidae	Fish	Kingcroacker	*Menticirrhus spp*	1	11.10		1	-18.80		MS	1988	Sullivan and Moncreiff 1990
Chordata	Sciaenidae	Fish	Sand weakfish	*Cynoscion arenarius*	2	11.00		2	-20.40		MS	1988	Sullivan and Moncreiff 1990
Chordata	Sciaenidae	Fish	Spot croaker	*Leiostomus xanthurus*	7	11.20		7	-21.00		MS	1988	Sullivan and Moncreiff 1990
Chordata	Sciaenidae	Fish	Spotted weakfish	*Cynoscion nebulosus*	1	11.80		11	-20.70		MS	1988	Sullivan and Moncreiff 1990
Chordata	Sciaenidae	Fish	American silver perch	*Bairdiella chrysoura*				1	-17.20		NC	1975	Thayer et al. 1978
Chordata	Sciaenidae	Fish	Spot croaker	*Leiostomus xanthurus*	8	12.37	1.47	8	-16.77	2.77	NC	2007	Wallace et al. 2009
Chordata	Sciaenidae	Fish	American silver perch	*Bairdiella chrysoura*	17	15.00	1.40	10	-19.60	1.30	FL(FG)	1992	Wilson et al. 2009
Chordata	Sciaenidae	Fish	Atlantic croaker	*Micropogonias undulatus*	30	13.80	0.70	16	-19.30	1.30	FL(FG)	1992	Wilson et al. 2009
Chordata	Sciaenidae	Fish	Sand weakfish	*Cynoscion arenarius*	9	15.20	1.40	5	-19.90	0.40	FL(FG)	1992	Wilson et al. 2009
Chordata	Sciaenidae	Fish	Spot croaker	*Leiostomus xanthurus*	22	14.20	0.60	15	-19.10	1.10	FL(FG)	1992	Wilson et al. 2009
Chordata	Sciaenidae	Fish	American silver perch	*Bairdiella chrysoura*	10	9.60	0.80	10	-17.00	0.40	FL(FG)	2007	Wilson et al. 2013
Chordata	Sciaenidae	Fish	American silver perch	*Bairdiella chrysoura*	18	12.20	1.20	18	-17.90	1.50	FL(FG)	2007	Wilson et al. 2013
Chordata	Sciaenidae	Fish	American silver perch	*Bairdiella chrysoura*	1	12.60		1	-16.10		FL(FG)	2007	Wilson et al. 2013
Chordata	Sciaenidae	Fish	Atlantic croaker	*Micropogonias undulatus*	6	10.90	1.10	6	-15.80	0.70	FL(FG)	2007	Wilson et al. 2013
Chordata	Sciaenidae	Fish	Atlantic croaker	*Micropogonias undulatus*	4	12.10	1.50	4	-15.30	2.50	FL(FG)	2007	Wilson et al. 2013

Chordata	Sciaenidae	Fish	Sand weakfish	*Cynoscion arenarius*	10	6.60	1.00	10	-16.80	0.70	FL(FG)	2007	Wilson et al. 2013
Chordata	Sciaenidae	Fish	Sand weakfish	*Cynoscion arenarius*	3	11.60	0.40	3	-15.40	2.50	FL(FG)	2007	Wilson et al. 2013
Chordata	Sciaenidae	Fish	Sand weakfish	*Cynoscion arenarius*	3	13.20	0.50	3	-13.50	0.60	FL(FG)	2007	Wilson et al. 2013
Chordata	Sciaenidae	Fish	Spot croaker	*Leiostomus xanthurus*	8	11.60	0.90	8	-16.10	0.80	FL(FG)	2007	Wilson et al. 2013
Chordata	Sciaenidae	Fish	Spot croaker	*Leiostomus xanthurus*	1	13.00		1	-13.10		FL(FG)	2007	Wilson et al. 2013
Chordata	Sciaenidae	Fish	American silver perch	*Bairdiella chrysoura*	4	14.69	1.98	4	-19.30	0.50	TX	1999	Winemiller et al. 2007
Chordata	Sciaenidae	Fish	Spot croaker	*Leiostomus xanthurus*	2	13.34	1.99	2	-13.50	0.10	TX	1999	Winemiller et al. 2007
Chordata	Sciaenidae	Fish	Spotted weakfish	*Cynoscion nebulosus*	8	13.23	2.21	8	-19.40	0.60	TX	1999	Winemiller et al. 2007
Chordata	Sciaenidae	Fish	Atlantic croaker	*Micropogonias undulatus*	63	15.50	0.40	63	-19.20	1.62	VA	2009	Xu et al. 2013
Chordata	Sciaenidae	Fish	Spot croaker	*Leiostomus xanthurus*	51	15.90	1.09	51	-20.70	1.09	VA	2009	Xu et al. 2013
Chordata	Sparidae	Fish	Sheepshead	*Archosargus probatocephalus*	1	7.42		1	-20.71		FL(FG)	2008	Abeels et al. 2012
Chordata	Sparidae	Fish	Pinfish	*Lagodon rhomboides*				2	-17.70		FL(FG)	1992	Chanton and Lewis 2002
Chordata	Sparidae	Fish	Pinfish	*Lagodon rhomboides*	5	9.72	0.91	5	-13.74	0.42	FL(FG)	1997	Chasar et al. 2005
Chordata	Sparidae	Fish	Pinfish	*Lagodon rhomboides*	23	10.71	0.53	23	-17.94	0.31	NC	2007	Deehr et al. 2014
Chordata	Sparidae	Fish	Pinfish	*Lagodon rhomboides*	3	13.40	1.91	3	-18.80	0.00	LA	2003	Fry and Chuchal 2012
Chordata	Sparidae	Fish	Pinfish	*Lagodon rhomboides*	13	11.80		13	-16.10		MS	1991	Moncreiff and Sullivan 2001
Chordata	Sparidae	Fish	Pinfish	*Lagodon rhomboides*				5	-17.00	1.40	FL(FG)	2007	Nelson et al. 2012
Chordata	Sparidae	Fish	Pinfish	*Lagodon rhomboides*	10	11.03	1.58	10	-16.59	1.77	TX	2006	Oakley et al. 2014
Chordata	Sparidae	Fish	Sheepshead	*Archosargus probatocephalus*	6	13.09	1.86	6	-18.57	1.81	TX	2006	Oakley et al. 2014
Chordata	Sparidae	Fish	Pinfish	*Lagodon rhomboides*	17	11.02	1.37	17	-19.25	2.64	FL(FG)	2006	Olin et al. 2012
Chordata	Sparidae	Fish	Pinfish	*Lagodon rhomboides*	14	9.69	0.64	14	-21.89	1.64	FL(FG)	2006	Olin et al. 2012
Chordata	Sparidae	Fish	Littlehead porgy	*Calamus proridens*	181	9.70	0.50	181	-16.00	0.80	FL(FG)	2010	Radabaugh et al. 2013
Chordata	Sparidae	Fish	Pinfish	*Lagodon rhomboides*	81	9.70	0.90	81	-16.80	1.00	FL(FG)	2010	Radabaugh and Peebles 2014
Chordata	Sparidae	Fish	Pinfish	*Lagodon rhomboides*	10	6.95	0.57	10	-13.23	1.26	FL(FG)	2000	Reynolds et al. 2001
Chordata	Sparidae	Fish	Pinfish	*Lagodon rhomboides*	12	14.87	0.83	12	-17.73	1.00	TX	2014	Rezek et al. 2017
Chordata	Sparidae	Fish	Pinfish	*Lagodon rhomboides*	27	8.00	1.30	27	-13.70	1.20	FL(FG)	2009	Rossman et al. 2015

Chordata	Sparidae	Fish	Pinfish	*Lagodon rhomboides*	20	9.00	0.70	20	-16.10	1.20	FL(FG)	2009	Rossman et al. 2015
Chordata	Sparidae	Fish	Sheepshead	*Archosargus probatocephalus*	15	9.00	0.80	15	-14.90	1.60	FL(FG)	2009	Rossman et al. 2015
Chordata	Sparidae	Fish	Pinfish	*Lagodon rhomboides*				2	-13.40		TX	1991	Street et al. 1997
Chordata	Sparidae	Fish	Pinfish	*Lagodon rhomboides*				2	-13.30		TX	1991	Street et al. 1997
Chordata	Sparidae	Fish	Pinfish	*Lagodon rhomboides*	6	9.60	1.80	6	-19.10	2.40	FL(FG)	1998	Sulak et al. 2012
Chordata	Sparidae	Fish	Pinfish	*Lagodon rhomboides*	4	10.10		7	-22.00		MS	1988	Sullivan and Moncreiff 1990
Chordata	Sparidae	Fish	Sheepshead	*Archosargus probatocephalus*	6	10.00		6	-21.20		MS	1988	Sullivan and Moncreiff 1990
Chordata	Sparidae	Fish	Red porgy	*Pagrus pagrus*	17	10.60	0.66	17	-16.20	0.66	NC	1990	Thomas and Cahoon 1993
Chordata	Sparidae	Fish	Spottail pinfish	*Diplodus holbrooki*	30	11.00	0.82	30	-17.70	0.66	NC	1990	Thomas and Cahoon 1993
Chordata	Sparidae	Fish	Pinfish	*Lagodon rhomboides*	10	5.70	1.70	10	-17.60	0.60	FL(FG)	2007	Wilson et al. 2013
Chordata	Sparidae	Fish	Pinfish	*Lagodon rhomboides*	8	11.40	0.60	8	-17.00	1.00	FL(FG)	2007	Wilson et al. 2013
Chordata	Sparidae	Fish	Pinfish	*Lagodon rhomboides*	11	11.50	0.20	11	-15.00	0.70	FL(FG)	2007	Wilson et al. 2013
Chordata	Sparidae	Fish	Pinfish	*Lagodon rhomboides*	12	9.01	1.72	12	-16.90	1.40	TX	1999	Winemiller et al. 2007
Chordata	Synodontidae	Fish	Inshore lizardfish	*Synodus foetens*				10	-17.60	0.47	FL(FG)	2007	Nelson et al. 2012
Chordata	Synodontidae	Fish	Inshore lizardfish	*Synodus foetens*	226	11.20	0.80	226	-17.30	0.60	FL(FG)	2010	Radabaugh et al. 2013
Chordata	Synodontidae	Fish	Inshore lizardfish	*Synodus foetens*	4	11.60	0.40	4	-15.00	1.20	FL(FG)	2007	Wilson et al. 2013
Chordata	Triglidae	Fish	Searobin	*Prionotus spp*	11	13.04	0.41	11	-18.70	1.84	AL	2008	Drymon et al. 2012
Chordata	Triglidae	Fish	Bighead searobin	*Prionotus tribulus*	8	11.40		8	-16.20		MS	1991	Moncreiff and Sullivan 2001
Mollusca	Buccinidae	Gastropod	Tinted cantharus	*Pisania tincta*	54	12.60		54	-19.20		MS	1991	Moncreiff and Sullivan 2001
Mollusca	Busyconidae	Gastropod	Lightning whelk	*Busycon sinistrum*	2	11.60		2	-17.10		MS	1991	Moncreiff and Sullivan 2001
Mollusca	Busyconidae	Gastropod	Whelk spp	*Busycon spp*	10	9.41	0.57	10	-17.01	0.70	NC	2007	Wallace et al. 2009
Mollusca	Calyptraeidae	Gastropod	Slipper snail	*Crepidula convexa*	3	8.86	0.34	3	-17.40	0.84	VA	2005	Douglass et al. 2011
Mollusca	Calyptraeidae	Gastropod	Eastern white slipper snail	*Crepidula plana*	177	8.70		177	-19.30		MS	1991	Moncreiff and Sullivan 2001
Mollusca	Cerithiidae	Gastropod	Sea snail	Cerithium lutosum				5	-13.40		TX	1991	Street et al. 1997
Mollusca	Cerithiidae	Gastropod	Sea snail	Ittibittium oryza				4	-15.30	0.79	NC	1975	Thayer et al. 1978
Mollusca	Columbellidae	Gastropod	Sea snail	Astyris lunata				4	-15.50	0.52	NC	1975	Thayer et al. 1978

Mollusca	Columbellidae	Gastropod	Sea snail	Costoanachis avara				6	-16.00	0.93	NC	1975	Thayer et al. 1978
Mollusca	Littorinidae	Gastropod	Marsh periwinkle	*Littorina irrorata*	3	8.30	0.17	3	-18.00	0.35	FL(FG)	2008	Baker et al. 2013
Mollusca	Littorinidae	Gastropod	Marsh periwinkle	*Littorina irrorata*	2	8.50	0.28	2	-14.00	1.41	LA	2008	Baker et al. 2013
Mollusca	Littorinidae	Gastropod	Marsh periwinkle	*Littorina irrorata*	3	9.40	0.17	3	-16.70	0.35	LA	2008	Baker et al. 2013
Mollusca	Littorinidae	Gastropod	Marsh periwinkle	*Littorina irrorata*	3	5.80	0.87	3	-19.30	3.81	MS	2008	Baker et al. 2013
Mollusca	Littorinidae	Gastropod	Marsh periwinkle	*Littorina irrorata*	1	3.80		1	-17.00		NC	2008	Baker et al. 2013
Mollusca	Littorinidae	Gastropod	Marsh periwinkle	*Littorina irrorata*	2	6.50	0.71	2	-16.30	0.14	NC	2008	Baker et al. 2013
Mollusca	Littorinidae	Gastropod	Marsh periwinkle	*Littorina irrorata*	3	8.00	0.80	3	-15.60	3.81	NC	2008	Baker et al. 2013
Mollusca	Littorinidae	Gastropod	Marsh periwinkle	*Littorina irrorata*	3	8.70	0.35	3	-14.50	0.69	TX	2008	Baker et al. 2013
Mollusca	Littorinidae	Gastropod	Marsh periwinkle	*Littorina irrorata*	3	9.20	0.35	3	-15.50	1.39	TX	2008	Baker et al. 2013
Mollusca	Littorinidae	Gastropod	Marsh periwinkle	*Littorina irrorata*	4	3.15	0.69	4	-16.03	0.65	NC	1992	Currin et al. 1995
Mollusca	Littorinidae	Gastropod	Marsh periwinkle	*Littorina irrorata*	3	10.80	0.69	3	-14.30	0.35	VA	1997	Knoff et al. 2001
Mollusca	Littorinidae	Gastropod	Marsh periwinkle	*Littorina spp*	65	6.29	0.62	65	-14.75	1.56	LA	2013	Olin et al. 2017
Mollusca	Littorinidae	Gastropod	Marsh periwinkle	*Littorina irrorata*	8	3.80	0.19	8	-15.60	0.88	MS	2006	Rush et al. 2010
Mollusca	Littorinidae	Gastropod	Marsh periwinkle	*Littorina irrorata*	8	6.50	0.30	8	-20.00	0.62	MS	2006	Rush et al. 2010
Mollusca	Littorinidae	Gastropod	Marsh periwinkle	*Littorina irrorata*				4	-21.60		MS	1988	Sullivan and Moncreiff 1990
Mollusca	Littorinidae	Gastropod	Common periwinkle	*Littorina littorea*				2	-18.80	5.40	AL	2010	Wilson et al. 2015
Mollusca	Littorinidae	Gastropod	Common periwinkle	*Littorina littorea*				10	-16.10	1.60	LA	2010	Wilson et al. 2015
Mollusca	Littorinidae	Gastropod	Marsh periwinkle	*Littorina spp*				1	-16.30		MS	2010	Wilson et al. 2015
Mollusca	Melongenidae	Gastropod	Crown conch	*Melongena corona*				1	-21.80		FL(FG)	1992	Chanton and Lewis 2002
Mollusca	Melongenidae	Gastropod	Crown conch	*Melongena corona*	1	4.30		1	-24.10		FL(FG)	2012	Denton et al. 2019
Mollusca	Melongenidae	Gastropod	Crown conch	*Melongena corona*	18	7.80	0.90	18	-19.90	2.20	FL(FG)	2012	Denton et al. 2019

Mollusca	Muricidae	Gastropod	Red-mouthed rock snail	*Thais haemastoma*	20	13.70		20	-16.60		MS	1991	Moncreiff and Sullivan 2001
Mollusca	Muricidae	Gastropod	Atlantic oyster drill	*Urosalpinx cinerea*	16	12.24	0.22	16	-17.78	0.29	LA	2007	Simonsen 2008
Mollusca	Muricidae	Gastropod	Sea snail	Eupleura caudata				1	-16.60		NC	1975	Thayer et al. 1978
Mollusca	Nassariidae	Gastropod	Eastern mudsnail	*Ilyanassa obsoleta*	3	7.07	0.38	3	-14.07	1.03	NC	1992	Currin et al. 1995
Mollusca	Nassariidae	Gastropod	Bruised nassa	*Nassarius vibex*	79	14.10		79	-16.30		MS	1991	Moncreiff and Sullivan 2001
Mollusca	Nassariidae	Gastropod	Bruised nassa	*Nassarius vibex*				1.00	-15.40		NC	1975	Thayer et al. 1978
Mollusca	Naticidae	Gastropod	Atlantic moon snail	*Polynices duplicatus*	1	11.40		1	-16.50		MS	1991	Moncreiff and Sullivan 2001
Mollusca	Naticidae	Gastropod	Atlantic moon snail	*Polinices duplicatus*	1	8.40		1	-18.10		MS	1988	Sullivan and Moncreiff 1990
Mollusca	Naticidae	Gastropod	Atlantic moon snail	*Polinices duplicatus*				1	-18.90		NC	1975	Thayer et al. 1978
Mollusca	Neritidae	Gastropod	Olive nerite	*Neritina usnea*	22	7.40	0.25	22	-20.90	0.50	MS	2006	Rush et al. 2010
Mollusca	Potamididae	Gastropod	Ladder horn snail	*Cerithidea scalariformis*	1	7.60		1	-19.10		FL(FG)	2012	Denton et al. 2019
Mollusca	Turbinidae	Gastropod	West Indian starsnail	*Lithopoma tectum*	6	4.47	0.72	6	-10.97	1.25	FL(FG)	1997	Behringer and Butler 2006
Plant	Cladophoraceae	Macroalgae	Filamentous green algae	*Cladophora spp*	1	8.91		1	-16.67		VA	2006	Douglass et al. 2011
Plant	Ceramiaceae	Macroalgae	Red algae	*Ceramium spp*	1	9.60		1	-13.07		VA	2006	Douglass et al. 2011
Plant	Cladophoraceae	Macroalgae	Green algae	*Chaetomorpha spp*	1	6.60		1	-21.70		NC	1992	Currin et al. 1995
Plant	Codiaceae	Macroalgae	Green sea fingers	*Codium fragile*	8	9.66	0.58	8	-15.34	1.25	VA	2010	Hondula and Price 2014
Plant	Codiaceae	Macroalgae	Green sea fingers	*Codium fragile*				2	-13.48	0.06	NC	1989	Raven and Osmond 1992
Plant	Dictyotaceae	Macroalgae	Forkweed	*Dictyota menstrualis*				2	-16.67	0.03	NC	1989	Raven and Osmond 1992
Plant	Dictyotaceae	Macroalgae	Forkweed	*Padina gymnospora*				2	-19.68	0.18	NC	1989	Raven and Osmond 1992
Plant	Ectocarpaceae	Macroalgae	Filamentous brown algae	*Ectocarpus spp*	1	7.58		1	-16.25		VA	2006	Douglass et al. 2011
Plant	Fucaceae	Macroalgae	Bladder rack	*Fucus vesiculosus*				2	-15.97	0.05	NC	1989	Raven and Osmond 1992
Plant	Gelidiaceae	Macroalgae	Red algae	*Gelidium spp*	3	7.84	0.07	3	-18.85	0.10	TX	2007	Gorga 2010

Plant	Gelidiaceae	Macroalgae	Red algae	*Gelidium spp*	3	10.07	0.11	3	-20.39	0.17	TX	2007	Gorga 2010
Plant	Gracilariaceae	Macroalgae	Red algae	*Gracilaria spp*				2	-20.30	0.57	FL(FG)	1992	Chanton and Lewis 2002
Plant	Gracilariaceae	Macroalgae	Red algae	*Gracilaria spp*	2	9.98	0.15	2	-17.11	4.66	VA	2005	Douglass et al. 2011
Plant	Gracilariaceae	Macroalgae	Red algae	*Gracilaria caudata*	1	5.90		1	-17.92		TX	1999	Herzka et al. 2002
Plant	Gracilariaceae	Macroalgae	Red algae	*Hydropuntia cornea*	1	7.70		1	-15.54		TX	1999	Herzka et al. 2002
Plant	Gracilariaceae	Macroalgae	Red algae	*Gracilaria vermicuphylla*	16	8.77	2.18	16	-18.03	2.59	VA	2010	Hondula and Price 2014
Plant	Gracilariaceae	Macroalgae	Red algae	*Gracilaria spp*	2	6.60		2	-13.00		FL(FG)	2011	Williams et al. 2014
Plant	Halymeniaceae	Macroalgae	Red algae	*Grateloupia spp*	10	6.77	0.66	10	-20.53	1.68	FL(FG)	2009	Prado et al. 2012
Plant	Macroalgae	Macroalgae	Benthic algae	*Unknown*	16	4.90	4.20	16	-20.40	4.10	TX	2004	Hoeinghau and Davis 2007
Plant	Macroalgae	Macroalgae	Macroalgae	*Gracilaria spp, Ulva spp*	2	7.45		2	-18.94		TX	2007	Howell et al. 2016
Plant	Macroalgae	Macroalgae	Macroalgae	*Gracilaria spp, Ulva spp*	2	9.21		2	-18.73		TX	2007	Howell et al. 2016
Plant	Macroalgae	Macroalgae	Epiphytic algae	*Unidentified*	4	5.90	0.90	4	-17.50	1.70	MS	1991	Moncreiff and Sullivan 2001
Plant	Macroalgae	Macroalgae	Benthic algae	*Unknown*	85	4.00	0.80	85	-19.30	2.70	FL(FG)	2010	Radabaugh et al. 2013
Plant	Multiple	Macroalgae	Macroalgae	*Ulva spp, Codium spp, Dictyota spp*	7	5.80	0.15	7	-17.13	0.35	NC	2007	Deehr et al. 2014
Plant	Multiple	Macroalgae	Macroalgae	*Sargassum spp, Gracilaria spp*	4	6.30	0.29	4	-19.27	0.83	NC	2007	Deehr et al. 2014
Plant	Multiple	Macroalgae	Sea lettuce, filamentous algae	*Ulva australis, miscellaneous macroalgae*	129	4.82	1.25				FL(FG)	1999	Dillon and Chanton 2008
Plant	Multiple	Macroalgae	Red algae	*Agardhiella subulata, Dictyota cervicornis, Gracilaria spp, Hypnea spp, Lomentaria baileyana, Solieria filiformis*	118	4.68	1.57				FL(FG)	2008	Milbrandt et al. 2019

Plant	Multiple	Macroalgae	Red algae	*Agardhiella subulata, Dictyota cervicornis, Gracilaria spp, Hypnea spp, Lomentaria baileyana, Solieria filiformis*	63	6.12	1.71				FL(FG)	2008	Milbrandt et al. 2019
Plant	Solieriaceae	Macroalgae	Red algae	*Agardhiella spp*	6	11.02	0.68	6	-16.85	0.40	VA	2006	Douglass et al. 2011
Plant	Solieriaceae	Macroalgae	Red algae	*Agardhiella subulata*	7	9.37	0.96	7	-18.84	2.88	VA	2010	Hondula and Price 2014
Plant	Ulvaceae	Macroalgae	Sea lettuce	*Ulva lactua*				3	-20.20	1.30	FL(FG)	1992	Chanton and Lewis 2002
Plant	Ulvaceae	Macroalgae	Sea lettuce	*Ulva spp*	1	8.10		1	-15.50		NC	1992	Currin et al. 1995
Plant	Ulvaceae	Macroalgae	Sea lettuce	*Ulva spp*	1	8.75		1	-17.10		VA	2005	Douglass et al. 2011
Plant	Ulvaceae	Macroalgae	Sea lettuce	*Ulva spp*	3	7.22	0.24	3	-19.01	0.10	TX	2007	Gorga 2010
Plant	Ulvaceae	Macroalgae	Sea lettuce	*Ulva spp*	3	8.52	0.12	3	-17.08	0.03	TX	2007	Gorga 2010
Plant	Ulvaceae	Macroalgae	Sea lettuce	*Ulva lactuca*	17	8.71	1.81	17	-20.76	2.67	VA	2010	Hondula and Price 2014
Plant	Ulvaceae	Macroalgae	Sea lettuce	*Enterpmoprha spp*	1	8.80		1	-16.20		MS	1991	Moncreiff and Sullivan 2001
Plant	Ulvaceae	Macroalgae	Sea lettuce	*Ulva lactua*	1	5.96		1	-18.54		TX	2006	Oakley et al. 2014
Plant	Ulvaceae	Macroalgae	Sea lettuce	*Ulva spp*	9	10.10	0.30				FL(FG)	2006	Oczkowski et al. 2011
Plant	Ulvaceae	Macroalgae	Sea lettuce	*Ulva spp*	5	6.77	0.13	5	-18.86	0.04	AL	2009	Prado et al. 2012
Plant	Ulvaceae	Macroalgae	Sea lettuce	*Ulva spp*	3.00	8.40	0.07	3.00	-15.40	1.54	LA	2016	Reeves et al. 2019
Plant	Ulvaceae	Macroalgae	Sea lettuce	*Ulva spp*	2	5.50		2	-12.80		FL(FG)	2011	Williams et al. 2014
Plant	Ulvaceae	Macroalgae	Sea lettuce	*Ulva spp*	3	6.50	0.40	3	-20.20	0.20	TX	1999	Winemiller et al. 2007
Plant	*Unidentified*	Macroalgae	Filamentous brown algae	*Unidentified*	4	10.60	0.02	4	-20.50	0.30	LA	2016	Reeves et al. 2019
Plant	*Unidentified*	Macroalgae	Filamentous green algae	*Unidentified*	2	10.20	0.59	2	-20.00	1.27	LA	2016	Reeves et al. 2019
Plant	*Unidentified*	Macroalgae	Filamentous red algae	*Unidentified*	3	8.80	0.05	3	-19.60	3.17	LA	2016	Reeves et al. 2019
Plant	Wrangeliaceae	Macroalgae	Red algae	*Wrangelia spp*				1	-21.60		FL(FG)	1992	Chanton and Lewis 2002
Plant	Cymodoceaceae	Seagrass	Manatee grass	*Syringodium filiforme*	1	3.70		1	-8.40		FL(FG)	1983	Harrigan et al. 1989
Plant	Cymodoceaceae	Seagrass	Shoal grass	*Halodule wrightii*	1	3.40		1	-12.80		FL(FG)	1983	Harrigan et al. 1989
Plant	Hydrocharitaceae	Seagrass	Turtle grass	*Thalassia testudinum*	1	3.70		1	-13.60		FL(FG)	1983	Harrigan et al. 1989
Plant	Cymodoceaceae	Seagrass	Shoal grass	*Halodule wrightii*				2	-14.45		FL(FG)	1992	Chanton and Lewis 2002

Plant	Cymodoceaceae	Seagrass	Shoal grass	*Halodule wrightii*	3	2.70	0.87	3	-12.10	0.35	FL(FG)	1998	Chasar et al. 2005
Plant	Cymodoceaceae	Seagrass	Shoal grass	*Halodule spp*	1	2.92		1	-12.26		NC	2007	Deehr et al. 2014
Plant	Cymodoceaceae	Seagrass	Shoal grass	*Halodule wrightii*	60	4.40	0.60				TX	2014	Delgado et al. 2017
Plant	Cymodoceaceae	Seagrass	Manatee grass	*Syringodium filiforme*	3	4.64	0.09	3	-5.25	0.19	TX	2007	Gorga 2010
Plant	Cymodoceaceae	Seagrass	Manatee grass	*Syringodium filiforme*	3	6.32	0.23	3	-10.82	0.14	TX	2007	Gorga 2010
Plant	Cymodoceaceae	Seagrass	Shoal grass	*Halodule wrightii*	3	5.39	0.11	3	-9.79	0.26	TX	2007	Gorga 2010
Plant	Cymodoceaceae	Seagrass	Shoal grass	*Halodule wrightii*	3	7.20	0.18	3	-5.20	0.08	TX	2007	Gorga 2010
Plant	Cymodoceaceae	Seagrass	Shoal grass	*Halodule wrightii*	1	3.68		1	-9.41		TX	1999	Herzka et al. 2002
Plant	Cymodoceaceae	Seagrass	Shoal grass	*Halodule wrightii*	16	5.47	0.37	16	-12.43	0.50	TX	2010	Lebreton et al. 2016
Plant	Cymodoceaceae	Seagrass	Shoal grass	*Halodule wrightii*	4	6.00	1.10	4	-12.20	1.20	MS	1991	Moncreiff and Sullivan 2001
Plant	Cymodoceaceae	Seagrass	Shoal grass	*Halodule wrightii*	4	3.50	1.24	4	-11.74	0.40	TX	2006	Oakley et al. 2014
Plant	Cymodoceaceae	Seagrass	Manatee grass	*Syringodium filiforme*	3	0.30	1.00	3	-8.80	0.40	FL(FG)	2004	Reich et al. 2008
Plant	Cymodoceaceae	Seagrass	Shoal grass	*Halodule wrightii*	6	-0.80	1.00	6	-10.80	0.20	FL(FG)	2004	Reich et al. 2008
Plant	Cymodoceaceae	Seagrass	Shoal grass	*Halodule wrightii*	5	6.58	0.10	5	-11.92	0.20	TX	2014	Rezek et al. 2017
Plant	Cymodoceaceae	Seagrass	Manatee grass	*Syringodium filiforme*	2	4.10		2	-6.90		FL(FG)	2011	Williams et al. 2014
Plant	Cymodoceaceae	Seagrass	Shoal grass	*Halodule wrightii*	2	1.40		2	-11.40		FL(FG)	2011	Williams et al. 2014
Plant	Cymodoceaceae	Seagrass	Shoal grass	*Halodule and Syringodium spp*	11	2.00	0.60	11	-8.80	1.60	FL(FG)	2007	Wilson et al. 2017
Plant	Hydrocharitaceae	Seagrass	Turtle grass	*Thalassia testudinum*	10.00	-0.07	1.08	10.00	-15.02	2.27	FL(FG)	2010	Barry et al. 2017
Plant	Hydrocharitaceae	Seagrass	Turtle grass	*Thalassia testudinum*	6	2.97	0.47	6	-6.97	0.53	FL(FG)	1997	Behringer and Butler 2006
Plant	Hydrocharitaceae	Seagrass	Turtle grass	*Thalassia testudinum*	13	3.57	1.42	13	-10.16	1.25	FL(FG)	1997	Chasar et al. 2005
Plant	Hydrocharitaceae	Seagrass	Turtle grass	*Thalassia testudinum*	69	5.77	2.28				FL(FG)	1994	Corbett et al. 1999
Plant	Hydrocharitaceae	Seagrass	Turtle grass	*Thalassia testudinum*	10	4.10	2.50	10	-10.60	1.10	FL(FG)	2012	Denton et al. 2019

Plant	Hydrocharitaceae	Seagrass	Turtle grass	*Thalassia testudinum*	10	6.00	0.95	10	-10.70	0.63	FL(FG)	2001	Fourqurean and Schrlau 2003
Plant	Hydrocharitaceae	Seagrass	Turtle grass	*Thalassia testudinum*	3	5.26	0.05	3	-9.34	0.03	TX	2007	Gorga 2010
Plant	Hydrocharitaceae	Seagrass	Turtle grass	*Thalassia testudinum*	3	5.59	0.11	3	-12.03	0.16	TX	2007	Gorga 2010
Plant	Hydrocharitaceae	Seagrass	Seagrass	*Thalassia testudinum, Cymodocea filiformis, Halodule beaudettei*	3	5.08	0.40	3	-8.12	2.49	TX	2007	Howell et al. 2016
Plant	Hydrocharitaceae	Seagrass	Seagrass	*Thalassia testudinum, Cymodocea filiformis, Halodule beaudettei*	3	6.37	0.81	3	-9.36	3.64	TX	2007	Howell et al. 2016
Plant	Hydrocharitaceae	Seagrass	Turtle grass	*Thalassia testudinum*	6	4.29	0.56	6	-10.46	0.73	FL(FG)	2010	Marco-Mendez et al. 2012
Plant	Hydrocharitaceae	Seagrass	Turtle grass	*Thalassia testudinum*	16	4.77	1.48	16	-10.21	0.52	FL(FG)	2009	Prado et al. 2012
Plant	Hydrocharitaceae	Seagrass	Turtle grass	*Thalassia testudinum*	3	1.40	1.20	3	-9.60	1.20	FL(FG)	2004	Reich et al. 2008
Plant	Hydrocharitaceae	Seagrass	Star grass	*Halophila engelmanni*	5	7.02	0.57	5	-13.96	1.79	TX	2014	Rezek et al. 2017
Plant	Hydrocharitaceae	Seagrass	Turtle grass	*Thalassia testudinum*	2	5.60	0.01	2	-7.70	0.14	FL(FG)	2011	Vander Zanden et al. 2013
Plant	Hydrocharitaceae	Seagrass	Turtle grass	*Thalassia testudinum*				8	-8.53	0.16	FL(FG)	2007	Williams et al. 2009
Plant	Hydrocharitaceae	Seagrass	Turtle grass	*Thalassia testudinum*	2	5.60		2	-6.80		FL(FG)	2011	Williams et al. 2014
Plant	Multiple	Seagrass	Shoal grass, Manatee grass, Turtle grass	*Halodule wrightii, Syringodium filiforme, Thalassia testudinum*	15	1.10	2.32	15	-12.90	1.94	FL(FG)	2001	Alves-Stanley et al. 2010
Plant	Multiple	Seagrass	Shoal grass, Manatee grass, Turtle grass	*Halodule wrightii, Syringodium filiforme, Thalassia testudinum*	15	1.40	1.16	15	-11.00	1.94	FL(FG)	2001	Alves-Stanley et al. 2010
Plant	Multiple	Seagrass	Shoal grass, Manatee grass, Turtle grass	*Halodule wrightii, Syringodium filiforme, Thalassia testudinum*	16	2.50	1.60	16	-14.80	3.20	FL(FG)	2001	Alves-Stanley et al. 2010

Plant	Multiple	Seagrass	Shoal grass, Manatee grass, Turtle grass	*Halodule wrightii, Syringodium filiforme, Thalassia testudinum*	164	2.19	0.65				FL(FG)	1999	Dillon and Chanton 2008
Plant	Multiple	Seagrass	Seagrass	*Unidentified*	5	6.02	1.00	5	-12.23	1.10	AL	2011	Kroetz et al. 2017
Plant	Zosteraceae	Seagrass	Common eelgrass	*Zostera marina*				1	-10.00		NC	1988	Canuel et al. 19997
Plant	Zosteraceae	Seagrass	Common eelgrass	*Zostera marina*	8	6.09	0.50	8	-10.01	0.89	VA	2005	Douglass et al. 2011
Plant	Zosteraceae	Seagrass	Common eelgrass	*Zostera marina*	22	6.55	0.68	22	-10.07	0.43	VA	2010	Hondula and Price 2014
Plant	Zosteraceae	Seagrass	Common eelgrass	*Zostera marina*	4	6.79	0.34	4	-9.37	0.55	VA	2014	Oreska et al. 2018
Plant	Zosteraceae	Seagrass	Common eelgrass	*Zostera marina*				12	-10.20	0.75	NC	1975	Thayer et al. 1978
Arthropoda	Multiple	Shrimp	Shrimp	*Unidentified*	5	10.87	0.57	5	-19.52	0.98	AL	2011	Kroetz et al. 2017
Arthropoda	Penaeidae	Shrimp	Northern brown shrimp	*Farfantepenaeus aztecus*	3	8.30	0.17	3	-17.10	0.17	FL(FG)	2008	Baker et al. 2013
Arthropoda	Penaeidae	Shrimp	Northern brown shrimp	*Farfantepenaeus aztecus*	3	9.60	0.17	3	-16.90	0.35	LA	2008	Baker et al. 2013
Arthropoda	Penaeidae	Shrimp	Northern brown shrimp	*Farfantepenaeus aztecus*	3	10.40	0.52	3	-19.10	0.35	LA	2008	Baker et al. 2013
Arthropoda	Penaeidae	Shrimp	Northern white shrimp	*Litopenaeus setiferus*	3	9.40	0.17	3	-16.90	0.35	LA	2008	Baker et al. 2013
Arthropoda	Penaeidae	Shrimp	Northern brown shrimp	*Farfantepenaeus aztecus*	3	7.30	0.17	3	-14.80	0.17	NC	2008	Baker et al. 2013
Arthropoda	Penaeidae	Shrimp	Northern brown shrimp	*Farfantepenaeus aztecus*	3	7.70	0.69	3	-15.60	0.52	NC	2008	Baker et al. 2013
Arthropoda	Penaeidae	Shrimp	Northern brown shrimp	*Farfantepenaeus aztecus*	3	8.20	0.35	3	-16.50	0.52	NC	2008	Baker et al. 2013
Arthropoda	Penaeidae	Shrimp	Northern brown shrimp	*Farfantepenaeus aztecus*	3	7.60	0.35	3	-15.30	0.52	TX	2008	Baker et al. 2013
Arthropoda	Penaeidae	Shrimp	Northern brown shrimp	*Farfantepenaeus aztecus*	3	9.00	0.35	3	-18.30	0.17	TX	2008	Baker et al. 2013

Arthropoda	Penaeidae	Shrimp	Northern brown shrimp	*Farfantepenaeus aztecus*	3	9.20	0.35	3	-17.20	0.52	TX	2008	Baker et al. 2013
Arthropoda	Penaeidae	Shrimp	Northern white shrimp	*Litopenaeus setiferus*	1	6.90		1	-15.40		TX	2008	Baker et al. 2013
Arthropoda	Penaeidae	Shrimp	Northern white shrimp	*Litopenaeus setiferus*	1	8.30		1	-17.10		TX	2008	Baker et al. 2013
Arthropoda	Penaeidae	Shrimp	Northern white shrimp	*Litopenaeus setiferus*	3	8.80	0.17	3	-17.00	0.52	TX	2008	Baker et al. 2013
Arthropoda	Penaeidae	Shrimp	Northern brown shrimp	*Farfantepenaeus aztecus*	3	10.90	0.35	3	-16.30	0.17	VA	2008	Baker et al. 2013
Arthropoda	Penaeidae	Shrimp	Northern white shrimp	*Litopenaeus setiferus*				19	-20.00		FL(FG)	1992	Chanton and Lewis 2002
Arthropoda	Penaeidae	Shrimp	Northern brown shrimp	*Farfantepenaeus aztecus*	11	8.65	0.66	11	-17.30		NC	2007	Deehr et al. 2014
Arthropoda	Penaeidae	Shrimp	Shrimp	*Penaeus spp*	4	10.87	0.56	4	-19.47	0.75	AL	2008	Drymon et al. 2012
Arthropoda	Penaeidae	Shrimp	Northern brown shrimp	*Farfantepenaeus aztecus*	19	10.10	0.31	19	-19.50	0.39	LA	2000	Duque 2004
Arthropoda	Penaeidae	Shrimp	Northern brown shrimp	*Farfantepenaeus aztecus*	310	9.30	1.76	310	-19.40	1.76	LA	2005	Fry 2011
Arthropoda	Penaeidae	Shrimp	Northern brown shrimp	*Farfantepenaeus aztecus*	175	9.87	0.97	175	-17.14	2.22	LA	2005	Fry 2011
Arthropoda	Penaeidae	Shrimp	Northern brown shrimp	*Farfantepenaeus aztecus*	71	9.94	0.60	71	-17.18	1.58	LA	1999	Fry 2011
Arthropoda	Penaeidae	Shrimp	Northern brown shrimp	*Farfantepenaeus aztecus*	71	12.20	0.45	71	-18.85	0.93	LA	2006	Fry 2011
Arthropoda	Penaeidae	Shrimp	Northern brown shrimp	*Farfantepenaeus aztecus*	74	12.84	0.68	74	-20.52	0.97	LA	2006	Fry 2011
Arthropoda	Penaeidae	Shrimp	Northern brown shrimp	*Farfantepenaeus aztecus*	45	8.82	0.62	45	-15.96	1.01	TX	1995	Fry 2011

Arthropoda	Penaeidae	Shrimp	Northern brown shrimp	*Farfantepenaeus aztecus*	18	13.90	0.85	18	-19.50	1.70	TX	1995	Fry 2011
Arthropoda	Penaeidae	Shrimp	Pink shrimp	*Farfantepenaeus duorarum*	177	6.96	0.95	177	-21.75	2.58	FL(FG)	1997	Fry et al. 1999
Arthropoda	Penaeidae	Shrimp	Pink shrimp	*Farfantepenaeus duorarum*	96	5.38	1.05	96	-12.11	1.50	FL(FG)	1997	Fry et al. 1999
Arthropoda	Penaeidae	Shrimp	Pink shrimp	*Farfantepenaeus duorarum*	74	6.56	0.79	74	-14.67	1.80	FL(FG)	1997	Fry et al. 1999
Arthropoda	Penaeidae	Shrimp	Pink shrimp	*Farfantepenaeus duorarum*	60	6.58	0.87	60	-14.67	1.07	FL(FG)	1997	Fry et al. 1999
Arthropoda	Penaeidae	Shrimp	Northern brown shrimp	*Farfantepenaeus aztecus*	49	10.15	0.58	49	-20.18	1.46	LA	2000	Fry et al. 2003
Arthropoda	Penaeidae	Shrimp	Pink shrimp	*Farfantepenaeus duorarum*	4	6.65	0.40	4	-23.20	0.25	FL(FG)	1983	Harrigan et al. 1989
Arthropoda	Penaeidae	Shrimp	Pink shrimp	*Farfantepenaeus duorarum*	4	5.40	0.50	4	-13.70	0.93	FL(FG)	1983	Harrigan et al. 1989
Arthropoda	Penaeidae	Shrimp	Northern brown shrimp	*Farfantepenaeus aztecus*	40	11.00		40	-17.70		MS	1991	Moncreiff and Sullivan 2001
Arthropoda	Penaeidae	Shrimp	Northern white shrimp	*Litopenaeus setiferus*	3	11.40		3	-19.60		MS	1991	Moncreiff and Sullivan 2001
Arthropoda	Penaeidae	Shrimp	Pink shrimp	*Farfantepenaeus duorarum*	8	11.20		8	-16.50		MS	1991	Moncreiff and Sullivan 2001
Arthropoda	Penaeidae	Shrimp	Roughneck shrimp	*Rimapenaeus constrictus*	29	11.40		29	-16.70		MS	1991	Moncreiff and Sullivan 2001
Arthropoda	Penaeidae	Shrimp	Yellow roughneck shrimp	*Rimapenaeus similis*	97	11.80		97	-17.90		MS	1991	Moncreiff and Sullivan 2001
Arthropoda	Penaeidae	Shrimp	Shrimp	*Penaeus spp*				5	-16.80	0.80	FL(FG)	2007	Nelson et al. 2012
Arthropoda	Penaeidae	Shrimp	Northern brown shrimp	*Farfantepenaeus aztecus*	16	8.65	1.48	16	-16.56	2.40	TX	2006	Oakley et al. 2014
Arthropoda	Penaeidae	Shrimp	Northern white shrimp	*Litopenaeus setiferus*	10	9.93	1.58	10	-17.45	2.56	TX	2006	Oakley et al. 2014
Arthropoda	Penaeidae	Shrimp	Penaeid shrimp	*Farfantepenaeus spp*	10	9.99	1.61	10	-17.39	1.87	TX	2006	Oakley et al. 2014

Arthropoda	Penaeidae	Shrimp	Shrimp	*Penaeus spp*	3	9.84	1.56	3	-17.10	0.83	TX	2006	Oakley et al. 2014
Arthropoda	Penaeidae	Shrimp	Northern brown shrimp	*Farfantepenaeus aztecus*	43	12.16	1.24	43	-16.54	1.23	TX	2014	Rezek et al. 2017
Arthropoda	Penaeidae	Shrimp	Northern brown shrimp	*Farfantepenaeus aztecus*				10	-20.50		MS	1988	Sullivan and Moncreiff 1990
Arthropoda	Penaeidae	Shrimp	Shrimp	*Penaeus spp*				10	-19.50	0.50	LA	2010	Wilson et al. 2015
Arthropoda	Penaeidae	Shrimp	Northern brown shrimp	*Farfantepenaeus aztecus*	9	8.00	0.50	9	-18.40	0.50	TX	1999	Winemiller et al. 2007
Arthropoda	Penaeidae	Shrimp	Northern white shrimp	*Litopenaeus setiferus*	5	10.10	3.30	5	-20.60	3.30	TX	1999	Winemiller et al. 2007
Arthropoda	Squillidae	Shrimp	Mantis shrimp	*Squilla empusa*	22	12.89	0.63	22	-18.66	0.70	VA	2006	Buchheister and Latour 2011
Arthropoda	Squillidae	Shrimp	Mantis shrimp	*Squilla empusa*	3	12.50	0.80	3	-18.78	0.67	AL	2008	Drymon et al. 2012
Arthropoda	Squillidae	Shrimp	Mantis shrimp	*Squilla empusa*	23	13.10		23	-16.90		MS	1991	Moncreiff and Sullivan 2001

Table B2. Summary of studies quantifying Kemp's ridley sea turtle diet composition throughout their range. Weighted means of these percentages were used as informative priors in the stable isotope mixing models. As most studies reported data for bivalves and gastropods within a single mollusc category, we split the weighted mean for molluscs evenly to generate informative bivalve and gastropod priors.

Source	State	Sample Type	Sample Size	Data Type	Turtle Carapace Length	Crustacean (%)	Mollusc (%)	Fish (%)	Macropalgae/ Seagrass (%)	Other/ Unidentified (%)
Schmid and Tucker 2018	FL(FG)	fecal	58	% dry matter	40.7 ± 8.5 cm SCL (24.2 - 63.7 cm)	80.60	0.30	0.10	0.10	18.90
Burke et al. 1993, 1994	NY	fecal	12	% dry matter	32.8 ± 4.8 cm SCL (24.7 - 42.6 cm)	80.40	4.00	0.00	9.90	5.70
Seney and Musick 2005	VA	whole digestive tract	18	% dry matter	36.7 ± 7.3 cm SCL (23.1 - 49.9 cm)	94.30	0.70	3.00	0.10	1.90
Servis et al. 2015	FL(FG)	stomach or entire GI contents	20	% wet volume	45.9 ± 3.1 cm SCL (23.6 - 65.0 cm)	70.70	5.20	8.70	0.00	15.40
Shaver 1991	TX	whole digestive tract	50	% dry matter	43.3 ± 2.2 cm CCL (5.2 - 71 cm)	95.40	1.56	0.08	0.14	2.82
Werner 1994	LA, TX	fecal	92	% dry matter	32.74 ± 7.14 cm SCL (21.6 - 59.5 cm)	61.57	8.66	13.65	4.35	11.77
Witzell and Schmid 2005*	FL(FG)	fecal	66	% dry matter	41.4 ± 5.8 cm SCL (28.2 - 52.5 cm)	34.90	2.60	0.00	0.10	62.40

*Excluded from analysis due to abnormally high *Other/Unidentified* percentage (i.e., high prevalence of tunicates in diet)

Table B3. Elemental concentrations of species representative of the prey groups included in the stable isotope mixing models. Data are from various geographic origin but we assumed taxonomy would be the primary source of variation.

Prey group	Common Name	Scientific Name	Sampling Location (State, Country)	Sample Size	%C	%N	Source
Bivalve	Eastern oyster	*Crassostrea virginica*	Virginia and Maryland, USA	525	43.45	12.63	Fertig et al. 2014
Bivalve	Eastern oyster	*Crassostrea virginica*	Maryland, USA	48	–	12.18	Fertig et al. 2009
Bivalve	Mussel	*Brachidontes exustus*	Florida, USA	120	47.33	11.14	Fry and Smith 2002
Bivalve	California mussel	*Mytilus californianus*	California, USA	8	42.60	12.80	Newsome et al. 2004
Crustacean	Blue crab	*Callinectes sapidus*	North Carolina, USA	4	38.61	12.00	Wallace et al. 2009
Crustacean	Portly spider crab	*Libinia emarginata*	North Carolina, USA	11	41.68	12.77	Wallace et al. 2009
Crustacean	Horseshoe crab	*Limulus polyphemus*	North Carolina, USA	10	43.35	12.30	Wallace et al. 2009
Crustacean	Unidentified	*Unidentified*	California, USA	3	42.30	12.00	Turner Tomaszewicz et al. 2017
Crustacean	Grass shrimp	*Palaemonetes vulgaris*	Georgia, USA	7	30.40	8.02	Parker et al. 2008
Fish	Capelin, blue runner	*Mallotus villosus, Caranx crysos*	California, USA	3	48.40	13.10	Turner Tomaszewicz et al. 2017
Fish	Spot croaker	*Leiostomus xanthurus*	North Carolina, USA	8	56.28	9.94	Wallace et al. 2009
Fish	Southern flounder	*Paralichthys lethostigma*	North Carolina, USA	10	44.89	12.65	Wallace et al. 2009
Fish	Atlantic sturgeon	*Acipenser oxyrinchus*	Florida, USA	36	47.23	14.62	Gu et al. 2001
Fish	Killifish	*Fundulus heteroclitus*	Georgia, USA	7	26.60	7.52	Parker et al. 2008
Fish	Miscellaneous	*Miscellaneous*	California, USA	24	40.30	12.40	Newsome et al. 2004
Fish	Capelin	*Mallotus villosus*	France	15	35.80	10.60	Cherel et al. 2005
Fish	Herring	*Clupea harengus*	France	15	42.60	12.50	Cherel et al. 2005
Fish	Speckled worm eel	*Myrphis punctatus*	Florida, USA	56	43.51	11.41	Vaslet et al. 2011
Gastropod	Whelk spp	*Busycon spp*	North Carolina, USA	10	44.76	13.09	Wallace et al. 2009
Gastropod	Mud snail	*Ilyanassa obsoleta*	Georgia, USA	6	34.10	8.02	Parker et al. 2008

Gastropod	Unidentified	*Unidentified*	Guadaloupe	5	44.50	7.50	Dromard et al. 2015
Macroalgae	Sea lettuce, red algae	*Ulva lactuca, Wranglia, Gracilaria*	Florida, USA	–	26.70	0.60	Wilson et al. 2010
Macroalgae	Sea lettuce	*Ulva spp*	Alabama, USA	–	31.67	1.95	Prado et al. 2012
Macroalgae	Bladder rack	*Fucus vesiculosus*	North Carolina, USA	–	28.69	0.87	Raven and Osmond 1992
Macroalgae	Forkweed	*Dictyota menstrualis*	North Carolina, USA	–	18.08	1.53	Raven and Osmond 1992
Macroalgae	Forkweed	*Padina gymnospora*	North Carolina, USA	–	17.54	0.94	Raven and Osmond 1992
Macroalgae	Green sea fingers	*Codium fragile*	North Carolina, USA	–	23.48	1.44	Raven and Osmond 1992
Macroalgae	Red algae	*Gracileria spp*	Maryland, USA	174	–	1.93	Fertig et al. 2009
Macroalgae	Red algae	*Bostrychia spp*	Georgia, USA	4	16.70	2.09	Parker et al. 2008
Macroalgae	Sea lettuce	*Ulva spp*	Georgia, USA	9	24.50	2.83	Parker et al. 2008
Macroalgae	Red algae	*Caloglossa spp*	Georgia, USA	5	15.60	1.76	Parker et al. 2008
Macroalgae	Red algae	*Grateloupia spp*	Alabama, USA	–	27.44	2.57	Prado et al. 2012
Macroalgae	Unidentified	*Dictyota pulchella*, *Acanthophora spicifera*	Guadaloupe	6	12.30	1.90	Dromard et al. 2015
Seagrass	Shoal grass	*Halodule wrightii*	Florida, USA	–	33.10	1.00	Wilson et al. 2010
Seagrass	Turtle grass	*Thalassia testudinum*	Florida, USA	10	36.38	2.08	Barry et al. 2017
Seagrass	Turtle grass	*Thalassia testudinum*	Texas, USA	108	–	1.84	Delgado et al. 2017
Seagrass	Turtle grass	*Thalassia testudinum*	Florida, USA	10	33.40	2.30	Fourqurean and Schrlau 2003
Seagrass	Turtle grass	*Thalassia testudinum*	Florida, USA	5	–	2.02	Goecker et al. 2005
Seagrass	Turtle grass	*Thalassia testudinum*	Florida, USA	5	–	2.24	Goecker et al. 2005
Seagrass	Turtle grass	*Thalassia testudinum*	Alabama, USA	–	34.37	2.47	Prado et al. 2012
Seagrass	Shoal grass	*Halodule and Syringodium spp*	Florida, USA	11	32.20	2.10	Wilson et al. 2017
Seagrass	Turtle grass	*Thalassia testudinum*	Florida, USA	134	39.20	1.90	Campbell and Fourqurean 2009
Seagrass	Shoal grass	*Halodule wrightii*	Florida, USA	70	43.40	2.30	Campbell and Fourqurean 2009
Seagrass	Manatee grass	*Syringodium filiforme*	Florida, USA	77	38.90	2.10	Campbell and Fourqurean 2009

Table B4. Statistical results for Kruskal-Wallis rank sum tests comparing prey stable carbon and nitrogen isotope ratios **(A)** within and **(B)** among regions.

Prey Group	$\delta^{13}C$			$\delta^{15}N$		
	X^2	*df*	P-value	X^2	*df*	P-value
(A) Within region comparisons						
western GoM	42.21	4	**<0.001**	60.13	4	**<0.001**
northern GoM	58.80	4	**<0.001**	53.13	4	**<0.001**
eastern GoM	59.73	4	**<0.001**	81.64	4	**<0.001**
southern Atlantic	23.35	4	**<0.001**	32.4	4	**<0.001**
northern Atlantic	15.47	4	**0.004**	26.24	4	**<0.001**
(B) Between region comparisons						
Crustacean	14.81	4	**0.005**	40.19	4	**<0.001**
Bivalve	22.55	4	**<0.001**	20.73	4	**<0.001**
Gastropod	11.03	4	**0.026**	7.59	4	0.108
Fish	30.28	4	**<0.001**	36.07	4	**<0.001**
Macroalgae/Seagrass	11.37	4	**0.023**	42.15	4	**<0.001**

Table B5. Statistical results for Wilcoxon rank sum tests comparing stable carbon and nitrogen isotope ratios among prey groups within regions.

	wGoM		nGoM		eGoM		NC		VA	
Comparison	$\delta^{13}C_{cor}$	$\delta^{13}N$	$\delta^{13}C_{cor}$	$\delta^{13}N$	$\delta^{13}C_{cor}$	$\delta^{13}N$	$\delta^{13}C_{cor}$	$\delta^{13}N$	$\delta^{13}C_{cor}$	$\delta^{13}N$
Crustacean vs. Bivalve	**<0.001**	0.969	**<0.001**	**<0.001**	**0.016**	0.823	**<0.001**	**0.008**	**0.027**	0.143
Crustacean vs. Gastropod	**0.010**	0.576	0.210	0.100	0.904	0.876	0.204	**0.003**	0.758	0.089
Crustacean vs. Fish	0.262	**<0.001**	**0.001**	0.015	**0.011**	**<0.001**	**0.050**	**0.004**	**0.003**	**0.002**
Crustacean vs. Macroalgae/Seagrass	**0.006**	**<0.001**	0.259	**<0.001**	**<0.001**	**<0.001**	0.324	**<0.001**	0.901	**<0.001**
Bivalve vs. Gastropod	**0.003**	0.502	**<0.001**	0.138	0.151	1.000	**<0.001**	0.699	0.095	1.000
Bivalve vs. Fish	**<0.001**	**<0.001**	**<0.001**	**<0.001**	**<0.001**	**<0.001**	**0.002**	**<0.001**	0.842	**0.003**
Bivalve vs. Macroalgae/Seagrass	**<0.001**	**<0.001**	**<0.001**	0.574	**<0.001**	**0.003**	**0.013**	0.177	**0.019**	0.246
Gastropod vs. Fish	0.092	0.070	**0.002**	**0.005**	0.212	**0.002**	**0.002**	**<0.001**	0.092	**0.051**
Gastropod vs. Macroalgae/Seagrass	0.856	**0.051**	0.699	0.153	**0.007**	**0.015**	0.926	0.66	0.933	0.381
Fish vs. Macroalgae/Seagrass	**0.018**	**<0.001**	**0.008**	**<0.001**	**<0.001**	**<0.001**	0.091	**<0.001**	**0.004**	**<0.001**

Table B6. Statistical results for one-way Analysis of Variance with post-hoc Tukey Honestly Significant Difference Test comparing Kemp's ridley bone stable carbon and nitrogen isotope ratios among regions.

Prey Group	$\delta^{13}C$		$\delta^{15}N$	
	Difference	P-value	Difference	P-value
wGoM vs. nGoM	1.49	**<0.001**	1.45	**0.004**
wGoM vs. eGoM	−0.44	0.600	4.23	**<0.001**
wGoM vs. NC	0.57	0.250	2.32	**<0.001**
wGoM vs. NC	−0.30	0.860	0.54	0.687
nGoM vs. eGoM	−1.93	**<0.001**	2.78	**<0.001**
nGoM vs. NC	−0.92	**0.032**	0.87	0.263
nGoM vs. VA	−1.79	**<0.001**	−0.91	0.276
eGoM vs. NC	1.02	**0.018**	−1.91	**<0.001**
eGoM vs. VA	0.14	0.994	−3.67	**<0.001**
NC vs. VA	−0.87	0.058	−1.78	**<0.001**

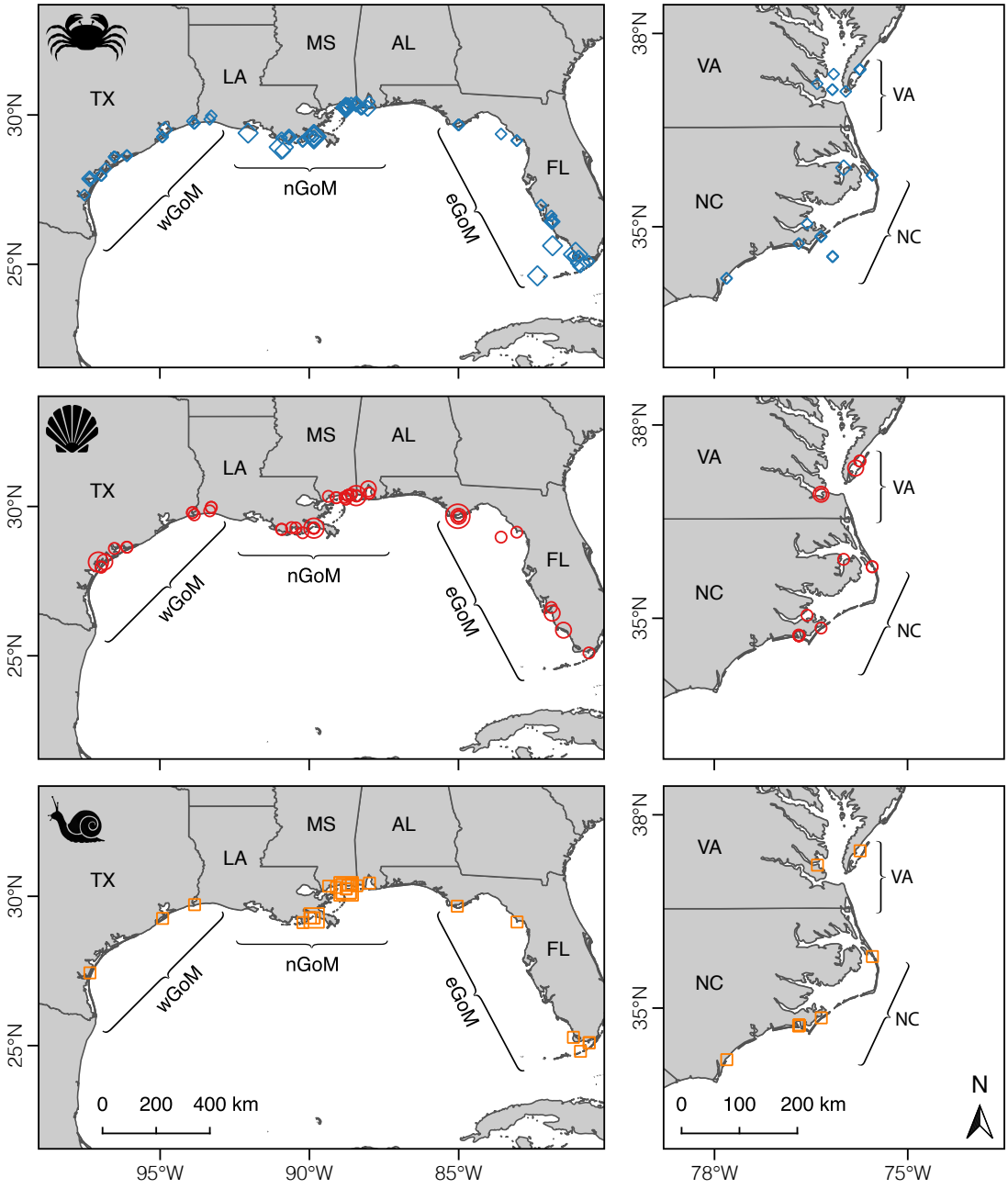

Figure B1. Map of sampling locations of invertebrate prey groups and geographic breakpoints used to cluster turtles and prey groups. Crustacean = blue diamonds, Bivalves = red circles, Gastropods = orange squares. Shape size scales with relative sample size for each study using bins of 0–25, 25–50, 50–100, and 100+.

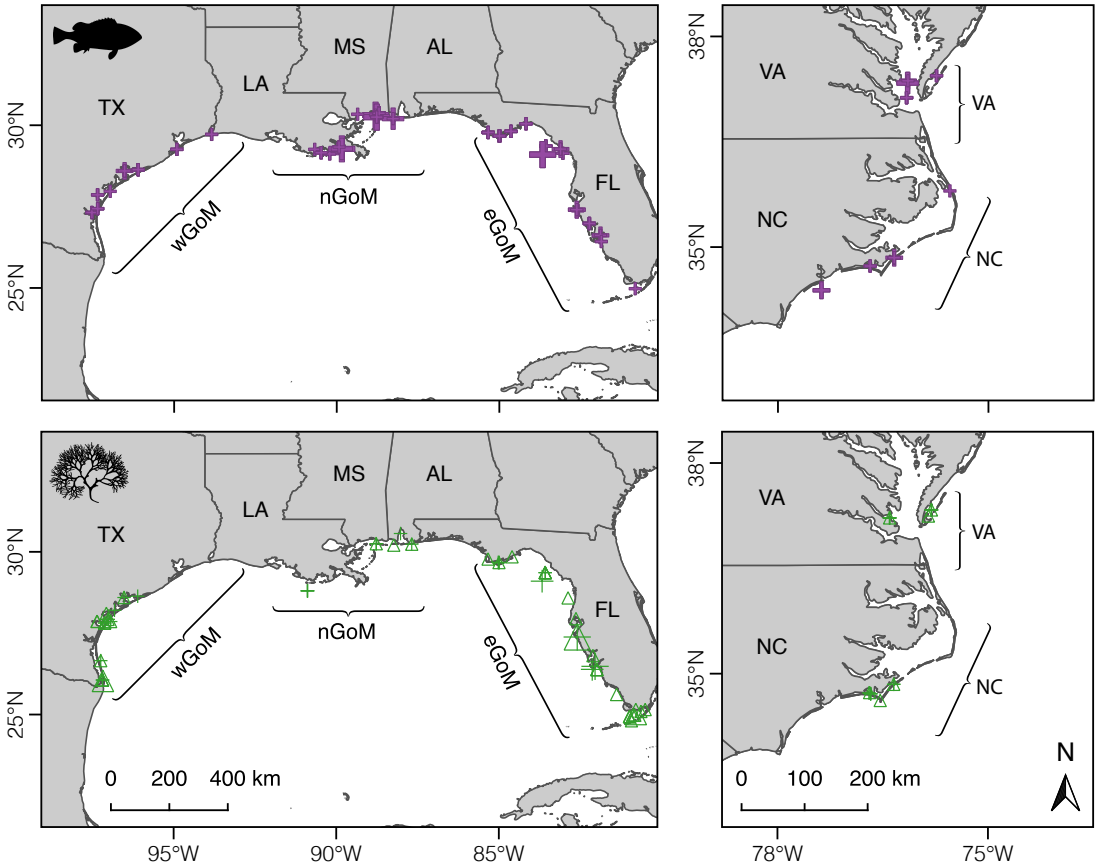

Figure B2. Map of sampling locations of fish and macroalgae/seagrass prey groups and geographic breakpoints used to cluster turtles and prey groups. Fish = purple plus signs, Macroalgae = green plus signs, Seagrass = green triangles. Shape size scales with relative sample size for each study using bins of 0–25, 25–50, 50–100, and 100+.

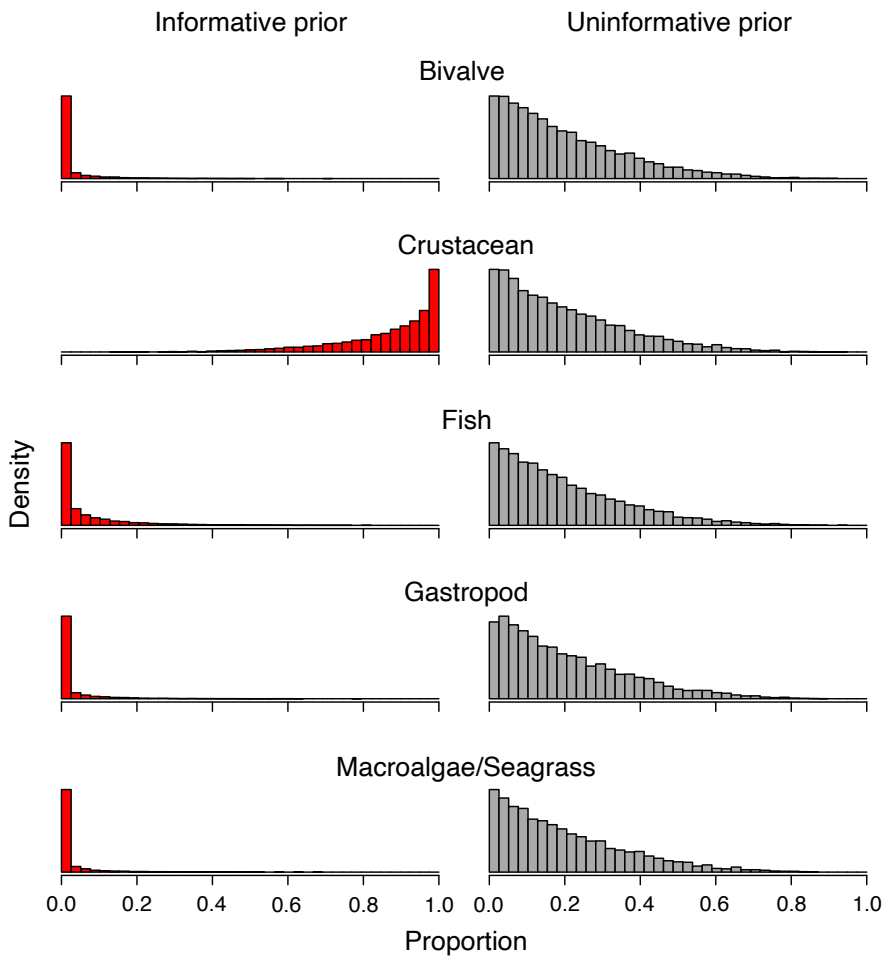

Figure B3. Informative and uninformative priors used in the mixing models.

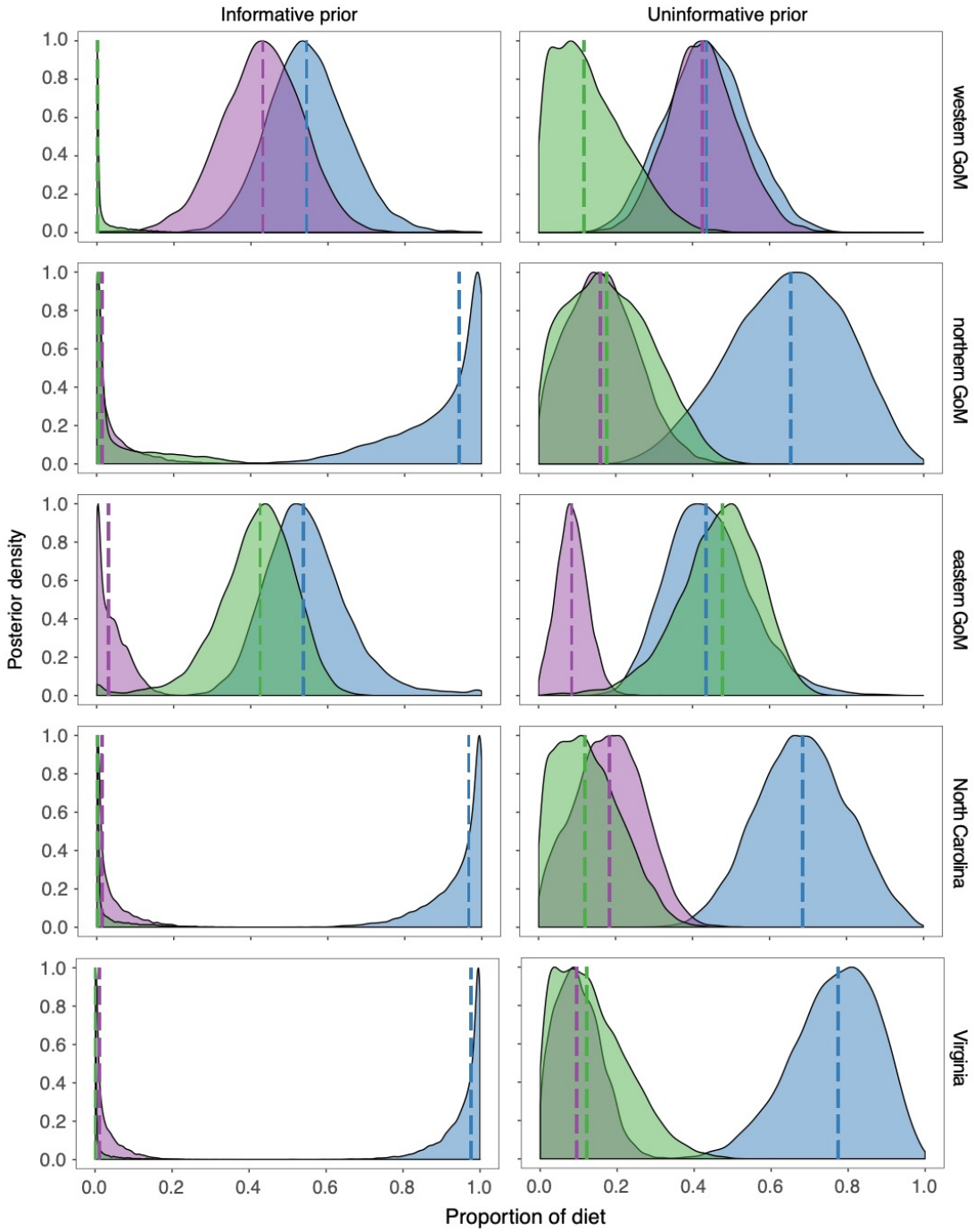

Figure B4. Posterior distributions for the proportional contribution of each prey group to Kemp's ridley sea turtle diets.
Blue = invertebrates, purple = fish, green = macroalgae/seagrass. Invertebrate prey groups (crustacean, bivalve, gastropod) were aggregated *a posteriori*. Medians are denoted by vertical dashed lines.

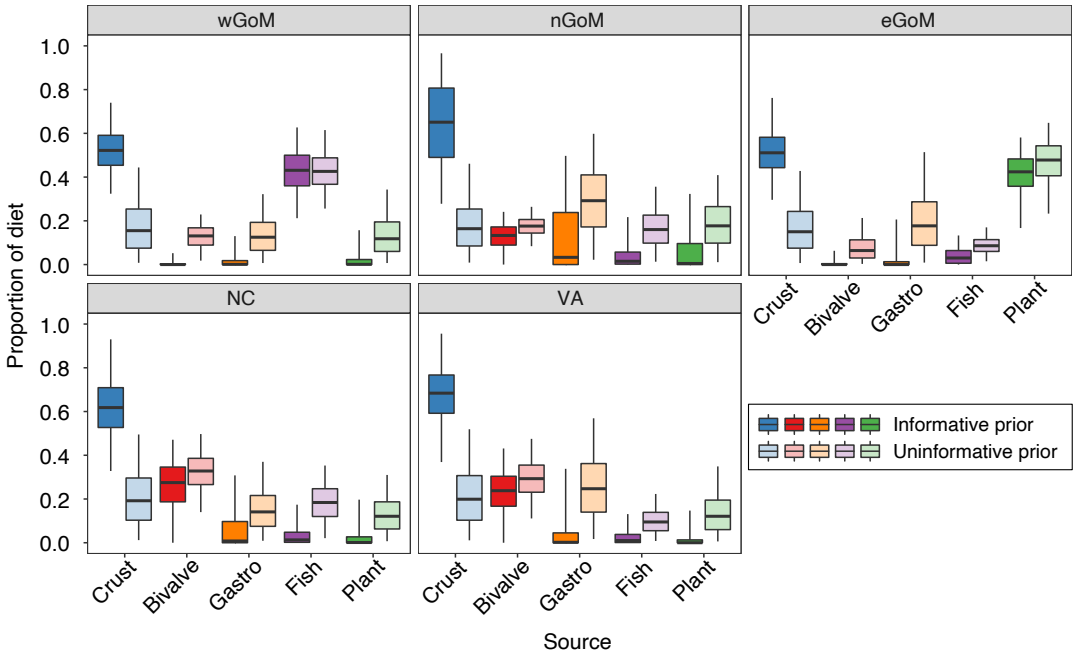

Figure B5. Proportional contribution of each prey group to Kemp's ridley sea turtle diets based on MixSIAR models that included an informative prior constructed from published diet proportion data and an uninformative prior that assigned equal probability to all prey groups.
Lines in boxes are medians, boxes are 50% credible intervals, error bars are 95% credible intervals.

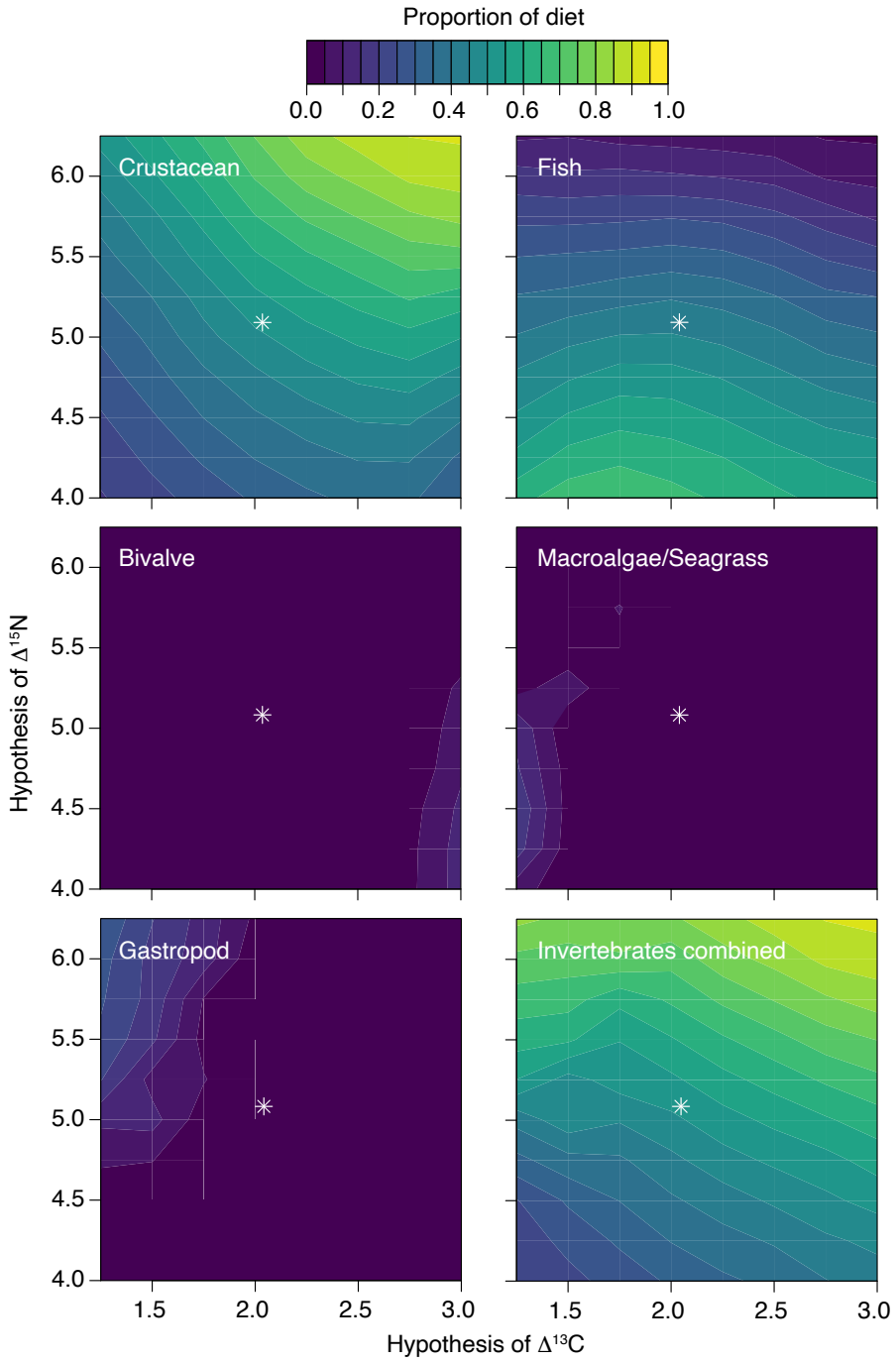

Figure B6. Sensitivity analysis showing how the proportional contribution of each prey group to western GoM-stranded Kemp's ridley sea turtle diets changes when trophic discrimination factors (TDFs) are varied. White stars denote mean TDF used in this study and plot areas represent approximately one standard deviation ($\Delta^{13}C$ = 2.1 ± 0.6, $\Delta^{15}N$ = 5.1 ± 1.1).

APPENDIX C: CHAPTER 4 SUPPLEMENTAL INFORMATION

		Predicted			
Model	Actual	ATL	GoM	% Correct	Model Evaluation
Scaled growth + trace element QDAs					
(A) trace element QDA_{full}	ATL	**30**	11	73.1	Wilk's $\lambda = 0.70$
	GoM	11	**21**	65.6	$F_{10,62} = 2.62$
	Total	41	32	69.8	$P = 0.010$
(B) trace element $QDA_{reduced}$	ATL	**31**	10	75.6	Wilk's $\lambda = 0.71$
	GoM	11	**21**	65.6	$F_{8,64} = 3.30$
	Total	42	31	71.2	$P = 0.003$
(C) trace element QDA_{growth}	ATL	**36**	5	87.9	ANOVA
	GoM	20	**12**	37.4	$F_{1,71} = 0.278$
	Total	56	17	65.8	$P = 0.599$

Table C1. Predicted regional assignment of Kemp's ridley sea turtles based on cross-validated quadratic discriminant function analysis (QDA). Models included (A) trace element QDA_{full} (scaled growth rate + 9 trace element concentrations), (B) trace element $QDA_{reduced}$ (scaled growth rate + 7 trace element concentrations), and (C) trace element QDA_{growth} (scaled growth rate only; see Table 4.4. Correct classifications are in **bold**. The most successful model is highlighted in grey. Final models were evaluated via (M)ANOVA. Atlantic (ATL) = Florida Atlantic Coast through Virginia, Gulf of Mexico (GoM) = Texas through Florida Gulf Coast.

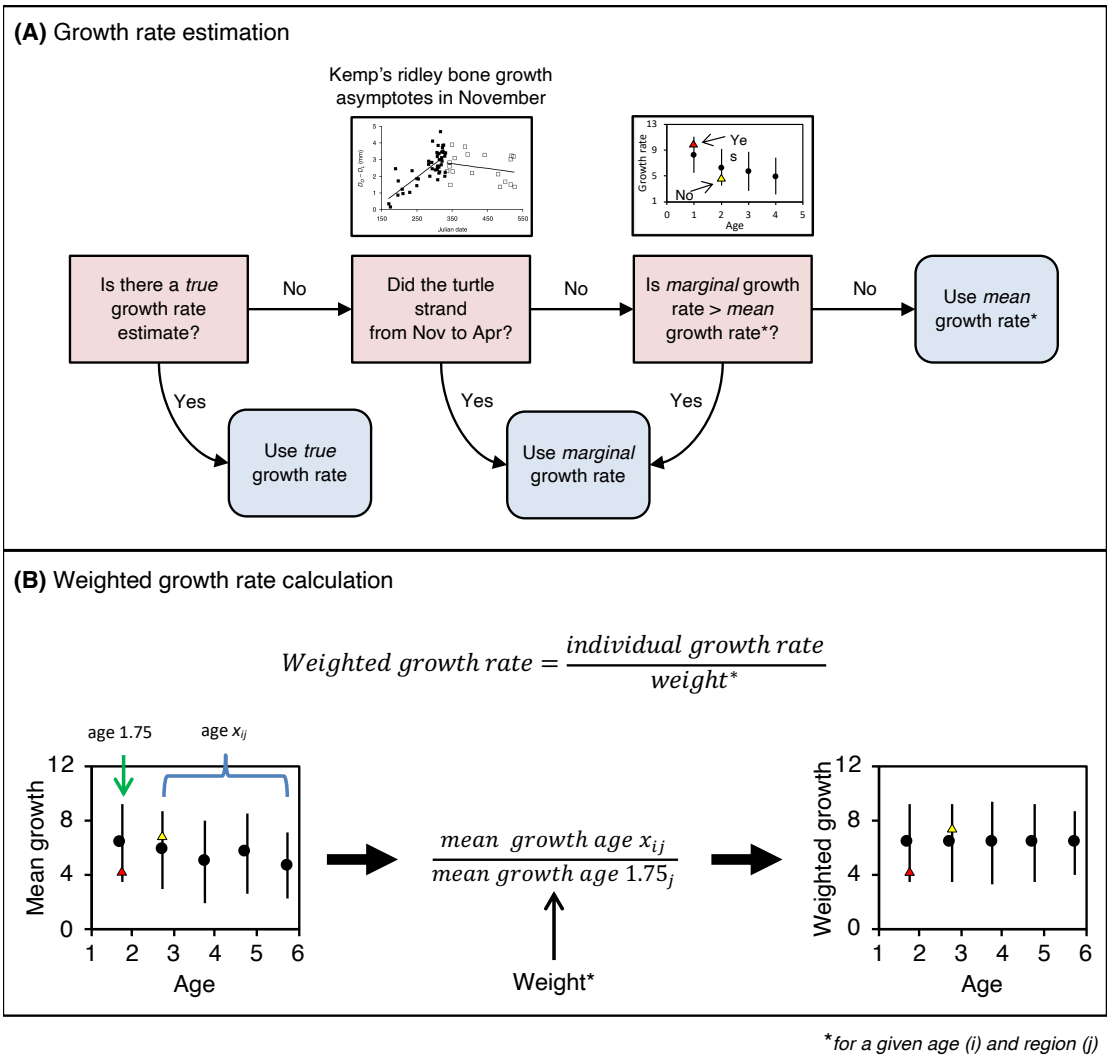

Figure C1. Conceptual diagram outlining **(A)** decision tree for estimating growth rates and **(B)** weighted growth rate calculation.

APPENDIX D: CHAPTER 5 SUPPLEMENTAL INFORMATION

Table D1. Annual nest and hatchling production from the three primary Kemp's ridley sea turtle nesting beaches in Mexico (Rancho Nuevo, Tepehuajes, Playa Dos). Data sourced from Gallaway et al. (2016) (originally provided by La Comisión Nacional de Áreas Naturales Protegidas, CONANP).

		Hatchlings					Hatchlings		
Year	Nests	Total	Corral	*In-situ*	Year	Nests	Total	Corral	*In-situ*
1966	5991	29100	29100	0	1988	842	62218	62218	0
1967	5519	24100	24100	0	1989	828	66802	66802	0
1968	5117	15000	15000	0	1990	992	74339	74339	0
1969	4018	28400	28400	0	1991	1178	79749	79749	0
1970	3017	31400	31400	0	1992	1275	92116	92116	0
1971	2012	13100	13100	0	1993	1241	84605	84605	0
1972	1824	14600	14600	0	1994	1562	107687	107687	0
1973	1643	23500	23500	0	1995	1930	120038	120038	0
1974	1466	23500	23500	0	1996	1981	114842	114842	0
1975	1266	11100	11100	0	1997	2221	141770	141770	0
1976	1110	36100	36100	0	1998	3482	167168	167168	0
1977	1036	30100	30100	0	1999	3369	211355	211355	0
1978	924	48009	48009	0	2000	5834	365479	365479	0
1979	954	63996	63996	0	2001	4927	291268	291268	0
1980	868	37378	37378	0	2002	5525	357313	357313	0
1981	897	53282	53282	0	2003	7604	433719	433719	0
1982	750	48007	48007	0	2004	6309	421684	413761	7923
1983	746	32921	32921	0	2005	9236	569963	555884	14079
1984	798	58124	58124	0	2006	11322	715002	688755	26247
1985	702	51033	51033	0	2007	13849	902290	709619	192671
1986	744	48818	48818	0	2008	17131	806079	731383	74696
1987	737	44634	44634	0	2009	19163	1025027	767633	257394

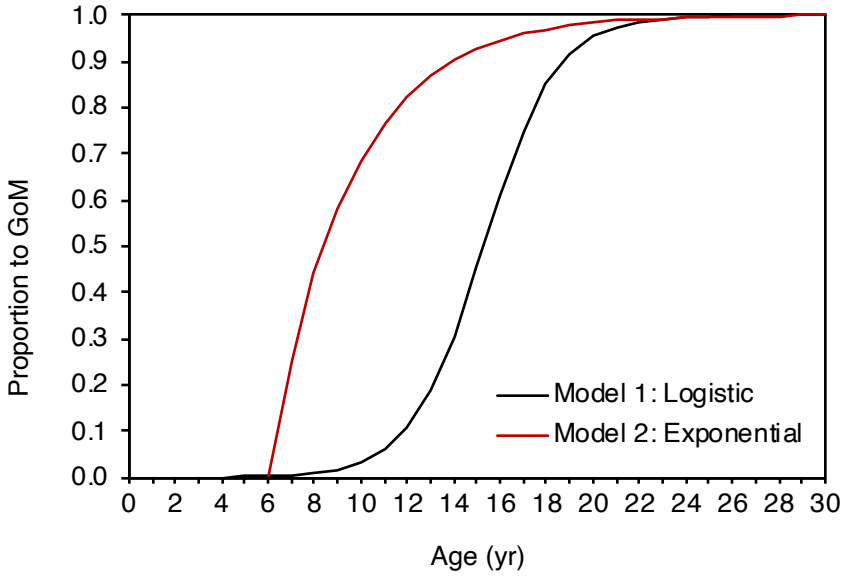

Figure D1. Transition probabilities for Atlantic-to-GoM ontogenetic shifts used in Model 1 (Atlantic turtles shift to GoM at maturation) and Model 2 (Atlantic turtles shift to GoM beginning at age 7).

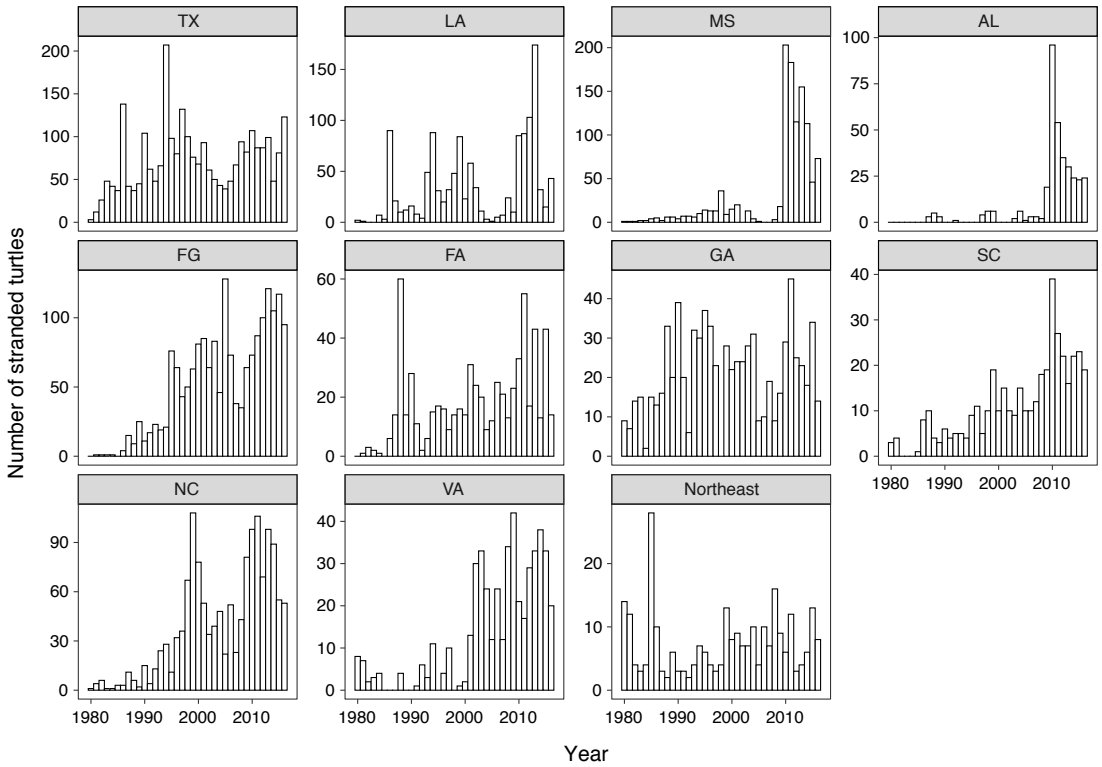

Figure D2. Kemp's ridley stranding counts by state and year.

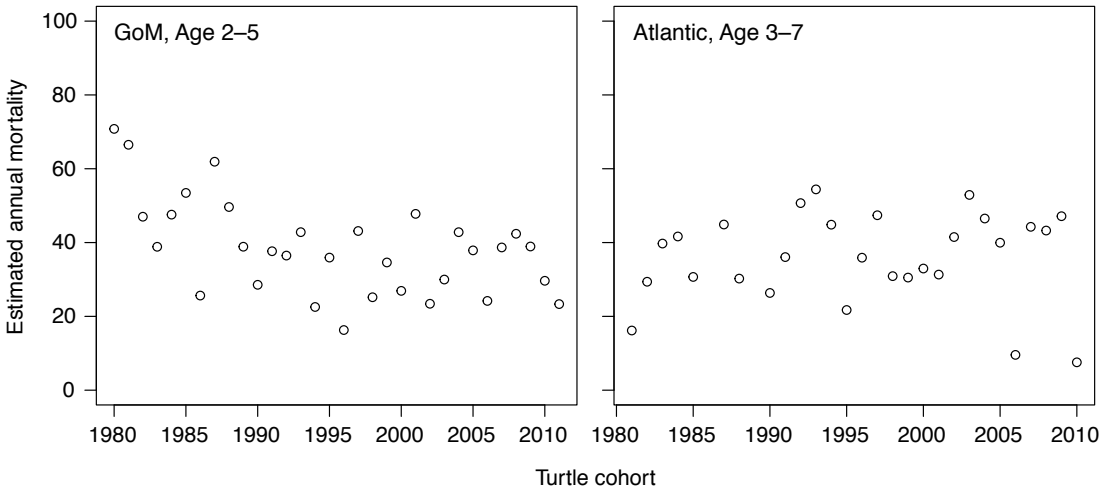

Figure D3. Estimated annual mortality estimates for Kemp's ridley stranding counts by state.

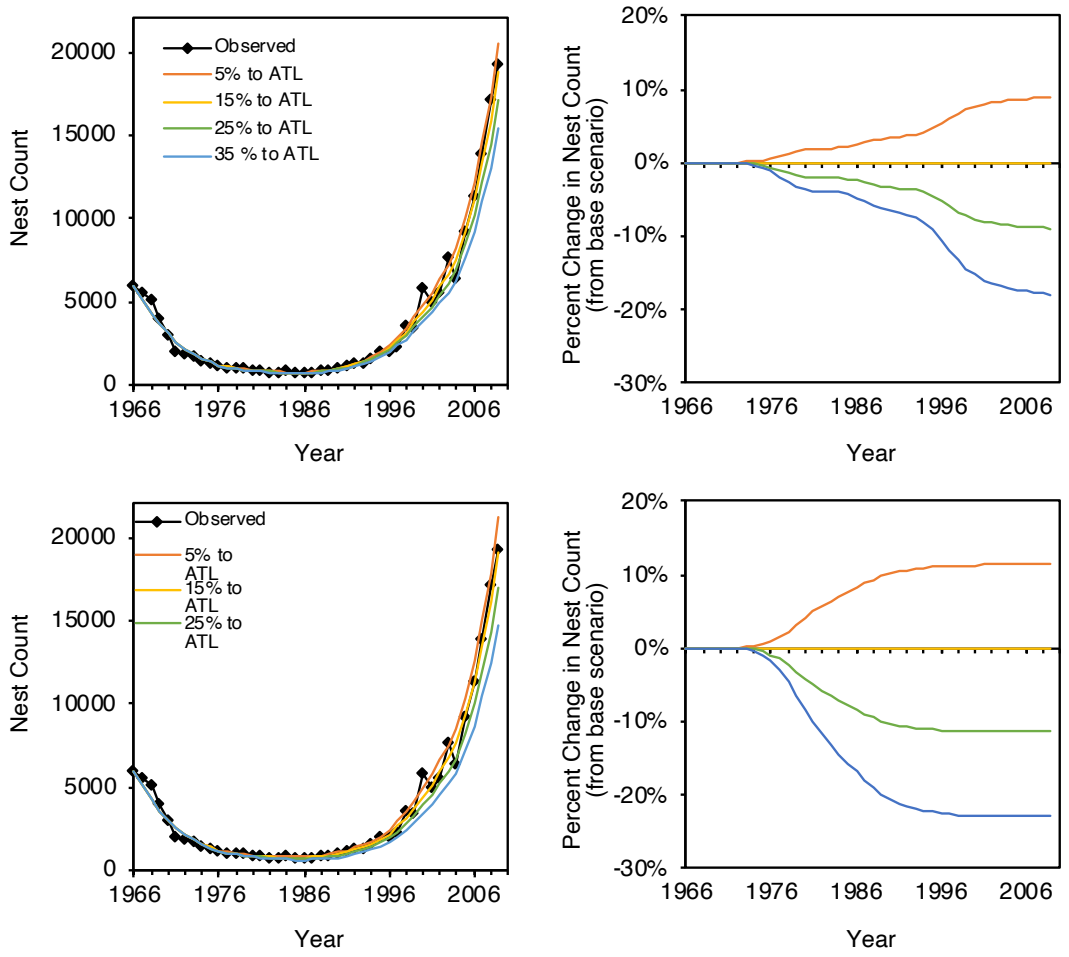

Figure D4. Predicted nest counts for Model 2 (upper panels; Atlantic turtles shift to GoM beginning at age 7) and Model 3 (lower panels; No Atlantic turtles shift to GoM) ran using varying proportions of turtles entering U.S. Atlantic life stages from the oceanic life stage. Bottom panel displays percent change in nests counts relative to the base scenario (base scenario = 15% to Atlantic, ATL, annually).